Cadas

ISPRS
MANAUS
1990

INTERNATIONAL SYMPOSIUM ON PRIMARY DATA ACQUISITION

TROPICAL HOTEL MANAUS

INTERNATIONAL ARCHIVES OF PHOTOGRAMMETRY AND REMOTE SENSING
ARCHIVES INTERNATIONALES DE PHOTOGRAMMETRIE ET DE TELEDETECTION
INTERNATIONALES ARCHIV FÜR PHOTOGRAMMETRIE UND FERNERKUNDUNG

Volume Volume Band 28 Part Tome Teil 1

Proceedings
Actes
Ergebnisse

Published by the Organizing Committee of the TC1 International Symposium on Primary Data Acquisition, MANAUS/1990

FOREWORD

To Symposia organizers, having the Proceedings ready before the event means always some challenge. **MANAUS/1990** has made it. More than twelve hundred pages, including the papers submitted for both the 6TH BRAZILIAN SYMPOSIUM ON REMOTE SENSING and the ISPRS Commission I's INTERNATIONAL SYMPOSIUM ON PRIMARY DATA ACQUISITION, have gone through printing and are in your hands.

Several institutions and people have contributed to this achievement.

In first place, the authors, which, in large majority, were strict in providing the manuscripts in time. Second, the organizing institutions, INPE, SELPER, and ISPRS/SBC, and the Commissions on Programs and Arts and Printing. Last but not least, the financing organizations, CNPq, FINEP and FAPESP, as well as the event sponsors: the Canadian Government, ESA, NASA, SPOT IMAGE, EOSAT, Carl Zeiss Jena, IBAMA and CNES.

It is thus with a lot of effort and no less in pride that we deliver to the scientific community the Proceedings of **MANAUS/1990**.

Paulo Roberto Martini

Paulo Roberto Martini
MANAUS/1990 Coordinator General

- **VI SIMPÓSIO BRASILEIRO DE SENSORIAMENTO REMOTO**
  - Workshop on Urban Settlements
  - Workshop SPOT
  - Workshop AVHRR
  - Workshop on Radiometry
  - Workshop on ERS-1 Applications
  - Workshop on Training and Education in Remote Sensing
  - Workshop on Digital Terrain Models
  - Special Session on the SPOT Applications Program (PAS)
  - III Workshop on Data Collection Platforms (PCD)

- **ISPRS Technical Commission 1's INTERNATIONAL SYMPOSIUM ON PRIMARY DATA ACQUISITION**
  - Special Session on International Remote Sensing Satellite Systems

June 24 to 29, 1990
Centro de Convenções do Hotel Tropical
Manaus - Amazonas
BRASIL

ORGANIZATION:

- Secretaria da Ciência e Tecnologia da Presidência da República - SCT / Instituto de Pesquisas Espaciais - INPE
- Sociedad de Especialistas Latinoamericanos en Percepción Remota - SELPER
- International Society for Photogrammetry and Remote Sensing - ISPRS / Technical Commission I
- Sociedade Brasileira de Cartografia, Geodésia, Fotogrametria e Sensoriamento Remoto - SBC

HONORARY PRESIDENT:

. José Goldemberg - Secretário de Ciência e Tecnologia da Presidência da República

STEERING COMMITTEE:

. Marcio Nogueira Barbosa - INPE's Director General

. Miguel Sanchez Peña - SELPER's President

. Kennert Torlegaard - ISPRS President

. Paulo E.M. Tavares - SBC President

EVENT COORDINATOR GENERAL:

. Paulo Roberto Martini

INTERNATIONAL SYMPOSIUM ORGANIZING COMMITTEE

. Marcio Nogueira Barbosa

. José Luiz de Barros Aguirre

. Paulo Roberto Martins Serra

BRAZILIAN SYMPOSIUM ORGANIZING COMMITTEE

. Roberto Pereira da Cunha

. Paulo Cesar Gurgel de Albuquerque

. Tania Maria Sausen

PUBLISHING COORDINATION:

. Comissão de Anais e Programas

. Comissão de Artes Gráficas e Impressão

COVER:

. Center Landsat-TM image produced by INPE

. Photos by courtesy of Abril Imagens

PRINTING:

Gráfica do INPE
Av. dos Astronautas, 1758
12225 São José dos Campos, SP
Phone: (0123) 22-9977 - Ext. 235

SUPPORT:

. Governo do Estado do Amazonas

. Prefeitura Municipal de Manaus

. FINEP - Financiadora de Estudos e Projetos

. CNPq - Conselho Nacional de Desenvolvimento Científico e Tecnológico

. INPA - Instituto Nacional de Pesquisas da Amazônia

. FAPESP - Fundação de Amparo à Pesquisa do Estado de São Paulo

INSTITUTO DE PESQUISAS ESPACIAIS - INPE

DIRECTOR GENERAL	: **Marcio Nogueira Barbosa**
HEAD OF STAFF	: **Sergio Sobral de Oliveira**
DIRECTOR OF SPACE SCIENCES	: **Volker W.J.H. Kirchhoff**
DIRECTOR OF ENGINEERING AND SPACE TECHNOLOGY	: **Mucio Roberto Dias**
DIRECTOR OF EARTH OBSERVATION	: **Luiz Gylvan Meira Filho**
ADMINISTRATIVE MANAGER	: **José Liberato Jr.**
INSTITUTIONAL RELATIONS MANAGER	: **Roberto Pereira da Cunha**

SOCIEDAD DE ESPECIALISTAS LATINO-AMERICANOS EN PERCEPCIÓN REMOTA - SELPER

PRESIDENT	: **Miguel Sanchez Peña - Argentina**
VICE-PRESIDENT	: **Roberto Pereira da Cunha - Brasil**
VICE-PRESIDENT	: **Walter Danjoy - Peru**
SECRETARY	: **Maria Cristina Serafine - Argentina**
TREASURER	: **Olga Florencia Casal - Argentina**
NATIONAL COORDINATOR	: **Paulo Roberto Martini - Brasil**

ISPRS - INTERNATIONAL SOCIETY FOR PHOTOGRAMMETRY AND REMOTE SENSING

OUNCIL 1988-1992:

PRESIDENT	: **Kennert Torlegaard**
FIRST VICE PRESIDENT	: **Gottfried Konecny**
SECOND VICE PRESIDENT	: **Ivan S. Katzarski**
SECRETARY GENERAL	: **Shunji Murai**
TREASURER	: **Keith Atkinson**
CONGRESS DIRECTOR	: **Lawrence W. Fritz**

ECHNICAL COMMISSION I: PRIMARY DATA ACQUISITION

PRESIDENT	: **Marcio Nogueira Barbosa**
SECRETARY	: **José Luiz de Barros Aguirre**

Working Group I/1: Optical Sensors for Remote Sensing

Chairman : **Hartmut Ziemann**

Working Group I/2: Digital Imaging Systems

Chairman : **Alexander Merametdjian**
Co-Chairman : **Xuan Jiabin**

Working Group I/3: Microwave Remote Sensing Systems

Chairman : **John Curlander**

Working Group I/4: Sensor Orientation and Navigation

Chairman : **José Bittencourt de Andrade**

Special Topic Working Group: Future Remote Sensing Missions and Early Results of New Systems

Rapporteur	: **Placidino Machado Fagundes**

Intercommission WG I/IV - International Mapping and Remote Sensing Satellite Systems

Chairman	: **Gottfried Konecny**

SOCIEDADE BRASILEIRA DE CARTOGRAFIA, GEODÉSIA, FOTOGRAMETRIA E SENSORIAMENTO REMOTO - SBC

PRESIDENT	: **Paulo E.M. Tavares**
VICE-PRESIDENT OF ADMINISTRATION AND FINANCE	: **Ney da Fonseca**
VICE-PRESIDENT OF TECHNICAL AND SCIENTIFIC SUBJECTS	: **Paulo R.M. Serra**
VICE-PRESIDENT OF INTERNATIONAL AFFAIRS	: **Hanns J.C. von Studnitz**
VICE-PRESIDENT OF REGIONAL AFFAIRS	: **Ernesto Baccherini**
SECRETARY GENERAL	: **Elaine R.dos Santos**

INTERNATIONAL SYMPOSIUM ON PRIMARY DATA ACQUISITION

COORDINATOR GENERAL : **Paulo Roberto Martini**

TECHNICAL COORDINATOR : **José Luiz B. Aguirre**

EVENTS STAFF:

. Andréa M.L. Machado

. Maria Etelvina Renó Dias Arbex

. Terezinha dos Santos Botelho

GRAPHIC ARTS AND PRINTING STAFF:

. Antonio José Garcia

. Carlos Alberto Vieira

. José Dominguez Sanz

AUDIOVISUAL AND VIDEO SUPPORT STAFF:

. Luiz Carlos de Souza

. Sills Bondezan

. Vanderlim Araújo Bastos

PUBLIC RELATIONS STAFF:

. Sherry Chou Chen

. Guy Loureiro

. Maria Magdalena Assaf

. Vera Lúcia Azevedo da Silva

. Simone Schulze

CONTENTS

--*

Optical Sensors for Remote Sensing

FULL GEOMETRICAL SYSTEM CALIBRATION OF METRIC AERIAL CAMERAS - RESULTS OF THE FIRST CALIBRATION FLIGHTS AT THE TEST RANGE BRECHERSPITZE

Karl Heiko Ellenbeck
Institut für Photogrammetrie
Universität Bonn
Nussallee 15, D 5300 Bonn 1, FRG

ISPRS COMMISSION I

Abstract

The setup of the three-dimensional test range Brecherspitze and the first results of system calibration under real working conditions are described. The high accuracy of the ground coordinates and the great elevation differences in the range permit a precise determination of the full interior orientation and of errors in the image plane.

1. Introduction

Nowadays the Global Positioning System becomes more important in photogrammetry not only for precise navigation of flight lines than for recording elements of outer orientation of each photo. The use of known coordinates of the projection centers in an aerial triangulation is supposed to reduce the number of terrestrial control points considerably. Thereby the information about the real inner orientation of the ariel camera will be significant. In the 1970's field calibrations for checking the inner orientation were mostlty carried out on flat test fields [4,5], omitting the focal lenght. Nowadays we need the full geometrical system calibration using mountainious test fields with elevation differences of more than a quarter of the mean flying altitude to break the high correlation between flying altitude and focal lenght in an adjustment of orientation elements.

2. The Test Range

The setup of the three-dimensional test range Brecherspitze and results of simulation computations were presented at the Kyoto congress [2].
The test range Brecherspitze is 1 km by 1 km large with differences of 380 m in elevation, that means about 50% of the mean flying altitude with a wide angel camera. The terrain feature looks like a slanted inverse pyramid. This geometrical feature fulfills the assumption for an ideal test range. The decision for choosing this test range was made because of the existence of the three-dimensional geodetic test-net of high accuracy of ±1 mm in each axis of the local carthesian coordinate system [6]. The geodetic net was built up by 6 concrete pillars situated in the corners and the top and the bottom of the test range.
The photogrammetric test field consists of 46 signal plates in a more or less regular arrangement, depending on footpathes in the area. 17 signals were coordinated in planimetry and elevation with an accuracy of ±2 to ±5 mm in each coordinate axis and 12 additional points were measured in elevaton only by nivellement of ±2 to ±3 mm accuracy. The remainding 17 signals serve for stabilizing the intersections of imaging rays in the adjustment.

3. Photo Flights and Measurement

The configuration of the photo-flights is a four-fold block along two flight lines crossing in the center of the area. The photo from this crossing covers the whole test field. That means a medium photo scale of 1:5000.
Up to now only two photo flights were measured: the flight of *Rheinische Braunkohlenwerke* (RB) from october 1987 with a *Zeiss RMK 15/23* and the fliht of *Aerowest* (AW) from August 1988 with a *Wild RC 10*. The measuring was done using the original B/W-negatives on an analytical plotter *Planicomp C100* with binocular monoscopic viewing. For increasing the pointing accu-

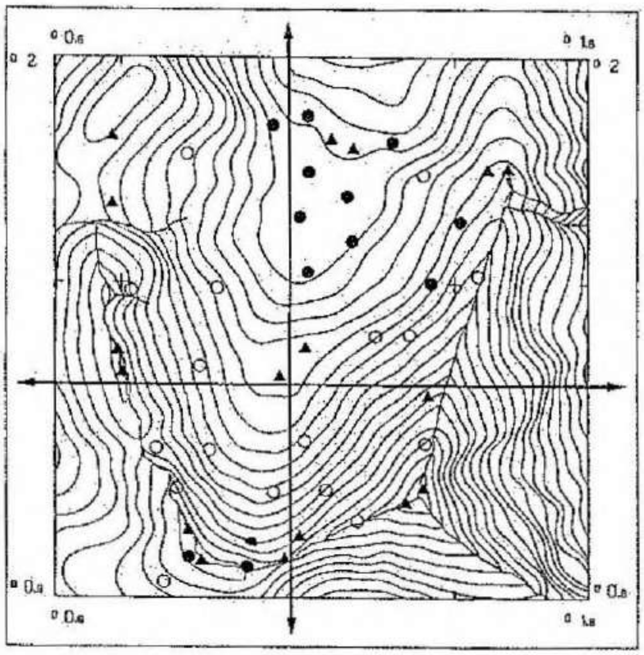

Figure 1
Testrange Brecherspitze
with flight strips

▲ full control points

● elevation control only

○ signals without ground coordinates

racy of the analytical plotter the measurement was done in four sets with a rotation of 90° between each set. This method is very fast and precise for coordinate measurement with analytical plotters.
Both photo flights consist of 20 images each, with 5 photos in each strip (side lap of 70% to 80%).

4. Calibration

The computation of calibration results were carried out with the programm CAP [3]: the matematical model is the bundle adjustment with the photo coordinates as obsevations and the terrain coordinates and the orientation elements as unknowns. The fitting of ground control is achieved by additional observation equations for known ground coordinates weighted by their known accuracy. The redundancy of such adjustment is about 1500 observation versus less than 300 unknowns.
The adjustments for the two photo flights were done in four versions.
In the *first version* the inner orientation was described by 7 unknown elements:
- focal length c
- principal point x_h, y_h
- 4 parameters for radial (A1, A2) and tangential (T1, T2) distortion:

$$dx = A1\ (r^2 - r_o^2)\ x + A2\ (r^4 - r_o^4)\ x + T1\ (y^2 + 3x^2) + 2T2\ xy$$
$$dy = A1\ (r^2 - r_o^2)\ y + A2\ (r^4 - r_o^4)\ y + 2T1\ xy + T2\ (x^2 + 3y^2)$$

with r = radial distance from image center ($r^2 = x^2 + y^2$)
and r_o = second zero of distortion function.

In the *second version* with altogether 21 elements of inner orientation the displacements in the image plane were described with a parameter set of BROWN [1]:

$$dx = A1\ (r^2 - r_o^2)\ x + A2\ (r^4 - r_o^4)\ x + A3\ (r^6 - r_o^6)\ x + B1\ x + B2\ y + (C1\ (x^2 - y^2) + C2\ x^2\ y^2 + C3\ (x^4 - y^4)\ )\ x\ /\ c + D1\ x\ y + D2\ y^2 + D3\ x^2\ y + D4\ x\ y^2 + D5\ x^2\ y^2$$

$$dy = A1\ (r^2 - r_o^2)\ y + A2\ (r^4 - r_o^4)\ y + A3\ (r^6 - r_o^6)\ y + (C1\ (x^2 - y^2) + C2\ x^2\ y^2 + C3\ (x^4 - y^4)\ )\ y\ /\ c + D6\ x\ y + D7\ x^2 + D8\ x^2\ y + D9\ x\ y^2 + D10\ x^2\ y^2$$

with

A1, A2, A3 for influence of radial distortion
B1,B2 for affine film shrinkage
C1, C2, C3 for unflatness of the image plane
D1 - D10 for unregular image displacement including non-radial distortion.

The third and fourth versions are for comparison: the elements of the inner orientation from laboratory calibration are fixed in the adjustments. The *third version* is a "normal" adjustment without additional parameters, in the *fourth version* the Brown parameters are the additional parameters.

Table 1: Results of calibration

Version	σ_o [µm]	c σ_c [mm]	xh σ_{xh} [mm]	yh σ_{yh} [mm]	m_X m_Y m_Z [mm]	σ_{X0} σ_{Y0} σ_{Z0} [mm]
RB1	3.3	153.4783 0.0057	0.0113 0.0027	-0.0274 0.0030	4.2 4.5 7.8	10-30 10-30 20-30
RB2 (Brown)	3.1	153.4709 0.0055	-0.0114 0.0019	0.0049 0.0016	4.0 4.3 7.4	10-30 10-30 20-30
RB3 (Labordaten)	3.7	153.481 0.0	0.001 0.0	-0.008 0.0	4.6 5.0 8.6	10-30 10-30 5-15
RB4 (Brown, Labordaten)	3.3	153.481 0.0	0.001 0.0	-0.008 0.0	4.1 4.5 7.8	10-20 10-20 5-15
AW1	2.3	153.0917 0.0048	-0.0025 0.0023	-0.0179 0.0025	3.3 3.3 6.1	10-30 10-30 20-30
AW2 (Brown)	2.3	153.0935 0.0048	-0.0020 0.0015	-0.0059 0.0014	3.3 3.3 6.1	10-30 10-30 20-30
AW3 (Labordaten)	2.8	153.09 0.0	-0.010 0.0	-0.011 0.0	4.0 4.0 7.4	10-30 10-30 5-15
AW4 (Brown, Labordaten)	2.4	153.09 0.0	-0.010 0.0	-0.011 0.0	3.4 3.4 6.3	10-30 10-30 5-15

σ_o = sigma naught of adjustment
c, σ_c = focal length and standard variation
x_h, y_h, σ_{xh}, σ_{yh} = principal point with standard variations
m_X, m_Y, m_Z = rms-values of the standard deviations of ground coordinates
σ_{Xo}, σ_{Yo}, σ_{Zo} = standard deviations of the projection centers

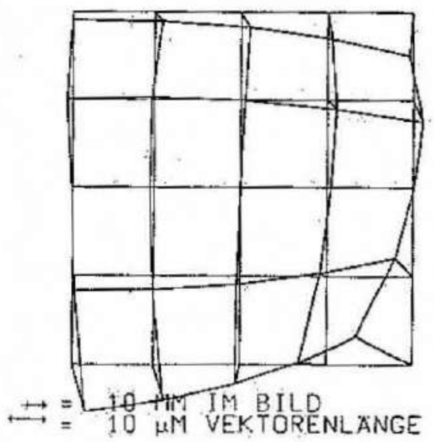

Figure 2:
Image displacement (Brown Parameter)
Flight RB with Zeiss camera

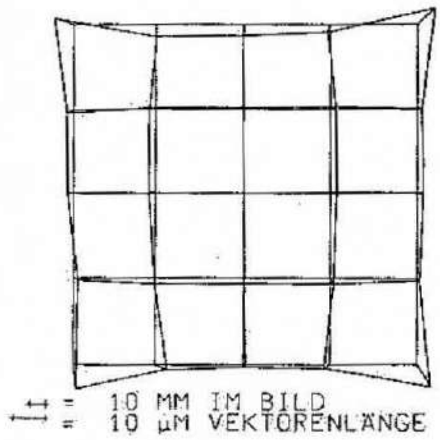

Figure 3:
Image displacement (Brown Parameter)
Flight AW with Wild camera

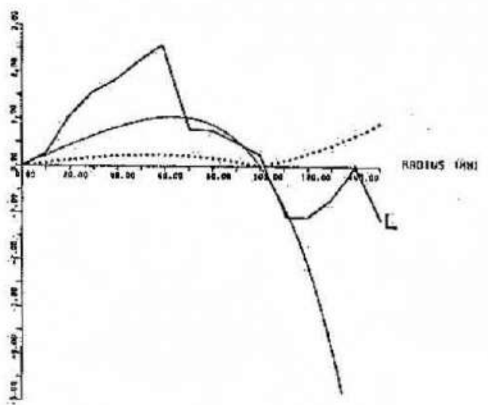

Figure 4:
Radial distortion and standard deviation (dotted) [µm]
Flight RB with Zeiss camera

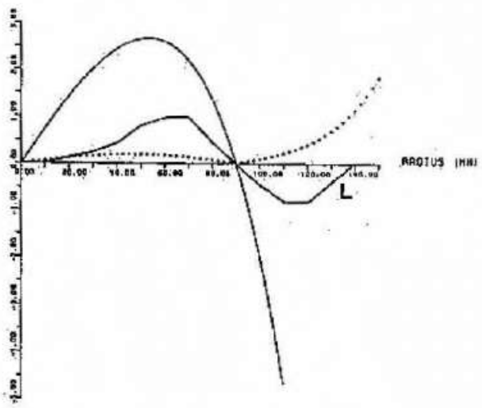

Figure 5:
Radial distortion and standard deviation (dotted) [µm]
Flight AW with Wild camera

5. Results of Calibration

The elements of inner orientation were computed with a high accuracy, better than supposed after simulation computations [2]. Reasons therefore are the actually better accuracy of the ground control and the higher number of photos used in the actual adjustments.

The adjusted focal length and Z_0-coordinates of the projection centers are correlated with coefficients between 0.86 and 0.96, according to the place of the photo in the strip.

The differences between now adjusted (versions 1 and 2) and laboratory-calibrated focal lenght are not significant. Thereby are the results of the versions 1 without additional parameters (RB1, AW1) closer to the laboratory calibration than the results of versions 2 with the Brown-parameters. That means, that the additional parameters describe scaling effects, which change the focal lenght.

Fig. 2 and fig. 3 show the image displacements of a regular grid in an useful area of 200 mm by 200 mm caused by the Brown-parameter (A1 to D10).

The position of the principal point is not homogeneous through the different adjustments. The differences between RB1 and RB2 result from significant parameters of tangential distortion T1 and T2 which are correlated with x_h and y_h respectivly with coefficients between 0.85 and 0.90.
The radial distortion computed with the parameters A1 and A2 is drawn in **fig. 4** and **fig. 5** and is compared with the polynom of radial distortion from the laboratory calibration (L).

Besides the inner orientation, **table 1** shows the accuracy of the adjusted ground coordinates and of the projection centers. The accuracy of ground coordinates is proportional to the σ_0 of the adjustment. The figures for the projection centers are all in the same level with the exception of σ_{Z0} the accuracy of the flying altitude: with fixed focal lenght (versions 3 and 4) the flying altitude is adjusted with a very high accuracy. In the calibration versions 1 and 2 the accuracy is much more worse, because of the correlation with the free focal lenght.
Remarkable differences are between the adjusted flying altitudes too (not shown in the table). There are differences of 30 mm to 60 mm between the versions 2 and 4. They are direct proportional to the differences in the focal lenght. The effects of the differences are compensated therefore. That means, that the flying altitude is not exactly determinable and the high accuracy in the version with fixed focal lenght is not reliable.

6. Closing Remarks

The calibration results of the first two flights over the test range Brecherspitze schow that a full geometrical system calibration is possible, though under bad conditions: worse illumination probably caused the lower accuracy level of the RB-Flight with the *Zeiss* camera versus the AW-flight with the *Wild* camera. Still field calibration is a feasable method of camera calibration. But for studying the accuracy and reliability of orientation parameters higher requirements are to be satisfied.
This could be done with larger or more precise differences in elevation, or with a combined adjustment of two blocks with different flying altitudes with GPS-measured differences between the hights.

References

[1] **Brown, D. C.**, The Bundle Adjustment - Progress And Prospects, Invited Paper ISP-Congress, Comm. III, Helsinki 1976

[2] **Ellenbeck, K.H., Kupfer, G.**, Full Geometrical System Calibration At The Test Range Brecherspitze, ISPRS-Congress, Comm. I, Kyoto 1988

[3] **Hinsken, L.**, CAP: Ein Programm zur kombinierten Bündelausgleichung auf Personal Computern, Bildmessung und Luftbildwesen (BuL 57), 1989, p. 92 -95

[4] **Kupfer, G.**, Zur Geometrie des Luftbildes, DGK Reihe C, Heft 170, München 1971

[5] **Mauelshagen, L.**, Teilkalibrierung eines photogrammetrischen Systems mit variabler Paßpunktanordnung und unterschiedlichen deterministischen Ansätzen, DGK Reihe C, Heft 236, München 1977

[6] **Schnädelbach, K.**, Erfahrungen mit einer räumlichen Triangulation hoher Genauigkeit, FIG-Congess, Montreux 1981

STANDARDS IN DATA ACQUISITION FOR PHOTOGRAMMETRY AND REMOTE SENSING: ARE THEY POSSIBLE AND HOW COULD THEIR SURVIVAL BE ASSURED?

Hartmut Ziemann

Senior Lecturer
Photographic Science and Sensor Physics
The Royal Institute of Technology (KTH)
S-100 44 Stockholm
Sweden

and

Institute for Navigation
University of Stuttgart
Postfach 10 60 37
D-7000 Stuttgart 10
West Germany

ABSTRACT:

Commission I of the International Society for Photogrammetry and Remote Sensing (ISPRS-I) has long been involved with the formulation of recommended procedures in regard to the calibration and testing of optical systems to be used in photogrammetry. This activity was precipitated by the desire to achieve an international agreement on how to test aerial cameras and on how to best report the obtained results. ISPRS-I has in the past in regard to the development and maintenance of these recommended procedures greatly benefited at no cost from extensive input provided by personnel from a no longer existing research group which was able to tie much of the performed work to efforts on a national level. ISPRS-I has further ventured into recommending a specification for aerial survey photography and established a formal liaison with one of the Technical Committees of ISO. The increasing use of images taken from outer space for mapping does not at present appear to be supported by general specifications

The paper attempts to summarize the present situation and offers suggestions in regard to an ISPRS involvement into the development and maintenance of standards or standard-related documents

KEY WORDS: Specifications, Recommended Procedures, Standardization

SYNOPSIS

Commission I of the International Society for Photogrammetry and Remote Sensing (ISPRS-I) has been involved approximately since the end of World War II with the development of recommended procedures in regard to the calibration and testing of aerial cameras. This activity was precipitated by the desire to achieve an international agreement in regard to testing and the reporting of the obtained results; it was at the time supported by the major national testing laboratories, by manufacturers of aerial cameras, by educational institutions such as the International Institute for Aerospace Survey and Earth Sciences (ITC), and at least one military research establishment in the USA.

The major traditional national camera calibration facilities (located at the United States Geological Survey (USGS) and the National Research Council of Canada (NRC) - others have been established in recent years) today represent much of the consensus achieved in the 1950's. At the same time, they use calibration philosophies essentially dating from that time and have failed to make major advances in regard to accommodating the consequences of some of the camera improvements made since. Both organizations provide a service mandated and in its content now determined by national mapping requirements and have in the past been rather resilient to make further equipment and/or procedural changes to bring about a better correspondence between results reported for identical cameras by either facility, a fact bothersome for camera owners outside North America how wish to use the services at either USGS or NRC with a decision being based on current calibration fees and exchange rates. The arguments brought forward are one of modification expenses and one of changes which might be necessary in the national mapping specifications; however, it is understood that the USGS is in the process of implementing at present a commercially available camera calibration software package.

The two mentioned facilities use photographic procedures for camera calibration and do either not provide any image quality data (NRC where resolution values were no longer considered to be critical in the early 60's when new equipment was taken into service; a change is now being sought by the federal mapping authority) or only high-contrast resolution numbers (USGS). The major manufacturers of aerial cameras use predominantly non-photographic procedures, and none provides image quality data in the form of optical transfer functions, leaving the photogrammetric community with little else than high-contrast resolving power data of possibly little relevance in regard to practical camera use and subjective judgement of image quality to go by in trying to select the lenses desired. The manufacturers have in the past had problems to see their cameras passed as fulfilling highest requirements at either USGS or NRC. Recent advances in camera design have led to the point where one manufacturer recalculates lenses using older procedures to pass a calibration at one of the facilities thus de facto eliminating from the calibration process a check on technological advances which the existing facilities is unable to cope with, and at the same time depriving the ultimate user of a camera in that country from taking full advantage of those technological advances.

In regard to the development and maintenance of recommended procedures for the calibration and testing of aerial cameras, ISPRS-I has in the past greatly benefited at no cost from extensive input provided by personnel at NRC, a "service" no longer available since the retirement of P.D. Carman (a former secretary of ISPRS-I) and the dissolution (in 1986) of the NRC Photogrammetric Research section. Organizational changes at NRC had de facto removed the running of the camera calibration facility from the influence of the photogrammetric community, and attempts are now being made there to arrange for outside personnel to assist in the carrying out of the calibration work. The situation at NRC is in particular regrettable since extensive efforts had been made in constructing a facility to derive optical transfer functions for aerial lenses and to use these as the base for modern image-quality-defining parameters. The intended use of the facility would have provided the possibility to consult with the manufacturers in regard to the obtained data and gain their cooperation in providing modern image-quality data to the photogrammetric community.

Efforts have further been made in recent years to establish a formal liaison to those Technical Committees of the International Organization for Standardization (ISO) dealing with areas of interest to photogrammetrists, namely Photography (TC 42) and Optics and Optical Instruments (TC 172); a formal liaison was established to the former but not the latter. In the case of TC 42 it was possible to provide newer lens transmission data than those given in a recently passed standard on aerial film speed (a somewhat embarrassing situation which ISPRS-I should help to prevent in future, arose). In the case of TC 172 it would have been possible to have photogrammetric concern be taken into consideration had an active participation in the development of standards for the determination of optical transfer functions, lens distortion and veiling glare existed.

ISPRS-I also saw fit to accept at the 1984 congress a specification for aerial survey photography heavily promoted by one national society to apparently meet their needs for an internationally sanctioned document. The development of this specification received the support of an ISPRS-I working group. However, technical suggestions not meeting with the approval of the sponsoring society were in the end brushed aside in spite of sound technical reasoning in their support. An approval process similar to that used by ISO would have assured that the document, if passed, would have been a compromise accommodating reasonable technical concerns of other than the sponsoring group(s).

Thus far the discussion was concerned with the use of aerial cameras and aerial photography. The availability of space images with a fairly high resolution has led in certain survey administrations to their use instead of that of aerial photographs. This use, primarily for updating purposes of maps at scales 1 in 50000 or smaller, has largely been on an experimental base, and the writer is aware of at least one country where the intended general use has now been limited to "non-significant" areas while it has been decided to use, against earlier intentions, aerial photographs for the updating of "critical" (e.g. built-up) areas. However, there appears to be no effort (on the international level) to develop recommended procedures or specifications for the use of space images for mapping. Should not ISPRS take an initiative here and lead such an effort?

Being able to see also how other learned societies deal with the issue of specifications, recommendations or standards, one must inquire about the seriousness with which ISPRS as a whole pursues this issue. It can be shown, e.g. on the example of the International Illumination Society (CIE), how a serious effort in regard to developing and passing standards can be mounted. There is no doubt in the writers opinion that ISPRS should engage into the development and passage of standards or related documents only under the following conditions:

(1) establishment of a permanent "secretary" with the mandate to represent or arrange for representation on behalf of ISPRS in such activities on a "permanent" base, i.e. independent of the periodic changes in the ISPRS administration,
(2) establish liaison to different standard bodies dealing with standards in technical areas of interest to ISPRS,
(3) actively participate in the activities of standard-creating agencies whenever standards of interest to ISPRS are being developed,
(4) take an active if not leading role in the development of specifications for the use of novel data acquisition techniques for mapping, and
(5) provide a certain amount of funding in support of the development and maintenance of standards and related documents.

Item (1) has been given its dominant position also in full awareness of the fact that attempts to solicit input from the member societies of ISPRS through the Commission I National Correspondents by mail have in recent years been rather unsuccessful.

CONCLUSION

The foregoing remarks will be expanded into a properly referenced paper to be submitted to the ISPRS Journal of Photogrammetry and Remote Sensing, which will also present the the current situation in regard to the standardization activities of interest to ISPRS in organizations such as the ISO; it will further be attempted to determine the extent of the development of specifications for mapping using images of the earth acquired from space vehicles.

IMAGE PERCEPTION ASPECTS OF AERIAL IMAGE QUALITY

Anders Boberg, MSc
Senior Lecturer, Department of Photogrammetry
Royal Institute of Technology, Stockholm, Sweden
ISPRS Commission I

ABSTRACT

A literature survey of the subject visual perception is presented as a basis for continued research in the field of aerial image quality assessment. Human and computer vision are compared, especially with reference to stereoscopic vision. Physical properties of an image, the resolution capability of the eye and interpretation quality parameters are discussed.

KEY WORDS: Visual Perception, Stereoscopic Vision, Computer Vision, Interpretability, Image Quality

1. TASKS OF VISUAL PERCEPTION

Perception comprises reception and extraction of information on the environment. Visual perception is performed either directly or indirectly. Indirect visual perception means perception of a scene via one or several images of it. But simultaneously, the picture is perceived directly. Thus, a two-dimensional image of three-dimensional objects may give a dualistic spatial representation. Image interpretation can be described as "a dynamic search for the best interpretation of available data" (Gregory 1972 p10). It is a continuous interaction between information from the image and information stored in our brain.

Man is confronted with and interacts with his environment more via images than via letters and words. Visual perception has two essential tasks in the interaction between man and his/her environment: to <u>recognize</u> objects and to help to <u>orientate</u> oneself in the environment.

The first task, to recognize, means that new visually perceived information is compared with stored knowledge. This requires a coding of the visual information to the same mental representation as the stored knowledge. The second task, to help to orientate, concerns judgement of spatial relations in a possibly unknown environment. It is yet more complex.

According to a cognitive attitude, man is active and constructive. He handles information in relation to a contextual system, which represents his knowledge of the environment. Perception is thus not a passive registration of incoming signals but is an active adaptation of the visual process.

Important questions to put is
–What is happening when we see an object or an image of it?
–How is what we see represented in our brain?
–Which influence can we expect from the quality of the image viewed and from the viewing conditions?

2. HUMAN AND COMPUTER VISION

Human vision is a very complicated process. One of the reasons to try to understand it better is the wish to imitate it in the form of computer vision. On the other hand, experiences of computer vision has in fact widened the understanding of human vision.

Eyes act like scanning devices, but in a more random way. The small saccadic movements appear to be dependent upon the importance of the image details. The eyes tend to fixate longer on patterns that are being searched for (Bedwell 1971). The search pattern and the choice of fixation points depend upon the purpose of examining the image (Orhaug 1971).

The human eye contains some 200 millions of photo receptors, each around a micron in diameter. The visual impression received by them is transmitted from the eye to the brain by some one million visual nerves. It is obvious, that the primary stimulus, in the form of a grey level image, can't be transferred to the brain without some form of preprocessing or compression. Most probably, vision requires several processes to be applied in modular, parallel form. At least two main steps may be discerned (See figure 1):
1) Light intensity is coded into pulse frequency
2) Properties of the two-dimensional image field are coded into responses from certain property detectors in the retina and in the cortex.

Moreover, before a conciousness of the environment is realized, the visual information must be transferred to an experience of the three-dimensional outer world using previous experience.

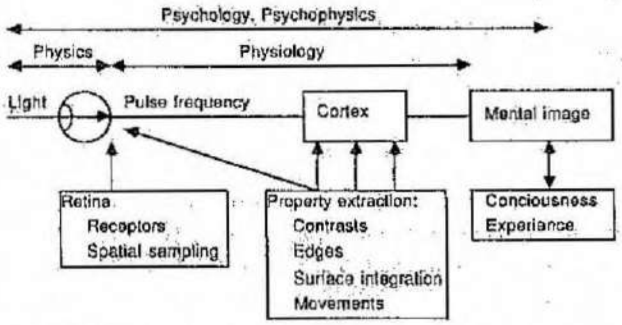

Figure 1. An outline of the human visual system (After Orhaug 1971)

Even between the photo receptors and the visual nerve a filtration of the signals is performed, leading to an amplification of the spatial variations in light intensity, a form of edge enhancement. Thus, a light spot hitting some nerve cells of the retina will either enhance or hamper the signals from adjacent nerve cells in a small receptive field (See figure 2). This function is rather similar to the photographic edge-effect or Eberhard effect.

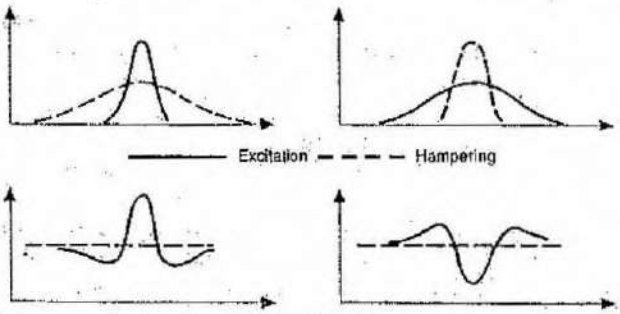

Figure 2. Two types of retinal receptive fields (After Orhaug 1971)

In computer vision, this effect has been modelled by a digital convolution filter, consisting of a Laplace-derivation of a Gauss-function. The Laplace-derivation is a rotation-invariant second derivation, transforming the Gauss-function into a shape somewhat like a Mexican hat, turned right side up or upside down. The resulting zero-crossings in the form of a binary image matrix may act as entrance data for other processing algorithms, e.g. for stereoscopic computer vision.

In order to treat intensity changes of different frequency, several filters of different sizes, i.e. with band-pass-characteristic, will have to be combined. Large filters will enhance slow or continuous intensity changes, small filters fine details. Sharp edges will be enhanced by all filters.

It has been shown, that zero-crossings in filtered images contain much information. In fact, image matrices, consisting of zero-crossings in different scales, were enough to reconstruct an original image without loss of information (Poggio 1987). In spite of this, the role of zero-crossings should not be over-estimated. They are merely possible candidates for an optimal coding system. Generally however, comparisons between biological and computational visual systems show correspondence in that changes of intensity at different scales play an important role in stereoscopic vision and in other visual processes.

3. IMAGE REPRESENTATION AND RECOGNITION

Cognition means apprehension, understanding or knowledge. According to a cognitive system model, the brain functions like several memories, interacting with each other, very much like in a computer (See figure 3). To a primary memory (a "CPU") two types of secondary memories are connected, a declarative memory containing facts, memories and rules and a procedural memory containing activities and logic. Information is regarded as being stored hierarchically in these memories, to avoid over-loading. The primary memory, which has limited capacity, contains information of current interest and relevance, including directly perceived information, visions and thoughts. There, problems are solved and conclusions are drawn.

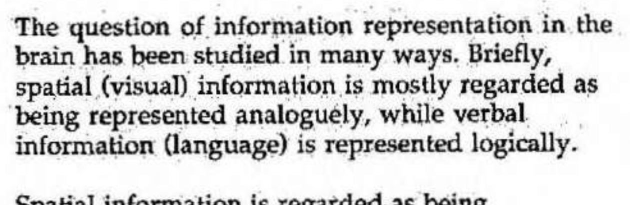

Figure 3. A cognitive model of the function of the brain (Backman & Eklund 1988)

The question of information representation in the brain has been studied in many ways. Briefly, spatial (visual) information is mostly regarded as being represented analoguely, while verbal information (language) is represented logically.

Spatial information is regarded as being represented via a limited number of basic geometric elements, like cylinders, cubes and cones. Together with attributes to these, like size, symmetry, edge type and axis curvature, they are called geons (geometrical ions, see figure 4). It is considered that 36 geons are enough to uniquely describe all possible geometrical forms (Backman & Eklund 1988).

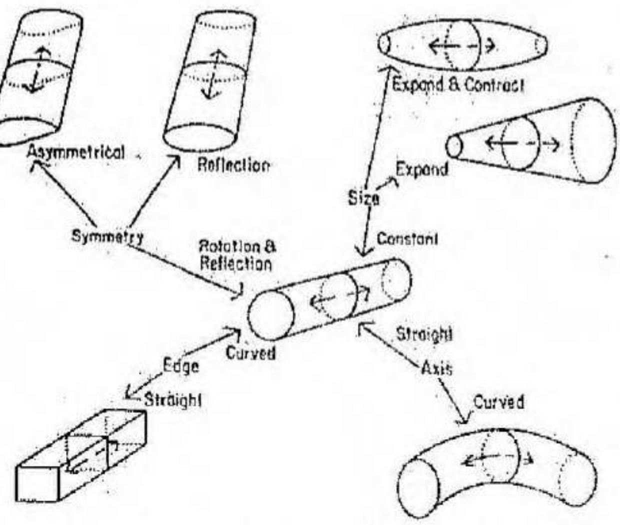

Figure 4. Example of analysis of an object by its geons(Backman & Eklund 1988)

The human ability to imagine absent objects is called mental imagery. Mental images may be rotated as if they were physically solid Thus, they have three-dimensional properties. Moreover, they may be enlarged to examine details, like on a mental projection screen. They therefore play an important role in recognition of features.

Mental imagery has three important functional properties:
1) It contributes to problem-solving and creativity
2) It improves our memory. A visual image requires smaller "memory space" than a verbal one, and is more associative
3) It can direct motor activities, like handling a photogrammetric instrument.

All these functions indicate that mental imagery is of great importance for image interpretation and photogrammetric mapping.

When visually perceiving an object or an image, edges and surfaces are localized by visual segmentation into regions. Simultaneously, so called nonaccidental properties, like colinearity, curvilinearity and symmetry, are perceived. In a two-dimensional image they are regarded as true reflections of the three-dimensional environment. These regions and properties are matched against existing object representations (geons) in the declarative memory. What we see is an interpretation of the external world.

A feature of this process is a preference for information that verifies existing hypotheses or expectations. This means that perception is biased. Certain channels between cortex and retina are activated, while other routes are blocked (de Haas et al 1966). On the other hand, provisional verifications are critically tested by new observations. In this way, the initial bias may be gradually and iteratively reduced, as the probability of the expectation is raised to certainty. In this process, property representations are more important than comparisons with mental prototypes (Orhaug 1971).

Recognition of forms and objects is governed by a set of four rules (Orhaug 1971):
1) The minimum surface law makes the smallest surfaces most easily interpreted as figures
2) The proximity law groups together image details close to another
3) The law of closure make surfaces with closed contours into figures
4) The law of the good curve prefer forms or patterns consisting of smooth curves or straight lines.

These rules may even contradict each other. Such and other types of ambiguities depend on the observer's experiences, associations and training. Therefore, no clear relationship may be established between stimulus and perception. This is a fundamental difficulty in computer vision.

4. STEREOSCOPIC VISION AND DIGITAL MATCHING

Stereoscopic depth perception is a good example of an application of visual pre-processing. When the eyes converge slightly, conjugate image details fall upon each Fovea Centralis, with image points falling at slightly different relative positions in each eye. This binocular disparity is transformed into depth perception. Four steps can be discerned (Poggio 1987):
1) The fovea must concentrate on a given spot
2) The same spot must be found by the other eye
3) The position of different image points on the foveas must be determined
4) From the location difference between the points, the depth is determined.

The derivation of three-dimensional perception is based not only on stereoscopic depth perception, but also on illumination and shadows, visual texture, movements, contours and overlaps.

The coordination of an image pair is not dependent on complete similarity of intensity of the points, neither on recognized forms or objects.

Figure 5. A random-dot stereogram (Poggio 1987)

This can be demonstrated by so-called <u>random-dot stereograms</u> (See figure 5), which are easily perceived stereoscopically although they don't show any recognizeable forms or patterns. Apparently, the human vision can quickly match the random-dot patterns.

An interesting question is, how fine a pattern or texture can still give a stereoscopic impression? Random-dot stereograms may be presented digitally as a rapid succession of points on two oscilloscopes, like the "snow" on a TV (Ross 1976?). Via a computer the stereoscopic shift between point pairs is determined. The stereoscopic effect was found to be maintained at an apparently unlimited rate of point display. Moreover, the point texture is integrated into a very definite, even idealized form perception, also in depth. This remains also when the disparity is continuously changed. Apparently, binocular perception is influenced by some form of visual memory, determining the framework for perception.

Although form perception is not necessary for maintaining stereoscopic vision, certain <u>properties</u> of the imaged or viewed physical surface are of importance for the possibilities to obtain it (Poggio 1987):
1) A given point on a physical surface should only have one three-dimensional position (Unambiguity criterion)
2) Physical objects are continuous and normally non-transparent (Continuity criterion).

The unambiguity criterion means, that each point pair will create only one binocular disparity. The continuity criterion implies, that the disparity changes continuously along a surface, abruptly only at the surface borders.

These surface properties may constitute a basis for a more formalized description of image properties, as a base for a better understanding of the process of vision, or for a formulation of digital operators in computer vision or digital matching. The grey-level image at the photo-receptors may be regarded as transformed into a representation, from which the brightness gradients' position, direction, extension and size can be derived. From this representation, the stereoscopic function of the brain can solve the problem of coordination and of reconstruction of the three-dimensional impression. The unambiguity criterion implies, that possible conjugate adjacent image details along the line of sight should hamper each other, while the continuity criterion implies, that adjacent points on the surface should amplify each other. Filtering and stereoscopic matching can be iterated, starting from the coarsest zero-crossing filter. The method functions also when one of the images is unsharp, which is another parallel to human stereoscopic vision.

According to the author's experience, stereoscopic fusion of image pairs is initially an active process, requiring image forms or details of sufficient size and contrast. As soon as one image detail pair is matched, however, stereoscopic vision is maintained "automatically", even without the normal linkage between convergence and accomodation, guiding direct stereoscopic vision of objects. This is evident when trying to fuse a stereoscopic image pair without the help of a stereoscope.

Stereoscopic vision acuity can be as much as 30 times higher than monocular visual acuity. This is easy to verify by looking "stereoscopically" at two identical images. The reason appears to be that stereoscopic perception is a cortical function (Bedwell 1971). Using a three-bar stereoscopic test, a stereoscopic acuity of approximately 6" was found to be an average for photogrammetric work, while the maximal visual acuity permits the separation of detail to 1' in a normal subject.

Experience of depth effect is regarded as partly innate art, although full binocular vision is not developed at birth. Within limits the ability can be learned and improvements can be obtained with practice, provided the basic visual ability is there.

5. IMAGE AND INSTRUMENTAL FEATURES

An image may be regarded as a transfer in time and space of some of the properties of the scene. The quality of the image therefore determines the quality of property transfer. Image quality may however not easily be unambiguously determined. It is dependent on the intended use of the image. Also, high quality as regards one property (e.g. contrast) may be combined with low quality in another (e.g. sharpness).

Three of the most important physical properties of an image are its contrast, its sharpness and its noise.

Image contrast is defined by two parameters, the density range and the number of discernible steps in it. Physical measures of contrast have to be correlated to subjectively experienced contrast.

Contrasts in the form of edges and contours play a very important role in image interpretation. This is obvious from the fact, that if a retinal image is brought to be stationary, it will disappear after a few seconds. The eye movements ensure, that the receptors continuously receive signal intensity changes, and thus don't cease sending signals to the brain. The minimal density difference that can be readily perceived may in practice vary from ΔD 0,01 to 0,05, depending on film and viewer (Graham & Read 1986).

Image sharpness has a definite influence upon the experienced information content of the image. Seen from a point of view of pure information theory, however, the information content is unchanged, provided the image is noise-free. Unsharp images may to a certain degree be restored.

Image grain noise reduces the number of discernible density steps and sets an accuracy limit for the determination of scene properties from the image. Perception of image graininess is measured as granularity. The information theoretical concept of Signal to Noise ratio (S/N) may be expressed as the relation between contrast and granularity in images.

Light, modulated by the scene or by an image of it, is information carrier to the eyes. As the resolution of the retinal image is dependent mainly on the pupil diameter and the imaging errors of the lens, it is dependent upon incoming light intensity. A bright illumination in photogrammetric instruments is therefore of great importance. However, instruments normally give very low levels of light. An illuminance of 4000 lux over the photographic plate was reported to have been reduced to 10 lux at the exit pupil (Bedwell 1971). This should be compared to recommended illuminance for reading, 1000-1500 lux, and to normal outdoor illuminance,10 000 lux (Ejhed 1990).

The resolution of the eye can be studied by different methods (See figure 6). The spatial

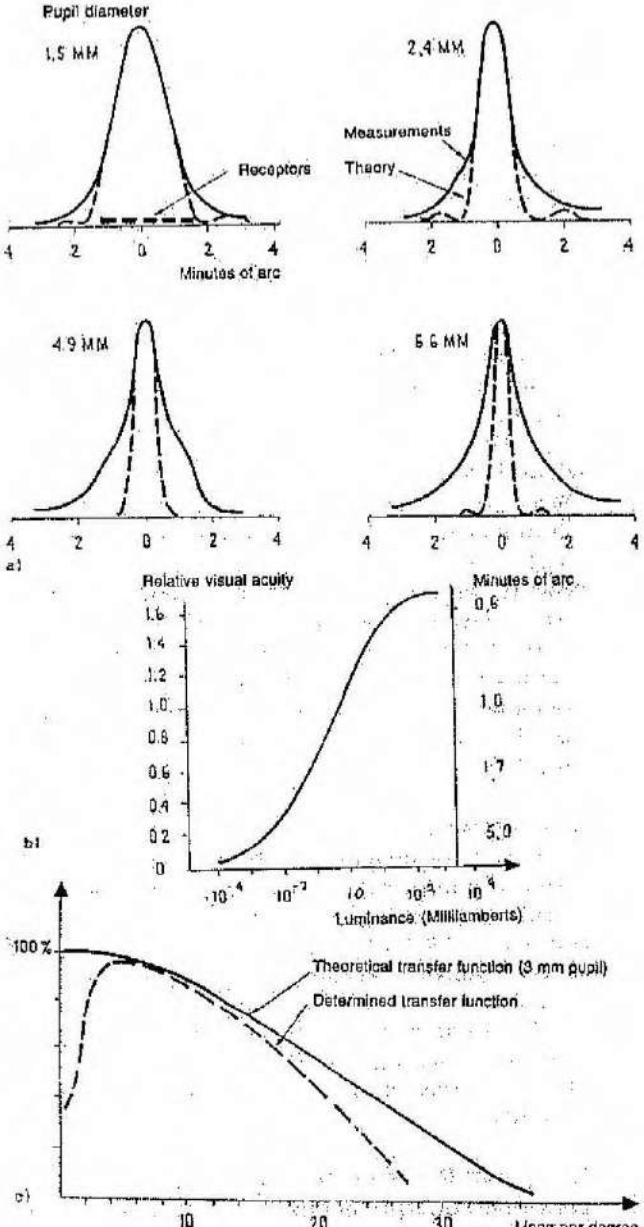

Figure 6. The resolution of the eye, studied by three different methods:
a) Point spread functions
b) Separability of two point sources at different illumination levels
c) A transfer function, based on sensitivity to sinusoidal line patterns

distribution of light at the retina from a point source at different pupil sizes shows a form of point spread functions. As expected, the largest pupil size deviates most from a diffraction-limited optical system. Separability of two point sources at different illumination levels gives a relation between resolution and illumination at daylight adaptation. Finally, the sensitivity to sinusoidal line patterns of different frequencies gives a transfer function for the eye. This transfer function has a maximum at a frequency of 5 line pairs per degree, which corresponds to a linear resolution of 1 lp/mm at reading distance or 10 lp/mm, viewed under 8x magnification. In this respect, the eye clearly differs from an optical system.

All these methods (the last at 50% transfer) point at a resolution capability of the eye of the magnitude of 3 minutes of arc.

The eye's ability to perceive contrast is a highly subjective function. Experienced illumination is approximately a logarithmic function of physical illumination. Adaptation of the eye covers in total a magnitude of 4-5 powers of ten. According to Weber's law, this is expressed by

$$DL = 0{,}02L$$

where L is background luminance and L+DL is object luminance. The linear range for perceiving a luminance difference or contrast between L and L+DL in a certain background luminance L_0 is however of a magnitude of only 2 powers of ten. A form of visual edge effect has been described above. It is easily demonstrated by a step tablet, and is also a reason for the form of the above-mentioned transfer function of the eye. It appears that these non-linear effects occur very early in the visual system.

In a number of experiments, physical quality parameters of images have been varied, and the result of interpretation tasks have been measured. Normal interpretation quality parameters are (Birnbaum 1962, Orhaug 1971):

1) R = number of correct interpretations (number of rights)
2) W = number of erroneous interpretations (number of wrongs)
3) O = number of omitted interpretations (number of omits).

Note, that (R + W) is the total number of performed interpretations, and that (R + O) is the total number of possible interpretations
From these, the following parameters may be derived:

4) Accuracy $A = R / (R + W)$
5) Completeness $C = R / (R + O)$
6) Efficiency $E = A \times C$.

Here, interpretation means either detection, identification or classification of objects in images.

-Efficiency of identification is logarithmically related to image resolution in (minutes of arc)$^{-1}$. At a resolution of 0,3(minutes of arc)$^{-1}$ or 3 minutes of arc, the improvement in efficiency decreases. Cf. the value for eye resolution above! Apparently, image resolution should be chosen with respect to eye resolution - and to the interpretation equipment.

-Image resolution was not found to correlate with accuracy, but highly and logarithmically with completeness of detection as well as with completeness of identification.

-Interpretatability (Completeness?) is linearly related to the number of image density levels up to a saturation level of around 8 levels.

-If the information content of the image, defined as a product of the number of density levels and the number of resolution elements, is kept constant, optimal probability of identification will be reached by increasing the density levels.

-In quality degraded images, physical image quality was measured as the area between a MTF curve and a visual TM curve and related to subjective image quality, measured via choice of best image. Good correlation (0,88) was experienced.

6. CONCLUSION

Understanding of human image perception is of great importance not only for development of image interpretation methods and for investigation of the basis for image quality assessment, but also for development of methods for computer vision and digital image matching. Computer vision and human vision are very much interrelated and can learn a great deal from each other. In both cases, the amount of information extractable is limited by the image quality, which has to be assessed in a relevant way.

REFERENCES

Backman J, Eklund S. 1988. Bilden i det kognitiva systemet. Rapport nr 8, Inst för bildlärarutbildning, Umeå University, Sweden

Bedwell CH. 1971. The Eye, Vision and Photogrammetry. Phot Rec 7(38), pp 135-156

Birnbaum A H. 1962. Effect of Selected Photo Characteristics on Detection and Identification. Int Arch of Phot, Vol XIV, pp 60-66. Uitgeverij Waltman, Delft

Ejhed J. 1990. Personal communication, KTH

Graham R, Read RE. 1986. Manual of Aerial Photography. Focal Press, London

Gregory A L. 1972. Öga och hjärna. Seendets psykologi. Aldus/Bonniers

de Haas WGL, Hempenius SA, Vink APA. 1966. Logical Thoughts on the Psychology of Photo-Interpretation. Int Arch of Phot, Vol XVI, pp I-43 – I-46. Éditions Technip, Paris

Orhaug T. 1971. Bilder Bildinformation Bildbehandling. FOA 2 rapport A 2538-51, Utgåva 2, Stockholm

Poggio T. 1987. Wie Computer und Menschen sehen. Wahrnehmung und Visuelles System / mit e. einf. von M. Ritter. Spektrum-der-Wissenschaft-Verlagsgesellschaft, Heidelberg

Ross J. 1976(?). The Resources of Binocular Perception. Scientific American, pp 80-86.

900510/ABg

Digital Imaging Systems

A SIMULATION STUDY ON POINT DETERMINATION USING MOMS-02/D2 IMAGERY

H. Ebner[1], O. Hofmann[1], W. Kornus[1], F. Müller[2], G. Strunz[1]

[1]

Chair for Photogrammetry
Technical University of Munich
Arcisstr. 21
D-8000 Munich 2
Federal Republic of Germany

[2]

Messerschmitt-Bölkow-Blohm GmbH
P.B. 801149
D-8000 Munich 80
Federal Republic of Germany

ABSTRACT

In the course of the second German Spacelab mission D2, which is scheduled for launch in early 1992, the MOMS-02 camera is intended to acquire digital threefold stereo imagery of the earth's surface from space. Extensive simulations were performed in order to examine the influence of the number and distribution of ground control points, the distance between the so-called orientation images, various arrangements of the three sensor lines in the focal plane of the camera and the precision of observed exterior orientation parameters on the resulting accuracy of point determination. Further investigations were carried out on using a given Digital Terrain Model as control information. The simulations are based on a bundle adjustment modified for the processing of three-line imagery.

The paper in hand briefly describes the mathematical model used for the computations. The project parameters of the simulations are outlined and the main results are given based on the theoretical standard deviations of the object point coordinates. Finally some conclusions are drawn from the results of the study.

KEY WORDS: MOMS-02/D2, Three-Line Imagery, Combined Point Determination, Simulation Study.

1. INTRODUCTION

MOMS-02/D2 is an experimental project for digital mapping from space, which is funded by the German Ministry for Science and Technology (BMFT). In the course of the second German Spacelab mission D2, which is scheduled for launch in early 1992, the MOMS-02 camera is intended to acquire digital imagery of the earth's surface *(Ackermann et al., 1989)*.

The special characteristic of the MOMS-02 camera is the combination of high resolution panchromatic images for three-dimensional geometric information with multispectral images for thematic information. In order to meet the requirements of the different users a modular optical concept based on a system with 5 lenses was chosen. The multispectral data acquisition will be performed by 2 lenses which allow for recording of a maximum of 4 spectral channels. The stereo module basically consists of 3 lenses with one CCD line sensor each, which provide a forward, a downward and a backward looking view. The central lens enables high quality image recordings with a ground pixel resolution of about $5*5\ m^2$. From the photogrammetric point of view the aims of the mission are mainly the production of high quality maps, the acquisition of digital data for geographic data bases and information systems and the generation of Digital Terrain Models (DTM) with an accuracy of 5 m or better. Moreover, the concept for completely digital photogrammetric data acquisition and evaluation shall be developed, realized at an experimental level and tested.

Simulations based on the MOMS-02 camera specifications and the D2 mission parameters were performed in order to obtain a survey of the attainable geometric accuracy and to give recommendations in the planning phase of the project concerning additional measurements during the mission and the technical design of the camera. The simulation study was ordered by the BMFT under contract No. 01 QS 8817 0 and the simulations were performed at the German aerospace company Messerschmitt-Bölkow-Blohm GmbH and the Chair for Photogrammetry of the Technical University of Munich.

In this paper the principle of photogrammetric point determination using digital data of three-line scanner systems is shortly reviewed. Then the simulation parameters are described and important results of the study and of additional simulations, performed by the Chair for Photogrammetry, are given. Finally the results are discussed and conclusions are drawn from the study.

2. PHOTOGRAMMETRIC POINT DETERMINATION USING THREE-LINE IMAGERY

The mathematical model for point determination using three-line imagery is based on the concept proposed by *(Hofmann et al., 1982)*. A detailed description of the model can be found e.g. in *(Ebner and Müller, 1986)*, *(Hofmann, 1986)* and *(Hofmann and Müller, 1988)*. For reasons of clarity the basic principle will be shortly reviewed.

A three-line opto-electronic scanner system consists of three linear CCD-sensors, which are arranged perpendicular to the direction of flight in the focal plane(s) of one or more lenses. During the flight the sensors are continuously scanning the terrain and the data are read out with a constant frequency. This dynamic mode of image recording results in a large number of successive images, each consisting of three lines (fig. 1).

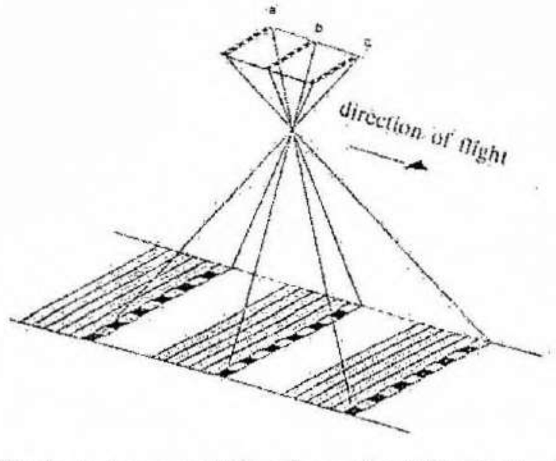

Fig. 1: *Image recording using a three-line scanner*

For the photogrammetric evaluation of these data conjugate points have to be determined. This task will preferably be accomplished or at least supported by digital image matching techniques *(Heipke et al., 1990)*. The simultaneous determination of object points and reconstruction of the exterior orientation of the three-line imagery is based on the principle of bundle adjustment. The exterior orientation, however, is calculated only for so-called orientation images, which are introduced at certain time intervalls. In between the parameters of every image are expressed as functions (e.g. linear interpolation functions) of the parameters of the neighbouring orientation images.

3. SIMULATION STUDY

3.1 Simulation parameters

The simulations are based on system parameters which fit to a large extent the specifications of the MOMS-02 camera and the flight parameters of the mission.

The following camera and flight parameters are assumed (see fig. 2).

- calibrated focal length:	$f = 660$ mm
- convergence angle:	$\gamma = 27.1933$ grad
- distance of 2 sensor lines:	$s = 300.418$ mm
- ground pixel resolution:	$5 * 5$ m^2
- flying height above ground:	$H = 334$ km
- base length:	$B = 152$ km
- strip width:	$W = 36$ km
- strip length:	$L = 606$ km

Unlike the stereo module of the MOMS-02 camera, which consists of three lenses with one sensor line each, a one-lens camera is used in the simulations.

A straight forward flight path is assumed with the attitude parameters of the camera being constant and equal to 0 grad.

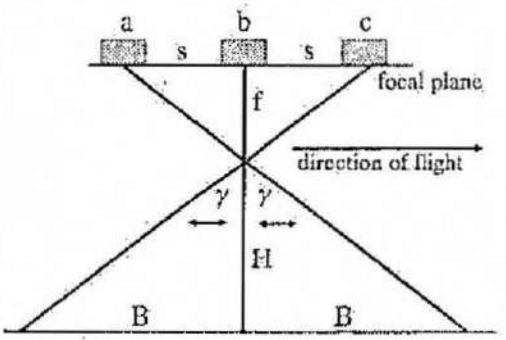

Fig. 2: *Camera and flight parameters of the simulation*

The following regular arrangement of the object points is used.

- distance of points along flight direction: 2 km
- distance of points across flight direction: 9 km
- height of all object points: 0 m

The total number of object points is 1520. They are arranged in 5 chains in the direction of flight with 304 points each. The points at the beginning and the end of the strip are projected into two images only, whereas every point at the central part of the strip, i.e. every point that is at a distance of more than one baselength from the beginning and the end of the strip, is projected into three images.

The object coordinate system is defined as a right handed cartesian system XYZ, with the positive direction of the X-axis parallel to the direction of flight.

A peculiarity of the MOMS-02 configuration is the extremely small image angle, which results in an unfavourable ratio between the strip width and the flying height of approximately 1:9. For point determination using three-line imagery principally no external information is necessary for rigorous object reconstruction. The above mentioned configuration, however, leads to rather poor accuracy. Consequently, observations of the exterior orientation parameters have to be considered in the evaluation process.

In order to obtain estimations of the achievable accuracy, the simulations are performed with variable parameters, which are described in the following.

a) Arrangement of the sensor lines in the focal plane:
   * parallel sensor lines,
   * convergent sensor lines ($\alpha \approx 14$ grad).
   Because preceding theoretical considerations *(Hofmann, 1986)* pointed out, that the geometric accuracy of point determination using three-line imagery can be improved, if the outer sensor lines are not parallel to the central line (fig. 3), the influence of the arrangement of the sensor lines on the resulting accuracy is investigated.

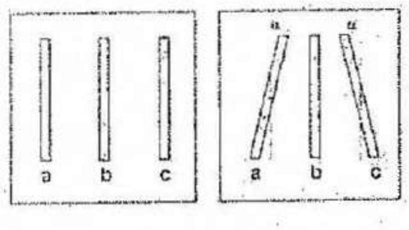

Fig. 3: *Arrangement of the sensor lines in the focal plane*

b) Distances between the orientation images:
   * 8.11 km (approx. 1 sec. flight time),
   * 15.60 km (approx. 2 sec. flight time),
   * 28.95 km (approx. 4 sec. flight time).
   When navigation data or orbit models of the D2 mission are available, the temporal position and attitude variations of the shuttle have to be analysed. Therefrom a time intervall has to be derived on condition, that during this intervall the camera orientation parameters are optimally approximated by the interpolation function, which is defined in the mathematical model. Because up to now practical data are not yet available, the values given above are used. The range they cover is expected to be realistic for the mission. In the simulations a linear interpolation function between the orientation images is assumed.

c) Observations of the orientation parameters of the images:
   * no camera orientation data available,

* standard deviations of position parameters: error-free, 2, 5, 10, 25 m,
* standard deviations of attitude parameters: error-free, 1, 2, 5, 10 mgrad.

In connection with MOMS-02 imagery, information about the parameters of the exterior orientation is of special interest. It will probably be derived from on-board navigation systems, from tracking data recorded during the space mission and from orbit models. The functional and stochastic models for tying these data in a combined adjustment have to be defined when the data are at hand. The simulations are performed with the simplified assumption that camera orientation data are given as observations for position and attitude of every orientation image. The data are treated as being uncorrelated, assuming various levels of precision.

d) Number of ground control points:
   * 4 XYZ control points (distance between control points: 302 km),
   * 10 XYZ control points (distance between control points: 75 km),
   * 18 XYZ control points (distance between control points: 40 km),
   * 34 XYZ control points (distance between control points: 20 km).

The control points are arranged in the threefold covered area of the strip. Their coordinates are treated as errror-free. Different numbers of available ground control points are assumed and the effect on the accuracy of point determination is investigated.

e) DTM as control information:
   * no DTM information available,
   * standard deviation of DTM: 20, 50, 100 m.

Additionally to or instead of control points a given DTM can be used in the adjustment as general ground control information. This information might originate e.g. from a height data base or from digitized contours of existing maps. The mathematical model for using DTM-information in a bundle block adjustment has been described in *(Ebner and Strunz, 1988)*. In the simulations different height precision levels of the DTM are assumed.

3.2 Estimation of the theoretical accuracy

Based on the described simulation model the image coordinates of all object points are generated. Then least-squares adjustments are performed according to the generalized model of bundle adjustment for three-line imagery.

The theoretical accuracy of the estimated parameters is described by their covariance matrix, which is composed of the cofactor matrix and the a posteriori estimate of the reference variance ($\hat{\sigma}_o^2$). The cofactor matrix of the parameters is obtained from the inversion of the normal equation matrix, whereas the estimate of the reference variance can be computed from the observation residuals and the a priori weight matrix of the observations. Since the simulations are performed with generated error-free observations, the a priori σ_o^2 is used instead of $\hat{\sigma}_o^2$. This means that the accuracy estimates are valid for the a priori assumed precision of the observations. The a priori σ_o is chosen as equal to the standard deviations of the image coordinates.

For all computations of the simulation study standard deviations of the image coordinates of $\sigma_o = 5\ \mu m$ are assumed. This accuracy of the image coordinates is mainly influenced by the precision of the image matching process and the effect of remaining interpolation errors. Interpolation errors are due to the approximation of the real variations of the position and attitude parameters by an interpolation function between neighbouring orientation images. By adapting the distance between the orientation images to the flight characteristics these errors have to be kept small.

3.3 Results

For the assessment of the theoretical accuracy of a particular simulation version the individual standard deviations $\sigma_{\hat{X}_i}$, $\sigma_{\hat{Y}_i}$, $\sigma_{\hat{Z}_i}$ of the estimated object point coordinates $\hat{X}_i$, $\hat{Y}_i$, $\hat{Z}_i$ are analysed. Because of the large number of simulations only the most important results will be presented in this paper.

First the theoretical accuracy limits for the used configuration are given. These values are achieved, if the parameters of the exterior orientation of all images are treated as error-free observations in the adjustment. This means that solely the geometric constellation of the intersection of the image rays and the precision of the image coordinates define the accuracy of the point determination.

In fig. 4 the accuracy limits for the heights of the object points are shown.

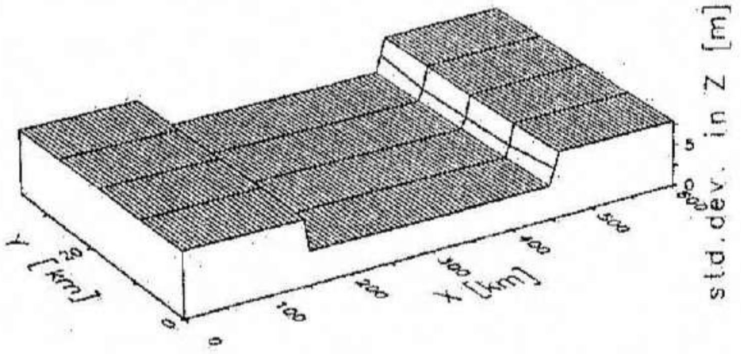

Fig. 4: *Theoretical standard deviations $\sigma_{\hat{Z}_i}$, assuming error-free observations of the exterior orientation parameters (accuracy limits), parallel sensor lines*

The theoretical standard deviations $\sigma_{\hat{Z}_i}$ obtained from simulation runs with parallel (fig. 5) and convergent (fig. 6) arrangement of the sensor lines, assuming a precision of position parameters of 10 m and of attitude parameters of 5 mgrad are given next.

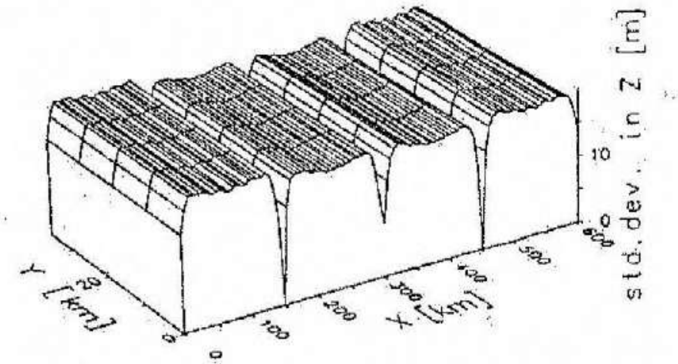

Fig. 5: *Theoretical standard deviations $\sigma_{\hat{Z}_i}$, assuming observed orientation parameters (standard deviations 10m/5mgrad), 4 ground control points, distance between orientation images: 8 km, parallel sensor lines*

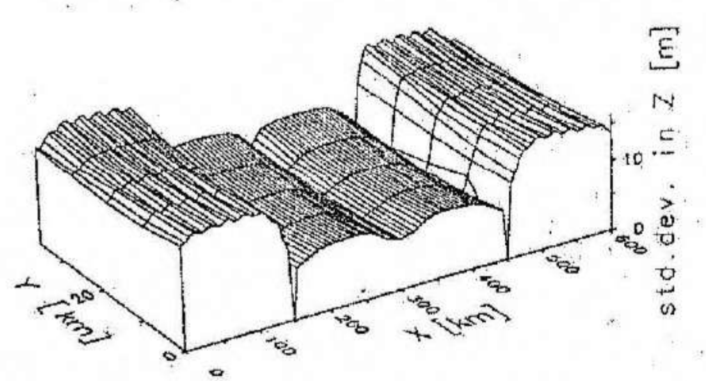

Fig. 6: *Theoretical standard deviations $\sigma_{\hat{Z}_i}$, assuming observed orientation parameters (standard deviations 10m/5mgrad), 4 ground control points, distance between orientation images: 8 km, convergent sensor lines*

Remark: In the figures 4-6 the values $\sigma_{\hat{Z}_i}$ of in each case 3 successive points in the direction of the X-axis are averaged and the strip width is enlarged by a factor of 10 compared to the strip length for clarity reasons of the graphic representations.

In order to present the results of the different computation versions in a compact form the root mean square (rms) values $\mu_{\hat{X}}$, $\mu_{\hat{Y}}$, $\mu_{\hat{Z}}$ of the theoretical standard deviations of all points, which are projected into three images, are calculated. Using these values, summarized accuracy measures for the respective simulation version can be given. In the following figures these rms values are shown graphically.

The following abbreviations are used in the figures:

- *par., conv.*:
  parallel or convergent arrangement of the sensor lines,
- *8km, 16km, 29km*:
  distances between orientation images,
- *error-free, 2m/1mgrad, ..., 25m/10mgrad*:
  standard deviations of observed orientation parameters,
- *no observ.*:
  no observations for the orientation parameters available,
- *4 GCP, 10 GCP, 18 GCP, 34 GCP*:
  number of XYZ ground control points,
- *DTM 20m, DTM 50m, DTM 100m*:
  standard deviations of the DTM used as control information.

Breaks in the graphic representations mean that the respective values are not given true to scale.

In the figures 7a-7c the influence of different precision levels for the observations of the position and attitude parameters of the orientation images on the resulting rms values $\mu_{\hat{X}}$, $\mu_{\hat{Y}}$, $\mu_{\hat{Z}}$ is shown.

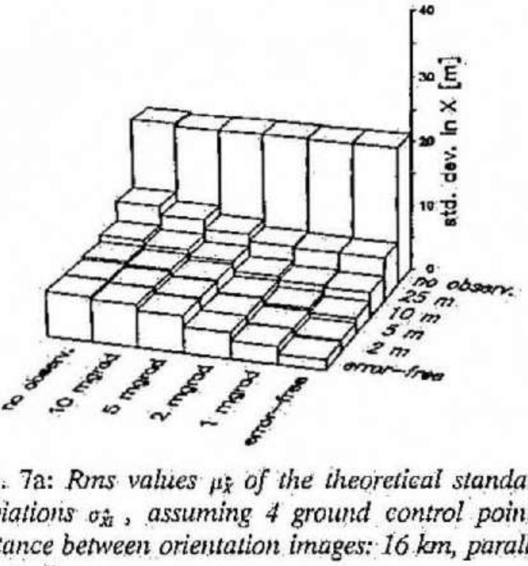

Fig. 7a: *Rms values $\mu_{\hat{X}}$ of the theoretical standard deviations $\sigma_{\hat{X}_i}$, assuming 4 ground control points, distance between orientation images: 16 km, parallel sensor lines*

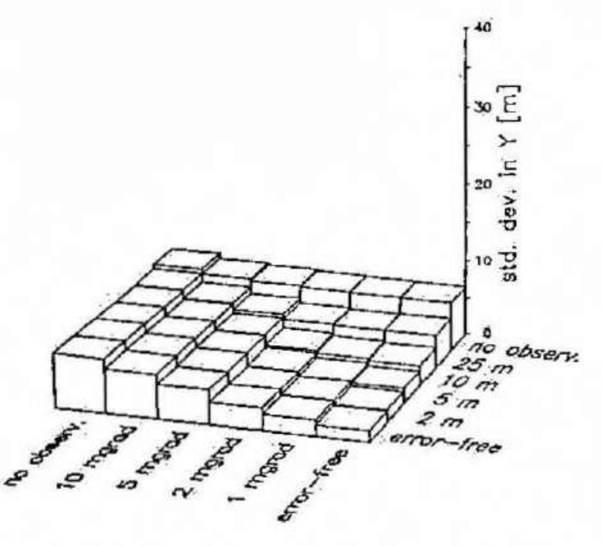

Fig. 7b: *Rms values $\mu_{\hat{Y}}$ of the theoretical standard deviations $\sigma_{\hat{Y}_i}$, assuming 4 ground control points, distance between orientation images: 16 km, parallel sensor lines*

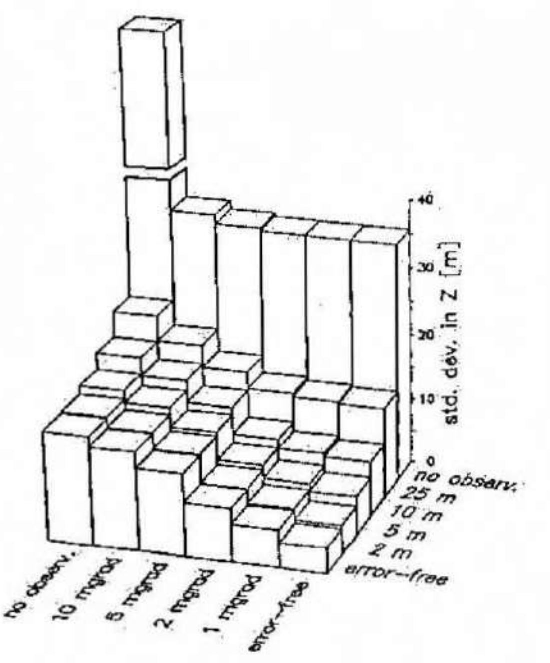

Fig. 7c: *Rms values $\mu_{\hat{Z}}$ of the theoretical standard deviations $\sigma_{\hat{Z}_i}$, assuming 4 ground control points, distance between orientation images: 16 km, parallel sensor lines*

In the figures 8-10 only the rms values $\mu_{\hat{Z}}$ are given.
The effect of different distances between the orientation images (fig. 8) and the influence of the

number of ground control points (fig. 9) for parallel and convergent arrangement of the sensor lines are presented in the next two figures.

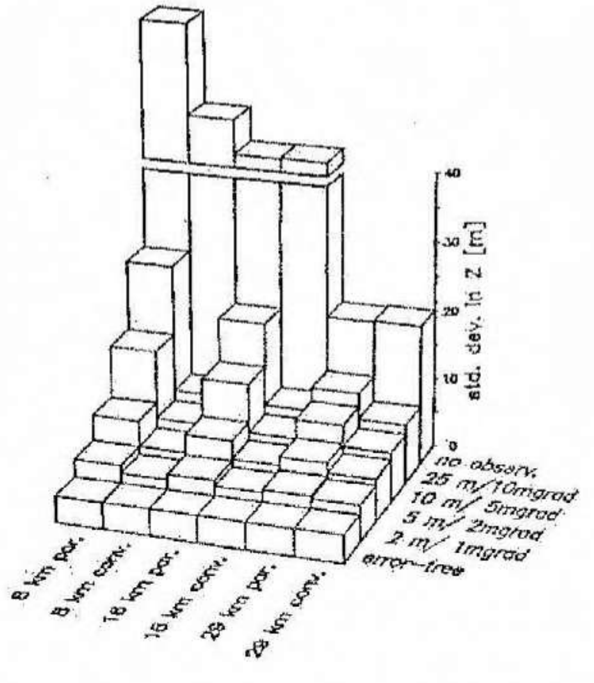

Fig. 8: *Rms values $\mu_{\hat{z}}$ of the theoretical standard deviations $\sigma_{\hat{z}_i}$, assuming 4 ground control points*

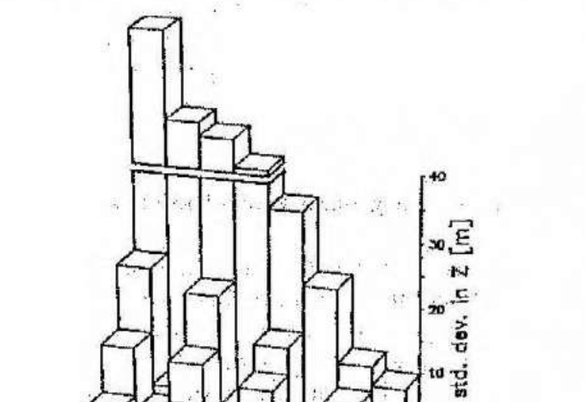

Fig. 9: *Rms values $\mu_{\hat{z}}$ of the theoretical standard deviations $\sigma_{\hat{z}_i}$, assuming distance between orientation images: 8 km*

In fig. 10 the influence of different precision levels of a given DTM used as control information on the resulting rms values $\mu_{\hat{z}}$ is shown.

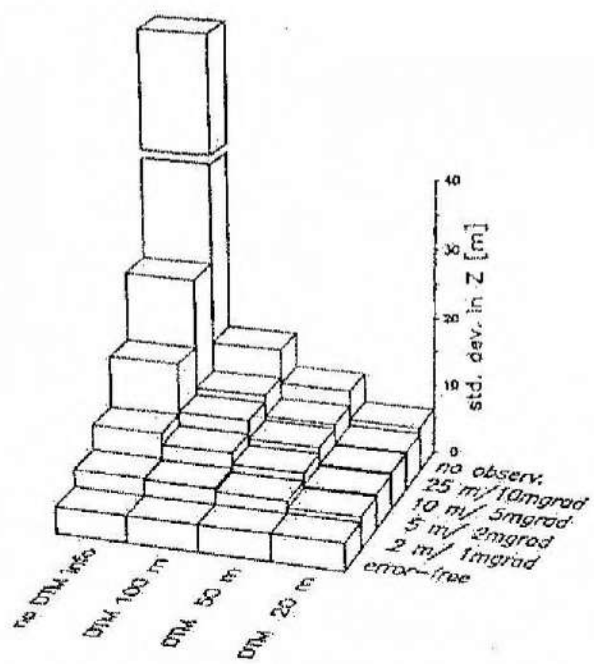

Fig. 10: *Rms values $\mu_{\hat{z}}$ of the theoretical standard deviations $\sigma_{\hat{z}_i}$, assuming 4 ground control points, distance between orientation images: 8 km, parallel sensor lines*

4. ANALYSIS

4.1 Theoretical accuracy limits of the object points

The following rms values for the theoretical accuracy limits of the object point coordinates are obtained from the simulations.
For points, which are projected into 3 images:
$\mu_{\hat{x}} = 1.5$ m, $\mu_{\hat{y}} = 1.5$ m, $\mu_{\hat{z}} = 3.9$ m,
and for points, projected into 2 images:
$\mu_{\hat{x}} = 2.5$ m, $\mu_{\hat{y}} = 1,8$ m, $\mu_{\hat{z}} = 7.9$ m.
In the graphic representation of the theoretical standard deviations $\sigma_{\hat{z}_i}$ in figure 4 the difference between points which are projected into two and three images is clearly visible. These values show, that only points in the threefold covered area satisfy the accuracy demands of the mission. Therefore in the following discussion mainly the resulting accuracies of these points are reflected.

4.2 Influence of the sensor arrangement

Comparing figure 5 with figure 6 it can be seen, that the standard deviations $\sigma_{\hat{Z}_i}$ of all object points are smaller, if convergent lines are assumed.
The accuracies for points which are projected into three images are in case of parallel lines slightly and in case of convergent lines significantly better than points projected into two images. This effect appears especially in connection with inaccurate observations of the exterior orientation parameters.
A review of the influence of the sensor arrangement on the photogrammetric point determination is given by the figures 8 and 9. For all distances between orientation images and for all versions of ground control points used in the simulations a distinct improvement of the accuracy is visible, if convergent sensor lines are used. The ratio between the standard deviations resulting from parallel and from convergent lines becomes better for the benefit of convergent lines the less precisely the observations for exterior orientation parameters are given, the shorter the distances between orientation images are assumed and the less ground control points are used.

Convergent lines on the ground can either be obtained by the convergent arrangement of the sensor lines or by inclining the shuttle across the direction of flight during the image recording. The roll angle ω, which corresponds to a sensor rotation α results from the formula:
$\sin(\omega) = \tan(\alpha) / \tan(\gamma)$
where γ denotes the convergence angle.
From this formula a sensor rotation of 14 grad corresponds to a roll angle of 33 grad. Additional simulations were performed, which resulted in no perceptible differences between an instrumental line convergency and the inclination of the shuttle in the rms values $\mu_{\hat{X}}$ and $\mu_{\hat{Z}}$. The values for $\mu_{\hat{Y}}$, however, got worse by the factor 2.

4.3 Influence of observations for exterior orientation parameters

The question, how precisely the parameters of the exterior orientation have to be measured in order to fulfill the accuracy demands, is of particular importance. The figures 7a to 7c show that the resulting accuracies improve with better precision of the position and attitude observations. If no observations are at hand the results are unsatisfactory. In particular, observations for the positions are important, because insufficient accuracies are to be expected even in case of error-free attitude observations (figures 7a and 7c). For the accuracy of the Y-coordinates (fig. 7b) that effect is less apparent.
The simulations were performed with idealized assumptions for the camera orientation data. In practice the data may be given with systematic offset or drift errors, e.g. if originating from an inertial navigation system. A simple approach to model that effect is a simultaneous determination of additional unknowns for offset and linear drift of the corresponding orientation data in the adjustment. This approach allows for the introduction of relative observations of the exterior orientation parameters. However, sufficient ground control information is necessary to determine these additional unknowns.

4.4 Influence of the distance between orientation images

It can be seen in figure 8 that the results become better with increasing distances between orientation images assuming a constant $\sigma_{\hat{Z}}$. The increase of the distance between orientation images, however, leads to higher interpolation errors. As mentioned in 3.1 already, the appropriate distance can only be chosen, when the practical data are available.

4.5 Influence of ground control information

From figure 9 it can be seen, that an increasing number of ground control points results in a better accuracy of point determination. But only in case of a dense network of ground control points one can renounce on precise exterior orientation observations, if the accuracy demands of the mission shall be fulfilled.
Because the availability of a large number of ground control points can not be ensured, a given DTM might be used as additional ground control information. Figure 10 shows a significant improvement of the resulting rms values of the standard deviations $\sigma_{\hat{Z}_i}$, even in case a DTM with low precision is introduced into the adjustment. If no observations of the exterior orientation parameters are available, sufficient height accuracy is achieved by DTM information with a precision level of 20 m or better.

5. CONCLUSIONS

From the photogrammetric point of view the major aim of the MOMS-02/D2 project is the three-dimensional point determination and DTM generation with high geometric quality. Based on the results of this study the following conclusions can be drawn.

The simulations showed that a convergent arrangement of the sensor lines results in significantly better accuracies than a parallel arrangement. However, since parallel sensor lines will be used for the mission, an improvement of the accuracy can be achieved by inclining the shuttle during the data recording.
Precise observations of the exterior orientation parameters are required in order to fulfill the accuracy demands of the mission. Therefore these data, which will be derived from on-board navigation systems, from tracking data and from orbit models, have to be introduced into the photogrammetric adjustment.
The exclusive use of ground control points is not recommended, because a dense network of control points would be required. The combination of ground control points with observations of the exterior orientation parameters and possibly general ground control information, e.g. from DTM, should be used in a combined adjustment of photogrammetric and non-photogrammetric data.

REFERENCES

Ackermann, F., Bodechtel, J., Lanzl, F., Meissner, D., Seige, P., Winkenbach, H. (1989): MOMS-02 - Ein multispektrales Stereo-Bildaufnahmesystem für die zweite deutsche Spacelab-Mission D2, Geo-Informationssysteme, 2(3), pp. 5-11.

Ebner, H., Müller, F. (1986): Processing of Digital Three Line Imagery Using a Generalized Model for Combined Point Determination, Int. Arch. of Photogrammetry and Remote Sensing, Vol. 26-3/1, pp. 212-222.

Ebner, H., Strunz, G. (1988): Combined Point Determination Using Digital Terrain Models as Control Information, Int Arch. of Photogrammetry and Remote Sensing, Vol. 27, Part B11, pp. III/578-III/587.

Heipke, C., Kornus, W., Gill, R., Lehner, M. (1990): Mapping Technology Based on 3-Line-Camera Imagery, Presented Paper, ISPRS Symposium Commission IV, Tsukuba.

Hofmann, O., Nave, P., Ebner, H. (1982): DPS - A Digital Photogrammetric System for Producing Digital Elevation Models and Orthophotos by Means of Linear Array Scanner Imagery, Int. Arch. of Photogrammetry, Vol. 24-3, pp. 216-227.

Hofmann, O. (1986): Dynamische Photogrammetrie, Bildmessung und Luftbildwesen, 54(3), pp. 105-121.

Hofmann, O., Müller, F. (1988): Combined Point Determination Using Digital Data of Three Line Scannner Systems, Int. Arch. of Photogrammetry and Remote Sensing, Vol. 27, Part B11, pp. III/567-III/577.

AIRBORNE DIGITAL DATA ACQUISITION TECHNIQUES

F.G. Bercha and J.A. Dechka
The Bercha Group
#250, 1220 Kensington Rd. NW, Calgary, Alberta, Canada T2N 3P5
Phone: (403) 270-2221, Facsimile: (403) 270-2014

ABSTRACT

Harsh conditions such as dense jungle and cloud cover, particularly in equatorial regions, have stimulated research for the development of new techniques to provide information in support of both engineering and natural resource projects. This paper describes methods developed for digital data acquisition and interpretation using microwave and laser data. Specifically, digital side looking airborne radar, spaceborne synthetic aperture radars, and pulse lasers are described. The methods developed help acquire information required for digital terrain models, resource management programs, and for the generation of products such as geologic information maps, vegetation thematic maps, and topographic and drainage maps.

1. INTRODUCTION

Contemporary remote sensing instruments such as side looking airborne radars, spaceborne radars, and microwave airborne profilers have become established as effective sensors for the generation of terrain and ocean information in frontier regions such as the tropics and the polar regions. Although the thermal characteristics of these two sets of regions represent the two extremes of the climactic spectrum, the regions have many environmental and operational common factors. The arctic and equatorial regions in many cases are inaccessible, are often covered with fog or cloud, and require that operations be carried out under day and night conditions. In addition, terrain in the tropical regions is covered with a dense vegetation canopy while terrain and oceans in the arctic regions are snow and ice covered. Thus, sensors which may be operated during day or night conditions, independent of weather or atmospheric conditions, and which can penetrate the jungle cover are ideal. Indeed, both side looking radar and laser profiling instruments are active sensors capable of being operated in virtually any atmospheric conditions during the day or night, and have various degrees of penetrability of atmospheric conditions and vegetation or snow cover.

Because the sensor itself is part of a complex platform, its interaction with the total system must be actively controlled, and where this is not possible, precisely monitored. Further, the data record from these high technology systems contains a wealth of information which can only be acquired through advanced digital data processing methods. An integral portion of the information generation process, from acquisition activities through to the final analyses, is a capability to digitally acquire and record sensor and system related data.

Specifically, digital data acquisition applications within the context of radar and laser operations may be considered to take place on three levels as follows:

(a) The operational level in which the instrument interacts with the platform and environment and must be adjusted or monitored through digital motion compensation, ground speed monitoring and slant range rectification.

(b) Near real-time processing in which the sensor data are processed directly after recording in order to eliminate data which are ultimately not required to obtain the desired information, and to obtain the desired information, and to permit real-time information generation.

(c) Ground-based processing in which the full information content of the data may be accessed utilizing a large variety of digital techniques.

The first of the above levels of data processing relates more to the instrument manufacture and operation and accordingly will not be further addressed in this paper except to say that digital processing is an integral aspect of contemporary remote sensing hardware construction and operation.

Acquisition and ground-based processing techniques will form the basis of the balance of this discussion. Specifically, each of these techniques will be discussed within the context of side looking airborne radars and laser ground profiling sensors. Finally, some conclusions drawn from current practices relating to the sensors will be drawn and recommendations for future work will be presented.

2. AIRBORNE RADAR DIGITAL DATA PROCESSING

2.1 Introduction to Side Looking Airborne Radars

Side looking airborne radar (SLR) is an active microwave imaging system which has the advantages of day or night, all weather airborne imaging capability, directional and depression angle control, and high-quality digital image data generation. In essence, side looking airborne radar generates a series of microwave pulses from platform to terrain, and records the return of these pulses in a digital format. These pulses are arranged to sequentially cover the terrain over which the aircraft is flying and can be directly digitally processed to present as radar image, such as that illustrated in Figure 1, obtained with the Bercha Group side looking airborne radar.

Two principal categories of side looking airborne radars are currently in use; namely, the real aperture side looking airborne radar, termed SLAR, and the synthetic aperture side looking airborne radar, termed SAR. The SLAR has a somewhat simpler digital processor than the SAR because it permits the recording of a variable width beam across range, resulting in a cross range variation of resolution. At the same time, it has the advantages of being more economical and is generally considered to provide a better image tonal quality or dynamic range. In terms of hardware, the SLAR is generally characterized by a longer antenna such as that of the Bercha Group SLAR depicted in Figure 2 where a 6 meter antenna is shown suspended from the Metro II aircraft. The operational level processing and recording of a Bercha SLAR image is shown in the block diagram in Figure 3. As may be seen, this particular SLAR system possesses two processing trains, an analog train and a digital train. Operationally, both trains are aircraft motion and ground speed rectified in real-time. The resulting digital image is an 8-bit format record on 9-track magnetic tape.

A current technology synthetic aperture radar system (SAR) is the ice and terrain mapping system (IRIS) manufactured by MacDonald Dettwiler & Associates and operated by the Bercha

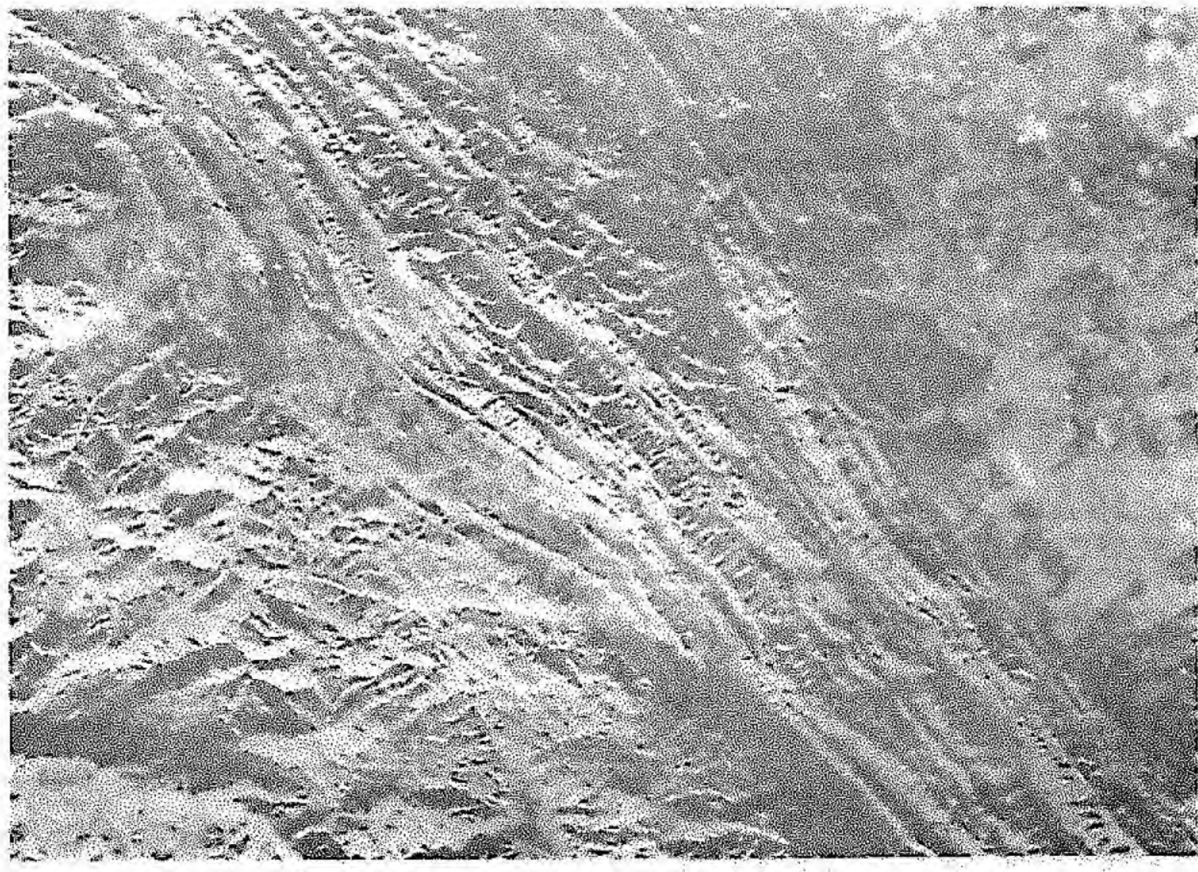

FIGURE 1: SLAR RADAR MOSAIC

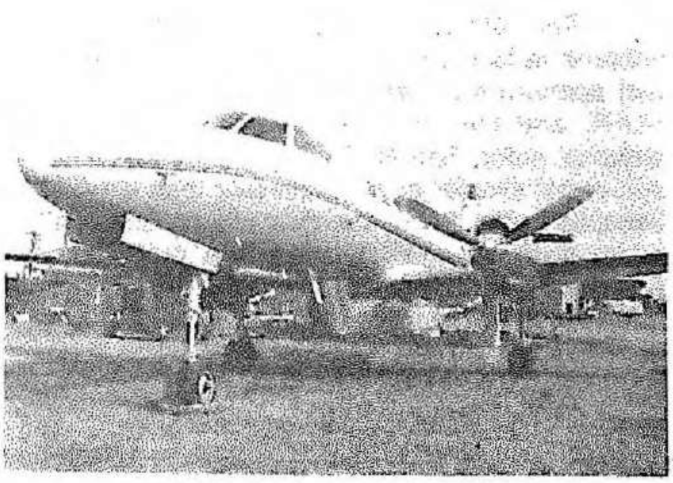

FIGURE 2: METRO II AIRCRAFT

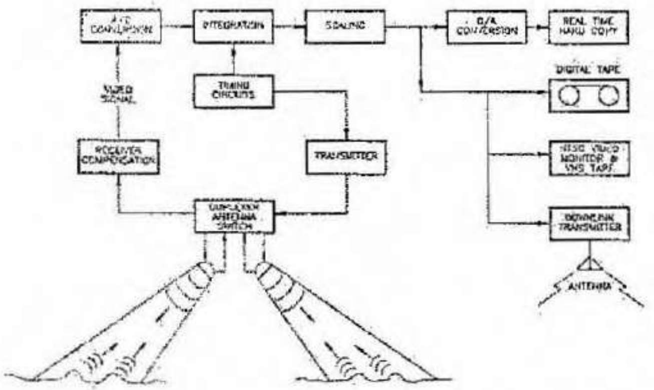

FIGURE 3: REAL-TIME RADAR DATA RECORDING

BLOCK DIAGRAM

Group in the CCRS owned Innotech operated Convair 580 aircraft shown in Figure 4, together with the acquisition and data generation processes illustrated in Figure 5.

2.2 Real-time SLAR Digital Processing Applications to Maritime Surveillance

Real-time monitoring of maritime operations including vessel, rigs, and the movement of potentially hazardous formations such as icebergs has been developed by the Bercha Group through an extensive series of commercial programs spanning five years and totalling over 6,000 SLAR mission hours. Specifically in developing a real-time maritime surveillance information extraction system for digital SLAR imagery, methods of isolating the positional and characteristic data for targets were developed to produce synoptic maps which can be transmitted in real-time through ordinary airborne facsimile transmitters which have the advantages of virtually no range limitation. Figure 5 illustrates a block diagram of the near-real time processing activities to provide maritime surveillance information based on data collected with the Bercha SLAR. In essence, an operator assisted digital interpretation process was implemented. In this process the SLAR image, digitally rectified in real-time, was placed on a digitizing tablet capable of automatically recording positional information and receiving inputs on target characteristics from a human operator. After the targets had been located and identified, the target information was automatically merged with positional models to generate a target map such as that shown in Figure 6 containing only the relevant maritime surveillance information. The map, then, was transmitted by telefax from the aircraft to selected offshore and ground stations. The entire interpretation process could be carried out within 15 minutes of target overflight, yielding target maps to any ground stations equipped with appropriate band facsimile receivers and appropriate security codes within half-an-hour of target overflight.

The Bercha Group has also carried out more comprehensive transmission activities in which the digital image itself with only positional information

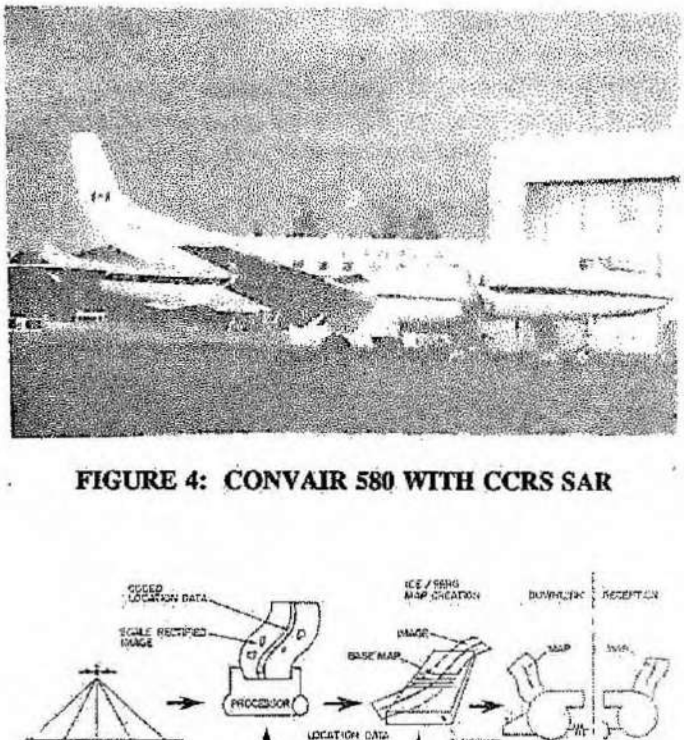

FIGURE 4: CONVAIR 580 WITH CCRS SAR

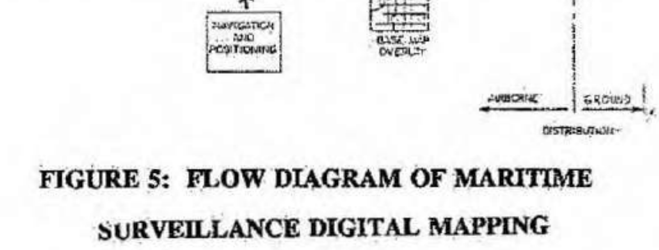

FIGURE 5: FLOW DIAGRAM OF MARITIME

SURVEILLANCE DIGITAL MAPPING

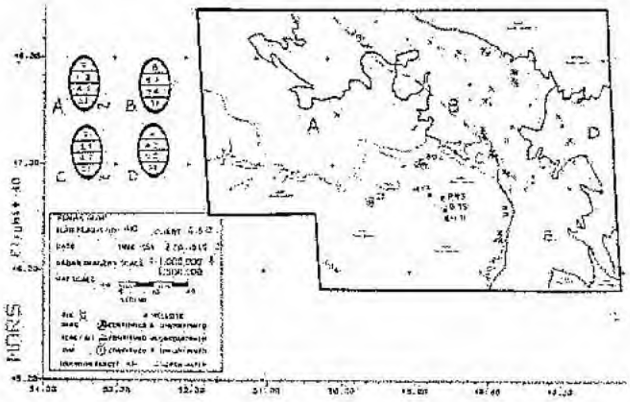

FIGURE 6: TYPICAL OFFSHORE TARGET MAP

has been transmitted by means of downlink. In the case of surveillance of more complex targets such as continuous troop movements, ocean surface conditions such as wave patterns or ice formations, and continuous phenomena such as floods or fires, it may be desirable to transmit the entire radar image rather than a real-time map generated as is optimal for point target information. To date, such digital transmissions have been carried out through line-of-sight transmission having the disadvantage of range restriction. That is for as given aircraft altitude the furthest ground station must be no further than the tangent point of a line from the aircraft to the earth surface. For a 10,000 meter ASL this is roughly 200 kilometres., Current developments, however, include transmission of digitized radar data to satellites with subsequent downlinking to ground stations thus removing, for all practical purposes, the range restriction. Figure 7 illustrates such as transmission technique for offshore maritime surveillance, clearly depicting the territorial advantage.

2.3 Ground-based Digital Analysis of Radar Imagery

2.3.1 General Discussion of Ground-based Digital Analysis of Radar Imagery

An integral element of digital data acquisition is the ultimate application to information extraction using digital interpretation techniques.

Techniques discussed in this section all pertain to ones which are generally carried out on a ground-based computer system in an operator interactive mode. The techniques are of two principal categories; namely, visual presentation techniques and digital information extraction techniques. As implied, visual presentation techniques are concerned primarily with enhancement of features in the radar image for subsequent graphic visual interpretation while information extraction techniques use the full potential of the data and involve the utilization of algorithms to extract information which may not be extracted by visual means alone. Visual interpretation techniques consist of those pertaining to single-band visual presentation, multi-band visual presentation and multi-sensor visual presentation. Examples of techniques pertaining to digital

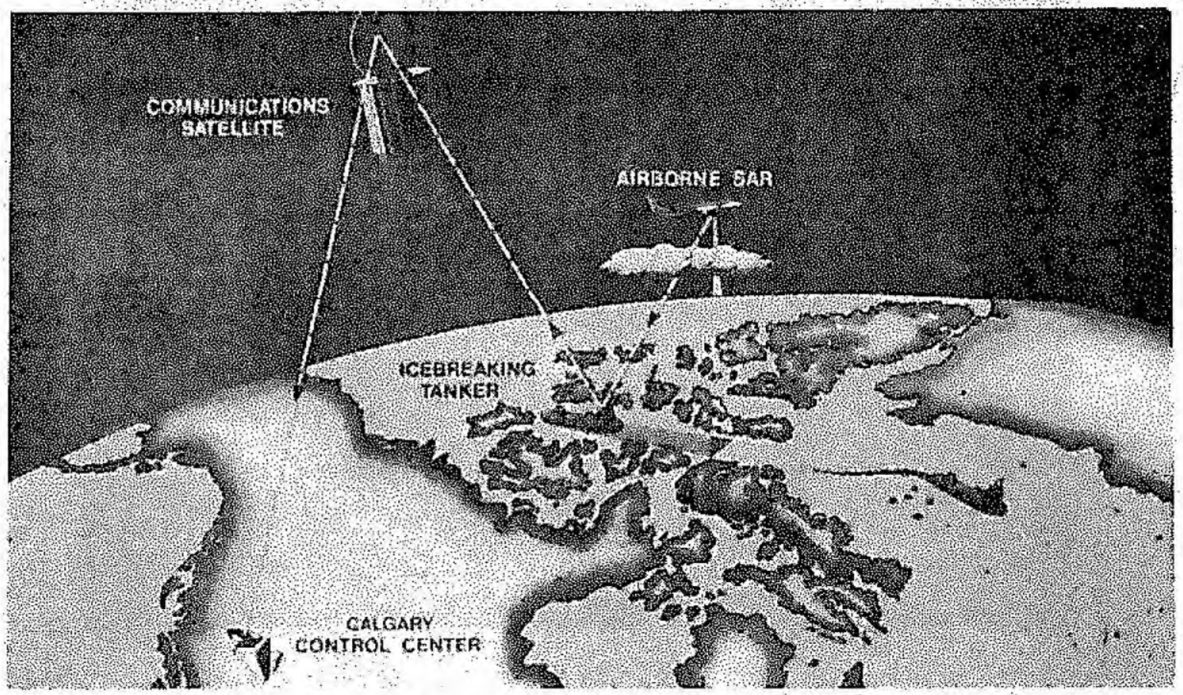

FIGURE 7: OFFSHORE DIGITAL RADAR DATA TRANSMISSION VIA SATELLITE

information extraction have been restricted to single-band considerations.

2.3.2 Data Interpretation Techniques for Visual Presentation

2.3.2.1 Single-band SLR Visual Presentation Techniques

Simple single-band visual presentation techniques include contrast stretching, polarization, spatial filtering, and colour presentation methods.

Contrast stretching is a simple manipulation which maps the range of pixel intensities in the original image to the full dynamic range afforded by the digital processing system. The process improves the contrast of the image and allows subtle feature differences to be distinguished in the image.

Polarization is the process whereby the pixel intensities are mapped inversely, so that black becomes white and white becomes black in the extreme. The approach is principally perceptual based upon concepts of figure and ground.

Spatial filtering utilizes spatial or equivalent frequency filtering techniques to highlight information of different spatial frequencies within the image. Especially useful is high-pass filtering which emphasized high-frequency features such as geologic linear structures and directional filtering which enhances specific directions of the image fabric. Filtering is also used to reduce image speckle.

The use of colour in enhancing an image facilitates visual recognition and interpretation of features as the human eye can discriminate far more colours than shades of grey. The use of colour in single-band enhancements is possible using as number of techniques including density slicing and split spectrum techniques.

A radar image acquired over Malaysia by the Bercha Group SLAR which has been enhanced by split-spectrum techniques is shown in Figure 8. This enhancement helps define three distinct lithologic units based on image colour and texture. Sedimentary rock structure is evident within the plunging syncline in the central part of the image, a zone of predominantly limestone can be seen below the syncline, and a massive crystalline structure composed of igneous rock can be delineated left of the river. Due to the differential erosion of the complete sedimentary rocks and the illumination geometry of the radar which highlights

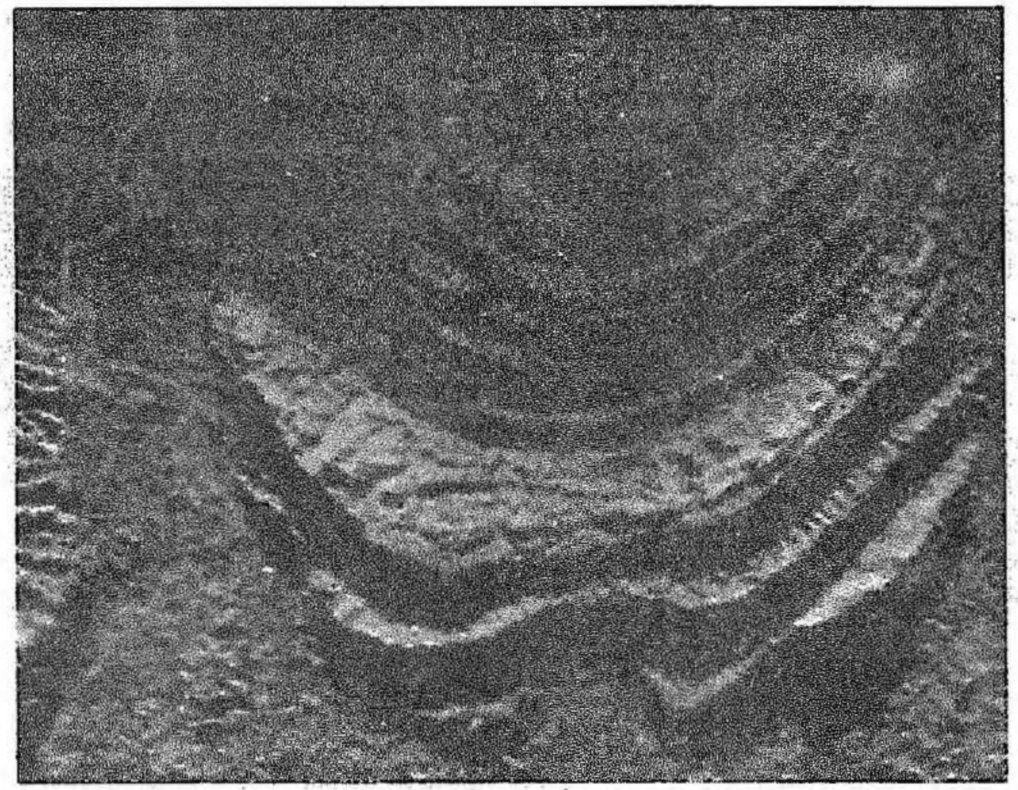

FIGURE 8: ENHANCED DIGITAL RADAR (SLAR) IMAGE, SOUTH LOOK

this erosional pattern, the dip of the beds toward the core of the syncline can easily be seen.

2.3.2.2 Multi-band SLR Data Interpretation Techniques

SLR systems may be configured to provide imagery from different look directions and incidence angles as with the Bercha SLAR, as well as different frequencies and polarizations as with the Convair SAR. Multi-band enhancement techniques can be utilized, for multiple SLAR passes over the same area, for the different look directions, incident angles, frequencies and polarizations. Each different image data set contributes unique information on the material and terrain providing greater detail for a particular target or set of features. Multiple SLAR bands can be effectively combined through a digital colour composite image in which the different colours or mixtures of colours represent unique information obtained from each band. Although colour composites provide a method for displaying multiple sources of information, they have limitations. First, only three bands can be displayed simultaneously, and secondly the method is restricted to the information inherent to a specific band. Mathematically transforming the data overcomes these limitations by extracting specific information for multiple bands and mapping them into fewer bands. The Bercha Group has developed expertise for carrying out such multi-band SLAR data transformations as reported in a series of papers by our Ottawa personnel, which may be made available upon request.

2.3.3.3 Multi-Sensor Combinations for Visual Presentation

Combining SLR data with other types of remotely sensed data will offer increased information, as the unique properties of each channel will complement the others when combined digitally. A number of enhancements which have been carried out by the Bercha Group for combination of LANDSAT MSS with IRIS SAR data are summarized in Table 1. As can be seen, different combinations of bands recorded during different seasons are used to emphasize different aspects of the terrain information required.

TABLE 1

LANDSAT MSS/SAR ENHANCEMENTS

DATA TYPE	ENHANCEMENT	PURPOSE
Winter LANDSAT/SAR	A. Product Images Band 7 x SAR - R** Band 5 x SAR - G Band 4 x SAR - B	Emphasizes topographic detail
Summer LANDSAT/SAR	Band 7 x SAR - R Band 5 x SAR - G Band 4 x SAR - B	Emphasizes biomass, land use patterns
	B. Colour Space Mapping (Taylor Enhancement	
Summer and Winter LANDSAT/SAR	Summer Band 7 used as a weighting function	Excellent drainage detail
Summer and Winter LANDSAT/SAR	SAR used as a weighting function	Emphasizes topographic detail
	C. Band Combination	
Summer and Winter LANDSAT/SAR	Summer band 7 - R Winter band 7 x SAR - G Winter band 4 x SAR - B	Emphasizes topographic detail

**Red, Green, Blue Colour Guns

2.3.4 Digital Techniques for SLR Data Information Extraction

The principal purpose of this category of techniques is to fully extract specific information quanta from imagery utilizing semi or fully-automatic methods for quantitative analysis. (Bercha et al., 1985; Shaw, 1986; Bercha et al., 1988). The types of information extracted include forest cover, soil types, hydrologic properties, biomass, and any other terrain, marine, or geological characteristics contained in the single or combined sensor data sets analyzed.

Generally, information from remotely sensed data is represented by spectral, spatial, temporal, and contextual properties of the scene. Spectral information is contained in pixel intensities which represent the reflected properties of the objects within a given resolution cell. Spatial information includes pixels within the neighbourhood which may be described by their textural and structural properties. Temporal information provided an indicator of the material and objects presented by their changing properties over time. Contextual information provides clues to the identification of an object by the presence of other forms, shapes and objects juxtaposed to the subject object or location within the scene. The general approaches to information extraction may be summarized as follows:

(a) Statistical approaches.
(b) Structural approaches.
(c) Artificial intelligence techniques.

Statistical approaches include the characterization and assignment of an element to a particular object on the basis of probability theory and statistics. Structural approaches view the object to be composed of simple patterns, where patterns are considered to have a structure of repeated elements that can be described by some mathematical model. Finally, a few artificial intelligence analysis systems, most of which are prototypes, are currently in existence dealing with remote sensing on the basis of artificial intelligence.

A variety of work for the identification of oceanographic phenomena including standing wave patterns, currents, and ice cover characteristics has been carried out by the Bercha Group utilizing cluster analytic statistical approaches, structural methods, and supported by the visual techniques. Such work is reported elsewhere and may be made available upon request.

3. LASER DATA DIGITAL PROCESSING

3.1 General Introduction to Laser Mapping Systems

Commercial, high-accuracy laser systems became available in 1980, although problems of generating an accurate ground and vegetation profile depended on the solution of timing, integration, and airborne platform positioning considerations.

A high-accuracy laser profiling system was implemented in a large-scale demonstration project of laser profiling, and topographic map product generation in Indonesia by the Bercha Consortium (Bercha, 1988). The laser mapping system consisted of an airborne data collection system and a ground-based data processing and automatic mapping system. Both the airborne and ground-based system components utilize current state-of-art proven and reliable technology.

The airborne platform was a Bell 206B helicopter equipped with specialized power, positioning, and racking equipment for the data acquisition program. As may be noted from the block diagram given in Figure 9, the principal sensing component consists of the lasers and the laser mirror. The navigational system is used to accurately provide planimetric and vertical coordinates for the platform at any given time, until 1988, initial survey systems were required while Global Positioning Systems used today facilitate acquisition efficiency. During acquisition both positional and platform to the canopy ground distance measurements are simultaneously recorded and delivered for first level processing. As may be seen from Figure 9, laser data and positional data are then merged to generate a ground profile. Next, the digitized ground profile is plotted, and map products may be generated utilizing a specialized software mapping package.

3.2 Laser Profile Generation Utilizing Digital Techniques

As shown in Figure 9, the real-time digitally processed data consists of two data sets, the positional data and the laser data. The positional data gives the X,Y, and Z coordinates of the platform at a high temporal frequency along the flightline. the laser data consists of a series of laser pulse measured distances between the platform and the terrain. As indicated earlier, distances from higher canopies also appear in this data set. In the ground-based processing necessary to generate a precise ground profile such as that shown in Figure 10, these two data sets are digitally merged to provide a true ground profile. The profiles are further digitally corrected from comparisons of positioning data and systematic ground truth location points.

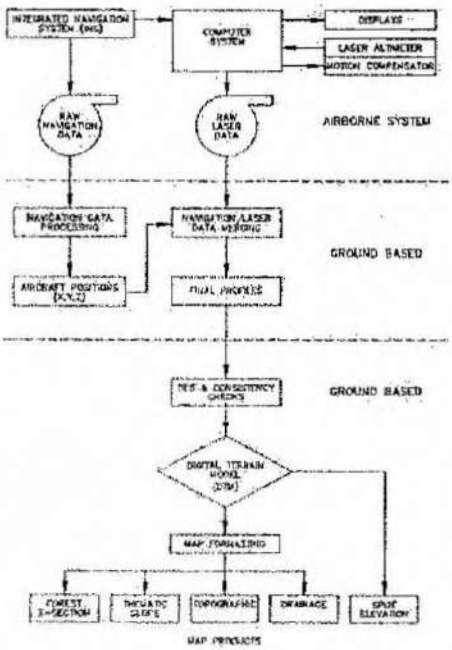

FIGURE 9: LASER SYSTEM BLOCK DIAGRAM

3.3 Digital Map Product Generation From Laser Data

The digitized ground profile is automatically read into the topographic mapping system. As may be seen from the block diagram of the mapping system in Figure 9, map products including slope, topographic, spot elevation, profile, forest profile and drainage maps may be generated. The first step in the map creation process is the creation of a digital terrain model (DTM) for the area to be mapped. The creation of the DTM for an area of roughly 100 sq. kilometres with a 100 meter profile grid takes approximately 46 hours. Creation of a file of contour lines for plotting is done by searching the regular grid for its upper and lower height and starting at the lowest, contour lines are interpolated throughout the grid. The contour file is then output to tape for plotting on a specialized map plotter, yielding products such as that shown in Figure 11.

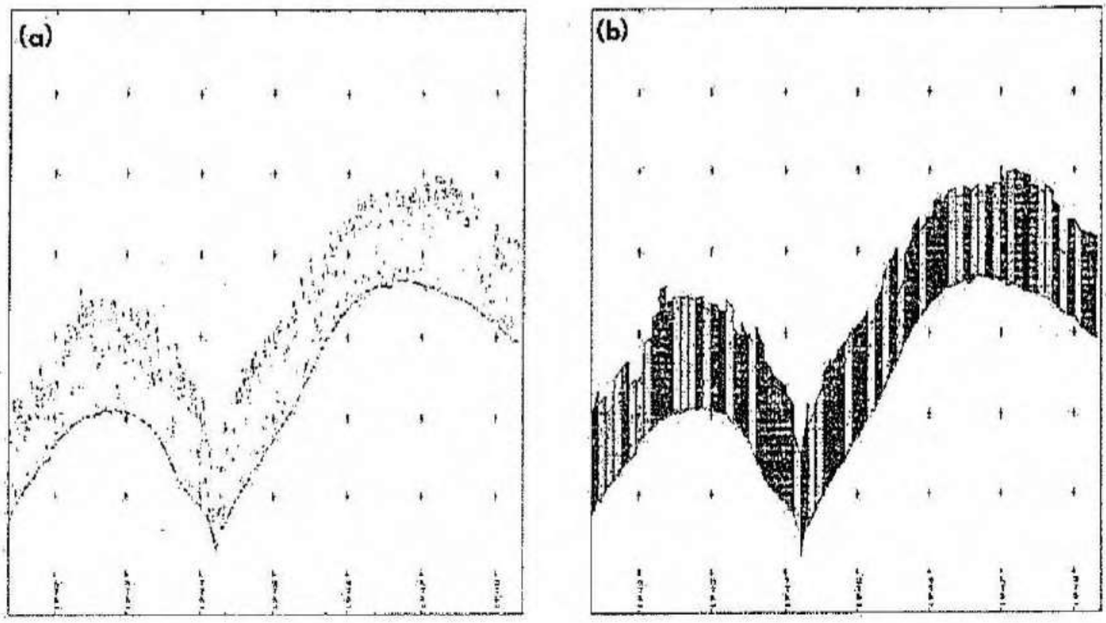

FIGURE 10: COMPARISON OF RAW AND PROCESSED DATA

Thematic maps may also be created from the DTM. First, forest profiles such as that shown in Figure 10(a) can be generated with processing to show cover classes as shown in Figure 10(b) (Bercha et al., 1989; Bercha et al., 1990). Using the grid nodes, specified slopes are identified and a file is created which is then output for plotting, to create thematic or slope maps. The utilization of a digital terrain model with a flexible profile data base which can be updated or corrected as required has substantial advantages permitting the generation of a variety of map products including the stated topographic and thematic map, spot elevation maps, drainage maps, the isometric or other orthographic projections of the three-dimensional terrain.

3.4 Statistical Laser Data Applications

In statistical laser data applications, positioning control accuracy may be relaxed because only a sample of profile or relative profile data needs to be acquired; that is, a sampling flight through the population area is only generally located since the results to be obtained include statistical data to serve as a basis for computation of frequencies, wave length, mean heights, and other characteristic parameters. To date, statistical applications of laser profilometry have included forest cross-section for forest volume computation, soil erosion or fluvial deposit variation assessment, and ice ridge or sand dune frequency and wave length evaluation. The airborne system used by the Bercha Group in these applications has generally consisted of the same basic laser as has been utilized for precise mapping, but in this case without the sophisticated motion compensation and positioning system needed for accurate planimetric and vertical control.

An instrument with a similar function in statistical applications is the airborne radar altimeter. Specifically, the forest penetrating radar for tropical zones, FPR 2, as developed by the National Research Council of Canada and operated

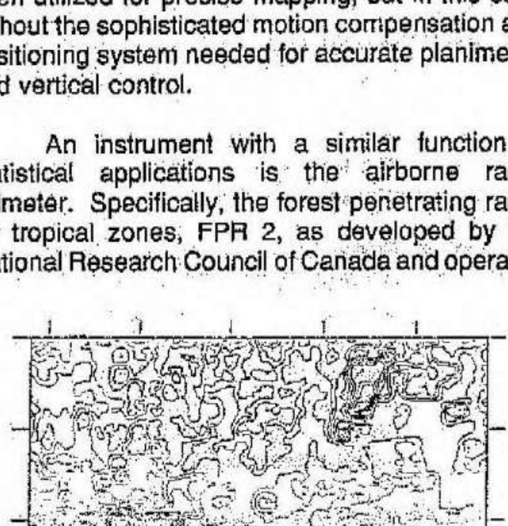

FIGURE 11: TYPICAL TOPOGRAPHIC MAP DIGITALLY GENERATED FROM LASER DATA

by Hauts Monts may be utilized to make altimetric measurements from a fixed wing aircraft, but with considerably less accuracy than the laser. Just as the laser, however, the radar altimeter penetrates multiple canopy foliage, to the ground, giving distance measurements from each canopy as well as from the terrain itself. Thus, a logical spinoff application is the computation of biomass from laser or radar profiles. This can be accomplished by combining typical trunk diameters with tree height measurements and processing transfer on appropriate biomass algorithms.

4. CONCLUSIONS

Major developments have recently occurred in civilian applications of digital methods to the acquisition, processing, and information extraction from radar and laser data. The following general conclusions may be summarized from the present corporate group's experience:

(a) Operational, real-time, and ground - based digital analysis of laser and radar data constitute a reliable and current state-of-the-art capability.

(b) Operational analysis of the sensor data generally falls within the manufacturer's domain as it involves sensor operation such as motion compensation, alignment, and other operational aspects.

(c) Radar real-time digital data analysis is particularly important in support of technical surveillance activities such as maritime surveillance and onshore security surveillance. It permits quick filtering of critical information from the image for virtually unlimited transmission range.

(d) Laser real-time data analysis currently involves creation of a position and distance file but should be extended to merge these two files in real-time.

(e) Ground-based processing capabilities are extensive for both radar and laser and it may well be concluded that virtually any application within the sensor spectral capability may be addressed with custom software and algorithm development.

(f) Radar ground-based analysis consists of visual enhancement techniques and digital information extraction for either single-band, multi-band or multi-sensor data sets.

(g) Because radar data are black and white although they do contain a very high dynamic range for the case of good quality radars, visual enhancement techniques utilizing colour are highly desirable to facilitate visual interpretation.

(h) Information digital extraction techniques for radar data represent a virtually unlimited potential for development although significant success has already been met in applying these to forest and vegetation classification, ocean and ice mapping, and maritime surveillance.

(i) Laser profiling and topographic mapping systems have been developed to a high level of accuracy and reliability and are capable of generating a diverse set of data for topographic maps, forest cross-sections and profiles, thematic maps, drainage maps, other map products based on the digital terrain model integrated into the map processing system.

5. RECOMMENDATIONS

The following recommendations are based on the above presentation:

(a) Manufacturers should more carefully consider the potential of operational real-time digital techniques in order to improve performance of radar, laser, and radar altimeter sensors.

(b) Other developments in real-time and near real-time radar data processing are desirable particularly for surveillance activities where a large part of the digital image storage volume is taken up by non-critical image pixels such as those corresponding to open water or bare terrain.

(c) Near real-time laser data processing should include a capability to automatically merge the positional information and planimetric sensor data to get a digital data base.

(d) Ground-based radar and laser data digital processing should be approached with optimism and confidence as virtually any application requirement can be met provided the positioning systems and sensors can generate accurate and reliable data records.

6. REFERENCES

Bercha, F.G., Hirose, T., and Harris, J., "Digital Techniques for SLAR Data Interpretation". Conference on Recent Developments in Remote Sensing Equipment and Technology, Singapore, June 10-15, 1985.

Bercha, F.G., "Kalimantan Laser Mapping Pilot Project", Proceedings of 3rd Asian Survey Congress, Bali, Indonesia, 1988.

Bercha, F.G., Shaw, V.L., and McRuer, W.H., "Auto Cross Correlation Analysis of Environment System and Target Parameters for Iceberg Detection Using Airborne Radar". IGARSS '88, Edinburgh, Scotland. Sept. 12-16, 1988.

Bercha, F.G., Currie, D.H., Dechka, J.A., Fuenning, P., and Jordan, P., "Multiband Interpretation Application in Sabah". Proceedings 10th Asian Conference on Remote Sensing, Kuala Lumpur, Malaysia, Nov. 23-29, 1989.

Bercha, F.G., Currie, D.H., and Dechka, J.A., "Multisensor Airborne Forest Inventory System". 23rd International Symposium on Remote Sensing of Environment, Bangkok, Thailand, April 18-25, 1990.

Currie, D.H., Shaw, V.L., and Bercha, F.G., "Integration of Laser Rangefinder and Multispectral Video Data for Forest Measurements". IGARSS'89, Vancouver, Canada, July 10-14, 1989.

Shaw, V.L., "Iceberg Detection Using SLAR", Proceedings of 10th Canadian Symposium on Remote Sensing, Edmonton, Alberta, May 5-8, 1986.

RADIOMETRIC INTERCALIBRATION BETWEEN SPOT AND SOME OTHER SATELLITES

M.DINGUIRARD (1), M.LEROY (2), P.HENRY (2), G.GUYOT (3) and X.F.GU (3)

(1) ONERA/CERT/DERO - 2, Avenue E.BELIN - 31055 TOULOUSE CEDEX FRANCE
(2) CNES - 18, Avenue E.BELIN - 31055 TOULOUSE - FRANCE
(3) INRA - BP 91 - 84140 MONTFAVET - FRANCE

ABSTRACT

This paper presents some results in the field of optical satellites radiometric intercalibration obtained by the French Spatial Agency CNES in collaboration with other institutes, ONERA CERT/DERO (Toulouse), INRA (Avignon) and LOA (Lille). Four main issues are reviewed in detail: (i) the intercalibration of a NASA hemispherical and CNES spherical large aperture preflight sources, (ii) the intercalibration between SPOT1 and MOS1 initiated in the framework of the MOS1 Preparation Program, (iii) the intercalibration of LANDSAT5-TM and SPOT1 on the test site of La Crau (South-East of France) using ground measurements of the ground reflectance and the atmospheric properties and (iv) attempts to intercalibrate the two satellites SPOT1 and SPOT2

KEY WORDS : Radiometric calibration, Remote Sensing cameras, SPOT, LANDSAT, MOS.

1 - INTRODUCTION

Absolute calibration of remote sensing cameras, that is, the conversion of digital instrument output into the observed radiance, is very important since it permits, if accurate, a good monitoring of a given phenomenon with time (multi-temporal calibration) as well as ability to mix informations issued from different cameras on-board different satellites.

As an accurate absolute calibration is a very difficult task, the French Spatial Agency CNES, in its SPOT program, has made in collaboration with other national institutes, ONERA CERT/DERO (Toulouse), INRA (Avignon) and LOA (Lille), a significant effort in cross-calibrating the SPOT instruments using many independent procedures as possible. The HRV cameras on board SPOT1 and now SPOT2 were carefully calibrated before flight in MATRA (SPOT manufacturer) laboratories. An on-board device including 2 different light sources (an halogen lamp + an optical fibre devices to conduct the solar irradiance onto the detectors) and continuous checks on orbit on defined sites with or without ground truth have allowed a good estimation of the temporal evolution of the cameras. Cross calibration with other remote sensing systems such as LANDSAT, MOS etc.. using the same ground standard or extrapolating absolute calibration from a camera to the other by comparison of quasi simultaneous images of the same area was also an aim of the program.

As a result, these different studies and experiments have turned out to be useful to define laboratory standards, signal models and calibration procedures, which may now be applicable with some generality to the new generation instruments in preparation in the various Agencies.

In section 2, general considerations on intercalibration are discussed and intercalibration coefficients defined. Following is a description of some experiments done, using the SPOT2 HRV cameras, in the aim of cross calibrating ground sources used by CNES and NASA (section 3) and, with SPOT1, cross calibrating SPOT1 with other cameras: MOS-1 (section 4), LANDSAT TM (section 5) and SPOT2 (section 6).

2 - GENERAL CONSIDERATIONS ON INTERCALIBRATION

We will adopt the SPOT signal model as described in the SPOT USERS HANDBOOK. Thus for a remote sensing camera (SPOT HRV, LANDSAT TM...), the average output signal corrected for dark signal is expressed as :

$$x_k = A_k \, G_{mk} \, L_k \qquad (1)$$

where k refers to the spectral band, A is the absolute calibration coefficient, Gm is the image analog gain and L is the equivalent spectral radiance defined as:

$$L_k = \frac{\int L(\lambda)\, S(\lambda)\, d\lambda}{\int S(\lambda)\, D\lambda} \qquad (2)$$

$S(\lambda)$ is the spectral profile of the considered spectral band k and $L(\lambda)$ is the spectral radiance.

$S(\lambda)$ is in relative units, x is expressed in digital numbers units and L in Watt meter^{-2} steradian^{-1} micrometer^{-1} as $L(\lambda)$.

For a given camera, the purpose of absolute calibration is to determine the Ak coefficients which allow the user to convert output signal in radiance units. This is usually done by direct measurement of a known radiance, a large integrating sphere in laboratory before flight or, when in orbit, by ground truth over well defined test sites (WHITE SANDS in NEW MEXICO USA or LA CRAU in the south of FRANCE).

The intercalibration coefficient is defined as the ratio between 2 absolute calibration coefficients. When estimated between two cameras in orbit, it provides an absolute calibration measurement for a given instrument (the other acting as a reference) or acts as a cross comparison by a different and independent mean of the absolute calibration of the 2 cameras (if absolute calibration coefficients are already available for the 2 cameras). In any case this cross information is useful for the users using different sets of images taken by different instruments.

In orbit, if no ground truth is possible, the comparison can be done between the images issued from the same ground scene viewed quasi simultaneously by the 2 cameras in the quasi identical spectral bands. If this cannot be achieved, because of system limitations, it is necessary to take into account the existing differences between the viewing conditions (time of over pass, view angle, atmospheric changes ...) and the spectral bands. Howe..., this leads to residual errors if all the model parameters are not perfectly known.

In fact the observed radiance depends on the equivalent ground reflectance ("viewed" at the top of the atmosphere) ρ_k, through the relation

$$L_k = \frac{1}{\pi} \rho_k \cos(\theta_s) E_k \tag{3}$$

where E_k is the equivalent normal solar irradiance (taking into account the sun-earth distance variation) and θ_s is the zenith solar angle.

The top of atmosphere reflectance depends on the atmospheric conditions. This is the reason why, when ground truth is not available, the time of overpass of the satellites to be compared must be as close as possible.

In order to achieve a good calibration accuracy, a careful choice of the site has been performed. Without ground truth, a suitable site for cameras intercomparison has to fulfil the following properties:

(i)- A high reflectance level, necessary to minimize the measurements errors.

(ii)- The site has to be reasonably flat to allow irradiance and viewing geometry corrections due to the differences between the 2 satellite overpass times.

(iii)- The spectral reflectance has to vary smoothly and slowly with wavelength to minimize the effects of possible differences between the 2 camera spectral bands.

(iv)- The site has to be large enough to avoid undesirable atmospheric environmental effects and also to allow statistical analysis of the image data.

In these conditions, one can suppose that the 2 cameras are looking at the same reflectance and the ratio of the absolute calibration coefficients is directly derived from the ratio of the cameras mean digital output:

$$\frac{A_{k2}}{A_{k1}} = \frac{x2}{x1} \; \frac{G_{m1}}{G_{m2}} \; \frac{\cos(\theta_s)_1}{\cos(\theta_s)_2} \tag{4}$$

3 - GROUND SOURCES INTERCALIBRATION

An intercomparison of a CNES integrating sphere (manufactured and calibrated by Labsphere USA) and a NASA GSFC integrating hemisphere was performed in the MATRA integration hall in Toulouse, FRANCE in October 1987. Their characteristics were tested against a standard laboratory spectroradiometer and against the SPOT2 satellite instruments.

This experiment was placed in the context of an increasing demand in the remote sensing community of the ability to cross calibrate various sets of remote sensing satellites as well as from other sources of data such as aircraft and ground radiometer measurements. Thus, this intercomparison has been viewed as a calibration link between the CNES SPOT2 satellite and the various radiometers calibrated by NASA GSFC. Besides, it provided a better characterization of the performance of each source and, as a by-product, a better insight into the range of accuracies of the characterization of the SPOT2 satellite performances.

The detailed description of the experiment is given in Leroy et al., 1990.

The measured absolute calibration coefficients for the 2 SPOT HRVs using the sphere and the hemisphere are listed in table 1. The discrepancies between the 2 sets of results range from 4% to 8%. These discrepancies decrease with increasing wavelengths and are nearly identical (to within less than 1%) for both HRVs, which is an indication of good experiment repetitivity as the 2 cameras are nominally identical.

		PA	XS1	XS2	XS3
SPHERE	HRV1	0,498	0,586	0,579	0,878
	HRV2	0,606	0,670	0,585	0,916
HEMISPHERE	HRV1	0,543	0,634	0,618	0,921
	HRV2	0,656	0,721	0,622	0,960
$\frac{A(sphere)-A(hemi)}{A(sphere)}$	HRV1	8,3%	7,6%	6,3%	4,7%
	HRV2	7,6%	7,1%	5,9%	4,6%

Table 1 : Ground sources intercalibration

It is instructive to elaborate an error budget of the experiment in order to attempt to explain the observed discrepancies. This is done in table 2, where one makes the distinction between bias (or deterministic) type errors and random type errors.

	PA	XS1	XS2	XS3
CALIBRATION BIAS $\Delta L(\lambda)$ (LABSPHERE-GODDARD)	+ 5%	+4%	+ 4%	+ 2%
LINEARITY BIAS	+ 1%	+ 0,6%	+ 0,8%	- 1%
TOTAL BIAIS	+ 6%	+ 4,6%	+ 4,8%	+ 1%
MEASUREMENT ERROR ESTIMATES	± 2%	± 2%	± 2%	± 2%
CALCULATION ERROR ESTIMATES	± 1%	± 1%	± 1%	± 1%
MAX. ERROR ESTIMATES	+3,8% to +8,2%	+2,4% to +6,8%	+2,6% to +7%	-1,2% to +3,2%
ACTUAL RESULTS	+ 8%	+ 7.5%	+ 6%	+ 4,6%

Table 2 : Error budget

The first bias taken into account concerns the calibration of the source itself. The results of table 1 were obtained using the Labsphere sphere calibration and the GSFC hemisphere calibration. The GSFC measurements of the sphere shows a +2% to 5% difference relative to the Labsphere sphere calibration, depending on wavelength.

The second bias to consider concerns the linearity issue. On the one hand, the functioning point of the sphere was not that where the sphere was calibrated, which is of consistence if the sphere is not perfectly linear. On the second hand, the radiance levels of the sphere and of the hemisphere during the experiment were not strictly the same which could have resulted in a slight bias if SPOT2 departs from a perfectly linear behaviour. A linearity analysis showed that non linearity can account to a 1% level bias.

The measurement errors have been estimated to the ±2% level peak to peak. They take into account the various temporal instabilities of the sources and of the HRV instrument.

The calculation errors, which include the reduction process of the images to obtain an average output signal and the various calculation steps leading to the equivalent radiance value L from models of $L(\lambda)$ and $S(\lambda)$, have been estimated to be within a ±1% level peak to peak.

In the error budget of table 2, the measurement and calculation errors have been summed quadratically and added linearly to the signed total bias. This results for each spectral band in a range of expected discrepancies between the values of the SPOT2 absolute calibration coefficients A obtained by the sphere A(sphere) or the hemisphere A(hemisphere), which can be compared to the actual results, taken as the results of table 1 averaged over the two HRVs. Table 2 shows that the actual result fit marginally the expected error range, with an overall tendency of the discrepancy to be higher than expected, as if an additional bias of unknown origin, of the order of 3%, existed.

4 - SPOT1 - MOS1 INTERCALIBRATION

The purpose of this experiment, detailed in Henry and Begni, 1989, was to determine the MOS1 absolute calibration coefficients using a simultaneous MOS/SPOT observation over an appropriate site.

The only possible sites fulfilling the criteria described in section 2 are sandy deserts or snowy plains. Besides, they have to be in the visible range of a MOS1 observation centre (SPOT using its on-board recorder).

The calibration of MOS1 using SPOT1 calibration coefficients was performed, according to these requirements, over a snowy area of MANCHURIA on February 16, 1988. The images have been recorded by MESSR2 and HRV1 in quasi vertical viewing with SPOT1 overpassing the site 17 minutes after MOS1. Close cooperation between NASDA and CNES has allowed a successful operation.

Common homogeneous area has been selected over the images (about 4 x 4 km2) and the radiometric average has been calculated for each spectral band.

The HRV1 absolute calibration coefficients have been computed for the viewing date using available data in CNES (Dinguirard et al., 1988). They allow to determine the equivalent radiance of the scene:

$$L_{SPOT} = \frac{X_{SPOT}}{AG_m} \qquad (5)$$

The HRV and MESSR spectral bands are not entirely identical, the HRV bandpasses being XS1 [0.50 - 0.59 µm], XS2 [0.6 - 0.68 µm], XS3 [0.79 - 0.89 µm], while the MESSR bandpasses are B1 [0.51 - 0.59 µm], B2 [0.61 - 0.69 µm], B3 [0.72 - 0.80 µm], and B4 [0.80 - 1.10 µm].

Assuming no change in the observed reflectance during the 17 minutes difference in the overpasses one can derive the equivalent radiance at the entrance of MESSR from that estimated by SPOT.

According to their similarity, direct comparison is possible between B1 and XS1, B2 and XS2. Thus the MESSR equivalent radiances in these bands can be provided by :

$$L_{MESSR} = L_{HRV} \frac{\cos\theta_{s_{MESSR}}}{\cos\theta_{s_{HRV}}} \qquad (6)$$

For B3 one can deduce the equivalent radiance from the one measured in XS2 and XS3.

For band 4 the SPOT measurement has to be extrapolated to 1.1 mm. A computation using the spectral reflectance of snow, the spectral solar irradiance and the spectral sensitivity of both instrument as a function of wavelength, provides the following equations :

$$L_{B3} = 0.49(L_{XS2} + L_{XS3}) \frac{\cos\theta_{s_{MESSR}}}{\cos\theta_{s_{HRV}}} \qquad (7)$$

$$L_{B4} = 0.89\ L_{XS3} \frac{\cos\theta_{s_{MESSR}}}{\cos\theta_{s_{HRV}}} \qquad (8)$$

Hence the MESSR2 absolute calibration coefficients can be determined as $A_k = x_k / L_k$.

The MESSR1 absolute calibration was achieved by an intercomparison between the 2 instruments made on the same area (over NAGOYA) recorded simultaneously by the 2 MESSRs on Feb. 28, 1988.

Table 3 gives the SPOT1 HRV1 calibration coefficients used in this intercomparison. Table 4 gives the MESSR absolute calibration coefficients as derived from SPOT HRV1 and the MESSR1/MESSR2 coefficients used to performed the calculation.

Table 5 gives an estimate of the error budget. According to table 5, The figures for the intercalibration accuracy range from 2% to 8% depending on the spectral band, while the absolute accuracy obtained for the MOS1 absolute coefficient ranges from 6% to 11%.

XS1	XS2	XS3
0.489	0.347	0.547

Table 3 : SPOT1 HRV1 absolute calibration coefficients

	B1	B2	B3	B4
MESSR2	0.417	0.396	0.266	0.337
MESSR1	0.412	0.420	0.272	0.311
MESSR1/ MESSR2	0.988	1.062	0.978	0.923

Table 4 : MESSR absolute calibration coefficient as deduced from HRV1 calibration.

	B1 (%)	B2 (%)	B3 (%)	B4 (%)
Measurement accuracy Method accuracy Atmospheric effects Snow effects	1 2 0,5 0,5	1 2 0,5 0,5	1 5 0,5 0,5	1 8 0,5 0,5
SPOT/MOS-1 intercalibration accuracy	2.3	2.3	5.1	8.1
SPOT coefficient accuracy	6	6	6	6
MESSR2 coefficient accuracy	6.4	6.4	7.9	10.1
MESSR1/MESSR2 intercalibration accuracy	5	5	5	5
MESSR1 coefficients accuracy	8.1	8.1	9.3	11.3

Table 5 : Absolute calibration coefficients error budget

5 - SPOT1 - LANDSAT5 INTERCALIBRATION

This intercomparison was done using ground truth over the French test site of LA CRAU (South-East of France).

In that case the calibration method has consisted in measuring the site reflectance and the atmospheric parameters during the satellite overpass, then apply a radiative transfer code named "5S" (Tanré et al, 1986) to derive the radiance of the site viewed by the tested camera. Radiometers adapted to SPOT spectral bands (Guyot, 1984) were used to determine the ground reflectance. The atmospheric parameters were evaluated by radio sounding data for water content, and tables were used for the Ozone content (London, 1976). The aerosol optical depth was deduced from Langley plots using a photometer developed by LOA (Laboratoire d'Optique Atmospherique, Lille France) taking into account a continental model according to LOA measurements.

Two campaigns were done during a common overpass (Sept. 30 and Oct.16, 1989). The results are displayed in table 6.

The last row in table 6 indicates TM/HRV1 intercalibration for the nominal analogic gains of SPOT (LANDSAT having no variable analogic gain), which is of better interest to compare similar images of the 2 instruments.

As simple models were used to determine

aerosol optical thickness, the obtained values of absolute calibration coefficients for the 2 satellites may be not very accurate, but the results of the intercomparison ($A_{k_{TM}} / A_{k_{SPOT}}$) are good.

The results show a good stability of the measurements (less than 2% variability).

The error budget for the intercalibration, where only differential errors between the 2 instruments are taken into account, is presented in Table 7. The overall accuracy is thus estimated to be 4.6%.

		XS1 or TM2	XS2 or TM3	XS3 or TM4
SPOT1 HRV1	09-30-1989	0.480	0.315	0.525
	10-16-1989	0.475	0.320	0.531
	mean	0.478	0.318	0.528
LANDSAT5 TM	09-30-1989	0.676	0.859	1.067
	10-16-1989	0.664	0.865	1.079
	mean	0.670	0.862	1.073
A_k TM / A_k HRV1		1.40	2.71	2.03
A_kTM / A_k G_{mk} HRV1		0.64	0.95	1.20

Table 6 : SPOT1 HRV1 and LANDSAT5 TM absolute calibration coefficient determined over LA CRAU French test site.

Mean radiometric image output estimate SPOT	2%
Mean radiometric image output estimate TM	2%
Atmospheric measurements: - water vapour - Ozone - Rayleigh - aerosols - environment effects	 0.5% 0.5% 0.2% 1% 0.5%
Ground reflectance measurements	2.5%
Solar irradiance (coupled with spectral bands uncertainties)	2%
Solar angles	1%
TOTAL (quadratic)	4.6%

Table 7 : SPOT-LANDSAT ERROR BUDGET

6 - SPOT1 - SPOT2 INTERCALIBRATION

The intercomparison between SPOT1 and SPOT2 was done by a ground truth campaign performed, during the SPOT2 in-flight assessment period, over the White Sands test site by the University of Arizona team conducted by P.N.Slater. These ground measurements were performed on February 6 and 7 (1990) when SPOT1 was overpassing the site, and on February 19 and 20 (1990) during a SPOT2 overpass. They allowed to determine the in flight values of A_k for SPOT2. This method was preferred to an extrapolation of the preflight calibration since sensitivity losses appear after launch and during the first days on orbit, certainly due to band filters outgassing (Dinguirard et al., 1988).

The HRV tested were for SPOT1 HRV2 in the Panchromatic mode and HRV1 in the multispectral mode while it was the reverse for SPOT2 (HRV1 in PA and HRV2 in XS).

The absolute calibration coefficients for the HRVs which have not been tested over White Sands were obtained by using common images taken, at the same time, over the same area by the 2 SPOT cameras. Several image couples recorded over various areas (snow fields, large cities or deserts) allowed, by histogram comparison, to estimate the relative sensitivity between HRV1 and HRV2 for SPOT1 and for SPOT2 (Dinguirard et al., 1988).

The results are given in table 8.

White Sands absolute measurements have an estimated accuracy of around 5 % (see table 9). This accuracy added to the HRV intercomparison one (around 2%) leads to an overall accuracy of ± 6% for the determination of the absolute calibration coefficients.

In parallel, in the same way as the intercomparison SPOT-MOS, common images have been taken the second and third days after SPOT2 launch, while SPOT2 was on a transitory orbit. This experiment is still under study and the results, when available, will be presented in a forthcoming paper.

		PA	XS1	XS2	XS3
SPOT1	HRV1	0.580	0.492	0.335	0.521
	HRV2	0.580	0.507	0.388	0.541
SPOT2	HRV1	0.488	0.517	0.424	0.754
	HRV2	0.595	0.573	0.420	0.739

Table 8 : Absolute calibration coefficients for SPOT1 and SPOT2.

Mean radiometric image output estimate	2%
Atmospheric measurements	3.7%
Reflectance measurements	2.5%
Solar irradiance	1.5%
Solar angles (including non lambertian effects)	1%
TOTAL (quadratic)	5.2%

Table 9 : White Sands measurement error budget

ACKNOWLEDGEMENTS

We wish to gratefully thank all the other persons who have worked on the various experiments:
B.Guenther, J.McLean and S.Guha from NASA GSFC and J.B.Bories from MATRA for the laboratory sources intercalibration.
K.Maeda and M.Shimada from EOC, NASDA for the SPOT-MOS comparison
R.Santer and E.Vermote from LOA (Lille France) and M. Verbrugghe from INRA (Avignon) for the SPOT-LANDSAT evaluation.
P.N.Slater, D.Gillman from the University of Arizona TUCSON, R.Jackson and S.Moran from ARS (USDA) PHOENIX and X.Briottet CERT/DERO for the SPOT1/SPOT2 experiments.

REFERENCES

Dinguirard M., Begni G., Leroy M., 1988. Analysis of the SPOT1 calibration after 2 years of flight. Proceedings SPIE 924. Recent advances in sensors, radiometry and data processing for remote sensing, ORLANDO.

Guyot G., Hanocq J.F; Buis J.P., Saint G. 1984. Mise au point d'un radiomètre de simulation de SPOT. C.R. 2ème Coll. Intl. Signatures Spectrales d'Objets en Télédétection, BORDEAUX 1983, Les colloques de l'INRA n°23:233-242.

Henry P., Begni G., 1989. MOSI absolute calibration using SPOT1 as an intermediate radiometer. Proceedings of the 3d symposium on MOSI verification program (MVP). Feb.1989 - II 348-359-NASDA

Leroy M., Henry P., Guenther B., Mc Lean J., 1990. Comparison of CNES spherical and NASA hemispherical large aperture integrating sources, to appears in Remote Sensing of the Environment.

London J., Bojkov R.J., Oltmans S., Kelley J.I., 1976. Atlas of the global distribution of total ozone July 1957-June 1967, NACAR Technical note n°113+STR

Slater P.N., Biggar S.F., Holm R.G., Jackson R.D., Mao Y., Moran S., Palmer J., Yuan B., 1987. Reflectance and radiance based methods for the in-flight absolute calibration of multispectral sensors. Remote Sensing of Environ., 22:11-37.

Tanré D., Deroo C., Herman M., Mororotie J., Perbos J., Deschamps P.Y., 1986. Simulation of Satellite Signal in the Solar Spectrum (5S) Proceedings of the 3rd symposium Signatures spectrales d'objets en télédétection held in Les Arcs, France, 16-20 December 1985, Ed. T.D. Guyenne, European Space Agency, ESA SP-247, March 1986, pp 315-319 (available from ESA, Division des Publications, ESTEC, Postbus 299, 2200 AG Noordwijk, The Netherlands).

Atmospheric effects on satellite imagery Correction algorithms for Ocean Color or Vegetation monitoring

E. Vermote, D. Tanre and M. Herman

Laboratoire d'Optique Atmosphérique, Université des Sciences et Techniques de Lille Flandres Artois Villeneuve d'Ascq, France

ABSTRACT

Earth Observation Satellite data generally have to be corrected from the atmospheric perturbation in order to provide measurements relevant to earth surface properties. A simple scheme is proposed that takes into account the perturbing atmosphere in simulations of the scattered sunlight as observed from a satellite. The scheme takes into account gaseous absorption, molecular and aerosols scattering, and illustrates the importance of the atmospheric perturbation in spaceborne observations. Then, by using this model, systematic corrections of satellite data are investigated. Two problems are considered: ocean color monitoring, in which case measurements at near infrared wavelengths may be used for estimating aerosols perturbation in the other channels, and earth surface observations for vegetative cover monitoring, in which case the satellite measurements are just corrected from the known molecular influence and from gaseous contamination, by using O_3 and H_2O climatologic estimates. Linear correction algorithms are developed and the accuracy of the derived products is examined; the errors in the retrieved ocean color are estimated as a function of viewing geometry, atmospheric turbidity, aerosols type, and wind velocity for the case of ocean observations.

INTRODUCTION

Satellite measurements are an important tool to survey the earth system. Whether or not one is interested in the atmosphere, one has to deal with its effects when using satellite data. In order to obtain measurements relevant to surface properties it's necessary to correct the reflectance at the top of the atmosphere, TOA reflectance, from atmospheric effects. This correction is necessary when looking to compare measurements performed at different time and/or at different places (monitoring of vegetative cover) or when looking for a quantitative estimate of parameters derived from spectral signature (eg the chlorophyll contents in ocean color problem). The problem of atmospheric correction is emphasized when using large field of view sensors, and in Ocean color monitoring when using short wavelength centered channels (eg 0.45µm).
This paper first describes very briefly the atmospheric effect modelling used in the radiative code 5S ("Simulation of Satellite Signal in the Solar Spectrum") developed by Tanre and al (Tanre 1986). This model allows us to estimate atmospheric effects and to elaborate correction strategy. Two operational correction methods are presented: ocean color, in which case measurement in the infrared (where water is "black") can be used to estimate the aerosol perturbations and retrieve water reflectance in the visible; land/vegetation observations, in which case there is no direct way to estimate and correct data from aerosol perturbation and where measurements are just corrected from the well known molecular influence and from gaseous absorption, using climatologic estimates of O_3 and H_2O integrated contents.

MODELLING

Within the signal observed in the solar spectrum by satellite sensors, the atmospheric and surface contributions are mixed. To retrieve surface reflectance, correction taking account gaseous absorption and molecule and aerosol scattering, has to be applied. Four gases absorb radiation in the solar spectrum (0.35µm to 2.2µm), O_2 and CO_2 which concentrations are stable in time and space, and O_3 and H_2O which concentrations are variable with time and space but can be estimated from climatologic data (London and al 1976, Tuller and al 1968). The influence of the molecules, or Rayleigh scattering, is well known and may be estimated accurately if ground pressure is known. The aerosol scattering properties vary according to the kind of aerosols, and of course with their abundance. The aerosol scattering parameters are variable in time and space and a climatology of these particles is not well established.
The modelling of atmospheric effects can be sum up by a very simple equation on which the 5S model is based. The reflectance at the top of the atmosphere, ρ^*, is given by :

$$\rho^* = Tg\left(\rho_a + T\frac{\rho_s}{1-\rho_s S}\right) \quad (1)$$

With:
Tg: The gaseous transmission on the double path within the atmosphere.
T: The total atmospheric transmission function on downward and upward path.
ρ_a: The intrinsic atmospheric reflectance observed at TOA when surface is "black".
S: The spherical albedo of the atmosphere (multiple surface-atmosphere interactions).
ρ_s: The surface reflectance.

CORRECTION SCHEME OVER LAND SURFACE

Principle

Figure 1 illustrates the expected atmospheric effects over vegetative cover. For a typical spectral signature of vegetative cover, we simulated ρ^*, for the four channels of $SPOT_4$-VGT (B_1 centered at 0.55µm, B_2 at 0.65µm, B_3 at 0.85µm and Mir, the Middle Infrared Channel, centered at 1.65µm), for a nadir viewing observation and for an edge of field of view observation. We also simulated the correction product, $\rho_{s+aerosols}$, i.e: the reflectance ρ^* corrected from gaseous absorption and molecular scattering.
Simulations are made for a moderate aerosol content corresponding to a visibility V=23Km. The major effects are the molecular scattering in the visible channels (B_1 and B_2), and the gaseous absorption in the infrared ones (mainly

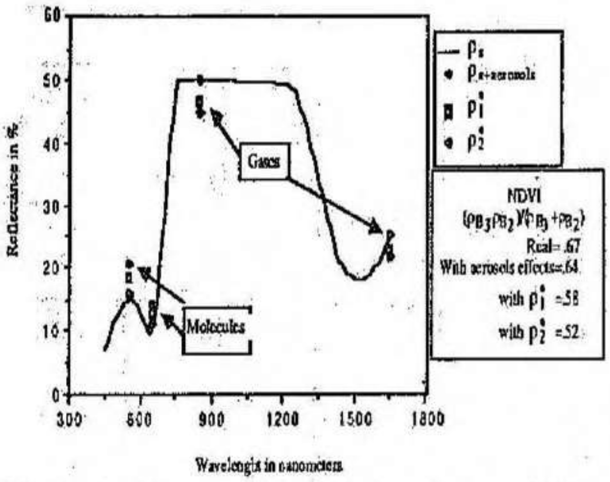

Figure 1: Atmospheric effects on vegetative cover Solar zenith angle 30°, principal plane, Continental Aerosols Visibility=23km, ρ_1^*: ρ^*(observed with θ_V=0°), ρ_2^*: ρ^*(observed with θ_V=60°).

H_2O in B_3). In this case, the perturbing effect of aerosols is not very high (compare ρ_s and $\rho_{s+aerosols}$) because their abundance is still reasonable for a horizontal visibility of about 23Km. Notice the large effect of the atmosphere on the vegetation index, NDVI, which is generally thought not to be atmospheric sensitive.

According to Figure 1, considering that the correction product $\rho_{s+aerosols}$ is generally near from ρ_s, we propose to just correct ρ^* from Rayleigh scattering and from gaseous absorption effects, that are known or may be derived from climatologic data. Of course, as a further step, the corrected data, $\rho_{s+aerosols}$ may be improved if some information about the aerosol content is available.

Formalism

Let us consider that measurements correspond to the "ideal" system presented figure 2a. The equivalent radiance observed by the satellite, L^*, (directly connected to observed digital count through calibration coefficient) is expressed by :

$$\rho^* = \frac{\pi L^*}{\mu_s E_s} \tag{2}$$

where E_s is the solar constant integrated over the spectral band and μ_s the cosine of the solar zenith angle.

Figure 2a

Figure 2b

The corrected reflectance $\rho_{s+aerosols}$, corresponds to the situation depicted in Fig 2b. Thus, assuming that the "aerosol plus ground" system is lambertian, according to eq (1), $\rho_{s+aerosols}$ is given by:

$$\rho^* = Tg_{CO_2} Tg_{O_2} Tg_{O_3} \left(\rho_R + T_R(\mu_s) \left[Tg_{H_2O} \frac{\rho_{s+aerosols}}{1 - S_R \rho_{s+aerosols}} \right] T_R(\mu_v) \right) \tag{3}$$

where the subscript $_R$ refers to molecular terms. The error budget developed in 3.d) shows that we can consider $1-S_R\rho_{s+aerosols} = 1$. Therefore, according to eqs (2) and (3), the corrected reflectance is a linear function of the observed radiance (or digital count), ie :

$$\rho_{s+aerosols} \cong AL^* + B \tag{4}$$

where A and B are given by :

$$A = \frac{\pi}{Tg_{H_2O} Tg_{CO_2} Tg_{O_2} Tg_{O_3} T_R(\mu_s) T_R(\mu_v) E_s \mu_s}$$

$$B = \frac{-\rho_R}{Tg_{H_2O} T_R(\mu_s) T_R(\mu_v)} \tag{5}$$

Operational Algorithm

Calculation of A and B The correction parameters, A and B, depend on quantities which exact computation is time consuming (gaseous transmission using Lowtran or 5S model) or insufficiently accurate (ρ_R with 5S). A special effort has been devoted on calculation of the ρ_R and Tg terms, looking for a compromise between accuracy and minimization of the computing time.

For each sensor (wavelength response) and for each absorbing component j (integrated content U_j), the gaseous transmission, $Tg_{i,j}$ have been calculated by using the semi-empirical expression:

$$Tg_{i,j} = \frac{1}{1 + a_{i,j}(U_j \times M)^{b_{i,j} + c_{i,j} \times Ln(U_j \times M)}} \tag{6}$$

where M is the total optical path ,that is

$$M = 1/\mu_s + 1/\mu_v \tag{7}$$

with μ_v the cosine of the view zenith angle

The parameters $a_{i,j}$, $b_{i,j}$, $c_{i,j}$ have been calculated by fitting the results of (6) to results given by 5S, by a least square criterion. The comparison of the two calculations is given on Figure (3) for the channel B_3 of $SPOT_1$ where the absorption effect is most important (water vapor).

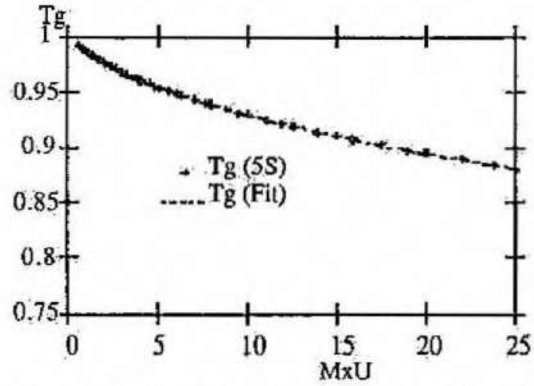

Figure 3: Comparison of gaseous transmission factor Tg_{H_2O} calculated by 5S and by formula (6) for B_3 channel.

	Temporal Interpolation		Spatial Interpolation		
	step in orbit number	Temporal Interpolation Error on A [‰]	Step in latitude	Step in Longitude	Spatial Interpolation Error on A [‰]
$A(B_1)$	80	0.78	1.5°	2°	1.37
$A(B_2)$	80	0.79	1.5°	2°	1.48
$A(B_3)$	80	0.76	1.5°	2°	1.25
A(Mir)	80	0.76	1.5°	2°	1.15
		Temporal Interpolation Error on B [10^{-3}]			Spatial Interpolation Error on B [10^{-3}]
$B(B_1)$	320	0.80	6.0°	2°	1.12
$B(B_2)$	480	1.00	9.0°	2°	1.00
$B(B_3)$	800	0.96	12°	4°	0.62

Table 1: Spatial and temporal resolution of interpolation grids, Interpolation Accuracy.

The ρ_R calculation is done by using a semi empirical formula based on the Chandrasekhar's X, Y functions (Chandrasekhar 1960). The computation time is very low, and comparison with accurate results derived from the Successive Order of Scattering method (Deuze 1989a) shows that the accuracy of the calculation is correct: The absolute accuracy on ρ_R is better than 5.10^{-4}.

The transmission term T_R is derived from the two stream method (Zdunkowski 1980), the resulting expression is:

$$T_R(\mu)=\frac{\left[e^{-\tau_R/\mu}\left(\frac{2}{3}-\mu\right)+\left(\frac{2}{3}+\mu\right)\right]}{\left(\frac{4}{3}+\tau_R\right)} \qquad (8)$$

The absolute accuracy is better than 10^{-3}.

Use of Interpolation methods In order to accelerate the correction process, the correction parameters are not computed for each pixel of the image. They are interpolated in time and space from a set of pre calculated grids of the A and B parameters. A specific study developed for $SPOT_4$ (Vermote 1990) shows that errors $\Delta B < 1.10^{-3}$ and $\Delta A/A < 1\%$ may be obtained by using interpolation grids corresponding to a data storage of 25 Megabytes, sufficient for one year of correction without recalculation, for the four channels of $SPOT_4$-VGT. To have a more precise idea about this work, Table 1 indicates the resolution in space (number of degree of latitude and longitude between two points of one interpolation grid) and in time (number of orbits between two interpolation grids) adopted for each $SPOT_4$ channel.

Error Budget Any data processing algorithm must be associated with a drastic error budget. The correction scheme [ie: basic eq. (3), using analytical formulations for ρ_R (Chandrasekhar 1960), T_R eq. (8), and Tg eq. (6)] is intended to be run for an assumed barometric pressure P_S=1020mbar, ground altitude z=0, and for climatologic values of the ozone and water vapor contents. Errors are induced at all levels, from the basic eq (3) to the interpolation process; we must also consider the uncertainties on parameters given by climatologic tables (U_{H2O}, U_{O3}, P_s). Then we can distinguish three classes of error sources:

(i) modelling errors
that are due to the use of the approximate eqs (6) and (8), approximate formulation of ρ_R, and basic eq (3) (because the aerosols+surface system is non lambertian); and to uncertainties on basic constants (ie; molecular anisotropy factor, spectroscopic constants in gaseous absorption).

(ii) differences between the assumed and the encountered atmospheric parameters P_s, U_{O_3}, U_{H_2O}.

(iii) systematic errors, due to the interpolation scheme.

The errors depend generally on the viewing geometry and on the ground reflectance. To evaluate these errors, the TOA reflectance, ρ^*, and the "ideal" reflectance $\rho_{s+aerosols}$ to be retrieved were calculated, by the accurate Successive Order of Scattering code, for different viewing conditions (nadir and edge of field of view), different seasons and different aerosol contents, by varying the error source terms successively within the expected range of variation (ie:±10% for spectroscopic data, ±20mb for P_s, ...). The correction algorithm was applied to ρ^* and the result was compared with the ideal $\rho_{s+aerosols}$ value. Moreover, we choose to evaluate algorithm performance in the same way that the $SPOT_4$ instrument performance are analyzed, because it's the most simple way to evaluate the quality of the final product (by adding Instrument and Algorithm noises) and because we think it's the more complete way to describe the quality of a image like product. The variation of the induced error is then

Table 2

	Low frequency biases 10km à 2000km	Temporal biases	Constant biases
Modelling	Uncertainties on Spectroscopic data (Tg 5S) Tg Formula (eq. 6) Uncertainty on δ_R (molecules depolarization Factor) ρR Formula (Chandrasekhar) *Separating molecules and aerosols* (eq. 3)	Uncertainties on Spectroscopic data Tg Formula (eq. 6) Uncertainty on δ_R ρR Formula (Chandrasekhar) Separating molecules and aerosols (eq. 3) Lack of topographic data	*Uncertainties on Spectroscopic data* Tg Formula (eq. 6) Uncertainty on δ_R ρR Formula (Chandrasekhar) Separating molecules and aerosols (eq. 3) *Uncertainty on* θ_s (computation method) Lack of topographic data
Variability of Atmospheric Parameters	Integrated contents in H_2O, O_3 Ground pressure P_s	Integrated contents in H_2O, O_3 Ground pressure P_s Solar Constant intrinsic variability E_s	
Interpolation Methods	Spatial Interpolation	Temporal Interpolation	

Table 3
Atmospheric correction Induced biases
(1) Modelling, (2) Atmospheric parameters Variability, (3) Interpolation

Channel	$\rho_{s+aerosols}$ $(x10^{-2})$	*Low Frequency biases* $(x10^{-3})$				*Temporal biases* $(x10^{-3})$				*Constant biases* $(x10^{-3})$	*Total error* $(x10^{-3})$
		(1)	*(2)*	*(3)*	*Tot*	*(1)*	*(2)*	*(3)*	*Tot.*		
B_1	15	4,6	3,4	0,8	5,8	14,2	5,9	0,9	15,4	2,8	16,7
B_2	10	2,3	2,2	0,7	3,3	7,3	3,9	1,1	8,3	1,1	9
B_3	50	1,1	9,5	0,7	9,6	4,2	16,5	1,3	17,1	4,8	20,2
Mir	25	0,1	3,1	0,7	3,2	1,3	5,4	1,2	5,7	0,5	6,6

FIGURE 4

Atmospheric Correction Error Budget

SATELLITTE :	SPOT4
INSTRUMENT:	VGT
CHANNEL :	B_1 (Vegetation)

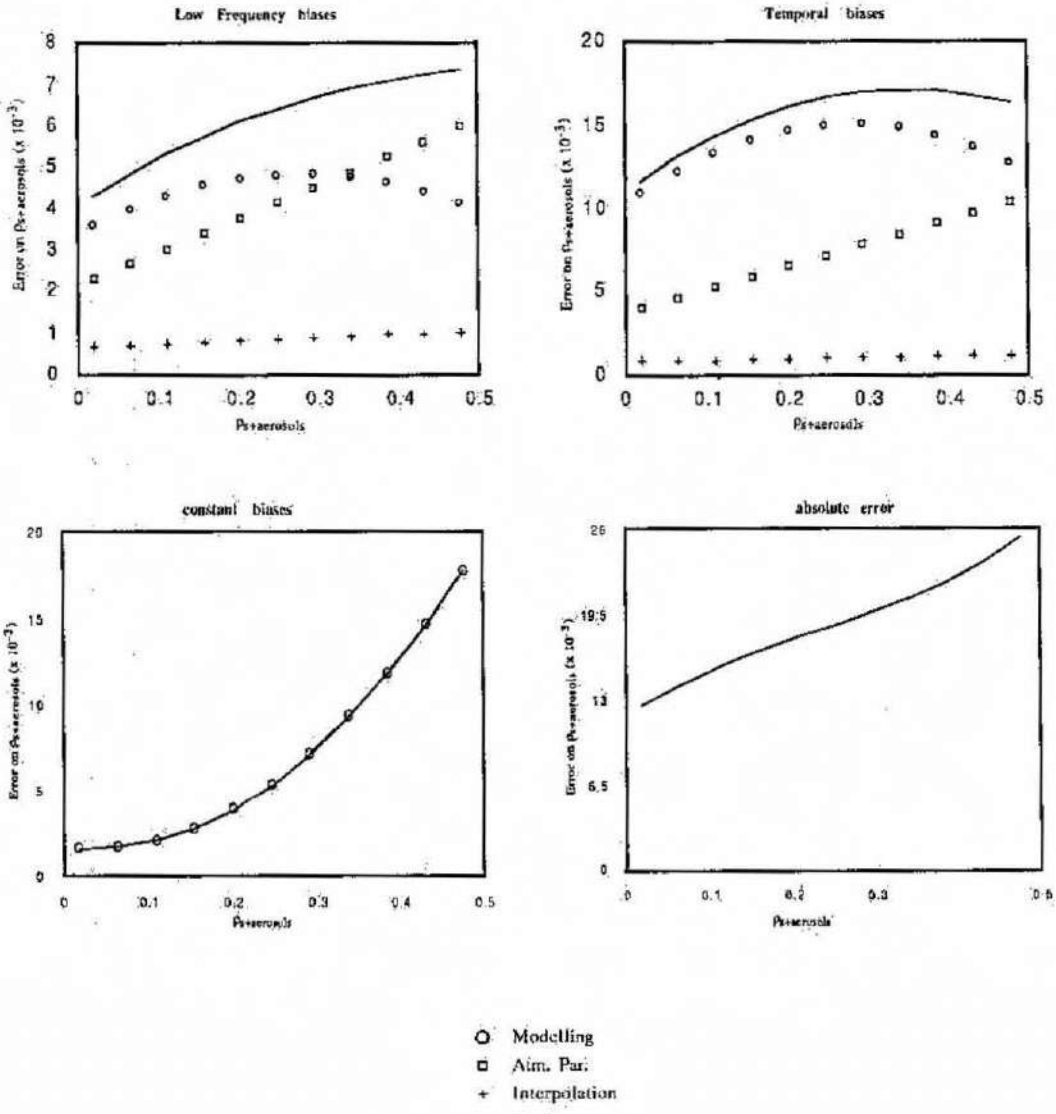

analyzed in term of temporal biases (temporal variation of the error), low frequency biases (variation of the error in the field of view) and the non variable part of the error is identified as constant biases. For each class of error, the relevant error sources where identified according to Table 2, and the total error was then calculated by adding in quadratic all independent biases. The error budget is just presented in its complete form for B_1 (Figure 4), we give in Table 3 the induced biases for all channels at the level of reflectance corresponding to the typical vegetative cover spectral signature presented in figure 1.

Conclusion

The error budget shows that the correction is rather good within the range of typical land observed reflectances, the upper limit of visibility we have taken is 23Km. Constant biases are relatively low. The low frequency biases and the temporal biases induced by the interpolation method are negligible. The most important biases result from the variability of atmospheric parameters and from the signal modelling (assuming ρ_s+aerosols is lambertian eq (3)).
An improved correction scheme would need more accurate H_2O and O_3 integrated contents and some information about the aerosols, but in this case the correction method would be more time consuming and more difficult to reverse.
The main interest of such a reversible method without external data is to provide a easy way to compare satellite data; moreover, the corrected products in most cases are very close from the true surface reflectances.

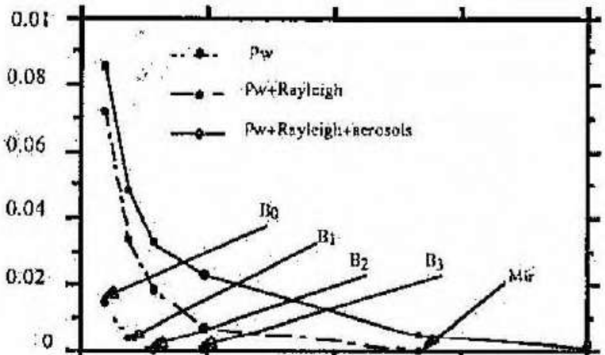

Figure 5: Decomposition of ρ^* for Ocean observations (without glitter and corrected from gaseous absorption).

OCEAN COLOR ATMOSPHERIC CORRECTION ALGORITHM

Principle

The influence of the atmosphere in the case of sea observations is illustrated by figure 5. For the $SPOT_4$-VGT Ocean mission, compared to the vegetation mission, one channel centered at 0.45µm (B_0) is added in order to evaluate the water turbidity. This channel is largely contaminated by Rayleigh Scattering which effect varies as λ^{-4}. The spectral dependance of aerosols can vary from λ^{-1} (Continental model) to λ^0 (Maritime model). Clearly, the retrieval of ρ_w is very sensitive to the modelling accuracy because ρ_w is only a minor part of the signal ρ^*. But for Ocean observations, ρ_w is null in B_3 and Mir, so that the reflectances in these channels, when corrected of the Rayleigh contribution, provide information about the aerosol influence. Then, these estimated influences in B_3 and Mir can be extrapolated in the visible channels (B_0, B_1, B_2) in order to correct ρ^* from all atmospheric effects and therefore to retrieve ρ_w.
In fact, the retrieval process is not so simple, particularly because of the sunglint (Gordon 1987) which is due to surface specular reflection on the agitated ocean. Although these results are not presented, simulations performed with different wind speeds show that, in a restricted "zone" located around the specular reflection geometry, the algorithm error prohibits correct retrieval of ρ_w.

Formalism

The correction strategy is done in three steps.

-Firstly, the observed reflectances in the five channels of the $SPOT_4$ Ocean color mission are corrected from gaseous transmission, Rayleigh scattering and glitter (The glitter contribution, ρ_G, is calculated for the case of a pure molecular atmosphere and for a wind speed of 10m/sec), according to:

$$\rho' = AL^* + B \tag{9}$$

with

$$A = \frac{\pi}{Tg_{H_2O}Tg_{CO_2}Tg_{O_2}Tg_{O_3}E_s\mu_s}$$

$$B = \frac{-\rho_R - \rho_G}{Tg_{H_2O}} \tag{10}$$

-Then, we estimate the aerosol reflectance in the visible channel, ρ^{vis}_a, from the corrected data ρ'_{Mir} and ρ'_{B_3}. Assuming that ρ^{vis}_a varies according to a λ^{-n} law we get:

$$\rho^{aerosols}_{vis} = \rho'_{B_3} \times \left(\frac{\lambda^{vis}}{\lambda^{B_3}}\right)^{-n} \tag{11}$$

where n is given by :

$$n = \mathrm{Log}\left(\frac{\rho'_{B_3}}{\rho'_{Mir}}\right) \Big/ \mathrm{Log}\left(\frac{\lambda_{Mir}}{\lambda_{B_3}}\right) \tag{12}$$

-Finally, we correct ρ'_{vis} from ρ^{vis}_a and from molecular transmission functions (aerosol transmission is put equal to 1) to get the estimated water reflectance ρ^{est}_w, by :

Figure 5a
$SPOT_4$ Case
Absolute error on retrieved ρ_w
Maritime aerosols
Correction Wavelength at $0.85\mu m$ and $1.65\mu m$

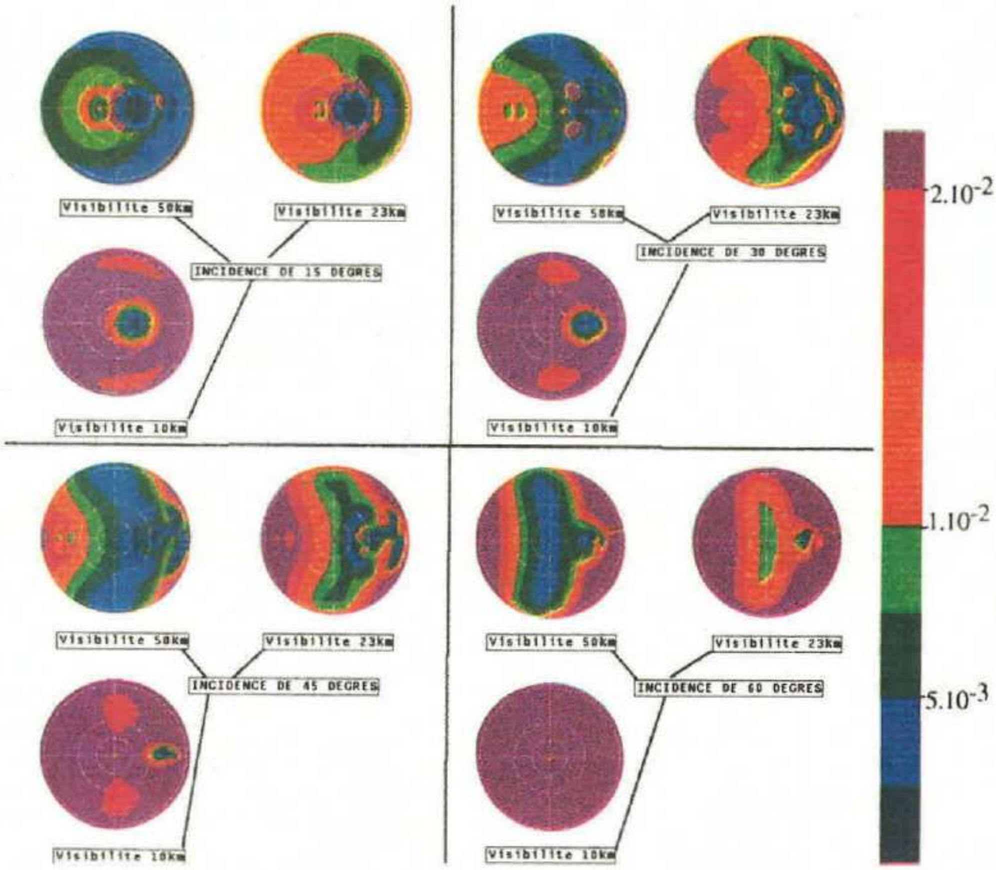

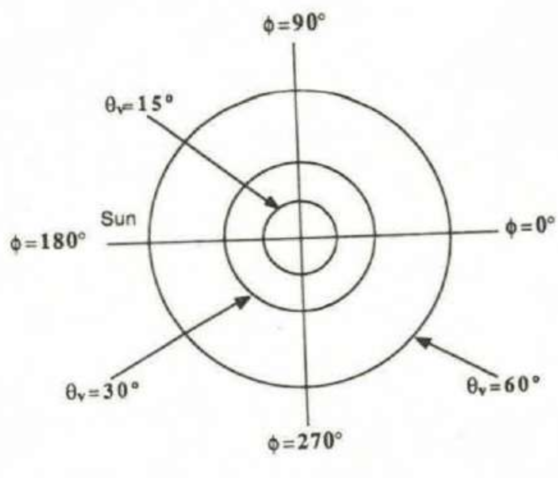

Figure 5b
MODIS Case
Absolute error on retrieved ρ_w
Maritime aerosols
Correction Wavelength at $0.75\mu m$ and $0.85\mu m$

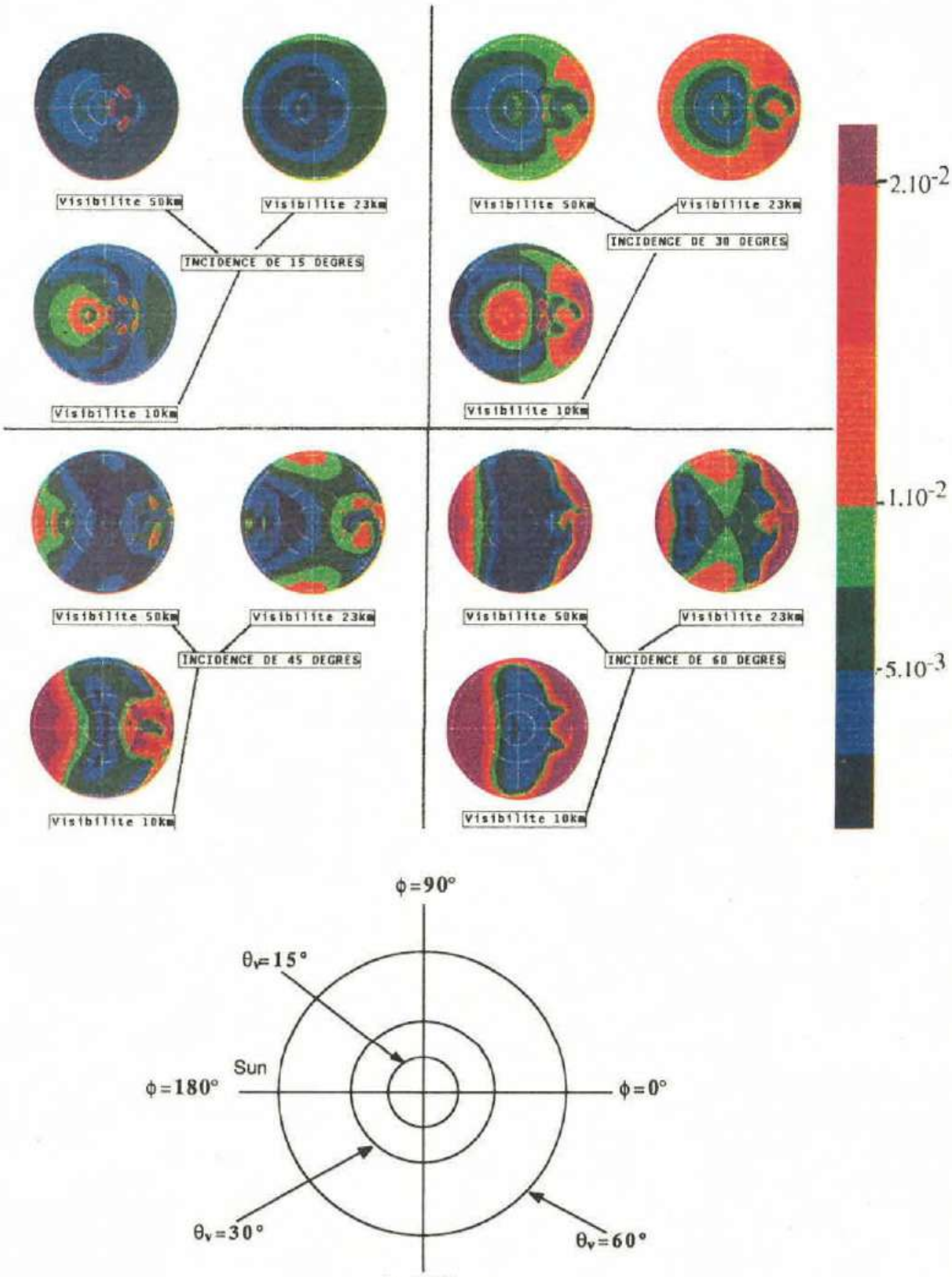

$$\rho_w^{est} = C\left(\rho'_{vis} - \rho_{vis}^{aerosols}\right)$$
with
$$C = 1/(T_R(\mu_s)T_R(\mu_v)) \qquad (13)$$

Simulation and analysis

By using the radiative code developed by Deuze and al (Deuze 1989a), ρ^* was simulated for the five channels of $SPOT_4$. Calculations were performed for different wind speeds, different water reflectance different aerosol types and abundances (Visibility of 50,23,10 Km), for four solar zenith angles (15°,30°,45°,60°), for view zenith angle varying from nadir to edge of field and for all azimuthal configurations. The previous correction algorithm was applied on this set of data, and we plotted on color polar graphs the maximum of the absolute resulting error on ρ_w. The results are presented for the case of maritime aerosols on Figure 5a, in the case of B_0 (where correction is hardest to perform, see figure 5), assuming that the wind speed is known. The results show that the error increases when the solar zenith angle and the view zenith angle are increasing. The error on ρ_w also increases with aerosol abundance and, for visibilities smaller than 23km, it becomes very difficult to get significant result. The interesting point is that the best results are obtained for viewing azimuths perpendicular to the sun incident plane. For continental aerosol model, the results (not presented here) are worst, due to the fact that the λ^{-n} behavior is not a good approximation for this kind of particles, within the 0.45µm to 1.65µm range. Therefore, we studied the correction algorithm results, by assuming that one 0.75µm centered channel was available (as it will be on the MODIS instrument) instead of the 1.65µm centered one which was primary devoted on $SPOT_4$ to the study of mineral resources. The results are given on figure 5b. The absolute error is divided by a factor 2 to 3 and the same performances are now obtained with Continental aerosols, in which case results are still acceptable up to visibility of 10km and incidence zenith angle of 45°.

DISCUSSION

Over land surfaces, the proposed correction algorithm allows to define a standard a comparison for satellite data. The correction removes the greatest part of atmospheric effects. The obtained product, $\rho_{s+aerosols}$, is in most cases very close from the true surface reflectance, and is improvable provided that data on aerosols are available. This standard can be computed by an operational, linear and reversible algorithm, which is associated with a detailed error budget. This method is now applied at the CISI (Brest) to correct a large set of AVHRR visible channel data.
Over the Ocean, we defined a operational correction scheme and the simulation allows us to evaluate and compare the performances for two different instruments $SPOT_4$ and MODIS.

To conclude, let us focus on the limit of atmospheric corrections. As shown previously the major problem is probably the estimate of the aerosol effect. Better aerosol estimates are needed in the studies of Ocean color where more detailed characterization of the aerosols should allow a better determination of ρ_w. But these estimates are especially needed in land surfaces observations, where direct information about the aerosol is lacking. In this case, promising methods are presently investigated, that are based on examination of the contrast degradation in satellite imagery (Tanre 1987, Kergomard 1989). These methods, however need high resolution sensor data so that their application at a global scale may be difficult. Polarization measurements may offer another possibility, that is now investigated with POLDER (Polarization and Directionnal Reflectance). This instrument, which a prototype has been developed at LOA, is intended to measure polarization and directionality of the Earth outgoing radiation. Because the polarized light reflected by vegetative covers does not depend on the wavelength (Vanderbilt 1985, Rondeaux 1990), polarization measurements could provide the required aerosol information over land surface. Over the Ocean, the characterization of aerosols by polarization (Deuze 1989b) and directionality is expected to allow a retrieval of ρ_w reducing absolute error by a factor 4 to 5 compared with the "classic" means.

ACKNOWLEDGEMENTS

This work was suported by the Centre National d'Etudes Spatiales (CNES) under contract number S4/NT/001/729/CN. We wish to gratefully thank M. Leroy, the CNES responsible of this study. The color polar graphs have been performed by using SPHINX (Satellite Process Handling Images uNder Xwindows) developed at the Laboratory by L. Gonzalez and C. Deroo.

REFERENCES

Chandrasekhar (1960). A Treatise on Radiative transfert. Ed. by D. Van Norstrand Company Inc., Princetown, New Jersey, U.S.A

Deuze J.L., Herman M. et Santer R. (1989a). Fourier Series Expansion of the transfert equation in the atmosphere ocean system. Journal of Quantitative Spectroscopy and Radiative Transfert, Vol 41, No. 6, 483-494

Deuze J.L, Devaux C., Herman M., Santer R., Balois J.Y, Gonzalez L., Lecomte P., Verwaerde C. (1989b). Photopolarimetric observations of aerosols and clouds from balloon. Remote Sensing of Environement., 29, 93-109

Gordon H.R and Castano D.J (1987). Coastal Zone Color Scanner atmospheric correction algorithm: multiple scaterring effects. Applied Optics, Vol 26., No. 11., p. 2111-2122

Kergomard C., Tanre D. (1989). On the retrieval of Aerosol Optical thickness over Polar Regions. Geophysical Research Letters, 16, 7, 707-710

London J., Bojkov R.D., Oltmans S. and Kelley J.I. (1976). Atlas Of the Global Distribution of total Ozone .July 1957-June 1967.
Ncar Technical Note, Ncar/tn/113+str,pp276

Rondeaux G. (1990). Polarisation de la lumiere reflechie par un couvert vegetal. These de Doctorat de l'Universite de Paris VII

Tanré D., Deroo C., Duhaut P., H M., Morcrette J.J., Perbo J. et Deschamps P.Y. (1986). Simulation of the Satellite Signal in the Solar Spectrum. User's guide, L.O.A. Lille.

Tanre D., P.Y. Deschamps , P. Duhaut, and M. Herman (1987). Adjacency Effect Produced by the Atmospheric Scaterring in Thematic Mapper Data. J. Geophys. Res., 92, 12000-12006

Tuller S.E. (1968). World distribution of mean monthly and annual precipitable water vapor. Monthly weather Review, 96, pp785-797.

Vermote E., Tanre D. et Herman M. (1990). Corrections atmosphériques applicables aux images Vegetation. CNES Internal Report: S4-NT-0B1-729-CN

Vanderbilt V.C., Grant L., Biehl L.,Robinson B.F. (1985)., Specular, diffuse and polarized light scattered by two wheat canopies. Applied Optics 24,2408-2418.

Zdunkowski W.G, Welch R.M, Korb G. (1980). An Investigation of the Structure of Typical Two-Stream for the Calculation of Solar Fluxes and Heating Rates in Clouds. Beitr. Phys. Atmosph., 53, no 2,p. 147-166

Microwave Remote Sensing Systems

NEW DEVELOPMENTS IN A FOREST PENETRATING RADAR

K.F. Link
Intera Kenting
Ottawa, Canada

R. Westby
F.P. Radars
Ottawa, Canada

P. Franco
Argus Aerolevantamentos S.A.
Rio de Janeiro, Brazil

ABSTRACT

Recent enhancements to the FPRII (Forest Penetrating Radar) promise to make the system an excellent tool for topographic mapping in dense tropical forests. Changes in the processing circuits now allow the system to be operated at higher altitudes where it is less affected by turbulence and yet maintain a high degree of accuracy. The "S" band radar's beam width is significantly reduced through unique circuit design producing a narrow footprint on the ground. This has allowed the system to utilize a smaller antenna. Sophisticated navigational and positioning systems including INS and continuous kinematic GPS allow the system errors to be minimized through post-flight computer processing.

Some of these design enhancements have been implemented and tested with encouraging results. The remaining positional correction is currently being implemented with tests over tropical jungles planned for this year. This test will compare maps produced from the radar with those developed from a detailed ground survey.

1.0 INTRODUCTION

Mapping systems involving the use of sensors other than photographic cameras are appealing in tropical areas with dense forest cover. Photographic sensors which operate in the visible portion of the spectrum are hampered by the natural elements (clouds, smoke, haze) and the inability to see beyond the tree tops. Research efforts have progressed over a number of years with an increasing degree of success. As the accuracy of the sensor information improves, it becomes critical to know the precise conditions affecting the data collection process. In the case of an airborne sensor, this refers to the attitude of the platform (roll, pitch, yaw) and the exact position to a high precision.

Systems such as radar altimeters have produced encouraging results due to their high sensitivity and operation at microwave frequencies. However, they have been limited by the need to fly relatively low where there is an increased likelihood of turbulence and only having a coarse knowledge of the aircraft position. In other words, the radar systems have been relatively accurate but the processing and recording information have limited their overall success.

The FPR2 system was developed to be part of an airborne topographic mapping system capable of making detailed maps of the ground beneath a dense forest canopy. The incorporation of state-of-the-art positional recording systems have eliminated many of the limitations mentioned earlier and promises to provide an operational tool for topographic mapping.

2.0 RADAR SYSTEM DESCRIPTION

The radar provides two recorded outputs on a strip-chart recorder. One output is the distance from the aircraft to the ground under the forest and the other is the distance from the aircraft to the forest canopy, along the flight path of the aircraft. After successfully testing the system over a tropical forest where the annual rain fall exceeds 3500 millimetres, it was evident that the radar, with the addition of ancillary equipment, could be a valuable instrument as an aid in topographic mapping the ground under tropical rain forests. A sample of the output obtained is shown in Figure 1.

2.1 Radar

The radar transmits a 0.7 microsecond pulse with a peak power of 2.5 kilowatts at a frequency of 3 gigahertz. This pulse duration is measured at the 10% level and the shape is shown in Figure 2.

At a frequency of 3 GHz more energy will be reflected, at times from the ground and at times more energy will be reflected by the foliage. The pulses from the ground and those from the forest canopy will be separated and coupled to a strip-chart recorder. Any intermediate pulses will be rejected. Some pulses, because of varying phases in the reflected energy, will be narrower than normal and will also be rejected.

2.2 Antenna

Operating at a higher frequency than 3 GHz allows the antenna to be smaller; however, but reduce foliage penetration. A lower frequency would call for an impractically large antenna. The 3 GHz frequency is a good compromise.

The antenna has a stepped parabolic reflector 112 centimetres in diameter, 9 centimetres in depth and a double dipole waveguide feed. The one way half power beam width is 6 degrees. The antenna pattern is shown in Figure 3. The antenna pattern from the 3 db points to the peak has been redrawn on a linear scale in Figure 4 to make it easier to understand the artificial narrowing described later.

2.3 Receiver

The receiver consists of a radio frequency amplifier, a crystal video (square law) detector and a video amplifier that employs a pulse by pulse automatic gain control. A curve of a typical crystal detector is drawn in Figure 5. Since the peak of the return pulse will be from the ground under the trees, from the forest canopy, or from somewhere in between, the action of the crystal detector will favour the peak of the received pulse.

The transmitter, modulator and duplexer are common components in many radar systems (see Figure 6). The output of the crystal detector, is coupled to the amplifier and pulse by pulse automatic gain control circuit. The action of the pulse by pulse automatic gain control can be seen in Figure 7. The gain has been adjusted so that only the peak of the receiver pulse exceeds the base line. The base line is then restored leaving only the peak of the received pulse. This peak is further amplified and coupled to a threshold triggered voltage comparator. Its output are square pulses leading and trailing edges determined by the peak of the pulse.

Many pulses, having varying amplitudes, were used to produce the photograph of the action of the pulse by pulse automatic gain control in Figure 7. The time of arrival of the peak can be obtained by measuring the time of arrival of both the leading edge and trailing edge and averaging the voltages.

The effective antenna pattern is narrowed since the energy transmitted at the centre of the antenna pattern is higher than the sides of the pattern, and the receiver circuit allows only the peak of the reflected energy to be present at the output.

3.0 INTERNAL SYSTEM PROCESSING

A sample of the transmitted pulse is a sync pulse for the timing circuit. The sync pulse is coupled through the calibrate and range circuit to the ramp voltage generator. The time of the linear voltage change is long enough to be several thousand feet in radar time -- the time for a pulse of energy to travel to the ground and return to the aircraft.

The ramp voltage generator is coupled to sample and hold circuits (1) and (2). The linearly changing voltage from the ramp voltage generator will be sampled then held. Voltage (1) is generated by the time of arrival of the leading edge of the peak and voltage (2) by the trailing edge of the received pulse.

The trailing edge of trigger circuit (2) activates trigger circuit (3) which generates a 20 microsecond sample period for sample and hold (3). The voltage that is equivalent to the time of arrival of the peak of the return pulse is now available at the output of sample and hold (3). Because of varying phases in the return signal, there will be times when the peak of the received pulse could be narrower than expected. A pulse length filter measures the duration of each pulse from Schmitt trigger and enables trigger circuit (3) only when the pulse duration exceeds a selected threshold.

The sync pulse derived from the sampler is coupled to a counter (min 10, max 100). To date, no forest has been encountered that requires a count higher than 100. The number selected is the number of return pulses to be examined by the peak detector circuits.

The voltage at the output of sample and hold circuit (3) is changing with each acceptable return pulse. One output of the peak detector circuit is the voltage that represents the shortest distance from the aircraft - the forest canopy. The other output is the voltage that represents the furthest distance from the aircraft - the ground. Immediately after the sample and hold circuit is switched back to the hold mode, the peak detector circuits are reset to be able to examine the next group of voltages from sample and hold circuit (3). The output from sample and hold (4) is the tree canopy and the output of sample and hold (5) is the ground under the forest.

These outputs are displayed on a two pen strip chart recorder. Two event markers are available to correlate other sensing devices such as photography and positioning with the recorded output of the radar. An output from the strip-chart for an analog to digital converter is also available.

A calibrate and range circuit has been built into the radar which provides a means of calibrating the output of the radar. The range of the radar can be switched in either 500 foot steps or 1000 foot steps. The full scale range of the strip-chart recorder is 1000 feet when the range circuit is switched in 500 foot steps and the full scale range of the strip-chart recorder is 2000 feet when the range circuit is switched in 1000 foot steps.

4.0 POSITION MEASURING EQUIPMENT

A number of new devices are presently being incorporated to enhance the overall accuracy of the system.

4.1 Global Positioning System (GPS)

GPS satellites have greatly increased the potential of surveying instruments and fairly common in airborne surveys. By simultaneously receiving the signals from several of the satellites and through triangulation calculations, it is possible to determine the position of the receiver to within 5 - 10 metres in X, Y and Z relatively easily. Receivers can be obtained from a variety of manufacturers which are suitable for airborne installations and provide digital outputs for recording.
Knowing the position of the aircraft to 5 - 10 metres in X and Y is a major improvement and adequate for many survey applications. However, the radar profiling system is trying to achieve accuracies of 2 - 3 metres and cannot tolerate the 5 - 10 metre error in the vertical Z component. Through the use of more elaborate recording and processing systems, it is possible to improve the aircraft positional accuracy to less than one metre. Continuous kinematic recording of the GPS signal records the phase of the carrier wave and through subsequent post-processing allows the radar antenna position to be computed.

Operation requires installation of antenna on the aircraft and calibration. Flights must occur during a GPS window when at least four and preferably five satellites are above the horizon. Four satellites should remain in continuous contact with the receiving antenna at all times. Loss of one of the signals may mean the loss of the critical Z component and negate the missions' data collection accuracy. The aircraft should return to the exact same position as it began the mission to close the loop.

This procedure is significantly more complex to operate and time consuming to process and correlate with the radar signal, however, it represents a major improvement in accuracy, eliminates the need for tracking cameras, and is consistent with the accuracy of the radar signal itself.

4.2 Attitude Sensor

The radar system effectively produces a narrow beam through the circuitry described above. When the aircraft is on a mission, it is regularly buffeted by winds which cause the radar footprint to vary from the desired nadir position. This mistracking can be a source of error, particularly in rugged terrain, unless a compensation procedure is incorporated.

Several methods exist which can minimize the effect on the position of the radar profile. These range from installing a gyroscopically steered antenna to discarding the signals outside of a set threshold.

For the upcoming tests we will be incorporating an inertial navigation system (INS) capable of digitally tracking the aircraft motion and discarding measurements taken during excessive turbulence. All data sets will be recorded on magnetic tape for subsequent processing and correlation.

5.0 SUMMARY

The FPR2 radar altimeter provides a recording of the distance between the aircraft and the tree canopy and simultaneously the distance from the aircraft to the ground under the forest. The recorded outputs are the forest and the ground along the flight path of the aircraft. Through the addition of state-of-the-art position measuring and recording instruments, like GPS and INS, the FPR2 is a comprehensive system for developing a ground profile through dense tropical forests. The specifications for the FPR2 are given below.

6.0 SYSTEM SPECIFICATIONS

Transmitter

Frequency - 3.0 GHz., Peak Power - 2.5 KWs., Pulse Duration - 0.7 usecs., Pulse Repetition Rate - 2000 Hz.

Antenna

Stepped Parabolic Reflector with double dipole feed, Half Power Beam Width - 6° conical, Diameter - 119 cms, Reflector Depth - 9 cms., Feed extends 34.5 cms below reflector.

RMS Error

Ground - 3 metres. Forest canopy - 6 metres.

Operating Range
300 metres to 3000 metres above the ground.

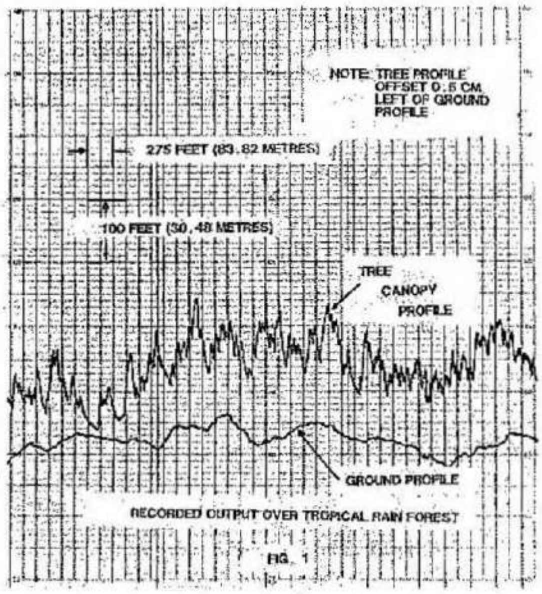

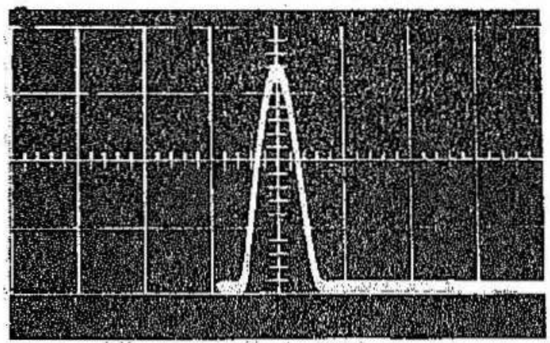

TRANSMITTED PULSE
FIG. 2

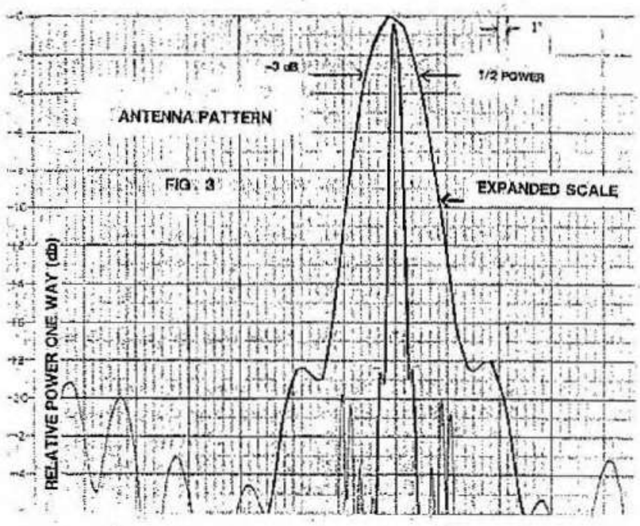

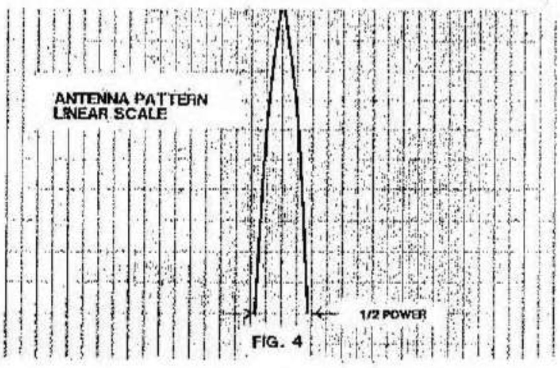

FIG. 4

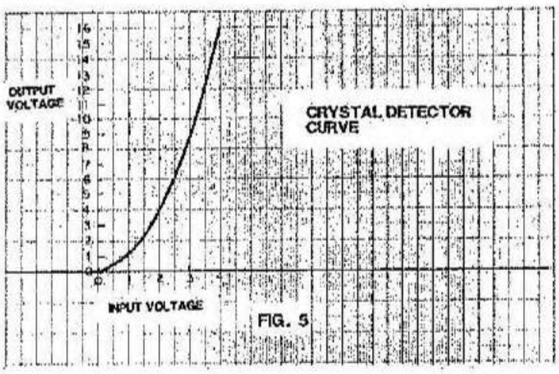

FIG. 5

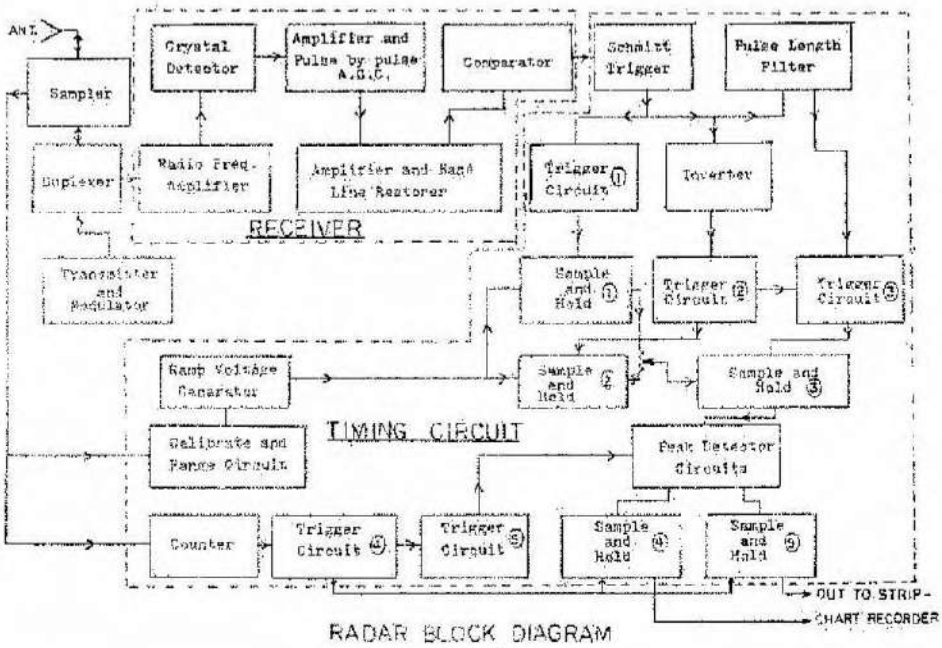

RADAR BLOCK DIAGRAM
FIG.6

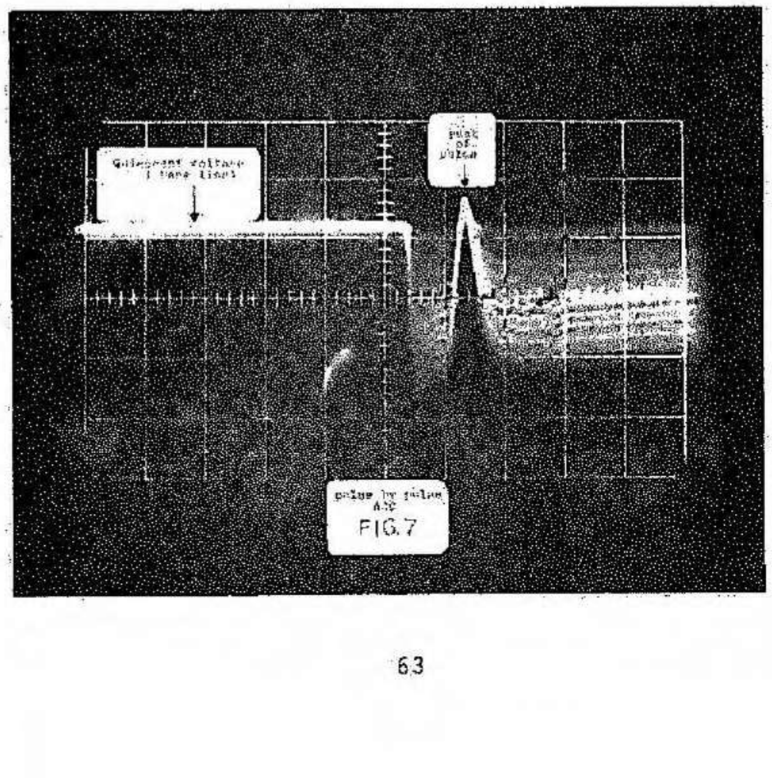

FIG.7

SYSTEM CONCEPTS FOR HIGH-RESOLUTION LAND AND ICE TOPOGRAPHIC MAPPING ALTIMETERS

Eastwood Im

Jet Propulsion Laboratory
California Institute of Technology
Pasadena, California 91109
U.S.A.

ABSTRACT

Global, high-resolution topography data set of land and ice regions on earth is of importance in a variety of geoscientific applications. In this paper two potential spaceborne radar instrument approaches, the scanning SAR altimeter and the interferometric SAR altimeter, for acquiring such data set are presented. The relative merits of and some technical issues associated with these two system approaches are discussed.

Key words : Topography, altimeter, resolution, SSARA, ISARA.

INTRODUCTION

Global land and ice topographic information is vital for earth system sciences, with applications in geology, geophysics, ecology, soil science, hydrology, botany, and glaciology. An overview on these applications can be found in the NASA Topographic Science Working Group Report (Topographic Science Working Group, 1988). Existing topographic data are available in the forms of contour maps and digital data, with digital data being digitized from existing maps. Figure 1 shows the existing topographic data in these two formats. It is clear from this figure that coverage is the major problem associated with the existing database, particularly in Africa, Asia, and South America. Other shortcomings are the uneven spatial scales and accuracies among different existing data sets. These shortcomings have reduced significantly the usability of such data sets for large-scale science studies.

With the limitations on the existing database, it is clear that a set of global, uniformly sampled, high resolution land/ice topographic data is needed, and that the space-based instrumentation is the only cost-effective means of acquiring such data set. Recently published report (1988) has indicated that such data set must possess spatial resolutions between 30 m to 100 m and height accuracies better than 10 m in order to provide useful information for most of the science applications.

Spaceborne radar altimeter is one of the promising instrument approaches for generating such global, high-resolution topographic map. Unlike the optical techniques (both stereophotography and laser altimetry), radar measurements are less susceptible to cloud covers and other weather conditions. In addition, radar's relatively fast pulse transmission rate and large swath coverage make it more attractive than the laser altimeters for acquiring spatially continuous data in a reasonable time period, and the altimetric processing time of the radar data is considerably less than that required for stereoscopic data. In this paper, two radar system approaches, the Scanning Synthetic Aperture Radar Altimeter (SSARA) and the Interferometric Synthetic Aperture Radar Altimeter (ISARA), that can meet the science requirements, will be presented. The relative merits and the technical issues associated with these two approaches will also be discussed.

SAR ALTIMETRY - GENERAL CONCEPT

A radar altimeter transmits short pulses and measure the round-trip propagation time of these pulses as they are reflected from the surface and detected by the radar receiver. With the accurate knowledge on the propagation time, the radar pointing, and the orbital altitude, the surface elevation can be reconstructed according to:

$$h = H - \rho \cos \theta \qquad (1)$$

where h is the surface elevation, H is the orbit height, ρ is the one-way range distance, and θ is the radar antenna pointing angle relative to nadir. For illustration purposes, H is chosen to be 400 km throughout this paper.

Because changes in land surface elevation can be significant over small distances, good surface spatial resolution and location determination of the acquired data are needed in order to detect such changes and obtain the desired height accuracies. With the synthetic aperture radar (SAR) systems, fine spatial resolution in the along-track direction

(r_a) can be achieved by generating a small effective along-track radar beam footprint

$$r_a = \frac{\lambda}{2\,L_{sar}}\rho \tag{2}$$

where λ is the radar wavelength and L_{sar} is the synthetic aperture size of the antenna. Conversely, L_{sar} can be determined from the specified r_a and instrument configuration. Of course, how large a L_{sar} can be achieved depends on the available dwell time, the number of azimuth looks needed for speckle noise averaging, the required swath coverage, and the orbital velocity.

SYSTEM APPROACH - SSARA

A graphical illustration of the SSARA approach is given in Fig. 2, and a set of system parameters is given in Table 1. The SSARA system operates at 94 GHz and utilizes one cross-track electrically scanned antenna with its short dimension oriented along the satellite track. The scan range (θ) of the antenna is ±0.57° relative to nadir in order to achieve an cross-track swath width (S) of 8-km. For a polar orbiting satellite operating at an altitude of 400 km, it is estimated that global surface coverage can be achieved over a 1-year period. With such antenna orientation, the narrow cross-track beam footprint (F_c) defines the cross-track spatial resolution (r_c). That is,

$$r_c = F_c = \frac{\lambda}{l_c}\rho\,. \tag{3}$$

In Eq. (3), l_c is the cross-track antenna dimension. At 94 GHz, H=400 km, and θ=0.57°, a cross-track antenna size of 12 m is required in order to obtain a r_c of 105 m, and a cross-track antenna size of 42 m is required in order to obtain a r_c of 30 m. With the anticipated technical challenges associated with large space antennas at 94 GHz, this strawman design settles for a spatial resolution of 105 m. In principle, for a given antenna size it is possible to operate SSARA at a higher frequency and/or in a lower orbit in order to achieve a better r_c. However, the atmospheric absorption (such as cloud and precipitation) associated with higher frequency operation, and the atmospheric drag and surface coverage reduction associated with lower orbit operation, may become prohibited.

The vertical resolution r_v for the SSARA system is achieved by radar pulses with short effective time width (τ_{eff}):

$$r_v = \frac{c\tau_{eff}}{2} = \frac{c}{2B} \tag{4}$$

where B is the instrument bandwidth and c is the speed of light. To illustrate, for B = 50 MHz, r_v = 3 m.

The along-track antenna beam footprint is

$$F_a = \frac{\lambda}{l_a}\rho \tag{5}$$

where l_a is the along-track antenna dimension. Notice that for SSARA $F_a > F_c$ because $l_a < l_c$. Consequently, the time-spread of a return echo (Δt) is primarily due to the range extent of F_a. For a terrain with a averaged slope δ over a reference plane along the sub-satellite track,

$$\Delta t = \frac{2\,F_a \tan\delta}{c} \tag{6}$$

Using Eq. (6) and from azimuth ambiguity consideration, it can be shown that

$$l_a > 4\,\eta\,V_{sc}\,(\tau + \frac{F_a \tan\delta}{c}) \tag{7}$$

where η is the doppler oversampling factor near unity, τ is the transmit pulse width, and V_{sc} is the spacecraft velocity (7.66 km/s). In deriving Ineq. (7), it has been assumed that the transmitted signal and received echo interleave one another. This inequality constrains the lower limit of the along-track antenna dimension. Using τ = 8 µs, η = 1.3 and δ = 12°, the minimum l_a required is 0.4 m.

The scan time (t_s) across the swath is defined such that a full scan is accomplished before the spacecraft moves an amount equal to F_a. Thus

$$t_s = \frac{\lambda\rho}{l_a V_{sc}} = 0.42\text{ s}\,. \tag{8}$$

Consequently, the maximum allowable dwell time over each resolution cell is:

$$t_d = \frac{t_s\,r_c}{S} = 5.4\text{ ms} \tag{9}$$

With r_c=r_a=105 m, L_{sar} can be determined using Eq. (2) to be ~6.5 m. The 1-look dwell time is, therefore,

$$t_d' = \frac{L_{sar}}{V_{sc}} = 0.85\text{ ms} \tag{10}$$

By combining Eqs. (9) and (10), the number of achievable azimuth looks is 6.

The signal-to-noise ratio (SNR) can be expressed in general as

$$\mathrm{SNR} = \frac{P_t\, G^2\, \lambda^2\, A_s\, \sigma_o\, L_s\, \gamma}{(4\pi)^3\, r^4\, k\ T\ B} \qquad (11)$$

where P_t is the transmit power, G is the antenna gain, A_s is the area illuminated by the pulse, σ_o is the surface backscattering coefficient, L_s is the system loss, γ is the pulse compression ratio, k is the Boltzmann's constant, and T is the noise temperature. The surface area illuminated by the pulse can vary substantially depending on the imaging geometry and surface slopes. In the SNR calculations, a pessimistic value of A_s

$$A_s = \frac{r_a\, r_v}{\sin\delta} = \frac{\lambda\ c\ \rho}{2\ l_c\ B\ \sin\delta} \qquad (12)$$

has been used. Using the parameters in Table 1 and assuming a σ_o of -3 dB at an 8° incidence, a "worst-case" SNR of +3 dB is achieved.

The height accuracy of the SSARA system depends strongly on terrain steepness and the processing algorithms. A previous study has indicated that centroid-type algorithms perform reasonably well for natural terrains (Rodriguez et al., 1986). By identifying the various error sources and with reasonable estimates of their contributions, an error budget was derived and tabulated in Table 2.

SYSTEM APPROACH - ISARA

Because of the limited cross-track antenna dimension the spatial resolution of the SSARA approach is limited to 105 m. In order to achieve a better spatial resolution, an interferometric SAR altimeter (ISARA) technique has been proposed (Zebker and Goldstein, 1986; Li and Goldstein, 1990). The surface imaging geometry of the ISARA approach is similar to that of the conventional SAR imaging radars except that in this case a second antenna is employed (see Fig. 3). The two antennas are of the same dimension and are separated horizontally. Pulsed signals are transmitted through one antenna and backscattered echoes are received by both so that phase difference between the two recorded surface images can be determined. This phase difference, being a function of the surface height within the same image pixel, can then be used to infer the surface topography.

The phase difference (ϕ) can be expressed as

$$\phi = \frac{2\pi D}{\lambda}\ \sin(\theta - \xi) \qquad (13)$$

where D is the baseline separation between the two antennas, and ξ is the angular offset of the antennas on a horizontal plane. From Eqs. (1) and (13) we can see that h can be derived by accurate knowledge of D, ξ, ρ, and H. Notice that ρ in this case can be derived directly and accurately from system clock timing. Whereas, ρ in the SSARA case must be estimated from the pulse flight time.

The ISARA design as shown in Fig. 3 operates at 35 GHz. The antenna dimensions are 5.5 m (along-track) by 0.4 m (cross-track), and the antenna beams are pointed at 25° off-nadir. The two antennas are separated horizontally by 10 m. The radar parameters for this ISARA system are shown in Table 1. Most of the SAR parameters can be derived in the similar fashion as that used in the previous section with a few exceptions. The cross-track spatial resolution, for instance, is obtained by the ground projection of the radar slant range resolution, and the swath width is the cross-track beam footprint size. For this particular system design, an spatial resolution of 30 m x 33 m, a cross-track swath width of 10 km, and a total of 24 looks (12 in azimuth and 2 in range) can be achieved. Assuming a σ_o of -10 dB at a 25° incidence, the SNR is calculated to be better than 11 dB.

Besides the errors in orbit determination and clock timing, the other major error sources in the ISARA approach are the phase noise (σ_ϕ), pointing error (σ_ξ), and the baseline determination error (σ_D). These error terms can be expressed as follows:

$$\sigma_h' = \frac{\lambda\ \rho\ \tan\theta}{2\pi D}\ \sigma_\phi\ , \qquad (14)$$

$$\sigma_h'' = \rho\ \sin\theta\ \sigma_\xi\ , \qquad (15)$$

$$\sigma_h''' = \frac{\rho\ \sin\theta \tan\theta}{D}\ \sigma_D\ . \qquad (16)$$

In Eq. (14), the height error decreases with an increasing D (first term of Eq. (14)). However, σ_ϕ increases directly with D due to the electromagnetic field decorrelation of the two received images. Consequently, an optimum D can be selected for a given system. In Fig. 4, the height error isopleths are plotted as the functions of the antenna baseline separation and the radar bandwidth. For this particular ISARA design, a height error contribution due to the phase noise is 2 m.

From Eqs. (15) and (16), the knowledge on system attitude and baseline separation must be accurate to 0.0003° and 2.3 mm, respectively, in order to obtain the required height accuracies. These knowledge requirements are reaching the state-of-art of the corresponding technical areas.

Another problem in measuring interferometric phase is the multiple 2π ambiguities in the phase measurements. For the system considered, a topographic change of n x 180 m will give rise to a n x 2π change in phase and make the measurements ambiguous. Fortunately, it is highly unlikely that any natural terrains will exhibit a 180-m topographic change in over a 30-m pixel spacing. Therefore, it is anticipated that the pixel-to-pixel phase change can easily be unwrapped.

The total height error budget for this ISARA design is tabulated in Table 3. For the described system, the topographic measurements can achieve height accuracy of ~3 m.

SUMMARY

In this paper two potential spaceborne radar instrument approaches, the scanning SAR altimeter and the interferometric SAR altimeter, for acquiring global, high-resolution land and ice topographic data are presented.

By operating at 94 GHz, the SSARA system can achieve spatial resolution of 105 m x 105 m and height accuracies of ~3 m (for gentle terrain) and ~10 m (for steep terrain). For the required system bandwidth, the instantaneous data rate is estimated to be ~800 Mbps. A rather sophisticated on-board data compressor must be employed such that the downlink data rate can be accommodated by the ground receive stations. Another major issue in implementation such system is the technology in fast, electronically scanned antennas at 94 GHz.

The 35-GHz ISARA system can achieve spatial resolution of 30 m x 33 m and height accuracies of ~3 m. The major technical issues associated with this approach are attitude and antenna baseline determination, and large, 2-dimensional space structure for antenna support.

ACKNOWLEDGEMENTS

The research described in this paper was performed by the Jet Propulsion Laboratory, California Institute of Technology, under contract with the National Aeronautics and Space Administration.

REFERENCES

Li, F.K. and R.M. Goldstein, 1990. Studies of multibaseline spaceborne interferometric synthetic aperture radars. IEEE Trans. Geos. & Remote Sensing, 28(1), pp. 88-97.

Rodriguez, E., K.E. Im and F.K. Li, 1986. Evaluation of land altimetry systems. Proc. of IGARSS' 86, pp. 1327-1330.

Topographic Science Working Group, 1988. Topographic Science Working Group Report to the Land Processes Branch, Earth Science and Applications Division, NASA Headquarters. Lunar and Planetary Institute, Houston.

Zebker, H. and R.M. Goldstein, 1986. Topographic mapping from interferometric synthetic aperture radar observations. *JGR*, *91*, pp. 4993-4999.

Parameters	SSARA	ISARA
Frequency (GHz)	94	35
Antenna		
Effective aperture (m)	12.0 x 0.4	0.4 x 5.5
Beamwidth (deg)	0.02 x 0.55	1.2 x 0.09
Peak gain at nadir (dB)	59	52
Angle from nadir (deg)	±0.57 (scan)	25
Transmit peak power (W)	200	250
Pulse duration (microsec)	8	87
PRF (kHz)	50	3.9
Bandwidth (MHz)	50	24
System loss (dB)	3.0	2.5
System noise temperature (deg)	2200	1200

Table 1. System parameters for SSARA and ISARA.

Source	Error (m) for gentle terrain	Error (m) for steep terrain
Attitude	1.1	2.7
Altimeter timing	3.0	10.0
Ephmeris	0.6	0.6
SAR processing	0.6	0.6
Atmosphere and ionosphere	0.3	0.3
Total (RSS)	3.3	10.4

Table 2. Error budget for SSARA.

Source	Error (m)
Phase noise	2.0
Baseline	0.9
Attitude	1.1
Clock timing	0.1
Ephmeris	0.6
SAR processing	0.6
Atmosphere and ionosphere	0.2
Total (RSS)	2.6

Table 3. Error budget for ISARA.

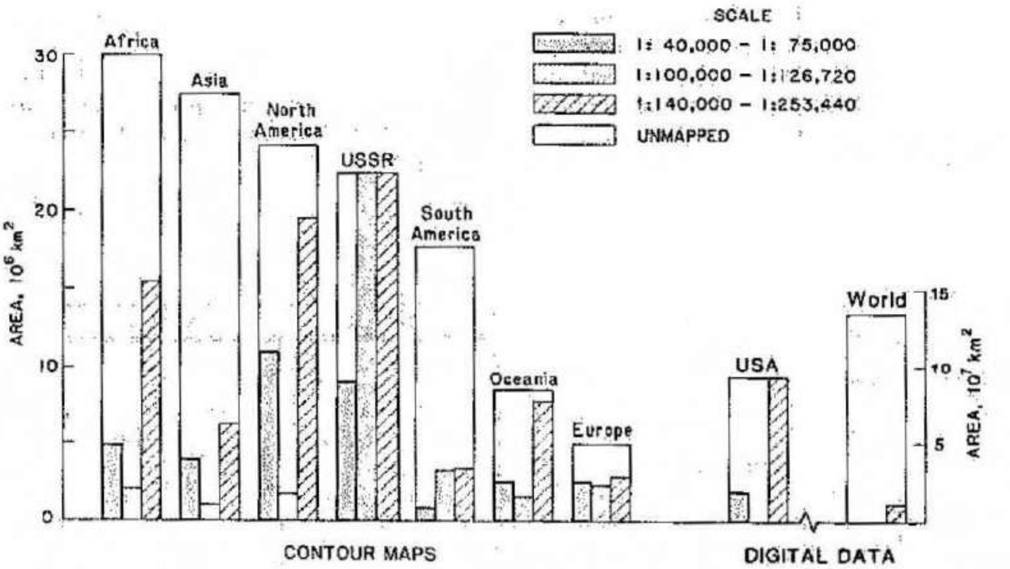

Figure 1. Existing topographic data at various scales in both contour map and digital form. Source: United Nations Development Project.

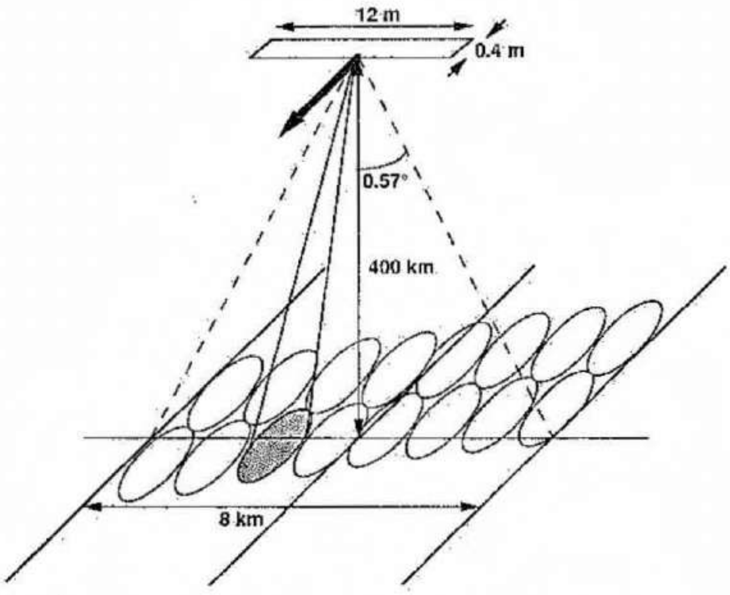

Figure 2. The conceptual design for SSARA.

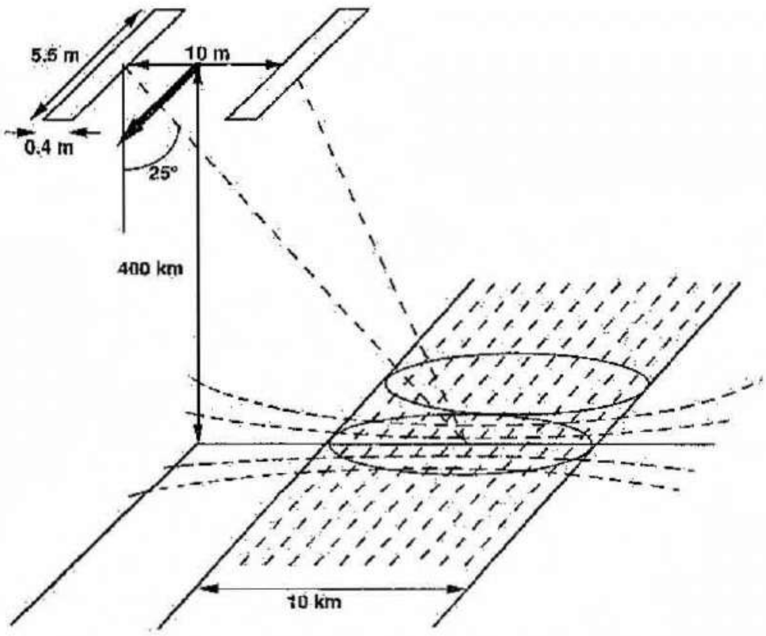

Figure 3. The conceptual design for ISARA.

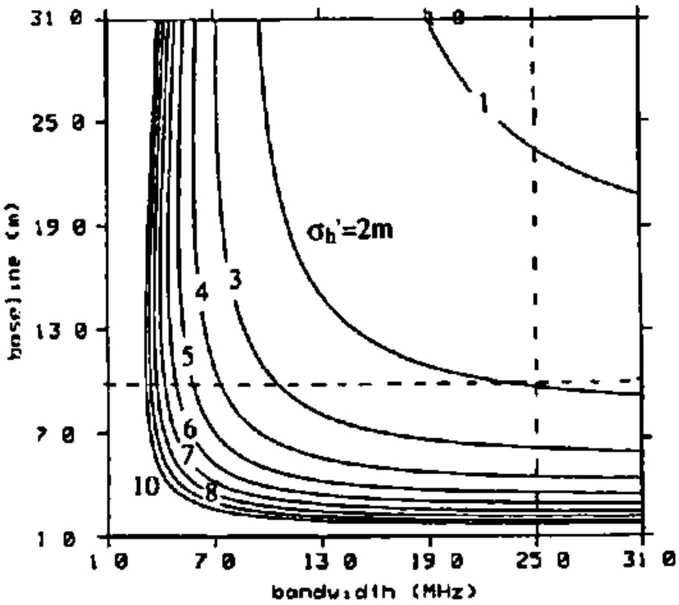

Figure 4. Height error isopleths for the SAR interferometers. The dashed lines correspond to the selected baseline and bandwidth for ISARA.

Sensor Orientation and Navigation

USE OF EXTERNAL DATA FOR AERIAL TRIANGULATION
AT INSTITUT GEOGRAPHIQUE NATIONAL - FRANCE

R. BROSSIER - C. MILLION

Institut Géographique National
2, avenue Pasteur
94160 ST-MANDE
FRANCE

COMMISSION I, WG I/4

ABSTRACT

IGN has realized during last years several trials in order to use for aerial triangulation external data provided by navigation means or auxiliary sensors. The major aim of these trials is to reduce ground preparation particularly for countries where displacements are difficult.

Best results were obtained with GPS system and pressure sensors. For instance a CROUZET 2100 pressure sensor was used is production surveys, in French Guyana and in Benin, with introduction of these data in aerial triangulation computation.

The paper presents the on-board equipment, the use of their data in different configurations, and the main results.

1 - INTRODUCTION

For several years IGN has been involved in developments about use of external data in aerial triangulation. The aim of these trials is to reduce ground preparation, which is very costly in countries with poor geographical and communication basic equipment. Several ways were explored :

- laser telemetry, already used for airborne profile recording and now applied to slant range measuring from aircraft to ground, as close as possible to the point of view.
- atmospheric pressure measurement by pressure sensor, in order to determine aircraft altitude.
- positioning and navigation system data, the most interesting being those given by GPS system.

These three kinds of data were used either separately or in association, for instance laser and pressure sensor or GPS and pressure sensor.

2 - THE ON-BOARD SENSORS

1) Laser telemeter

It is a TAY 130 telemeter, built by CILAS french company. This equipment was already described in a previous publication (ref 1) related to ground profile recording. Let us remind its main performances :

- Maximal range measurement : 15 km
- Maximal measure frequency : 20 Hz
- YAG laser transmitter
  - . Emission wavelength 1.06 μ m
  - . Maximal energy per pulse 40 mJ
  - . Pulse duration 18 ns
- Field of emission 0.5 mrad
- Field of reception 8 mrad
- Measure accuracy 0.50 m

2) Pressure sensors

Two pressure sensors, built by CROUZET France company, were used during the trials. Both equipments are based on the same principle i e deformation measurement of a diaphragm placed in a vacuum chamber and connected to a static pressure port. But the deformation measurement device is quite different for the both sensors.

a) Crouzet 44 model

This sensor is controlled by a force balance. The pressure to be measured creates diaphragm deformation which moves an arm. This displacement is balanced by an electromagnetic force generated by a current in an adjusting coil located in an air-gap of a permanent magnet. An electronical circuit continuously maintains the balance ; the current in the adjusting coil passes through a measuring resistance which delivers a tension proportionnal to the pressure to be measured.

b) Crouzet 2100 model

On this sensor diaphragm deformation is not measured by an electromagnetic force ; the arm connected to the diaphragm strains a quartz monocristal. The resonance frequency of the quartz is a function of the applied constraint and the piezo-électric effect is used for measuring resonance frequency. In addition a resistive sensor located inside the device allows to measure its temperature and therefore to correct pressure measurement by means of an integrated microprocessor.

During the trials these both sensors were used together and they provided very similar results.

In practice the measurements are performed by a sequence of six pressure recordings, at a frequency of 1 Hz, centered on the exposure pulse of the RC 10. The average value of these measures is kept after elimination of aberrant values, if necessary. From these measures a calculated altitude for each point of view is determined, referred to isobaric surface, by means of an appropriate model. Finally the following linearised least square model was used, with one unknown (B) for each flight axis

$$M = AZ + B$$

where M : sensor measure

Z : calculated altitude

$$A = \frac{dM}{dZ} = -\frac{gM}{RT}$$

g : gravity acceleration

R : perfect gas constant

T : absolute outside temperature (in °K)

These altitudes Z can be introduced directly in aerial triangulation computation.

3) GPS navigation system

IGN used a TR5S-B GPS receiver, built by SERCEL-France company, for several trials done either on low speed twin engine Aerocommander aircraft, or on fast speed twin jet Falcon 20. This receiver was already described during a previous presentation in Stuttgart, in 1986 (ref 2). Let us remind this equipment comprises an antenna with its preamplifier, a receiving processing unit, a colour CRT display unit and a control keyboard. The receiver can simultaneously process all the signals coming from up to 5 satellites, on L 1 frequency (1.57542 GHz) and C/A code. It is designed for measuring pseudo-distance and phase at a rate of 0.6 second in each of the 5 channels. TR5S-B receiver is equipped of an internal processor for computing in real time a complete 3 D + T position solution using pseudo-ranges smoothed by phase.

For flights at large scale on Aerocommander aircraft the equipment was the same than for previous maritime applications. But trials on Falcon 20 aircraft needed a special omnidirectional DORNE-MARGOLIN antenna of which aerodynamism was compatible with the aircraft speed (350 Knots).

4) Aerial survey equipment

All the surveys were performed with a WILD RC 10 camera, equipped with a UAg lens cone of focal length 152 mm. This cone is modified for picking up exposure pulse on the reed-switch which commands exposure mechanism of the lens cone. But this operation occurs with a delay which can be determined experimentaly in laboratory : it is a constant for a given lens cone and a given exposure time.

For the laser experimentations, an auxiliary 35 mm camera was used. Its optical axis is rigorously parallel to the laser emission beam. The images given by this camera allow to localize the point of impact on ground of the laser beam and to transfer this point on the associated 24 x 24 cm stereoscopic survey.

3 – TEST FLIGHTS

Each of the previously described equipment was used during test flights, in order to determine its interest for the needs of aerial triangulation.

1) Laser and pressure sensors

TAY 130 laser telemeter has been used for several years for airborne profiling. But this method is very heavy and it needs many manual and costly operations.

Another application of laser telemetry consists of direct measurement of slant range between the exposure station and an identifiable point on ground. These data, corrected from atmospheric refraction provide a scaling for each negative, in addition to pressure measures for the determination of altitude of the exposure station.

In practice this method comes up against many difficulties. Identification of the points of impact is not the least, due to the use of the 35 mm camera and the delay between exposure times of this auxiliary camera and the RC 10 one. This delay was measured in laboratory : its value is 84 milliseconds i e a distance of about 15 meters in case of a Falcon 20 survey. Despite of all precautions taken in the succession of operations it was not possible to reach a good precision for the localization of the point of impact.

Another difficulty is occured by the fact we cannot select the point of impact which can fall on any topographical detail. That implies an important percentage of unusable points : for others the accuracy is a function of the ground slope and the vegetation coverage.

Nevertheless a full test was done on the 1:50 000 sheet of la Souterraine, with a survey at a scale of 1:30 000. Results can be summarized as follows :

- Number of exposure stations : 60
- Number of usable laser measurements : 36
- RMS on slant range between exposure station and ground compared to the calculated range issued from aerial triangulation : 1.80 m
  (accuracy of the calculated range itself is about 0.70 m)

Usable laser data and pressure measures have been introduced in aerial triangulation computation where they brought interesting results as illustrated hereafter :

- standard deviations on check points

with a full network of control points	with a few control points* and external data
X Y : 0.70 m	No check
Z : 0.45 m	0.50 m

* it concerns a normal adjustment block with side overlaps of 20 %. Therefore a minimal control point network should be kept, i e if n is the number of flight axis :

- 2 points for planimetry
- n + 2 points for altimetry

These trials were not carried on, due to the previously recalled difficulties. But some improvements would be studied such as :

- reduction of delays between 35 mm camera and RC 10 exposure times.
- suppression of the auxiliary 35 mm camera.

Yet it remains that the measures are available only on bare and flat ground and it is difficult to automate elimination of faulty points (trees, roofs,...).

2) GPS data

Use of GPS data in aerial triangulation was already described in a previous paper (ref 3) relative to the results of two experimental surveys over the 1:50 000 sheets of Lunel and Vichy. For these missions two TR5S-B SERCEL receivers were used :

- one on a stationary point at Creil airport
- the other, on-board the aircraft

GPS data were exploited in trajectography mode by means of a software which uses pseudoranges, phase and beat counting for Doppler shift. This computation provides geographical coordinates of the aircraft trajectory, at a rate of 0.6 second. Coordinates of exposure stations are linearly interpolated then transformed in Lambert projection before introduction in aerial triangulation computation.

Results can be summarized as follows :

with a full network of control points	with one X.Y.Z control point and GPS data
Lunel X Y = 0.75 m	0.75 m
Z = 0.45 m	0.50 m
Vichy X Y = 0.55 m	0.55 m
Z = 0.45 m	0.60 m

Remark : stiffness of the adjustment block was enhanced by two north - south flight axis. In these conditions one X Y Z control point is enough with GPS data.

These results show that GPS data, in association with only one control point, allow to avoid heavy ground preparation network and give comparable accuracy, at medium scale. In addition it is not necessary to put a receiver on the site what is generally impractical in countries where meteorologic conditions are poor for aerial surveys.

However, GPS data will be really usable for photogrammetry when GPS constellation is complete and only if satellite emissions remain accessible for the civil community. To-day, GPS association with other sensors allows to extend acquisition periods. Some trials were done in this way, using a pressure sensor in addition with GPS for 1:30 000 surveys on two 1:50 000 sheets, Albertville and Manosque. Over these sheets 3 satellites only could be received, leading to a 2D + T solution i e planimetric coordinates and time. Then GPS data are completed by pressure data and this solution is suitable when satellites are low on horizon. One can summarize the results given by this method.

- Standard deviations on check points

with a full network of control points	with a few control points GPS and pressure data
Albertville	
X Y = 0.90 m	1.05 m
Z = 0.80 m	1.00 m
Manosque	
X Y = 0.90 m	1.20 m
Z = 0.70 m	1.00 m

Remarks

a) The Albertville sheet is situated in mountainous area (it's a part of the 1992 Olympic Winter Games site !). The important heights explain high enough values of standard deviations in case of a full network determined by classical ground preparation.

b) For the Manosque sheet it is rather the oldness of ground preparation (transferred on 1987 survey) which explains high values of standard deviations.

c) The Albertville and Manosque adjustment blocks do not have any transversal flight. The control point network must be the following one :

- 2 points for planimetry
- n + 2 points for altimetry (n number of flight axis)

d) Over these both sheets use of GPS, even in lowered configuration, and pressure data, leads to results of which quality is hardly lower than these obtained from a full control point network.

3) Pressure sensor only

The good results obtained with association of a pressure sensor, either with GPS or with laser telemetry allow to consider the use of pressure sensor only. Some trials were simulated from Lunel and Vichy data ; then two real applications were conducted, the one over French Guyana coast in 1987, the other in Benin, in 1989.

French Guyana survey was done at a scale of 1:30 000, over a zone where displacements were very difficult. Due to this fact ground preparation was limited to the coast and the main coastal streams. Pressure measures were therefore very useful for completing altimetric network for the inside adjustment block to bridge the gap between control point lines along the rivers.

The contribution of these pressure measures is tested for instance over the St-Laurent du Maroni block (124 stereo pairs) where many altimetric points are available. Some of these points are not used for controlling but kept for checking. In these conditions results are as follows :

- Z standard deviations on check points

Without pressure data : 1.90 m
With pressure data : 1.25 m

The Benin survey, at a scale of 1:30 000 covered a part of the Ouémé valley, in order to do a preliminary cartography for dams setting up. That involves a dense savanna with trees where ground penetration is difficult due to the lack of tracks. As in French Guyana pressure sensor data allow to ensure the continuity of altimetric network.

4 - CONCLUSIONS

The different experimentations conducted by IGN during last years allow to draw some conclusions on the interest of external data for aerial triangulation.

At first, it does not seem that laser telemetry have a great future except on bare and desert ground due to the problems to spot the point of impact and the burden of office work of its use.

Pressure sensor is already most interesting : despite of its low volume, low weight, low price, it provides directly usable data for aerial triangulation. Its accuracy remains compatible with medium scale survey and it can be associated with other sensors such as GPS or laser.

However, among all the external data tested at IGN for photogrammetric needs it is GPS which brings the best results. They will contribute strongly to reduce ground preparation when satellite constellation is complete.

But don't forget that the trajectography mode, with two receivers, only brings suitable results, particularly when GDOP factor moves quickly. At medium scales it is not necessary to place a stationary receiver close to the survey site ; it is enough to put it on an easy access point where all logistics are available. At large scales this method becomes inadequate and it is necessary to operate in kinematic mode with a stationary receiver inside the survey site. In this direction, IGN plans to do a densification of a geoditic network by photogrammetry and GPS.

At any scale GPS will allow to reduce strongly ground preparation and costs of surveys and will generate deep changes in all the photogrammetric line of production.

BIBLIOGRAPHIC REFERENCES

1. Applications of laser airborne telemetry at IGN - France
by R. BROSSIER, IGN - France
ISPRS symposium, commission I, Stuttgart 1986

2. Use of TR5S-B GPS receiver in airborne photography surveys.
by R. BROSSIER, IGN - France
G. NARD, J. RABIAN, R. GOUNON, Sercel SA - France
ISPRS symposium, commission I, Stuttgart 1986
3. Photogrammetric applications of SERCEL GPS TR5S-B receiver at IGN - France
by R. BROSSIER, C. MILLION and A. REYNES IGN - France
ISPRS congress, commission I, Kyoto 1988
4. The use of auxiliary airborne data in space-photogrammetric block adjustments
by JAR BLAIS and MA CHAPMAN
in "The Canadian Surveyor" vol 38 n°1 - 1984
5. Airborne laser topographic mapping results
by WB KRABILL, JG COLLINS, LE LINK, RN SWIFT, ML BUTLER
in "Photogrammetric engineering and remote sensing" vol 50 n° 6 - 1984
6. Profilomètre laser - inertiel (PLI) : un essai qualitatif en terrain boisé
par R. MOREAU
in "Le géomètre canadien", vol 40, n°1 - 1986
7. Empirical accuracy of positions computed from airborne GPS data
by P. FRIESS (RFA)
ISPRS congress, commission III, Kyoto 1988
8. Kinematic relative positioning using GPS code and carrier beat phase observations
by A. KLEUSBERG
in "Marine geodesy", vol n° 10 - 1986

BUNDLE BLOCK ADJUSTMENT USING KINEMATIC GPS-POSITIONS

Jacobsen, Karsten;   Li, Keren,   University of Hannover

ABSTRACT:

The University of Hannover has carried out a photo flight with kinematic GPS positioning using a dual frequency receiver with P-code in the aircraft and a reference station on the ground. Checked by precise block adjustment, the accuracy of the GPS-positions relative in the strips has reached following standard deviations: Sx=±18cm, Sy=±19cm, Sz=±10cm. But problems with the ambiguity solutions have caused systematic shifts of the positions in the strips.

The systematic effects have been respected by bundle adjustment with program system BLUH in using additional parameters separately for any photo strip. Based on 3 control points in a line crossing the flight directions the bundle block adjustment using the GPS projection centre coordinates has reached an accuracy of ±10cm in all components determined by accurate check points. After elimination of the systematic shifts of the GPS positions, block adjustments without control points have been possible also with just 20% sidelap.

Following problems have not been solved sufficiantly up to now:
- loss of reference caused by cycle slips, even if this effect can be determined by selfcalibration
- exact recording of the exposure instant
- synchronus mode of GPS registrations and photo exposure
- exact calibration of the antenna and camera system

The number of satellites will be completed within 2 years. After complete coverage, the use of GPS projection centre coordinates will become a standard application because also with the today existing problems the number of ground control points can be reduces drastically.

KEY WORDS: block adjustment, kinematic GPS positioning, minimizing number of control points

INTRODUCTION

The expenditure for the ground survey of control points for block adjustment is not negligible. Sometimes the cost for the ground survey is the same like for the whole block adjustment. It is possible to reduce the number of necessary control points with additional strips of photos crossing the main photo flight direction. But with known projection center coordinates determined by kinematic GPS positioning the number of control points can be minimized, also block adjustments without control points are possible. The economic meaning has lead to the realisation of a test block with kinematic GPS positions. This resulted in the projection of the first applications.

GPS TEST BLOCK BLUMENTHAL

A photo flight over an area with a high number of accurate known ground points has been made by the University of Hannover in July 1988 with kinematic GPS positioning in the aircraft in relation to a ground station in the block area. 5 strips with 80% endlap, 20% sidelap have been flown in the scale 1:6370 using a TI4100 (dual frequency, P-code).

UNIVERSITY OF HANNOVER PROGRAM SYSTEM BLUH
GPS BLUMENTHAL p = 60% q = 60%

1.1 69 photos, 248 control points (no GPS positions), p=80%, q=60% differences at control points:
Sx=+/- 4.2cm Sy=+/- 4.2cm Sz=+/- 5.0cm

1.2 69 photos, 4 control points (no GPS positions), p=80%, q=60% differences at 263 check points:
Sx=+/- 21.0cm Sy=+/- 8.7cm Sz=+/- 35.6cm
maximal differences in height: 290.2cm - with 4 control points the block is very unstable, no computation is possible with 4 control points and only 20% sidelap

table 1: results of bundle block adjustment with program BLUH, without GPS positions:

The ambiguity problem of the kinematic GPS positioning has been solved "on the way" based on linear combinations of the dual fre quency phase measurements and the dual frequency P-code (Seeber, Wuebenna 1989). After this, the full carrier phase accuracy was used. The noise level has been high, this can be explained by a multipath effect. So the solution for one strip was not correct with a systematic shift of approximate 3m. A comparison of the photo orientations determined by bundle adjustment with control points and the GPS positions resulted in:

	systematic differences GPS - bundle adjustment			mean square differences after stripwise elimination of shifts			
	dx	dy	dz	sx	sy	sz	
strip 1:	-3.56	-1.27	1.69	±.17	.16	.09	[m]
strip 2:	-3.81	-1.21	1.98	.14	.21	.14	
strip 3:	.31	2.96	1.68	.14	.26	.08	
strip 4:	-2.99	-1.34	2.55	.14	.17	.10	
strip 5:	-4.00	-1.21	1.46	.26	.12	.09	
mean				± .18	.19	.10	

table 2: accuracy of kinematic GPS positions

The systematic differences between GPS and bundle adjustment can be explained by the time period between the recorded and the effective instant of exposure. This difference in time could not be avoided because no registration of the center of the exposure time was possible. The recorded time was depending upon a diode located close to image plane.

	distance in flight direction	corresponding time difference
strip 1	3.52 m	59 ms
strip 2	3.71 m	62 ms
strip 3	3.08 m	51 ms
strip 4	3.87 m	65 ms
mean		59 ms

table 3: systematic difference of GPS positions

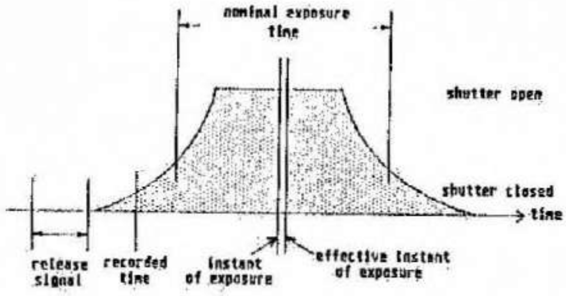

instant of photographic exposure

figure 2:

In addition to the error in time, there is a shift of strip 3 in X and Y and a shift of strip 4 in Z. The shifts have been determined by bundle adjustment with selfcalibration using additional parameters (focal length, principal point x,y separate for any strip) with 3 to 4 control points. With just one control point, the determination of the shifts have not been accurate, the shift in Z could not be identified for the individual strips. The offset between antenna and camera has been respected in the bundle adjustment program of the University of Hannover BLUH corresponding to the individual photo orientations. But the camera was not fixed to the aircraft, so a changed yaw angle of the camera has caused errors of the X and Y- coordinate not exceeding 0.1m.

The control points should be distributed to the different strips. It is better to have a line of control points across the strips than control points at the corners of the block. Based on a line of control points, the systematic shifts of the individual strips can be determined by additional parameters in the block adjustment (see fig. 1).

photos	p	q	control points	SX	SY	SZ
69	80%	60%	4	± 11.0	10.1	23.1 [cm]
69	80%	60%	1	± 23.1	54.5	44.1
35	60%	60%	3	± 11.7	9.1	19.4
35	60%	60%	1	± 24.5	36.1	51.2
21	60%	20%	2	± 14.3	18.7	28.5
21	60%	20%	1	± 21.2	34.1	58.4

table 4: results of bundle block adjustment with BLUH, including GPS positions, without individual precorrection of the GPS positions, accuracies computed with independent check points

Bundle adjustments without control points have been possible also just with 20% sidelap. The results are influenced by the shift of the kinematic GPS positions (table 2).

photos	p	q	control points	SX	SY	SZ
69	80%	60%	4	± 9.8	7.1	9.7 [cm]
69	80%	60%	1	± 9.7	10.4	10.1
69	80%	60%	0	± 10.1	10.6	17.7
35	60%	60%	3	± 10.4	13.5	23.2
35	60%	60%	1	± 9.6	12.4	21.7
35	60%	60%	0	± 11.1	13.6	17.9
21	60%	20%	2	± 11.5	15.3	25.7
21	60%	20%	1	± 10.8	14.8	34.7
21	60%	20%	0	± 12.9	16.0	23.5

table 5: Results of block adjustment with stripwise precorrection of the GPS positions, computed with independent check points

For these computations the systematic shifts of the GPS positions of the projection centers have been eliminated stripwise in advance. This is corresponding to a GPS positioning without loss of reference or with correctly determined ambiguity.

The results are strongly depending upon the used control point(s). If just 1 control point will be used, the individual differences of the ground coordinates are influencing the whole block. The main influence of the number of control points is the determination of systematic shifts. After elimination of the systematic differences in the coordinates between the adjusted object points and the check points, only negligible differences in the corresponding data sets have been achieved after stripwise preparation of the GPS positions with different control points.

p=80%,	q=60%	Sx=± 9.3cm	Sy=± 8.7cm	Sz=± 9.9cm
p=60%,	q=60%	Sx=± 8.4cm	Sy=± 11.2cm	Sz=± 17.3cm
p=60%,	q=20%	Sx=± 8.8cm	Sy=± 13.4cm	Sz=± 24.3cm

table 6: relative accuracy of determined ground coordinates Standard deviations determined at independent check points after elimination of shifts in the ground coordinates X, Y, Z (mean value, independent from number of control points)

SUMMARY

With the today technology of kinematic GPS positioning of projection centers during photo flight it seems not to be possible to avoid systematic errors changing from photo strip to photo strip. Also with relative positioning using also a GPS receiver in or close to the flight area, shifts up to 4m cannot be avoided.

Based on a small number of control points GPS positions obtained by relative positioning with one receiver in the aircraft and a reference station on the ground stripwise shifts can be identified and respected by block adjustment with selfcalibration by additional parameters. By theory just one control point is sufficiant if the block geometry is stabilized by at least one crossing strip. Only by reasons of reliability more than one control point is necessary in such a case. The accuracy which can be reached today is sufficiant for all mapping purposes. Without control points shifts cannot be avoided, but the internal accuracy of such a block is usually satisfactory.

Systematic errors are not only caused by the GPS positioning also the inner orientation of the cameras is not known accurate enough. A 15 microns change of the focal length can be caused just by influence of the temperature. This is corresponding to a vertical shift of 0.01 % in the case of a wide angle camera - the usual level of accuracy. Errors in the principal point can be compensated with opposite flight directions.

Constant errors in time recording also can be identified by block adjustment using photo strips with opposite flight directions. Such errors cannot be avoided. Only the new camera Zeiss RMK TOP supplies a signal of the midpoint of exposure for data recording (Zuegge 1989). But even this can be affected by systematic differences caused by the characteristic of film (figure 2). The camera release signal should not be used for recording. Even if no rotary shutter is used, affected by the use of the shutter the temperature will be changed causing a change of the delay between release signal and the instant of exposure within some milliseconds (Merchant 1989).

Accuracy will be lost by the interpolation of the projection centers between the GPS recordings. The time difference between instant of exposure and GPS

recording should be small as possible. If the camera is not used in a simultaneous mode the recording intervall should not exceed 1 second. High speed photo flight will raise these problems.
The offset between camera and GPS antenna in the aircraft should be small as possible. This offset can be respected in the bundle block adjustment if the relation between camera and aircraft is not changed during photo flight. That means also the drift angle should not be respected for the camera orientation during photo flight, otherwise a recording of changed orientation of the camera in relation to the aircraft is necessary. This problem also can be avoided if the antenna is located exactly above the camera.

The attitude data can be determined by block adjustment. There is no advantage of an inertial navigation system together with GPS positioning if the problem of cycle slips can be solved.

CONCLUSION

The power of kinematic GPS positions has been demonstrated. Even with the today not avoidable systematic errors it can be used in a combined bundle block adjustment. With just one control point a sufficiant accuracy also for large scale mapping can be reached. Only because of reliability more than one control point should be used. The block adjustment should be done with the bundle method, like with usual blocks the independent model adjustment will not lead to the same accuracy. The today bottleneck of a not sufficiant satellite coverage will be solved within the next 2 years. It can be possible that the GPS system will be supplemented by the USSR GLONAS system which is very simillar to GPS.

User friendly bundle block programs for combined adjustment with GPS data are available. But the programs for the kinematic GPS computation still have to be improved. The GPS ambiguity problem will be reduced with a higher number of available satellites. The enormous economic advantage of block adjustment with GPS projection center coordinates has lead to the first projection of comercial applications.

REFERENCES

Ackermann, F. 1986: Use of Camera Orientation Data in Photogrammetry - A Review, ISPRS Com I, Stuttgart 1986

Andersen, O. 1989: Experience with Kinematic GPS during Aerial Photography in Norway, 42nd Photogrammetric Week Stuttgart

Baustert, G., Hein,G.W., Landau,H. 1989: On the Use of GPS in Airborne Photogrammetry, Hydrographic Applications and Kinematic Surveying, 5th International Geodetic Symposium on Satellite Positioning, Las Cruces, New Mexico 1989

Brossier, R., Million,C., Reynes,A. 1988: Photogrammetric Applications of Sercel GPS TR5S-B Receiver at Institut Geographique National, ISPRS Kyoto 1988

Columina, I. 1989: Combined Adjustment of Photogrammetric and GPS Data 42nd Photogrammetric Week, Stuttgart 1989

Cortes, F., Heimes, F.J. 1988: A Comparative Study of Dynamic Positioning by GPS, ISPRS Kyoto 1988

Friess, P. 1988: Empirical Accuracy of Positions Computed from Airborne GPS Data, ISPRS Kyoto 1988.

Gruen, A., Runge, A. 1988: The Accuracy Potential of Self-Calibrating Aerial Triangulation without Control,ISPRS Kyoto 1988

Hein, G.W. 1989: Precise Kinematic GPS/INS Positioning: A Discussion on the Affiliations in Aerophotogrammetry, 42nd Photogrammetric Week, Stuttgart 1989

Jacobsen, K. 1990: European Progress on GPS Photogrammetry, ASPRS, Denver 1990

Jacobsen, K., Li, K. 1990: Bündelblockausgleichung mit kinematischer GPS-Positionierung, Zeitschrift fuer Vermessungswesen

Lighteringk, G.H. 1988: A Study on the Improvement of Photogrammetric Blockadjustment Procedures, ISPRS Kyoto 1988

Merchant, D.C. 1989: Positioning of the Photo Aircraft by the Global Positioning System, ACSM/ASPRS Annual Convention Baltimore 1989

Seeber, G., Wuebenna, G. 1989: Kinematic Positioning with Carrier Phases and "on the way" Ambiguity Solution, Fith Int. Geodetic Sympos. on Satellite Positioning, Las Cruces New Mexico 1989

Straub, J., Thiel, K.-H. 1989: Further Development of the GPS and GPS Receivers, 42nd Photogrammetric Week, Stuttgart 1989

van der Vegt, H.J.W., Boswinkel, D., Witmer, R. 1988: Utilisation of GPS in Large Scale Photogrammetry, ISPRS Kyoto 1988

Zuegge, H. 1989: RMK TOP - the new Aerial Survey Camera System from Carl Zeiss, 42nd Photogrammetric Week, Stuttgart 1989

QUALITY ENHANCEMENT IN ACQUISITION OF AIRBORNE REMOTE SENSING DATA

FRANZ PLISCHKE

I N T E R F L U G
Division for Remote Sensing,
Industry and Research Flights
Airport Berlin-Schoenefeld
GDR - 1189

A B S T R A C T

Besides the single transmission levels also the correlations between atmosphere, aircraft, imaging system and data carriers diminish the quality of remote sensing data.

The most important sources of quality reserves are the improvement of acquisition of orientation data, of navigation and attitude stabilization of aircraft, dynamic or/and electronic compensation of bluring and distortion influence of angular (rotatory) movements, and the increase of specific information content of remote sensing recordings in connection with the corresponding image data carrier.

Furhter qualitative and economical effects can be produced by the use of multisensors in connection with multidata concepts.

KEY WORDS: Data quality, sensor orientation, piloting, angular motion, on-line-compensation.

1. Problems of the interaction between atmosphere, aircraft and imaging system

The development test results obtained on the ground under laboratory conditions and under given flight conditions were in practical routine flights not generally achieved. Therefore, the aim was to investigate the causes of the negative influences under practical conditions and to initiate optimum counter-measures.
A worldwide accepted criterion of image quality is the modulation transfer function MTF (cf. /1/), whose advantage is that the MTF total value can be formed by multiplication of the transfer values of the discrete items. However, as was recognized in this connection, this does still not justify the procedure to consider these discrete items independently of each other (object, atmosphere, camera system with optics and sensor, motion of the camera system, data carrier and reproduction instruments).
Because of the mutual interrelation and the dependence on each other the total process must be treated as a complex unified system, which requires an interdisciplinary cooperation.

These cooperative relations have been established in the GDR between the instrument industry, academic research institutions, civil aviation enterprise, data users and analysts an the producers of data carriers (e.g. film) and are further developed between research and production.

In the following, a few selected investigation results shall be presented.

2. Improvement of aircraft piloting

For aerial photogrammetry implemented with smaller aircraft visual navigation is still worldwide predominantly used for maintaining the fixed flight strips, whereas for electronic scanner and side-looking radar systems larger aircraft with primarily instrumental navigation is employed. The reason of this lies on the one hand in the recording principle and, on the other hand, in the financial ratio of the entire aircraft to its instrumentation. Proof was furnished that the investment costs for automatic highly precise navigation which at first glance seem to be high are quickly amortized by highly qualitative and significant economic advantages. This becomes evident by the following consideration: When the prices for remote sensing products are fixed on the basis of a definite quantity and quality it is with reliably exact flight line navigation and attitude stabilization of the aircraft possible to minimize the expenses by the reduction of lateral overlap of flight strips or swathes and the reduction of the reflight rate.
For remote sensing applikation in aeroplanes a modern navigation system has to fulfil two basic tasks:

- the highly precise, realiable and optimum, i.e.cost-effective performance of flight and

- the output of data of outer orientation (position coordinates, attitude angles) for the on-line control of the imaging systems and for synchronous recording on the data carrier of the remote sensing system.

For fulfilling the first aforementioned task in compliance with internationally valid accuracy requirements relative to a whole frame block we sonsider it according to our own investigations necessary to achieve in the near future an accuracy of outer orientation as to the flight path in a route relative to its centre line or regarding its middle flight attitude and the routes of a frame block relative to each other, with the following values:

For the relative on-line position accuracy:

in plane $\Delta x, \Delta y < n \cdot 15$ m; n=1 for h<2 km
in height $\Delta z < n \cdot 20$ m; n=2 for h=2..4 km etc.

for the dynamic on-line attitude stability in each flying height:

angular speed about all three axes
(pitch $\dot{\varphi}$, roll $\dot{\omega}$, yaw $\dot{\varkappa}$) $< 0{,}2\ ^\circ/s$.

and for the relative on-line attitude accuracy in each flying height:

pitch angle φ, roll angle ω, yaw angle $\varkappa < 0{,}5^\circ$
(for photographic and CCD-matrix cameras)

While the position accuracy can be realized by the aircraft alone, it is with respect to the accuracy of the attitude angles and there dynamic stability after the prestabilization by a flight control system possible that a dynamic angles-stabilized platform performs the fine stabilization for the particular recording system except for the above-mentioned residual values.

A future-oriented navigation system capable of meeting the above requirements is intended to be used in a satellite-based global positioning and navigation system such as GLONASS (USSR) or GPS-Navstar (USA), which may give a considerable impetus to the increase of quality and quantity in remote sensing and particularly in photogrammetry.

By means of a reference signal and a phase metering of interferometer unit the GPS Navstar is also in the civil C/A code capable of automatically controlling more exactly (c.f./2/) and more effectively than hitherto both the flight parameters of route guidance and attitude angles via a flight control system (including autopilot) and the recording system according to image-sequence, direction and attitude with an on-line total accuracy of the above-mentioned values as well as the restitution instruments with the recorded orientation data. Since the orientation data are acquired with a considerably higher accuracy than the on-line values to be realized according to Section 2, it is also possible to carry out a highly accurate off-line post-rectification and a geometric allocation of the pixel to the terrain.

3. Minimization of motion influences

On principle, three groups of significant relative motions can be distinguished between recording system and objekt scene:

- forward motion of the aircraft,
- angular (rotary) vibrations excited especially by air turbulences,
- translatory vibrations arising from the aircraft engines and the atmosphere.

The latter group has a negliable influence on the image quality.

The influence of forward motion need no longer be dealt with, since on the one hand it is well known and on the other hand the number of aerial cameras without forward motion compensation (FMC) is declining. For these cameras the shutter time limitation involved has still to be taken into consideration. But also with camera system with FMC (e.g. LMK, MKF-6 and MSK-4) it is because of the previously inferior angular motions still not allowed to fully eliminate the limitation of long shutter times. However, the limitation is based on completely other laws than for forward motion. It is for the same angular motions independent of the flying height. The effect of angular aircraft vibrations on the image data was analyzed according to /3/.

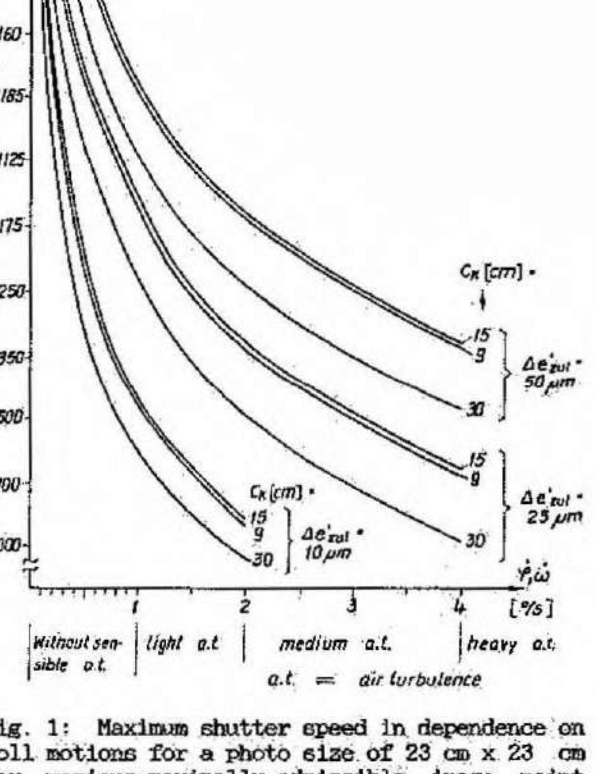

Fig. 1: Maximum shutter speed in dependence on roll motions for a photo size of 23 cm x 23 cm for various maximally admissible image point migrations

In Fig.1 a diagram is shown representing the maximum shutter time as a function of the particular speed of angular motion and of the maximally admissible image blur to be expected in the image corners.

The angular motions of an aircraft or helicopter are besides their stochastie nature largely of a periodic nature and can be described by a sum of two or three superimposed sinusoidal or quadratic functions. Their typical frequencies, which exert the largest effect on the image, lie between 0.1 and 1 Hz and their angular speed amplitudes are significantly dependent on turbulences. Under conditions of a quiescent flight (without noticeable turbulences) the roll motion of aeroplanes with a take-off weight of abt. 3 t to 6 t without autopilot system reaches amplitudes of angular speed of up to 1°/s and at medium turbulences of up to 4°/s. As against the roll motion as the strongest and most influential angular component the other angular components of pitch and yaw increase the maximum total image motion by about 25 %. Due to the vectorial addition and depending on the phase position of the angular vibrations the maximum of image point motion occurs at least in one point at the image edge or in one of the 4 image corners. The latter case is illustrated by an example in Fig. 2, for which the maximum of the three angular speed components are just in phase.

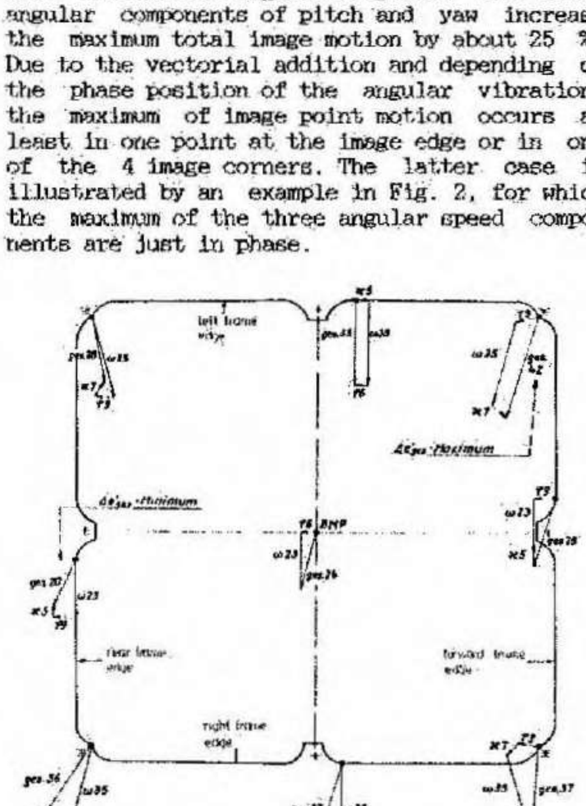

Fig. 2: Determination of total angular pixel bluring for various photo coordinates according to image orientation in the aircraft.
Example of LMK-15 at a medium turbulence ($\dot{\omega} = 3\,°/s$, $\dot{\varphi} = \dot{\varkappa} = 1\,°/s$) and a shutter time $t_s = 1/350$ s or at a scarcely noticeable turbulence ($\dot{\omega} = 1°/s$; $\dot{\varphi} = \dot{\varkappa} = 0{,}4\,°/s$) at $t_s = 1/120$ s); the drift is compensated, i.e. $\varkappa_0 = 0°$;
$\dot{\omega}, \dot{\varphi}, \dot{\varkappa}$ -maximum in phase; in the image ω stands for $\Delta e'(\dot{\omega})$ etc; the following numbers are the amounts of migration (bluring) given in µm.

On the other hand, for the instantaneous vibration state: $\dot{\omega} = \dot{\omega}_{max}$ and $\dot{\varphi} = \dot{\varkappa} = 0°$ in the middle of exposure, the maximum image blur would be evident approximately on the whole left and right image edges and the minimum blur on the whole image centre line in flight direction.

Through the influence of a real photographic shutter with an efficiency between 70 % and 80% the image motion being actually evident in the image is according to /11/ in contrast to a theoretically determined image motion of 50 µm for an ideal shutter (lens shutter efficiency = 100 %) reduced by abt. 25 %, so that in connection with the above-mentioned 25 % increase conclusions to a first approximation can be drawn in practice from the roll motion alone to the image motion. In any case, however, the image motion is due to all angular motion components subjected to a random process from image to image, since there is no connection between the temporal course of the angular speed amplitude and the moment of exposure.

Therefore, it may happen that one or several photographs of highest or high resolution with long shutter time are directly followed by one being intolerably unsharp. Normally it is so that with adherence to the given shutter time limitation the statistical distribution of sharp and less sharp photos still occurs, but the highest image blur will then no longer exceed the admissible measure. Thus, in a reasonable system conception the stochastic influence of the angular image motion has to be considered already in the instrument design in order that a waste of means is avoided, when for example an imaging system with highest resolution, which is well suited for the quiescent flight of a satellite, can on the other hand in an aircraft statistically reach the maximum resolution only in one of n photographs.

In the case of scanners the angular motion-induced distortion within one line can be neglected, but between adjacent lines it must absolutely be taken into consideration especially because of occurring scanning gaps, in particular when a small exposure time is choosen in relation to the line cycle frequency in favour of a small pixel bluring. Overlapping or multiple scanning as illustrated by way of example in Fig. 3 can be rectified aferwards, but missing object details with dimensions smaller than or equal to the particular scanning gap in consequence of underscanning cannot be regained in the following image processing, so that at least for this an online compensation technique has to be applied.

Such motion compensation techniques were suggested on the basis of latest knowledge described above and developed up to maturity of invention with the partners mentioned at the beginning. They concern a dynamically angle-stabilized platform according to /4/ for all recording systems, the choice of the instant of exposure in phases of minimum angular motion

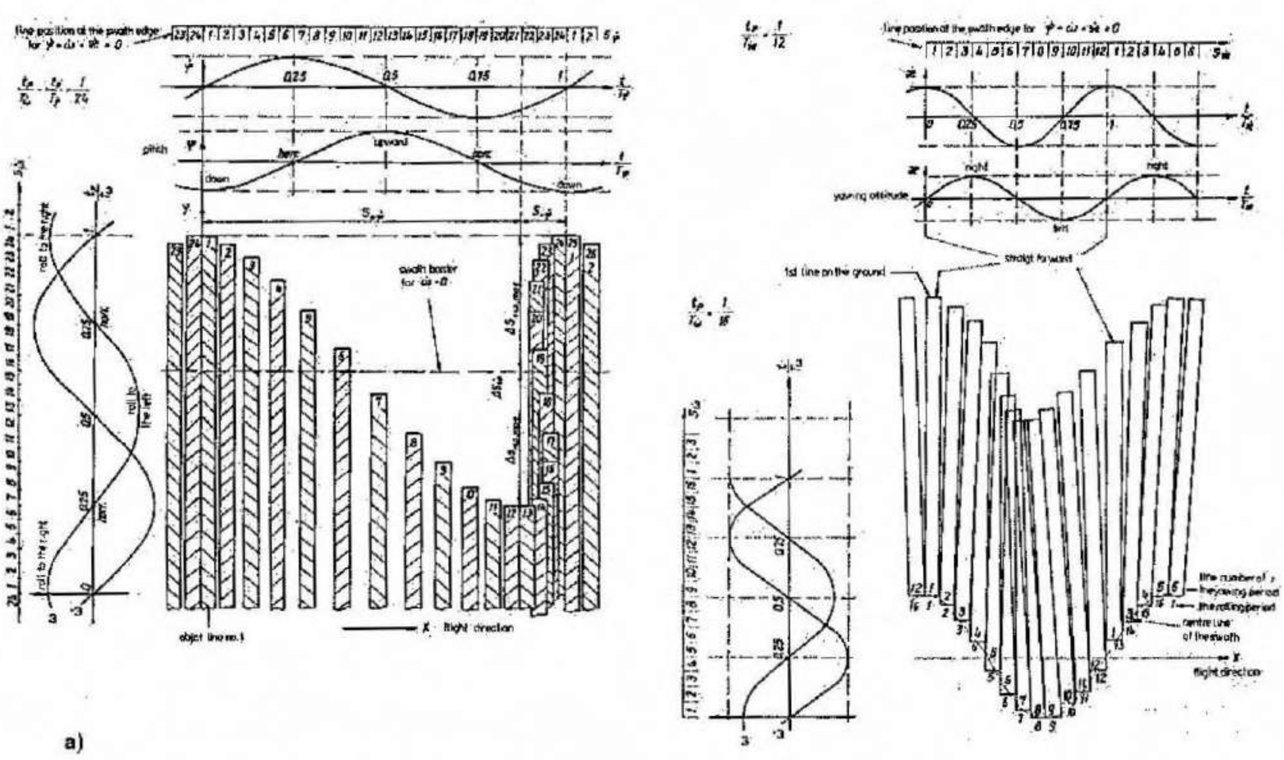

a)

b)

Fig. 3: Distortion of scanning on ground
(detector exposure time t_B << scanning period t_p << angular motion period T)
a) with simultaneous influences of roll and pitch motions ($\dot{\omega}$ and $\dot{\varphi}$)
b) with sumultaneous influences of yaw and roll motions ($\dot{\varkappa}$ and $\dot{\omega}$)

according to /5/ for photographic camera systems and the electronic selection of detector elements of an array for an instantaneous desired scan line which corresponds to the desired flight attitude according to /6/ and Fig. 4 for scanners.

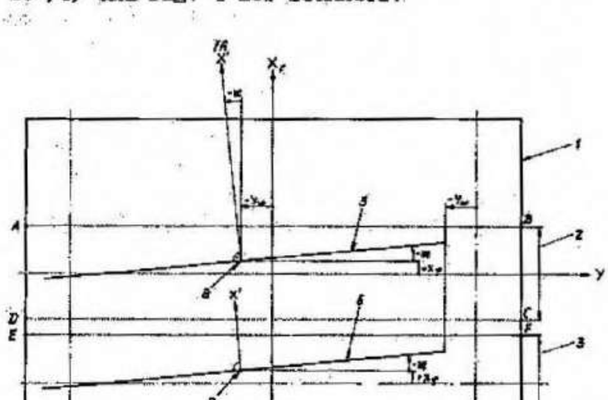

Fig. 4: Detector array (1) with a nominal scan line directed vertically downward (5) and one looking ahead (6) with the motion ranges (2,3,4,7 and 10)

4. Maximization of the usable image information density

The usable image information density is defined as the processable information quantity stored on a remote sensing data carrier per unit area; this information quantity is differentiated by the geometric resolution (or image modulation), the radiometric resolution (grey value, temperature stages and others) and the spectral resolution (band width per channel). In photographic recording systems their maximization would be the achievable gamut of grey values per film area and the maximum spatial frequency in resolved lines per millimeter and would inter alia be synonymous with the optimization of aerial image exposure (cf. /7/).

In modern aerial films with strongly reduced emulsion thicknesses (e.g. ORWO-VF 45 or KODAK PANATOMIC-X Aerographic II), the resolving power is only weakly dependent on contrast, so that we plead for the full utilization of the possible density volume in the image on the linear portion of the characteristic curve of abt. 1.6 density units for the VF 45 type as compared with the previous constant limitation to 0.85.

In conjunction with the details given in Section 3 this extension of the density volume, an improved differential exposure measurement and the use of microcomputers on the basis of refined computation algorithms with regard to the photographic systems could render it possible to achieve maximization of the recorded image infomration density.

In this connection one has also to consider the technology of aerial film development, for the aforementioned measures require a film development at a nominal gradient being controllable within the film. For this purpose a continuous processing machine has to be modified so that the rate of travel of the film is automatically controlled by the data carrier which is to be scanned synchronously to the film or on the film (cf. /10/).

5. Multi-sensor concept

With the sumultaneous use of different supplementing recording systems which operate either independently of each other or in an enhanced version coupled together, the interpretation reliability and information capability of the remote sensing data can considerably be increased, with the added effect that their acquisition becomes more economic. The multiconcept in remote sensing which had already been suggested years ago by leading scientists of various countries can now be realized with the present state of microelectronics. This was stated in 1988 at the 16th Congress of the ISPRS in Kyoto/Japan and recommended to all countries for application. With the conduction of the "GEOEX" complex experiment of the international INTERCOSMOS cooperation first steps were undertaken from 1986 on in direction of a multisensor use in the Remote Sensing Division of the INTERFLUG which were then continued by the creation of a ZKE-2 coupled block for the sumultaneous use of the MSK-4 Multispectral Camera and an LMK Aerial Camera operated from one control unit (cf. /9/) and which shall be followed by a thematically programmable optoelektronic multispectral imaging system (TOMAS) would have to be controlled by radiometric, spectral, meteorologic, geometric, orientation and motion data from the advanced object line field which are supplied by an advanced field sensor as it is suggested in /8/.

The degree of automation of the recording systems is further increased in order to simplify operation and to reduce the number of operators needed for the recording system in the aircraft.

References

/1/ Rüger, Pietschner, Regensburger: Photogrammetrie, Verlag Bauwesen, Berlin, 5. Auflage 1988

/2/ Hartl, Schoeller: Application of GPS-Receivers for Earth Observation. Proc. ISPRS-Symp., Com. I, Stuttgart 1986

/3/ Plischke: Der Einfluß von Luftfahrzeugbewegungen auf die Qualität von Fernerkundungsaufzeichnungen, Vermessungstechnik, Berlin 35 (1987) 8

/4/ Klose, Plischke: Anordnung zur dynamischen Lagestabilisierung einer Luftbildmeßkammer, DDR-WP G01c/280127 4, Nr. 240595A1, Berlin 1985

/5/ Plischke, Rempke, Zeth: Verfahren zur Elimination von Bildverwischungen. DDR-WP G01c/312306.0, Berlin 1988

/6/ Plischke, Bach, Nopirakowski: Verfahren zur aktiven Korrektur der bewegungsbedingten Verzerrungen bei Scanneraufnahmen aus Luft- und Raumfahrzeugen. DDR-WP G01c/303434.0, Berlin 1987

/7/ Plischke: Optimierung der Luftbildbelichtung. TIZL Berlin 24 (1988) H. 2

/8/ Bach, Kruspig, Nopirakowski, Plischke, Scheele: Aufnahmesystem zur Gewinnung von Fernerkundungsdaten. DDR-WP G03B/322340-0, Berlin 1988

/9/ Plischke, Hanelt: Rationelle Luftbildgewinnung durch gekoppelte Aufnahmesysteme. Berlin TIZL 24 (1988) und Vermessungstechnik 36 (1988) 2

/10/ Braunschweig, Diete, Plischke, Voß: Verfahren und Vorrichtung zur optimalen Entwicklung fotografischer Bilder. DDR-WP G03D/317485.8 Berlin 1988

/11/ Zeth, Diete: Test Technique for Checking the Forward Motion Compensation Device in the LMK Aerial Survey Camera System. Proc. 16. ISPRS-Congr. Kyoto 1988, Com. I (Part B1)

ASPECTS AND FIRST RESULTS OF THE APPLICATION OF ANGULAR MOTION COMPENSATION (AMC) IN THE LMK AERIAL PHOTOGRAPHIC SYSTEM

Norbert Diete, Carl Zeiss Jena, GDR

ABSTRACT:

Image quality enhancement is one of the main concerns of improving the instruments for logging of primary photographic data. Considerable progress was achieved thanks to the simultaneous applications of high performance optics, photographic material of strongly enhanced resolution and the compensation for the aircraft forward motion (FMC).

Now, more and more the surrounding conditions of taking aerial photographs revealed to have a limiting effect on the further and general quality enhancement. The logical consequence of the preceding scientific-technical process was the development of the BM2000 gyro mount as part of the LMK standard equipment in order to compensate for any image motions as complete as possible.

Based on the results of a flight using simultaneously both a conventional and a stabilized mount, the present paper tries to give a first answer to the question for the effect of such measures on the image quality improvement achievable under dynamic conditions. Compared with photograms taken without stabilization, the photograms obtained with AMC showed an increase in resolution to 130% at a flight height of h_g=1200 m and 162% at h_g=600 m, calculated from the evaluation of high contrast test patterns.

The considerable reduction of both the maximum and the average image blurr thanks to the application of stabilized mount was generally proved.

(Original not received in time for publication)

Future Remote Sensing Missions and Early Results of New Systems

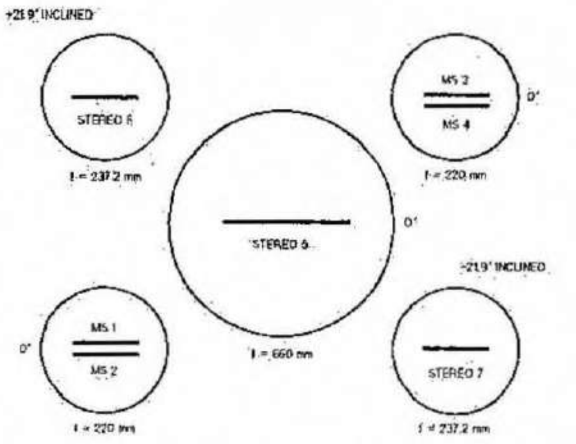

Figure 1. MOMS-02 Optical concept

Figure 1. shows a schematic representation of the MOMS-02 optical concept. In order to be able to fulfill the different user requirements a modular concept, which was already sucessfully proven by MOMS-01, was selected. The system consists of five lenses, three of which are intended for the stereoscopic images, and the other two for the multi-spectral images. The central lens, with a focal length of 660 mm, forms the core of the camera system. It makes possible the high resolution imagery with a ground pixel size of 4.5 X 4.5 m. In order to attain a sufficient swath width with such high resolution, two linear sensors are optically joined to each other in the focal plane. In connection with the central high resolution lens, there are two other stereo lenses, each with a focal length of 237.2 mm. Because of their pitch of $+21.9^{\circ}$ and -21.9°, respectively, relative to the direction of flight, three-fold stereoscopic imagery is achieved. The focal length of these lenses was so chosen, that there is an integral relationship between the ground pixel sizes seen by the high resolution channel and the two inclined channels of 1:3.

In addition, two other lenses, each with a focal length of 220 mm, enable the multi-spectral imaging of a total of four channels. In order to achieve this, there are two sensors in the focal plane of each lens, together with their corresponding filters. In order to ease the image data analysis, the relationship of the ground pixel size of the high resolution channel with that of these multi-spectral channels is also selected to be 1:3.

Figure 2. shows the total MOMS-02 imaging geometry, and the ground track resulting from it. The swath width for the high resolution channel can be as much as 37 km, depending on the recording mode, and for the other channels, as wide as 78 km. These values are relative to a nominal orbit altitude of 296 km. Because of the viewing angle of 21.9° in the two outer stereo channels, the image swath on the earth's surface for these channels is separated from the swath of the nadir channels by about 140 km.

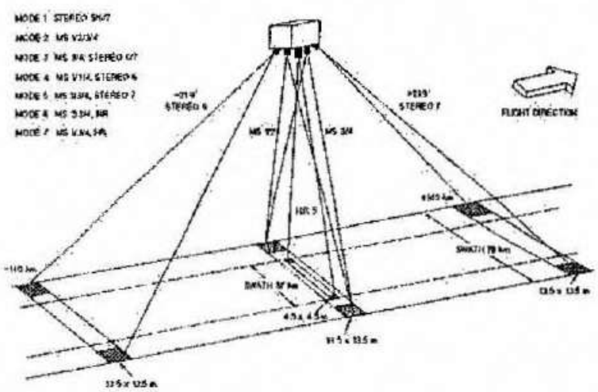

Figure 2. MOMS-02 Imaging geometry

In the coverage areas, because of the size relationships of the ground pixels, it takes nine picture elements of the nadir viewing high resolution channel to fill the area of one of the multi-spectral pixels. The same holds for the ground pixel area relationship between the high resolution channel and the two angled stereo channels.

Table 2. lists the most important optical parameters of the MOMS-02 camera. The center wavelengths of the seven channels are distributed over a range between 472 nm and 790 nm. The corresponding bandwidths, of the multi-spectral channels, vary between 35 nm and 65 nm. The stereo channels all cover the same panchromatic region, a bandwidth of 240 nm with a center wavelength of 640 nm. The high optical quality of the lenses allows the values of the modulation transfer function to be read out at the Nyquist frequency.

CHANNEL	FOCAL LENGTH (MM)	f/D	CENTER WAVELENGTH (NM)	BANDWIDTH (NM)	FOV (DEG)	MTF AT NYQUIST FRQ.
1	220	4.2	472.5	65	± 7.76	≥ 0.65
2	220	4.2	552.5	45	± 7.76	≥ 0.60
3	220	4.2	662.5	35	± 7.76	≥ 0.65
4	220	4.2	790	40	± 7.76	≥ 0.65
5	660	4.5	640	240	± 3.5	≥ 0.60
6	237.2	5.6	640	240	± 7.2	≥ 0.60
7	237.2	5.6	640	240	± 7.2	≥ 0.50

Table 2. MOMS-02 Optics performance data

Figure 3. illustrates the MOMS-02 stereo imaging principle and the associated difficulties of later image data interpretation. The three viewing angles already discussed make it possible to image a point A on the earth's surface, at three different times, and with the three different viewing angles. This scenario makes the later stereoscopic interpretation possible. The fact that the three images are recorded with a lag time of about 20 seconds makes it very difficult to correlate the images, because of the intervening movement of the platform. In order to later be able to model, and thus compensate for these movements, other appropriate supplementary data must be available. These are for one, the position data given by TDRSS tracking, and for another, the attitude data delivered by the Shuttle navigation system (IMU). The latter are supposed to be recorded directly with the MOMS-02 image data during the flight.

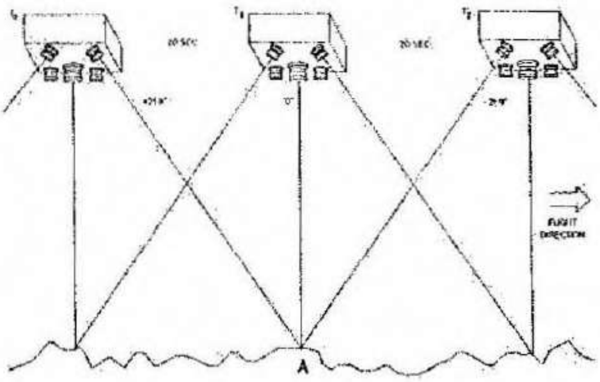

Figure 3. MOMS-02 Stereo imaging

The strict requirements placed on the imaging quality of the camera require the use of modern CCD sensors. Table 3 lists the most significant parameters of the applicable Fairchild linear arrays.

SENSOR	FAIRCHILD CCD 191
NO. OF ELEMENTS PER SENSOR	6000
PIXEL SIZE	10 x 10 μm
NO. OF SIGNAL OUTPUTS	2
FULL WELL CAPACITY	> 750 000 e⁻
READOUT NOISE	35 - 50 e⁻
DYNAMIC RANGE	> 15 000 : 1 (up to 30 000)
SATURATION OUTPUT VOLTAGE	3 - 4.5 V
CHARGE TRANSFER EFFICIENCY	.999999
MTF AT NYQUIST FREQUENCY	60 %
SPECTRAL RANGE	400 - 950 nm

Table 3. MOMS-02 Sensor characteristics

Special emphasis should be given to the wide dynamic range of 6000:1, as well as the charge transfer efficiency of .999999, which assures a high modulation transfer function.

The high data rate of the MOMS-02 channels, gives rise to certain operational limitations during the mission. The maximum data recording rate of the on-board magnetic tape recorder is 100 Mbit/sec, which means that all the channels cannot be operated simultaneously. In order to be able to manage the high data rates, data compression is necessary, especially in the high resolution channel, which is compressed from the original 8 to 6 bits. It was determined that the compression procedure would not impair the ability to interpret the stereo imagery. The multispectral channels can be recorded without compression, with the full radiometric resolution of 8 bits. The adaptation of the image to the current lighting conditions occurs by a switching of the electronic amplification factors.

Table 4 lists the seven operational modes proposed for the mission. In addition to the two purely stereo and multispectral modes, several combinations of these are possible. In modes 6 and 7, only half the high resolution channel (designated by 5A in the table) is used. This limitation of the swath width is due to a limited data rate. The choice of operational mode during the flight is determined by the corresponding overflight landscape type.

MODE	CHANNEL COMBINATION		SWATH (KM)
1 STEREO		STEREO CHANNELS 5 + 6 + 7	37 / 40
2 MULTISPECTRAL	M/S CHANNELS 1 + 2 + 3 + 4		78
3 M/S STEREO	M/S CHANNELS 3 + 4	STEREO CHANNELS 6 + 7	78
4 M/S STEREO	M/S CHANNELS 1 + 3 + 4	STEREO CHANNEL 6	78
5 M/S STEREO	M/S CHANNELS 1 + 3 + 4	STEREO CHANNEL 7	78
6 M/S HR	M/S CHANNELS 2 + 3 + 4	HR CHANNEL 5A	43 / 27
7 M/S HR	M/S CHANNELS 1 + 3 + 4	HR CHANNEL 5A	43 / 27

Table 4. MOMS-02 Operation modes

The magnetic tape recorder allows a maximum recording time of 5.5 hours, corresponding to a data capacity of 2.5 X 10^{12} bits. With this recording capacity, 8-10 million km^2 can be covered, depending on the combination of operational modes used.

Figure 4. shows the MOMS-02 system configuration. The camera, developed by MBB, comprises four modules. These are the optics module with the five lenses and the associated control and read-out electronics for the CCD

sensors, a power supply box, a logic box, and the magnetic tape recording equipment. The magnetic tape recorder is in a sealed container, since during operation, a slight residual atmosphere is necessary.

The entire system is mounted on a bridge structure, and meets free space conditions. Because the bridge is not accessible during the flight, the magnetic tape cannot be changed.

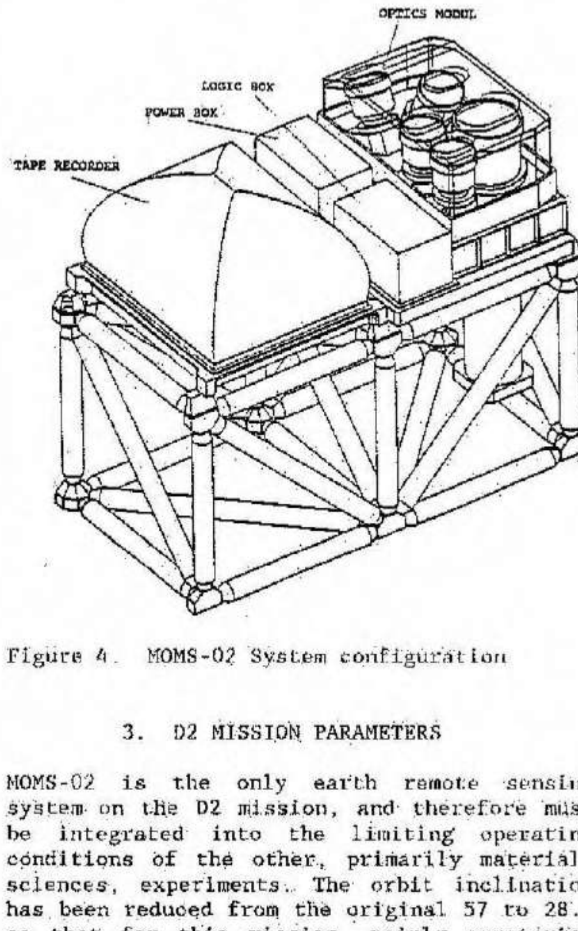

Figure 4. MOMS-02 System configuration

3. D2 MISSION PARAMETERS

MOMS-02 is the only earth remote sensing system on the D2 mission, and therefore must be integrated into the limiting operating conditions of the other, primarily materials sciences, experiments. The orbit inclination has been reduced from the original 57 to 28.5 so that for this mission, mainly equatorial regions will be covered. The current launch date of the STS 52 flight is set for March 1992; the projected launch time is 16:00 UTC.

The necessary recording conditions for MOMS-02, with a solar altitude of between 20° and 70°, will be shifting from the northern latitudes to the south during the course of the mission. Because of this, the overflight surface areas desired for photogrammetric interpretation, are only accessible at the beginning of the mission.

Figure 5. shows a typical orbit path, as well as the borders of the possible coverage area. The boxed-in areas are the regions of primary interest for the scientists participating in the mission.

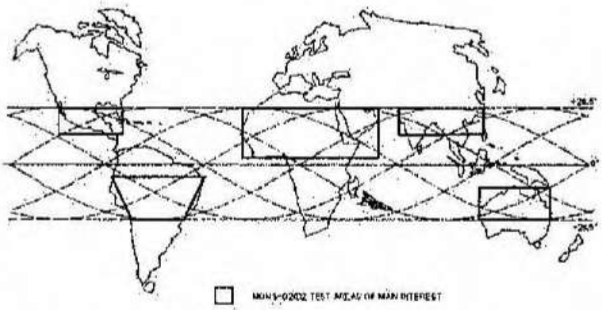

Figure 5. MOMS-02/D2 coverage

4. DATA CONCEPT

During the seven day flight of MOMS-02/D2, a total of about 2 X 10^{12} bits of data, from the operational modes previously described, will be recorded on high density magnetic tape. The recorded tape will be taken out of the container after the landing, and flown to Germany for further processing.

Figure 6. shows an overview of the data processing concept developed for MOMS-02/D2. To get a quick overview of the raw data, a Quicklook data set is planned. This image data set will have a strongly reduced resolution, reduced by a factor of 5 for both the rows and columns. Because of the large quantity of data, it is planned to store the Quicklook data on an intermediate optical disk. From this optical disk, the Quicklook images can be readied for single CCT copies, and/or produced on film. The Quicklook images are to be used, for one, to check the quality of the recorded images, and, for another, to select especially interesting images for further processing. The Quicklook images also represent the groundwork for the preparation of a data catalog, which, for later users, will streamline the selection process of images of interest.

After the Quicklook preprocessing is completed, the actual image processing will begin. The beginning will be the conversion of the HDT data into Level 0 computer compatible form. This process will run on a specially adapted Gould computer. Within this process, the decompression of the data, which was compressed on-board, will take place, in order to restore the original 8 bit format in the three stereo channels. In case the MOMS-02/D2 flight attitude data from the INS navigation system is recorded along with the image data, the plan is to generate a separate CCT with the data conversion, which will also contain

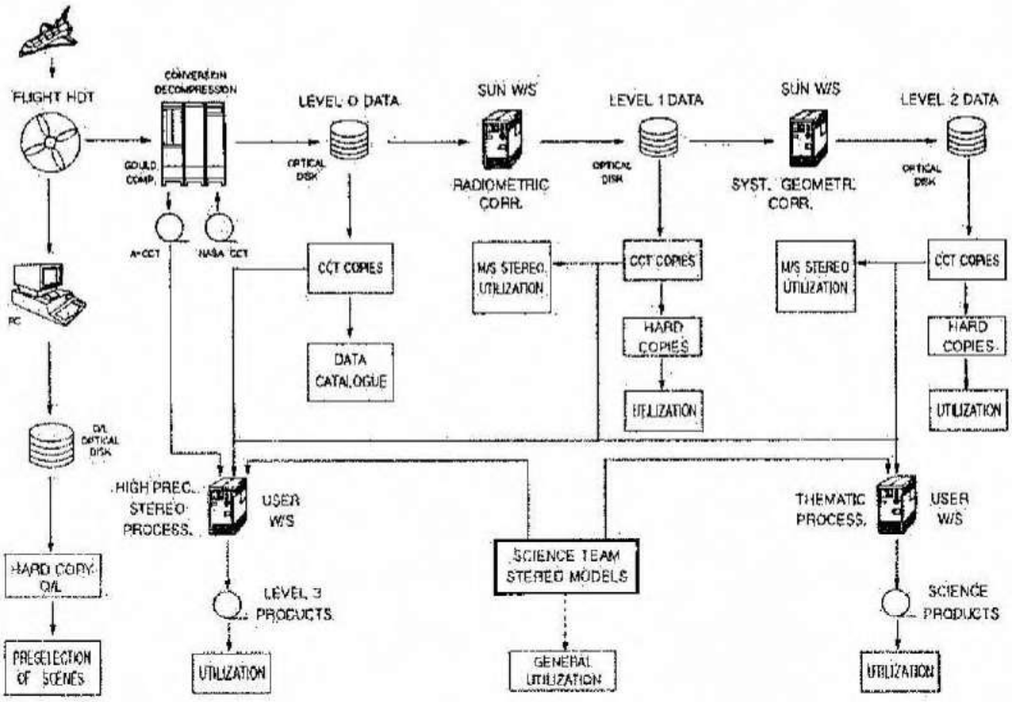

Figure 6. MOMS-02 ground segment

the attitude data. This so-called A-CCT will serve as the input data for later modelling of the Shuttle flight attitude. Additionally, at this first processing point, supplemental data made available to the project by NASA, can be coordinated into the MOMS-02 data stream. The converted data will also be stored on an optical disk, in order to simplify the manageability of the great quantity of data. The data format is compatible with the pertinent DLR standards, since the subsequent image data sets are proposed to be processed on the DLR-WT-DA FIRE system. From there, the data can be distributed to the users.

Just as the first data conversion takes place on a specially adapted mainframe computer, all the subsequent processing steps are planned for so-called workstations. This concept offers the advantage of increased processing speed, which is critical in light of the large quantity of MOMS data. In addition, this concept offers the possibility of more parallel processing. The standardization of the computing concept with respect to routine preparation of the image data, and with respect to the users, simplifies software exchange and to possible editing problems.

The Level 1 data comes about in the framework of the first systematic correction step, whereby the data which had already been radiometrically corrected on board, would undergo any necessary fine radiometric correction on the ground. The data storage will be, as in the previous steps, on optical disk. With the Level 1 data, useable data is available to the users for the first time.
In the next step, systematic geometric corrections, necessitated by the curvature of the earth and the earth's rotation, will be made. The storage and distribution of these systematically corrected Level 2 data conform with the previously described procedures. The project goal is to have the data conversion and all systematic correction completed within a period of one-half year after the flight.

Figure 6. illustrates the general use of the Level 0 through Level 2 data. Because the Level 0 data is of such limited value, the use of the data will be concentrated on the radiometrically and/or geometrically corrected data. In many areas of thematic application, these data are directly usable in image and CCT form.

In the next higher analysis level, for the examination of atmospheric influences or the specification of altitude dependent phenomena, there will be, along with the systematically corrected data, stereo analysis models, drawn upon for the production of level 3A and 3B data.

The production of high accuracy digital landscape models constitutes the core of the MOMS-02/D2 data analysis. Within the framework of preparing for the D2 flight, the necessary software packages will be developed by the Science Team, and will be tested using MEOSS aircraft flight data. An integrated stereo work site is planned to be built within the DLR Institut fur Optoelektronik, where all the software packages from the participating scientists will be integrated. In addition to supporting the specialized work of the participating institutions, this work site will enable users to use all the software packages developed for the project. The Level 4 data products, which in addition to the stereo models, contain the integrated supplementary orbit and shuttle attitude data, represent the scientifically most demanding application of the MOMS-02/D2 data.

The integrated stereo work site will also be available to those users who were not participants in the project, after a successful test phase.

5. SCIENTIFIC GOALS OF THE MOMS-02 MISSION

The scientific guidance of the MOMS-02 D2 project is realized in the form of a Science Team, made up of scientists in the areas of photogrammetry and thematic mapping.

The Team's objectives are to define, from a scientific viewpoint, the necessary requirements for the MOMS-02/D2 hardware, and to oversee its conformance to the MOMS-02 specifications throughout the duration of the project. The Science Team is supported by the project manager. The team defines the scientific goals of the mission and specifies, during the preparations phase, all conditions for the later use of the mission data. With the 3-line arrangement in the panchromatic region, a stand-alone photogrammetric stereo interpretation of high resolution should be possible. The following functions are to be differentiated:

- The possibility of the stereoscopic visual image or the corresponding automatic image processing providing better interpretation, for topographic as well as for thematic contents.

- The high resolution of less than 5 m ground pixel size will afford the manufacture of high quality research maps, and not, as before, at a level of reduced standards of quality.

- Over and above cartographic requirements, MOMS-02/D2 will create an outstanding data source for the production of topographic / geographic data bases and for the development of geographic information systems.

- For the future, the MOMS-02 system will offer the pre-requisites needed to develop photo-maps, that is, photo/map combinations adapted to demanding, specialized points-of-view.

- An original, important task will be the manufacture of digital terrain models with an accuracy of 5 m or better. A significant goal of the mission is to examine and prove this performance capability.

- Independent of other uses, MOMS-02 will be the foundation of the development and testing of a fully digital photogrammetric imaging and analysis system, and thus will lay the groundwork for the digital photogrammetry of the 90's.

The emphasis of the thematic science objective lies in the linking of high resolution stereo data with simultaneously acquired multispectral data. The seven different operational recording modes of MOMS-02 enable the examination of a wide range of differing thematic areas. Scientific experiments can be optimized in different applications over land and over water because of the flexibility of the sensors. Such experiments in the development and testing of analysis models and in the combining of different sensors illustrate the expansion of the utility of remote sensing methods. This expansion will carry through to the solution of problems in the observation and analysis of the changes in our earth's surface. Examples of these problems include desertification, vegetation index, deforestation of the tropical rain forests, geochemical and hydrological changes in the soil, and examination of the concentration of mineral resources. In many international programs (European Community and UN), pilot projects and experimental contributions for the future better use of spaceflight technology can be realized with MOMS-02.

The stereoscopic mode enables connecting digital three dimensional data with multispectral data, thereby improving conventional image interpretation. This connection will allow, for the first time, pilot experiments on synchronously acquired data sets in different applications areas over land surfaces to be carried out. The comparison of images taken from different viewing angles (forwards, backwards, nadir) makes it possible to examine the angle dependence of surface signatures as well as the examination of the surface behavior in coastal oceanographic areas (e.g., transparence or water depth).

MOMS-02, with its modular concept, its variable recording modes, and its high spatial and spectral resolution, enables definition of optical sensors for future operational applications. Special attention in this regard is application to future ecological observation systems in connection with imaging spectrometers such as MERIS and HIRIS.

6. REFERENCES

Meissner D., Seige P., 1985: The Modular Optoelectronic Multispectral Scanner (MOMS-01) Test Flights on STS-7 and STS-11: SPIE Proceedings, Instrumentation for Optical Remote Sensing from Space, Vol. 589, pp 2-8, Cannes, France

Meissner D., 1982: Modular Optoelectronic Multispectral Scanner (MOMS) Development: Paper presented at 20th Goddard Memorial Symposium and 4th Joint AAS/DGLR Symposium, Goddard Space Flight Center, Greenbelt, Maryland

Bodechtel J., Meissner D., Seige P., Haydn R., Winkenbach H., 1984: MOMS-01 on STS-7 and STS-11 - mission and results, Proc. of IGARSS Symp. Strassbourg, France, ESA SP-215, ESTEC, pp. 29-32

Lanzl F. 1989: The Monocular Electro-Optical Stereo Scanner (MEOSS) Satellite Experiment in High Precision Navigation, Springer Verlag ISBN 3-540-50921-6

Lanzl F. 1986: The Monocular Electro-Optical Stereo Scanner (MEOSS) Satellite Experiment: Int. Arch. of Photogrammetry and Remote Sensing, Vol 26-1, pp 617-620, Stuttgart

Ackermann F., Bodechtel J., Meissner D., Kaufmann H., Seige P., Winkenbach H., 1988: Development of MOMS to a future multiband and stereoscopic sensor. Proc. of the Int. Symp. of Spectral Signatures of Objects in Remote Sensing, Aussois, France, Jan. 18-22, ESA SP-287, ESTEC, pp 479-482

Meissner D. 1989: Critical Design Review of MOMS-02 for D2 Mission, Doc. No.: MOMS-02.RP.0020, MBB Muenchen

Ackermann F., Bodechtel J., Dorrer E., Ebner H., Kaufmann H., Koch B., Konecny G., Lanzl F., Seige P., Winkenbach H., Zilger J., 1989: MOMS-02/D2 Wissenschaftsplan, DLR pp 85

PREPARING THE USE OF ERS-1 DATA FOR TROPICAL FORESTS SOIL MAPPING

Frédérique Seyler and Boris Volkoff, ORSTOM, Cameroon

ABSTRACT:

An airborne SAR experiment has been carried with a C-band radar (DLR system, German Aerospace Research Establishment, Germany) to prepare the use of high resolution imaging SAR which will be launched with ERS-1 satellite.

The aim of the study is the evaluation of the microwave data use for the mapping of South Cameroon forest lateritic soils. The scale of topographic and thematic data which are needed for this mapping have to be compatible with the size of the lateritic systems spatial variations. Usually, in yet unknown regions, aerial photographies are in use. For humid tropical areas, this usual method cannot be improved due to the everlasting clouds cover.

A first experiment has been carried out in the south of France on a forested area of medium size relief, seeming for the topography and the thick forested cover to the South Cameroon modeling. The C band SAR data, acquired in August of 1989, have been tested by a comparison with the great amount of auxiliary data available for the chosen area (soil map, vegetation map, digital terrain model, SPOT image data).

(Original not received in time for publication)

SPOT 2 - FIRST IN-FLIGHT RESULTS

Patrice Henry, CNES, France

ABSTRACT:

SPOT 2, the second satellite of the SPOT family, will be launched mid-january 1990.

A two month check out period is foreseen, to perform an overall assessment of the image quality both in terms of geometric and radiometric performances, and to confirm the good results of the ground tests.

This paper presents the very first in-orbit results, and a comparison with the system specification allows to verify how the requirements are met. As far as service continuity is concerned, the SPOT 2 results are compared to SPOT 1. A particular emphasis is put on the oportunity of using easily both SPOT 1 and SPOT 2 data for a given application.

Thus, the follow-on of the SPOT program ensures, to the remote sensing community, the long term availability of high resolution images.

(Original not received in time for publication)

International Mapping and Remote Sensing Satellite Systems

INTERNATIONALIZATION OF REMOTE SENSING

Yvonne C. Lodico
United Nations
New York, NY
USA

ISPRS number 199

Abstract

The remote sensing industry is rapidly expanding, governments, private entities, research institutions, database services, to name a few, will invest hundreds of millions of dollars in the technology. Considering the global coverage of remote sensing systems and their data and the ever increasing interdependence of economic, environmental and political systems, international cooperation is essential. Thus, to make the operation of the satellite systems financially profitable, to avail the systems to all possible users, particularly to those in the developing countries and to promote international harmony, the establishment of cooperative arrangements among national organizations and private entities will promote the widest application and the most successful ventures in using remote sensing to monitor our Earth's environment.

Introduction

Following the launch of the Landsat satellite in the early 1970's, new earth observation remote sensing systems were launched that introduced different sensors and quality of resolutions that expanded the amount of data and information about our environment and natural resources. In almost twenty years, the remote sensing industry has grown tremendously, representing a significant element of the international space business with revenues expected in the billions for the 1990's. Despite the technological progress in remote sensing, obstacles exist. These obstacles include developing the remote sensing systems, educating users about the data and establishing legal standards. These obstacles result from the fact that designing, launching and using a sophisticated satellite remote sensing system is a very costly enterprise. Also, the present and potential user community have diverse needs and have various preferences for legal norms. Therefore, this paper reviews present availability of earth resource remote sensing technology, the market for the data, the existing international legal and political structure regarding access to data, and some relevant international cooperative organizations that may offer insight to promoting international use of remote sensing.

This paper does not necessarily represent the views of the United Nations.

Current and Potential Use of Remote Sensing Systems

Since the launch in 1960 of the United States TIROS (Television and Infra-Red Observations Satellite), the first dedicated meteorological satellite, better and more diverse images have been obtained from space about the Earth's surface. Although other meteorological satellites were launched, including the Soviet Cosmos and Meteor satellites, in 1972, the United States launched the first satellite designed to conduct remote sensing, the Earth Resources Technology Satellite, (ERTS) or as it became known, the United States Civil Land Observation and Satellite Programme (LANDSAT). Following Landsat 1, the United States government launched Landsats 2 and 3, and in the 1980's it launched Landsats 4 and 5 that provided higher resolution (30m) thematic mapper sensor in addition to the original multi-spectral scanner (80m). The Landsat system is expected to continue with the launching of Landsat 6 in 1991.

In 1974, the USSR launched its Earth observation system with the Meteor-Piroda series. Also, the Soviet Union carried out extensive Earth observations programs during several manned Soyuz and Saylut missions with a sophisticated Multispectral Cosmic Photographic (MKF) camera developed jointly with the German Democratic Republic. Also, the Soviet Union obtains data currently from the MIR space station and Resurs satellite using the KFA-1000 camera that produces very high (up to 2m) resolution. (Space News). Other remote sensing satellite systems include the French remote sensing satellite SPOT first launched in 1986. To ensure continual operation of the Spot system, France launched Spot 2 in January 1990. The Spot system provides high resolution (10 m and 20 m) and allows varying observation angles which offer the advantages of repeated observation and stereoscopic viewing. In 1988, India launched its remote sensing satellite, the Indian Remote sensing Satellite (IRS), that carried sophisticated instrumentation and with a ground resolution of 72m and 36m in the visible and near-visible infra-red regions. Also, the European Space Agency (ESA) has carried two major remote sensing experiments on the Spacelab and expects to launch its Earth Resource Satellite (ERS-1) in late 1990 to provide an all-weather remote sensing facility capable of observing and monitoring the ocean, coastal zones, land and polar regions using microwave technology. The ERS-1 will comprise a complex systems of sensors including a synthetic aperture radar for improved meteorological information system through the collection data on weather conditions above the oceans. Other systems for the very near future include the Canadian Radarsat planned for launch in 1994 to provide for a space based radar system exploiting the applications of synthetic aperture radar and the Japanese Earth Resource Satellite (JERS-1) and Advance Earth Observation platform, ADEOS, planned for launch in 1995. Thus, since the launching of Landsat, the availability and quality of earth observation remote sensing data have increased tremendously and with expected international launches of remote sensing satellites in the 1990's there will be even greater and more diverse amount of data.

Market Potential

With the advent of remote sensing technology, land use planners, meteorologists, environmentalists and other development specialists, have expanded their knowledge about the quality and extent of the Earth's natural resources. In addition, private entities and local governments are beginning to apply remote sensing data. According to a United States Commerce Department study (Department of Commerce) the revenue from sales of non-enhanced and value added data will grow from $7.2 billion to $9 billion dollars from 1987 to 1997.

Major commercial users of remote sensing include oil and mineral exploration concerns, engineering and construction companies, agribusiness, forestry, ocean transport and fishing industries, land development, cartography, research and academic community, state and local governments. In addition to serving commercial needs, it is possible through remote sensing to monitor the effects of commercial activities such as the movement of oil slicks to icebergs, the effects of acid rain on forests and lakes, and the influence of ground erosion on farmlands. Also, the legal profession has discovered that remote sensing can provide supportive evidence in cases dealing with illegal waste dumping, oil and gas disputes and in alternative dispute resolution cases. (Marks, B.) In addition, the development of Geographic Information Systems (GIS) that can combine remotely sensed data with other types of data such as a map, census, and property ownership is expected to accelerate demand. There are over 20 state operated systems in the United States, many universities have implemented a GIS and within the United Nations there are several remote sensing data bases, such as the United Nations Environment Programme's Global Resource Information Database (GRID) and the Global Environmental Monitoring System (GEMS). Therefore, economic potential for various applications is great and should increase with greater knowledge about the applicability of the data.

Commercialization

With such grand market revenue projections, national governments have established private (or quasi-private) commercial companies to market remote sensing data.

The United States Land Remote Sensing Commercialization Act represented the first effort to completely commercialize a remote sensing system. To ensure against exploitation of the conversion of remote sensing data to a commercial commodity, the act specifies that private company must provide for nondiscriminatory access to unenhanced, civilian data for all potential users, and must honor its international obligations (See Land Remote Sensing Commercialization Act of 1984, 15 U.S.C. secs. 4201-4292 Supp. 1989). The Act provided for the sale of Landsat to the private sector, with the intention that Landsat 5 would be the last remote sensing satellite fully that the United States government would fund. The government awarded the Earth Observation Satellite Company (EOSAT) the contract to assume operation and market Landsat products. Although the Landsat almost came to a termination, funding was renewed and United States government will construct Landsat 6.

Other nations support remote sensing commercial activities. Although the French CNES owns Spot, the private company, Spot Image manages, markets and distributes the data. Since its inception, Spot Image sales have risen steadily, from $3 million in 1986 to $22 million in 1989 and the company expects a 25 per cent growth over the next three years. (Space News). Also, the Soviet Union has established a marketing company, Soyuzkarta, to distribute its remote sensing data. It is likely that as other governments implement new remote sensing systems they will establish some type of commercial mechanism to market and sell the data.

The Legal Order for Remote Sensing Activities

With the widening use of remote sensing data, international legal and political implications have intensified over access and ownership of sensed objects or territories. Due to its wide scope of coverage, remote sensing affects practically all nations, either as operators, users or objects of remote sensing applications. Nations have differed over who has the right to retrieve sensed data, who may distribute it and whether a sensed state should have any priority over access to the data about its territory.

The exploration and use of outer space is a global problem affecting the entire international community. Therefore, the United Nations has provided the forum for establishing rules and treaties governing activities for outer space, including remote sensing. Since 1971, following the United Nations General Assembly Resolution 2778, (U.N. Doc. A/RES/41/65, 22 January 1987) the Committee on Peaceful Uses of Outer Space (COPUOS) has included the agenda item of satellite remote sensing. In attempt to establish a legal order for remote sensing, the United Nations General Assembly in 1986 adopted resolution 41/65 entitled the <u>Principles Relating to Remote Sensing of the Earth from Space</u>.

The Principles on Remote Sensing derive from the doctrine set forth in the various outer space treaties. According to Principle I, the term "remote sensing" as the sensing of the Earth's surface from space for the purpose of "improving natural resources management, land use and the protection of the environment." Principle I also defines the terms primary data, processed data and analyzed information. Principle II requires remote sensing activities to be carried out for the benefit and in the interests of all countries. This is similar to article 1 in the Outer Space Treaty (1967 Treaty on Principles Governing the Activities of States in the Exploration and Use of Outer Space, Including the Moon and Other Celestial Bodies) that calls for the exploration and use of outer space, including the moon and other celestial bodies, to be carried out for the benefit and in the interests of all countries." Principles III and IV essentially provide that remote sensing should be conducted in accordance with international law, Principle IV adds that remote sensing activities should not be carried in a manner that is detrimental to sovereign rights. Principles V through VIII generally call on states to cooperate in equitable and mutually acceptable terms. Principle IX provides that states conduct their remote sensing programs according to Article IV of the Registration Treaty (1974, The Convention on Registration of Objects Launched into Outer Space) and Article XI of the Outer Space Treaty.

Also, the Principles contain general provisions regarding a state's sovereign rights over information about its resources. According to Principles X and XI, sensing states need to disclose any information that would assist another state to avoid or mitigate a natural disaster or avoid harm to the Earth's environment. Principle XII, considered critical to the Principles, provides the sensed state with access to the primary and processed data concerning its own territory. The remaining Principles require states to consult with sensed states to provide ways for their participation (XIII), recognizes states responsibility for national remote sensing activities in space (XIV), and provides for a dispute resolution mechanisms through established procedures (XV).

The Principles on Remote Sensing establish a fairly broad mandate and leave unclear the issue of sovereignty and territorial jurisdiction and the role of private operator as it relates to sensing of natural resources (DeSaussure, H. 1989). Principle IV's provision that calls for states to not conduct their activities in a manner detrimental to rights of states over their own natural resources raises a question about national sovereignty, that is, the extent that information about natural resources applies to territorial jurisdiction over natural resources. Principle XII that provides for equal access to the data, may imply that a sensed state does not have priority over data about its own natural resources. It also leaves ambiguous proprietary rights over analyzed information. Principle XIII requires only states to consult with other sensed states, it does not address the role of the private sector and whether the private operator has a duty to consult with a target state. Also, Principle XV provision for dispute resolution may not be relevant for a private company that may avoid taking a claim to foreign court system.

For comparison, remote sensing laws in the United States Landsat Act illustrate a national government's effort to establish a legal regime for remote sensing. With the establishment of this Act, two policies of "Open Skies" and "Nondiscriminatory Access to Data" became law. The "Open Skies" policy is based on the principle that non territorial sovereignty extends into outer space (National Aeronautics and Space Act of 1958, 42 U.S.C. secs. 2451-2484 Supp.V. 1987). This is similar to article 1 of the Outer Space Treaty. The Act also embodies a policy of Nondiscriminatory Access. According to the Act, unenhanced data (15 U.S.C. sec. 4204 supp.II 1984), data that is "unprocessed or minimally processed signals or film products collected from civil remote sensing space systems must be made available to all potential users "without preference, bias or any other special arrangement... regarding delivery, format, financing or technical considerations that would favor one buyer or class of buyers over another." The same information that a foreign nation could receive, an private company could also receive at the same price.

The governments of developing countries, that do not have the financial resources to purchase remote sensing data or the technological capabilities to process and interpret the data have an unfair advantage. Even though the data is made equally available to all nations, some nations lack the ability to analyze the data. For some countries, outsiders with access to remote sensing data may know more about the third world and its resources than nations do themselves. This is the reason that developing countries urged the right prior consent to the sensing, as well as the right of first access to the data. The Land Remote Sensing Commercialization Act rejected the right of disclosure. To ensure, however, that remote sensing remains within the bands of international law, the United States Landsat commercialization provides the Secretary of State with the requisite authority for ensuring that private commercial earth remote sensing activities are conducted in strict accordance with recognized international space law.

Obstacles

The future growth for remote sensing may depend largely upon educating the potential buyer because many potential buyers do not yet know how to use the data nor do they appreciate its applicability. For developing countries, the obstacle are worse in terms of education due to the costs and lack of training in the use of the data. Remote sensing data, however, are particularly pertinent for their economic development as well as for the support of the world's ecological balance.

In addition to data dissemination and education obstacles in developing remote sensing systems, a remote sensing system requires exorbitant financial and technological commitments. Along with the satellite system that can cost over $200 million, the sensed data that is transmitted to Earth require special ground receiving station equipped with suitable decoding facilities are needed. Earth observation satellites such as the United States Landsat missions require ground stations that cost about $15 million in capital investment, with annual expenses running at a level between $1 and $2 million. In addition, to use these facilities requires fairly advanced technical and scientific knowledge.

The enormous technological and financial investment for a remote sensing system even hinders commercialization efforts. The United States Landsat program, despite the establishment of Eosat and the mandate of the Landsat Commercialization Act, has nearly terminated on several occasions. For a purely private company to stay competitive, it is necessary to invest in new spacecraft to deliver timely high resolution products. At the same time, a private company must sell lots of products and make a profit and this is difficult in light of competition from other companies that receive support, financial, technical and political, from their governments. Therefore, it appears that the requisites for building the remote sensing industry require more than commercialization, but also some form of cooperative arrangement with a governmental or international institution.

In addition to the technological and cost aspects, no uniform regulations exist. As more nations launch and develop remote sensing programs, their domestic laws governing their remote sensing systems will extend along with the remote sensors beyond territorial borders. To ensure international harmony, norms and standards for international compatibility must exist. In an effort to implement international guidelines for remote sensing activities the United Nations established the Principles for Remote Sensing. The United Nations Principles, though provide for a basis for international cooperation, do not establish any mechanism for international order of remote sensing. These obstacles point to the need for establishing some form of international coordination or cooperative for remote sensing.

Promoting Internationalization of Remote Sensing - Cooperative Arrangements

To ensure the widest possible use of remote sensing technology, multinational or even bi-national alliances may facilitate technological development and data distribution. Within the United Nations, there are various programs initiated to assist developing countries. The United Nations Outer Space Affairs Division, as part of its Programme on Space Applications sponsors meeting, seminars, training courses and workshops on remote sensing for participants in developing countries. Its efforts are often in cooperation or collaboration with other United Nations organizations and specialized agencies. Not one international organization, however, deals specifically with space-borne remote sensing activities. It is possible, however, that some type of international cooperative arrangement could be established and those organizations like INTELSAT, INMARSAT or ESA may offer some insight in establishing such an arrangement. Although established outside of the United Nations, these institutions have incorporated the basic tenets of international space law that the uses of outer space should benefit all mankind.

The launching of communications satellites and the anticipated demand for international communications prompted the establishment of the International Telecommunication Satellite Organization (INTELSAT). With the interim agreement signed in 1964 and the definitive arrangements signed in 1971, the organization's purpose is to make available global communications on a non-discriminatory basis in light of the technical and operation expertise and significant level of financial investment required for satellite communications.
The organizational operates as a not-for-profit cooperative, with its ownership and investment to finance capital expenditures based on actual use of the system. Revenues which derive from utilization charges, with all users paying the same charges, are distributed to Signatories in proportion to their investment shares.

The structure involves both governments and telecommunications entities. The organization has a four tier structure consisting of Assembly of Parties, The Meeting Of Signatories, the Board of Governors and the Executive Organ. The Assembly of Parties consists of sovereign states and considers general policy. The Meeting of Signatories of the Operating Agreement considers future programs and their financial implications. The Board of Governors, is responsible for the design, development, construction, establishment and operation of the INTELSAT space segment. The organization began with 11 nations signing an interim agreement and at the end of 1989, more than 117 nations belonged to INTELSAT.

The International Maritime Satellite Organization (INMARSAT) established in 1979, provides satellite telecommunications services for the shipping and the off-shore industry, including communications for distress and safety at sea, efficiency and management of ships and aircraft, maritime and aeronautical services. The objective of INMARSAT is similar to that of INTELSAT in that its seeks to provide global, though for maritime use, communications to all users on a non-discriminatory basis. Therefore, the users of INMARSAT, do not pay a differentiated scale of charges and regardless of level of development, they can benefit from the use of satellite technology.

Although the organization operates also as a cooperative, it has the characteristic of being both public and commercial enterprise in that each INMARSAT Party is required to either sign the Operating Agreement or to designate a competent entity, public or private, subject to the jurisdiction of that Party. The Organization is required to operate on a sound economic and financial basis having regard to accepted commercial enterprise. Like INTELSAT, Signatories, in proportion to their investment shares, receive capital repayments and compensation for use of capital. Unlike a commercial enterprise, however, when there is a surplus of revenues, space segment utilization charges must be reduced. The structure consists of an Assembly of Member states to consider policy, a Council composed of Signatories that donate the largest investment shares together with four members to ensure equitable representation, and a Directorate that is responsible for operating the communications system.
private

To promote European cooperation and use of outer space, a Convention was ratified in 1980 to form the European Space Agency (ESA). Presently ESA includes 13

Member States: Federal Republic of Germany, Austria, Belgium, Denmark, Spain, France, Ireland, Italy, Norway, the Netherlands, the United Kingdom, Sweden, Switzerland and an Associated State, Finland. Canada is bound to ESA though a cooperative agreement and participates in several optional agreements. Like INTELSAT and INMARSAT, ESA seeks to ensure equitable representation. The average income of Member States is calculated to form the basis for determining contributions to the budget and each state, regardless of its financial and technological capabilities, has one vote for matters concerning finance, science and technology, unless the vote is on an optional program. According to ESA's Convention, however, for optional programs, such as the ERS-1, only participating States vote and finance optional programs.

Conclusion

Although not all countries have equal technological access, they are part of and participate in the international, interdependent framework. Thus, it seems that remote sensing information that provides global coverage, detecting all the various elements of the world's resources as well as the changes that we cause, should receive the greatest international utilization.

In other areas of space technology, international cooperative arrangements have been established. These organizations haved operated successfully, in terms of financial and international cooperation, because of the need for efficient communications technologies. Although INTELSAT, INMARSAT and ESA are institutions outside the United Nations structure, they have an affect on the harmonizing international space co-operation.

In addition to well established international cooperatives, however, there is growing trend for multinational space efforts. Due to the level of financial and technological expertise required for space projects, governments have found that they need to collaborate. This requisite, along with international efforts and legal support, may set the foundation for cooperative arrangements for promoting the internationalization of remote sensing.

References

Bourley, M. 1988. Legal Problems Posed by the Commercialization of Data Collected by the European Remote Sensing Satellite ERS-1. J. of Space Law. 16:2, 130-146.

de Cerf, P.L. 1987. International Satellite Telecommunications and EEC Law. Proceedings of the 30th Colloq. on the Law of Outer Space. 341-349.

Danilenko, G. 1989. International Law-making for Outer Space. Space Policy. 321-329.

Department of Commerce, Office of Space Commerce, An Industry Assessment, p. 69, 1988.

DeSaussure, H. 1989. Remote Sensing Satellite Regulation By National and International Law. Rutgers Computer & Technology Law Journal. 15:351-381

Marks, B. 1989. Dispute Resolution in the Space Age: Forensic Applications of Earth Observation Satellite Data Through Adaption of Technical Standards Similar to DNA Fingerprinting. Journal of Dispute Resolution. 5:1 1989

"Remote Sensing Market Place Becomes Crowded" Space NewsApril 16, 1990, p. 18)

Global Monitoring

A Review of Remote Sensing for Tropical Forest Management to Define possible RADARSAT contributions

F. J. Ahern
R. K. Raney
Canada Centre for Remote Sensing
1547 Merivale Road
Ottawa, Ontario, Canada

R. V. Dams
Intera Technologies, Ltd.
Calgary, Alberta, Canada

D. Werle
Aerde Environmental Research
Halifax, Nova Scotia, Canada

ABSTRACT

Approval of RADARSAT for construction and launch brings the dream of an active microwave satellite dedicated to operational earth resources management closer to reality. Following the example of the Landsat and SPOT series, RADARSAT is designed to make remotely sensed data available to earth resources managers on a routine basis at a reasonable cost.

Tropical forests are one of Earth's most valuable resources, from both economic and ecological perspectives. Their large areas and frequent cloud cover make them promising candidates for management strategies which incorporate RADARSAT data. Optical satellite data should also play an important role provided less frequent coverage is acceptable.

We have reviewed much of the published literature concerning the use of optical and microwave data for vegetation assessment in the tropics, and discuss how both data sources can contribute information for mapping and monitoring of resources over a very wide range of scale and coverage.

RADARSAT will provide data in three basic modes: ScanSAR (500 km swath, 100 m resolution), Standard (100 km swath, 28 x 30 m resolution), and High-Resolution (55 km swath, 8 m resolution). This range of capabilities, coupled with frequent revisit possibilities, will enable RADARSAT to contribute to tropical forest resource management over the full range of scale and coverage. We have also identified information which can be provided by low and high resolution optical satellite sensors and by airborne SAR.

In order for RADARSAT and other data sources to become an integral part of tropical forest management, work is required to better understand the information content of these data sources, to develop information enhancement and extraction techniques, and to foster technology transfer to agencies with mandates for tropical forest management.

1. INTRODUCTION

Tropical forests are one of Earth's most valuable resources. From an ecological perspective, they play a major role in the hydrological cycle and in recycling atmospheric carbon dioxide. They stabilize soil and prevent excess runoff of silt and dissolved substances into streams. Their effects on climate through energy and water exchange with the atmosphere are not well understood but are expected to be very significant. Much of the Earth's species diversity is represented by the plants and animals which make up tropical forest biomes.

The alarming rate of destruction of tropical forests has been widely documented and publicized (Myers, 1986, Nelson, et al., 1987, Repetto, 1988 and 1990, Booth, 1989, Ellis et al., 1988, Wilson, 1989). For most tropical countries deforestation has become a drain of an increasingly valuable resource. Local and overseas interests alike have over-exploited forest resources. Failure to collect royalties, export taxes, and related fees has led to a cronic undervaluation of tropical forest resources (Repetto, 1990).

The pattern of tropical forest conversion varies from one country and region to another. In some cases there are deliberate conversions to small or large scale farming or ranching. In other cases clearcutting is practiced, or partial harvesting of commercially valuable trees causes enough damage to prevent recovery of the original forest. In yet other cases, construction of roads, canals, or railways permits access into previously sparsely populated areas, and the subsequent influx of migrant farmers causes degradation of the original forest environment.

In most cases tropical forests are much less likely to regenerate to their pre-disturbance plant and animal communities than temperate latitude forests because of severe loss of nutrients, seed sources, and vitality, vigourous competition by early seral species, the inability of late seral, shade tolerant species to become established in large open areas, and the lengthy time required to reach climax stability.

While it is apparent that improved management of tropical forests requires substantial economic, political, and institutional changes, it also requires additional information about the forests themselves and changes which are happening in and around them. Much of the additional information can be supplied by satellite and airborne remote sensing systems (with adequate field checking).

The purpose of this paper is to identify some of these information requirements for tropical forests, and examine the contribution that the Canadian RADARSAT system may make in conjunction with other readily available data sources.

2. POTENTIAL ROLES OF REMOTE SENSING

Information about tropical forests is required over a range of areas and levels of detail. In other words it is a multiscale problem which must be addressed with sensors having a range of fields of view and spatial resolutions. International agencies such as the United Nations Food and Agricultural Organization, the World Bank, and the World Resources Institute require "strategic" data at national, continental, and global scales (10^6 and smaller). Global scale environmental programs such as the International Geosphere Biosphere Program and the National Aeronautics and Space Administration Mission to Planet Earth also require data at continental and global scales. These organizations place considerable emphasis on monitoring activities. For these organizations, data must be acquired frequently, when needed, not when weather may permit. Frequent, reliable coverage is essential.

Sound tropical forest management by national and state agencies begins with regional baseline data about undisturbed areas before development if at all possible. Information about topography, geomorphology, drainage networks, and vegetation cover requires data with higher spatial resolution, on the order of 10 to 100 m, than that considered by the international agencies. However, the area to be covered for specific sites is smaller. A baseline inventory does not need frequent temporal coverage, so the data volume remains manageable. Once an area is opened to human access, changes in vegetation cover are often rapid. Frequent, reliable coverage of active areas at high resolution is required. At the same time, there is often a requirement to monitor changes on a regional scale (state/province, and nationwide) for governmental resource management and policy formation.

In order to assess the potential contributions of remotely sensed data to effective tropical forest management, we have reviewed published accounts describing applications of optical and microwave data sources to tropical forest management.

Our review, although by no means complete, includes accounts of aerial photography, the Landsat Multispectral Scanner (MSS) and Thematic Mapper (TM), and the Système pour l'Observation de la Terre (SPOT), as well as reports of airborne and spaceborne imaging radar data. Proven abilities and limitations of various optical and microwave data sources are indicated, leading to predicted roles of RADARSAT in combination with other readily available data sources.

2.1 Studies with optical data

Aerial photography Aerial photography has been used in the tropics for many years, just as in temperate latitudes. The difficulties of storing and using film in hot humid environments are described by Leshack (19??). Additional problems such as frequent cloud cover and turbulent air are well known and also mentioned by Leshack. These problems have meant that aerial photography has been much less extensively employed in the tropics than in temperate latitudes. Nonetheless, it seems safe to say that aerial photography of tropical forests can be acquired if it is essential, given sufficient patience and persistance, and a budget which can accommodate high standby costs.

As in temperate latitudes, aerial photography is particularly useful for information regarding vegetation inventories, including species composition (Myers and Benson, 1981, Stellingwerf et al., 1986) and for environmental and forest resource management plans (Terchunian et al., 1986). Large scale photography can also be used for forest mensuration, such as heights and diameters of crowns (Aldred, 1976). However, crown diameter generally cannot be used to infer trunk diameter, as is often possible in temperate latitude forests. The review by Stellingwerf et al. also demonstrates the use of aerial photography for mapping mangrove forests, forest damage and drainage, mapping plantations, and detecting and mapping roads and land use change.

Landsat Multispectral Scanner Data The ready availability of Landsat Multispectral Scanner (MSS) data following the launch of Landsat 1 in 1972 resulted in a significant number of studies and attempts to use that revolutionary new data source for tropical forests. Many of the early results were reviewed by Baltaxe (1980 and 1987). The majority of successful applications of Landsat data to tropical forestry have relied predominantly on visual interpretation of black-and-white single band images, colour composites, and computer enhanced colour images.

Stellingwerf et al.,(1986) illustrated the use of Landsat MSS data in tropical forests. They showed how MSS data could be used to map broad vegetation classes in Indonesia and Colombia, as well as vegetation change and land use change in Colombia.

As in temperate latitudes, Landsat MSS data have been found particularly well suited for mapping broad vegetation classes in previously unmapped areas. Examples of successes for this application have been documented in Brazil (Novaes, 1979), Bolivia (Baltaxe, 1980), Papua New Guinea and the Phillipines (Williams and Coiner, 1975), and Peru (Sadowski and Danjoy, 1980), while Keech et al.,(1978) used Landsat MSS data for a more detailed vegetation inventory in Brazil.

Mangrove forests represent a particularly important but threatened resource in many parts of the tropics. A number of studies, including one by ERIM (1979) have demonstrated that the Landsat MSS can be used to map mangrove forests.

Landsat MSS data have been utilized for mapping regional drainage networks and roads in Indonesia (Stellingwerf et al.,1986).
Changes in vegetation related to agricultural conversion, settlement, and harvesting have been interpreted in Landsat images of Columbia (Stellingwerf et al.,1986), Brazil and Thailand (Baltaxe, 1980).

Joyce and Sader (1986) have reviewed studies of Landsat MSS data for deforestation in the tropics and conclude that forest clearing can be detected and mapped at scales of 1:200 000 and smaller, for detecting plantations of 4 ha and larger, but that it has only marginal utility for partial cutting, successional changes or detecting changes caused by insects, disease, or other stress agents.

Landsat Thematic Mapper and SPOT HRV Data
Relatively few results have been published of studies with the Landsat Thematic Mapper and SPOT HRV sensors for tropical forestry applications. Those that have appeared suggest that the significant increase in capability of these sensors relative to the MSS will generally be valuable in the tropics.

Rosenqvist et al.,(1989) used three dates of Landsat TM, MSS, and SPOT imagery to identify deforested and landslide-affected areas in Thailand. The intent was to identify the causes and effects of the heavy rainfalls, flooding, and severe landslides that had affected a large area in southern Thailand. Digital analysis techniques were used to show that over 3500 ha of forest had been cleared, and bare soil exposure had increased by over 230% during the four year monitoring period prior to the disastrous flooding and landslides.

Guillon (1989) used Landsat TM (Bands 2,3 and 4) for pine plantation mapping in inaccessible areas of Argentina. Broad classes of pine plantation cover, age, and densities could be identified on the TM imagery.

Artieda (1989) analyzed multitemporal Landsat MSS and TM imagery in the Ecuadorian Amazon for the purpose of deforestation monitoring between 1977, 1985, and 1986. Both visual and digital analyses were employed to identify 16 different forest and land cover types, which were compressed to six types (forest, cultivation, forest/pasture, pasture/cultivated, open water, wet areas) for the purpose of change detection between years. A 58% reduction in forest cover was measured between 1977 and 1986. The large area covered per scene, the periodic revisit of the same study areas, ease and efficiency of the digital analysis approach and cost effectiveness compared with conventional air photo and field approaches were listed as definite benefits.

Ekstrand (1986) was able to map 8 vegetation classes with the Thematic Mapper in Ethopia, compared to only 4 with the MSS. Both visual and digital techniques were combined to give 80% classification accuracy.

Wilkie (1990) used TM data to detect and map small settlements near the Okapi Rain Forest Reserve in Zaire. The author was able to distinguish active from abandoned settlements, and also to suggest which of the settlements were agriculturalist, and which were gold miners' camps.

Khan et al. (1983) found that visual interpretation of simulated SPOT multispectral images could be very effective in monitoring the condition of mangroves in the Ganges delta of Bangladesh. They were able to detect deforestation, afforestation, original forest, dykes, roads, and other features important for this densely populated and vulnerable area.

Low Resolution Optical Sensors With increasing concern over tropical deforestation, researchers have examined data from a number of low resolution, wide area sensors to explore the utility of these instruments to provide timely information over wide areas for national and international agencies.

Their findings, plus others not specifically mentioned, are summarized in Table 1. This summary is not intended to be exhaustive, but simply to portray the most important applications which have been demonstrated with optical sensor data when applied to tropical forests.

Justice et al. (1985) demonstrated that low spatial resolution, high temporal frequency AVHRR data are useful for monitoring temporal dynamics for the entire globe. Normalized vegetation index images were analyzed to study the phytophenology of the African grasslands, Indian tropical forests, and forest clearance in Brazil. Nelson and Holben (1986) compared three low resolution data sources (1 km AVHRR, 4 km AVHRR, and data from the spin-scan radiometer on the Geosynchronous Operational Environmental Satellite, or GOES) with the Landsat MSS for detecting forest clearings in Brazil. They found the GOES and 4 km AVHRR data to be too coarse for meaningful estimates. However, they found that the 1 km AVHRR data could be used to map forest clearings in Rondonia adequately.

Building on Nelson and Holben's work, Woodwell, et al., (1987) used the MSS to determine the forest/non-forest threshold in AVHRR band 3 radiance and then used the AVHRR scene to estimate the deforested area for the entire state of Rondonia. Their estimate was consistent with other data sources.

Matson and Holben (1987) investigated the use of AVHRR data for detection of tropical burning. They showed how band 3 (3.55 to 3.93 micrometres) can detect sub-pixel fires, while the use of bands 3 and 4 (10.30 to 11.30 micrometres) can be used to estimate both the temperature and area of the burn. They found that the larger burns were associated with decreased values of the Normalized Difference Vegetation Index (NDVI, the difference between the band 2 and band 1 intensities, divided by their sum), indicating a decrease in vegetation greenness in areas which had been extensively burned.

Malingreau and Tucker (1987) summarized the main contributions of the AVHRR sensor as detection of fires and detection of cleared areas over wide regions of active forest clearing. They indicate that band 3 is more suitable than the NDVI for differentiating cleared from uncleared areas.

2.2 Studies with microwave data

The advantage of radar remote sensing to operate independently of solar illumination and in areas of persistent cloud cover, such as the tropics, was demonstrated in the successful completion of the first imaging radar mission over Darien Province of Panama in the late 1960s (Wing, 1970).

Numerous studies of the application of radar remote sensing in the tropics have been carried out since then. Most of the tropical experience with radar has been "on the job learning" as part of operational surveys, in contrast with temperate latitude studies, which have been generally of a formal research nature. A few reviews of the use of radar for forestry applications have been published, including those by Churchill et al., 1985, Simonett et al., 1987, and Werle, 1989b.

Airborne SAR and SLAR surveys Airborne Synthetic Aperture Radar (SAR) and real aperture Side Looking Airborne Radar (SLAR) imagery of tropical areas around the globe have been acquired during more than 50 major commercial reconnaissance surveys, employing mainly X-band SLAR and SAR systems with HH polarization and to some extent a K_a-band SLAR system with HH and HV polarizations. Regional and nationwide surveys in Southeast Asia, and Africa as well as Central and South America to-date exceed more than 15 million km^2 in areal coverage. With the exception of more recent investigations employing digital SAR data, image analysis procedures have mainly relied on visual interpretation techniques. During the 1970s, most data sets were collected by the Westinghouse SLAR, the Motorola/MARS SLAR and the Goodyear/GEMS SAR systems. The data were optically correlated and processed on image film suitable for qualitative image analysis. The primary objective was the assessment of natural resource, terrain mapping and map revision, whereas in many instances the analysis of tropical vegetation was of secondary importance (Werle 1989a).

The development of digital SAR imaging and processing technology by Canadian industry and the Environmental Research Institute of Michigan (ERIM) during the early 1980s resulted in advanced operational systems. Digital SAR data with a spatial resolution as good as 6 meters and offering high geometric and radiometric fidelity were used in computer assisted image analysis procedures, for the construction of image mosaics, and in topographic mapping programs. Since the mid 1980s, Intera Technologies of Calgary has employed airborne SAR systems in the tropics for a variety of commercial forestry and land cover surveys including those with a focus on natural vegetation (Thompson and Dams, 1990).

Regional and nation-wide tropical vegetation surveys, primarily using X-HH data, have been reported by a number of investigators, e.g. Thompson and Dams, (1990), Furley (1986), Parry & Trevett (1979), Trevett (1986), Gelnett et al. (1978). Major vegetation formations and to some extent zones experiencing ecological transition and stress within the tropics have been identified including savanna, dense and open tropical forest and woodland mosaics. Difficulties were encountered in identifying specific formations in hilly or mountainous terrain. De Molina and Molina (1989) were able to map thirty different vegetation cover types in Colombia at a scale of 1:40 000. Areas of selective logging and differing tree crown densities were also identified.

There is further evidence that mangrove forest environments can be mapped accurately because of their generally strong radar backscatter compared to surrounding forest stands (Lewis 1977, MacDonald et al., 1971). Thompson and Dams (1990) report success discriminating primary and secondary forests, and in mapping a variety of forest cover types, including mangrove/Nypa palm swamp, beach forest, peat swamp forest, hill dipterocarp forest, high scrub forest, tea tree and wallum cover, eucalyptus forest, and mimosoid legume and palm forests. Their data source was high quality black and white stereo prints made from X-Band HH digital SAR data with resolutions of 6 x 6 m and 6 x 12 m.

Plantation types which have been distinguished on airborne SAR imagery include palm and bananas (Dellwig et al. 1978, Thompson and Dams, 1990), and pine, eucalyptus, and rubber (Thompson and Dams, 1990).

Several studies indicate that forest disturbance can be detected and mapped (Dams et al. 1987, de Molina & Molina 1986, de Molina et al. 1973, Sicco Smit 1978, Thompson and Dams, 1990).

Airborne radar data acquisition was almost exclusively restricted to the dry season and hardly any multi-temporal data sets have been obtained so far. Trevett (1986) noted that significant changes in radar backscatter were identified comparing dry and wet season imagery acquired during the Nigerian NIRAD survey. These changes were mainly attributed to moisture differences.

Spaceborne SAR investigations Spaceborne SAR imagery of tropical terrain has been acquired during the experimental SEASAT (1978), SIR-A (1981) and SIR-B (1984) missions. These radars operated at L-band with horizontal transmit and receive polarization (L-HH). The spatial resolution achieved by each system varied between 25 meters, 40 meters and 18-60 meters, respectively. SIR-A and SIR-B provided only relatively narrow swath coverage of 50 km and 15-40 km, respectively. The combined total coverage in the humid and seasonally humid tropics exceeded a land area of 1.5 million km^2.

Multi-temporal SAR data is extremely limited and is restricted to some repeat coverage of the SEASAT SAR within the mask of the Merrit Island, Florida, receiving station, and to occasional overlap of SIR-A and SIR-B image swaths. With the exception of one study (Pope 1987), this has virtually precluded the use of existing spaceborne SAR data for change detection within tropical forest environments. The few studies that have been carried to assess environmental conditions and dynamic land use phenomena thus relied on single date spaceborne SAR data.

Both computer assisted and visual interpretation procedures were employed in the analysis of spaceborne SAR data for tropical vegetation and lands use investigations. Most of them suffered from a lack of ground information and knowledge of specific environmental and target parameters at the time of data acquisition thus limiting the accuracy of interpretation results.
The imagery acquired during the SIR-A mission in November, 1981 provide a useful yet little known source of information for examining forest conversion in all major tropical forest regions of the globe. There is evidence that SIR-A imagery (L-HH) at a scale of 1:250,000 is suitable for identifying the nature and extent of tropical forest conversion such as commercial timber harvesting operations, man-made grasslands for cattle ranching projects as well as natural grassland successions, and, to a limited extent, settlement colonization and agricultural schemes (Werle 1986 and 1989a).

Stone & Woodwell (1987) and Stone et al. (1989) found evidence that clearings within the tropical forest of Amazonia may exhibit different radar backscattering behaviour as a function of age and clearing practices. They found that L-band would be helpful in determining primary forest composition, but their data were insufficient in areal coverage to determine exact rates of deforestation.

Hoffer & Lee (1989) evaluated the potential of multi-temporal SEASAT and SIR-B data for defining areas of forest change, different forest categories and reforestation sites in Florida. Primary categories of forest change such as deforestation and reforestation were identified with relatively high accuracy. Reforestation stages were detected with modest success.

Ford & Casey (1988) distinguished and mapped swamp and lowland forest, tidal forest, wetland and clearcut areas in the coastal rainforest of Borneo using SIR-B data at two different incidence angles. Radar backscatter values for swamp areas were noted to change as a function of incidence angle. The SIR-B data were not suited for discriminating between different forest types within the mountainous interior of Borneo.

Imhoff et al. (1986) have studied multi-incidence angle SIR-B data of Bangladesh in order to characterize forest canopy and assess radar penetration capabilities. They were able to map flood boundaries beneath mangrove vegetation canopies. Breaches and holes in the natural canopy structure were also easily detected.

De Molina & Molina (1986) examined SIR-A data as part of a multi-sensor study for forest classification in the Colombian Amazon. Although their forest typing exercise met with no success, a clear discrimination of forested and non-forested areas was noted. Boundaries between savanna vegetation, tropical forests, floodplain vegetation and clearings were delineated without difficulty.

Ford and Da Cunha (1985) examined the radar backscatter properties of floodplain vegetation using multi-frequency SAR data. Alluvial forest areas were clearly identified on SIR-A L-band data, but could not be separated from surrounding forest areas on X-band airborne SAR data.

Pope (1987) was able to monitor seasonal flooding of lowland terrain in tropical forests of Guatemala using multi-temporal SEASAT SAR as well as airborne SAR data. Radar backscatter values of vegetated flooded terrain was found to be at a maximum under small incidence angle illumination.

These findings and others are summarized in Table 2, which shows that, as in the case of optical sensors, many different kinds of information useful for tropical forest management can be obtained from suitable radar data.

Studies at C-band are noticably absent from Table 2. With both ERS-1 and RADARSAT including C-band SARs, there is a serious knowledge gap about the capabilites at this frequency.

3. POTENTIAL ROLE OF RADARSAT

3.1 Characteristics of RADARSAT

The Government of Canada announced on 13 September, 1989 that RADARSAT, Canada's planned earth resources remote sensing synthetic aperture radar (SAR) satellite, was fully approved for construction and operation, with a design lifetime of five years from its 1994 launch. The approved design is outlined in this section (Langham, et al., 1989). (More complete discussion of RADARSAT may be found in a companion paper (Raney, et al., 1990).

The SAR is an advanced multi-mode instrument (see, for example, Luscombe 1989) that operates at 5.3 GHz (C-Band) having a wavelength of about 5 cm. It has a choice of three transmitter pulse bandwidths and numerous beam selections (and thus incidence angles) to give images with a variety of swath widths and resolution (see Table 3). The beam positions and swath widths are electonically selectable, and each rapidly accessible in response to a variety of user requirements during each orbit. Although the RADARSAT mission has been optimized for ice surveillance in Canada's north, it includes characteristics which are very favourable for a variety of applications around the globe.

The SAR can be turned on several times per orbit to a maximum accumulation of 28 minutes. Most parts of the world are accessible for observation from RADARSAT within a three day period although the repeat cycle is 24 days. (If an area needs coverage at a specified incidence angle, the larger number applies.)

The NASA launch of RADARSAT from California is scheduled for 1994 using a medium-class expendable launch vehicle. RADARSAT will use a sun synchronous dawn-dusk orbit. Perhaps the greatest operational advantage of the dawn-dusk orbit is that the SAR can be turned on at any time without consideration of conserving battery power. This means that there is no distinction between ascending and descending passes from an applications point of view. Another operational advantage is that the data reception periods for RADARSAT will not conflict with other remote sensing satellites most of which use near mid-day orbit timing.

3.2 Three levels of use

In approaching the use of RADARSAT, airborne SAR, and optical data for tropical forest management, it is very helpful to recognize a relationship between the area for which information is required, and the level of detail desired (see Section 2).

There are also corresponding relationships between the area covered by a sensor and its spatial resolution (see Table 3), and between the spatial resolution of sensors and the level of detail available from them (see Tables 1 and 2 and the review by Molina, 1981). These relationships result in natural groupings between the information requirements of various agencies, and the appropriate sensors to satisfy the information requirements. We have emphasized three such groupings in Table 4, where we match information requirements with the sensors which appear, at present, appropriate to satisfy the information requirements.

Strategic forest management information is required at global, continental, and national scales. Typical mapping scales range from $1:10^6$ to $1:10^7$, with appropriate resolutions in the range 0.1 to 10 km. Strategic information requirements are wide in scope but quite general in nature. As indicated in Table 4, the information about tropical forests is related to the overall characteristics of the vegetation, and can be supplied by low resolution sensors. The use of the NOAA/AVHRR for mapping broad vegetation classes, monitoring vegetation growth and vigour, and detecting large areas of significant vegetation change has been very well documented (see Table 1). In the ScanSAR mode (500 km swath, 100 m resolution), RADARSAT should be able to detect cases of vegetation removal over large areas.

Numerous studies have shown microwave backscatter to provide information about vegetation which is complementary to the information provided by optical sensors (e.g. Ahern et al., 1978, Guindon et al., 1980, Brisco et al., 1983, Wu, 1985). It is reasonable to expect, therefore, that RADARSAT data will also prove useful as a complement to optical data for mapping broad vegetation classes over wide areas.

The second level of detail requires a variety of information by national, state and provincial natural resource, environment, and parks departments. Because of the diversity of their mandates, these agencies require a wide variety of information. Mapping scales of $1:10^4$ to $1:10^6$ are typical, and spatial resolutions of 10 to 1000 m are appropriate.

For this level of detail, RADARSAT data in the standard (28 x 30 m resolution) and high resolution (8 m resolution) modes will contribute valuable forest management information. Again, its utility may be enhanced further when combined with optical data. High resolution airborne SAR can provide additional information on forest type and density by depicting the texture of the canopy. RADARSAT data in the standard and high resolution modes will probably be valuable for mapping drainage networks including, in some cases, standing water under tropical forest canopies (as in the case of mangrove swamps). It will probably also be useful for mapping roads, settlements, plantations, agricultural conversion, and other evidence of intensive land use. Since SAR imagery, particularly at high incidence angles, depicts topography very clearly, RADARSAT data may be particularly effective when combined with high resolution optical data from the Landsat and SPOT satellites in a way which allows interpreters to visualize topography when mapping vegetation classes from optical images.

The ability of RADARSAT to provide relatively high resolution images whenever desired will allow government agencies to closely monitor areas which are developing rapidly through the road-building and land clearing activities associated with development. Such timely information will enable governments to deal with deviations from approved forest managment plans much more quickly and therefore much more effectively than has been possible in the past. RADARSAT data will also enable forest management agencies to monitor forest inventory depletions due to clearcutting, but selective cutting will probably not be detectable with RADARSAT data, although access roads may be visible.

The persistance of haze, smoke, and cloud cover in the tropics makes it virtually impossible to monitor large areas with high resolution optical sensors over short periods of time. Nevertheless, these sensors may contribute to mapping diverse vegetation types and vegetation condition, and to initial mapping and to map revision at less frequent intervals.

It is worth noting that such mapping information can also be obtained through aerial photography, as indicated in Table 1. However, we believe that the use of satellite data will prove to be far more cost effective for most of the information at this intermediate scale.

In compiling Table 4, we have emphasized the Landsat Thematic Mapper even when the Landsat Multispectral Scanner or SPOT HRV multispectral data are likely to provide suitable information.

Our experience in Canada, has shown that sales of TM data to the forestry sector greatly exceed MSS and SPOT multispectral sales. TM is preferred over MSS because its spatial resolution and spectral bands provide more information than either MSS or SPOT multispectral data. SPOT panchromatic data are chosen when their superior spatial resolution is deemed important enough to justify the higher cost per unit area.

The third and most detailed level of information is required by natural resource companies, engineering companies, and local governmental and non-governmental organizations. Very detailed information about timber resources and the conditions such as topography, vegetation cover, and drainage is required.

Stereo aerial photography has been the remote sensing technique of choice for such information for many years, and is likely to remain so for some time to come, because much of the information needed requires stereo imagery with resolution in excess of that available from foreseeable satellite sensors or commercial airborne SARs. However, the multispectral data available from Landsat and SPOT can often supplement aerial photography for detailed vegetation mapping. RADARSAT high resolution data may provide supplementary information on topography and may also prove particularly useful for revealing standing water under the vegetation cover. Recent experience with high resolution airborne SAR is beginning to suggest that this data source can provide much of the information traditionally expected of medium scale aerial photography.

This assessment shows that RADARSAT is expected to contribute information at all three levels of detail because of its wide area coverage and range of spatial arn temporal resolutions. At present, RADARSAT's most important role appears to be for monitoring deforestation and other signs of human activity at a wide range of scales. It will probably also provide information which complements optical data for general and possibly detailed cover type mapping at scales from 1:20 000 to $1:10^7$.

4. PROBLEMS TO BE OVERCOME AND RECOMMENDATION FOR FUTURE ACTION

The experience we at the Canada Centre for Remote Sensing have had over the last fifteen years in developing remote sensing for improved forest management in Canada can serve as a guide to the steps necessary to help introduce microwave and optical remote sensing into the tropical forest management process. One lesson is particularly clear from our experience: introducing new technology, even very cost-effective technology, is a slow, painstaking process.

Five areas of activity must all be pursued to realize the potential of remote sensing for tropical forest management.

The first is to establish a detailed understanding of the information requirements of the agencies with mandates for various aspects of tropical forest management. It is not essential that all of the requirements for many agencies be itemized in detail from the outset. This can be done initially for a few agencies, with the others following as their interest and project resources permit.

The second area is one of research: to identify the information content of operational microwave and optical sensors. As can be seen from Tables 1 and 2, much information is already available. However, large areas of uncertainty remain. There is almost no experience with C-band SAR in tropical forests. This can be overcome through investigations with C-band airborne data and data from the ERS-1 satellite, followed by actual RADARSAT data. More experimentation is needed to address the information content of various optical and microwave sensors in the context of the detailed information requirements of particular agencies. Finally, most of the results reported to date are qualitative; more quantitative assessments of forest variables that can be measured, and mapping accuracies achievable are needed to assure prospective customers that information derived from remote sensing data can satisfy their needs.

The third area, a companion area of research, is the development of information extraction techniques. Once the information content of various sensors is known, the appropriate information extraction techniques may be obvious, but this is not always the case. Research will probably be needed to enhance and extract the important tone, texture, and pattern information on SAR imagery. Much experimentation may be necessary to develop effective ways to combine microwave and optical data and to extract the desired information from the combined data sets.

The fourth area of activity is the development of suitable infrastructure in the agencies responsible for tropical forest management. It is generally accepted that remote sensing data is best utilized when combined with natural resource information in digital form on a geographic information system. The Canadian provincial forest management agencies have found that a very large effort is necessary to convert a detailed existing forest inventory into digital form on a GIS. Developing countries may be at an advantage in this respect since they may have the opportunity to establish their resource management data base in digital form at the outset. GIS technology itself has come down in price recently, and systems covering a wide range of sizes and costs are available from a multitude of vendors.

The final activity is technology transfer: the adoption of the technology by the resource management agency. Experience has shown that this is most effective when the resource management agency becomes a partner in the technology development process at an early stage. The most appropriate time is often as part of the determination of the detailed information requirements of the agency. Agency personnel can then either follow the technology development process as observers, or participate more actively. Participation can include contributing to investigations of information content and accuracy to be expected from the data from various sensors, and specifying the system they will need to use the remotely sensed data operationally.

4.1 Recommendation

One effective way to carry out activities in the five areas described above is through a partnership between organizations supplying remotely sensed data, organizations with tropical forest management mandates, and organizations specializing in the development of remote sensing technology and applications. In preparation for the RADARSAT mission, the Canada Centre for Remote Sensing is proposing investigations of the information content of C-band SAR data, optical data, and information extraction technology to be carried out jointly with nations having responsibility for management of tropical forests. Such joint projects could pave the way for increasing activities of this nature, leading to widespread operational use of microwave and optical data for improved tropical forest management.

6. ACKNOWLEDGEMENTS

The authors wish to thank L. Brown-Woods, L. Marcotte, T. Potter, and E. Storie of Horler Information Incorporated for their continued assistance in indexing and cataloguing the RESORS collection and helping us retrieve immense amounts of material from it.

7. REFERENCES

Agatsiva, J. L., J. P. Delsol, and J. M. Terres, 1989. Monitoring forest cover transformation on Kikuyu Escarpment using remote sensing data, Proceedings of the Fourth Latin American Symposium on Remote Sensing, Bariloche, Argentina, pp 239-249.

Ahern, F.J., D.G. Goodenough, A.L. Gray, R.A. Ryerson, R.J. Vilbikaitis, and M. Goldberg, 1978. Simultaneous Microwave and Visual Wavelength Observations of Agricultural Targets, Canadian Journal of Remote Sensing, 4(2):127-142.

Ahmad, W.Y.W., F. MacCallum, R.V. Dams, S.B. Mokhtar, and H.G. Cheah, 1988, Landsat MSS, SPOT, and SAR for Tropical Forestry Applications in Malaysia, Ninth Asian Conference on Remote Sensing, Bankok, Thailand, Nov 23-29, 1988, pp Q-23-1 to Q-23-8.

Aldred, A. H. 1976. Measurement of tropical trees on large-scale aerial photographs, Canadian Forestry Service Forest Management Institute Information Report FMR-X-86, 39pp.

Artieda, A. G., 1989. Analisis multitemporal de imagenes Landsat deforestacion de la region amazonica ecuatoriana, Proceedings of the Fourth Latin American Symposium on Remote Sensing, Bariloche, Argentina, pp 209-222.

Baltaxe, R. 1980. The application of Landsat data to tropical forest surveys, United Nations Food and Agriculture Organization contract report, Swedish Funds-in-trust For:TF/INT/333 (Swe).

Baltaxe, 1987. The application of remote sensing to tropical forest cover monitoring: a review of practices and possibilities, Remote Sensing Yearbook, pp 34 - 51.

Booth, W. 1989. Monitoring the fate of the forests from space, Science 243: 1428-1429.

Brisco, B., F. T. Ulaby, and M. C. Dobson, 1983. Spaceborne SAR data for land-cover classification and change detection, IGARSS'83 Technical Digest, IEEE Geoscience and Remote Sensing Society, San Franscisco, August 31 - September 2, pp PS-2 1.1 - 1.8

Churchill, P.M., A. Horne & R. Kessler 1985. A review of radar analyses of woodland, EARSeL Workshop Proceedings, ESA SP-227, pp. 25-32.

Dams, R.V., D. Flett, M.D. Thompson, and M. Lieberman, 1987. SAR image analysis for Costa Rican tropical forestry applications, II Simposio Latino Americano Sobre Sensores Remotos, Bogota, Columbia, pp 22-28.

Dellwig, L.F., J.E. Bare, and R. Gelnett, 1978. SLAR - for clear as well as cloudy weather, Proceedings of the International Society of Photogrammetry and Remote Sensing, Freiburg, Federal Republic of Germany, pp 1527-1546.

de Molina, I., L. Mosquera, M. Molina and R. Deagostini 1973. SLAR in the mapping of humid tropical forests of Columbia. Proceedings, 1st Panamerican Symposium on Remote Sensing, Panama City, pp 231-272.

de Molina, G.I. and L.C. Molina 1986, The use of SLAR and SIR-A images for the classification of forest types in the tropics, (unpublished paper), 11 pages.

de Molina, G.I., and L.C. Molina 1989. The use of high resolution radar imagery in forest inventories in tropical forests of cativo (Prioria copaifera), Proceedings of 4th Latin American Symposium on Remote Sensing, San Carlos de Bariloche, Argentina, November 24-26.

Disperati, A.A. and M.A. Keech, 1978. The value of using SLAR, satellite imagery and aerial photographs for a forest survey in the Amazon basin, in: Collins, W. G., and J. L. van Genderen (eds.), 1978, Remote Sensing Applications in Developing Countries, Remote Sensing Society, Reading, UK. pp 48-55.

Ekstrand, S., 1986. Thematic mapper in tropical forest inventories: a comparison with landsat MSS data, panchromatic aerial photography, and colour infrared aerial photography, Proceedings of the 20th International Symposium on Remote Sensing of Environment, Environmental Research Institute of Michigan, Nairobi, Kenya, Dec 4-10, pp 1299 - 1307.

Ellis, W. S., W. A. Allard, and L. McIntyre, 1988. Brazil's Imperiled Rain Forest. National Geographic, 174(6):772-799.

ERIM, 1979. Bangladesh training programme in the processing of Landsat digital data for land accretion, boro rice inventory and forestry applications, Bangladesh Landsat Centre and Environmental Research Institute of Michigan Final Report, United Nations Food and Agricultural Organization, UNDP/FAO/DP/BGD/75/029-1/AGOF, 216 pp.

Ford, J.P. and R. da Cunha 1985. Shuttle radar images for geologic mapping in tropical rainforest. Proceedings, Fourth Thematic Conference: Remote Sensing for Exploration Geology, San Francisco, CA., pp 669-676.

Ford, J.P. and D.J. Casey 1988. Shuttle radar mapping with diverse incidence angles in the rainforest of Borneo, Int. J. Remote Sensing, 9(5):927-943.

Ford, J.P. and F.F. Sabins 1985. Space Shuttle radar investigations in Indonesia, International Symposium on Remote Sensing of Environment, Fourth Thematic Conference on Remote Sensing for Exploration Geology, Environmental Research Institute of Michigan, San Francisco, pp 113 - 122.

Furley, P.A. 1986. Radar Surveys for resource evaluation in Brazil: an illustration from Rondonia, in: Eden, M. J., and J. T. Parry (eds.), 1986, Remote Sensing in Tropical Land Management, London, New York, Sidney, Toronto, pp 79-99.

Gelnett, R.H., L.F. Dellwig and J.E. Bare 1978. Increased visibility from the invisible - a comparison of radar and LANDSAT in tropical environments. Proceedings of the 12th International Symposium on Remote Sensing of Environment, Environmental Research Institute of Michigan, Manila, Philippines, Vol 3, pp 2205-2216.

Grainger, A. 1984. Quantifying changes in forest cover in the humid tropics: overcoming current limitations. Journal of World Forest Management 1(1):3-63.

Guindon, B., J. W. E. Harris, P. M. Teillet, D. G. Goodenough, and J.-F. Meunier, 1980. Adaptive filtering and image segmentation for SAR analysis, Proceedings of the Fouteenth International Symposium on Remote Sensing of Environment, Environmental Research Institute of Michigan, San José, Costa Rica, pp 1673 - 1690.

Guillon, L., 1989. Relevamiento forestal en cordoba mediante imagen Landsat TM, Proceedings of the Fourth Latin American Symposium on Remote Sensing, Bariloche, Argentina, pp 181 - 189.

Hoffer, R.M and K.S. Lee 1989. "Forest change classification using SEASAT and SIR-B satellite SAR data", IGARSS '89 Symposium, Vancouver, Proceedings, Vol. 3, pp. 1372-1375.

Hunting Technical Services Ltd. 1984. Study of a land use of synthetic aperture radar, Report to ESA/ESTEC, Vol. 1-2, (Contr. No 5778/83/NL/MS), Borehamwood, England.

Imhoff, M.L., Story, C.H. Vermillion, F. Khan and F. Polcyn 1986. Forest canopy characterisation and vegetation penetration assessment with spaceborne radar, IEEE Transactions on Geoscience and Remote Sensing, GE-24(4):535-541.

Joyce, A. T., and S. A. Sader, 1986. The use of remotely sensed data for the monitoring of forest change in tropical areas, Proceedings of the Twentieth International Symposium on Remote Sensing of Environment, Environmental Research Institute of Michigan, Nairobi, Kenya, December 4-10, pp363-378.

Justice, C. O., J. R. R. Townsend, B. N. Holben, and C. J. Tucker 1985. Analysis of the phenology of global vegetation using meteorological satellite data, International Journal of Remote Sensing 6(8):1271-1318.

Keech, M. A., A. A. Disperati, and O. Ganzel, 1978. The delineation of *Araucaria angustifolia* in the forests of southern Brazil using satellite imagery, in Hildebrandt, G. and H. J. Boehnel (eds.), Proc. International Symposium on Remote Sensing for Observation and Inventory of Earth Resources, Freiburg: 1805-1811.

Khan, F. A., M. A. H. Pramanik, Blasco, Kerr, M. Lavenu, G. Begni, and P. N. Paschaud, 1983. Results of SPOT simulation in Bangladesh - Application to coastal and mangrove problems, Proceedings of the fourth Asian Conference on Remote Sensing, Colombo, Sri Lanka, November 10-15, pp E-8-2 to E-8-13.

King, R.B. 1985. Comparison of SLAR, SIR and Landsat imagery for mapping land systems in Kalimantan, Indonesia. Proceedings, International Conference of the Remote Sensing Society and the Centre for Earth Resources Management, 9-12 Sept. 1985, London, pp 381-390.

Langham, E. J., E. Shaw, and R. K. Raney, 1989. RADARSAT: Canada's Microwave Satellite, IEEE Geoscience and Remote Sensing Society Newsletter, November, pp 19-21.

Lewis, A.J. 1977, Coastal mapping with radar. Geoscience and Man, 18:239-247.

Leshack, L. 1971. Automated data processing of forest imagery, Photogrammetric Engineering, 37(8):885-896.

Lewis, A. J. and H. C. MacDonald, 1972. Mapping of mangrove and perpendicular oriented shell reefs in southwestern Panama with side looking radar, Photogrammetria, 28:187 - 199.

Lowry, R.T., P. van Eck, and R.V. Dams, 1986. SAR for forest management, Proceedings of International Geoscience and Remote Sensing Symposium, Zurich, Switzerland, pp 901 - 906.

Luscombe, Anthony P., 1989. The RADARSAT Synthetic Aperture Radar System, Proceedings of the 1989 International Geoscience and Remote Sensing Symposium, Vancouver, B.C., Canada, 10-14 July, pp 218-221.

MacDonald, H. C., A. J. Lewis, and R. S. Wing, 1971. Mapping and landform analysis of coastal regions with radar, Geol. Soc. Am. Bull., 82, pp345 - 358.

Macdonald, H. C., W. P. Waite, and J. S. Demarcke, 1981. Seasat radar geomorphic applications in coastal and wetlands environments, southeastern U. S., Fall Technical Meeting, American Society of Photogrammetry, San Francisco, September 9 - 11, pp 181 - 190.

Malingreau, J. P. and C. J. Tucker, 1987. The contribution of AVHRR data for measuring and understanding global processes: large-scale deforestation in the Amazon basin.

Matson, M., and B. Holben, 1987. Satellite detection of tropical burning in Brazil, Int. J. Remote Sensing, 8:509-516.

Molina, L. C. 1981. The application of remote sensing for the classification and survey of tropical forests, Proceedings of the First Symposium on Remote Sensing in Colombia, Bogota, Columbia, July 27-31, pp 63 - 70.

Myers, N. 1986. Tropical Forests: Patterns of Depletion, in Prance, G. T. (ed), Tropical Rain forests and the World Atmosphere, American Association for the Advancement of Science Symposium, Westview Press, Boulder, Colorado, pp 9-32.

Myers, B. J. and M. L. Benson, 1981. Rainforest species on large-scale color photos, Photogrammetric Engineering and Remote Sensing, 47(4)505-514.

Nelson, R., and B. Holben, 1986. Identifying deforestation in Brazil using multiresolution satellite data, International Journal of Remote Sensing 7:429-448.

Nelson, R., N. Horning, T. A. Stone, 1987. Determining the rate of forest conversion in Matto Grosso, Brazil, using Landsat MSS and AVHRR data. International Journal of Remote Sensing, 8(12):1767-1784.

Novaes, R. A. 1979. Recent accomplishments and expectation of remote sensing appluied to forest in Brazil, cyclostyled paper, Instituto des Pesquisas Espaciais, San José dos Campos, Brazil, 18pp.

Parry, D.E. and J.W. Trevett 1979. "Mapping Nigeria's vegetation from radar", In: Geographical Journal 145, No. 2, pp. 265-281.

Pope, K.O. 1987, unpublished manuscript), Radar remote sensing of seasonal inundation in the Bajos near El Mirador, Peten, Guatemala.

Raney, R. K., R. Pereira da Cunha, and K. Link, 1990. Radar Processing, RADARSAT, and Technology Transfer Issues, International Symposium on Primary Data Acquisition, Amazonian Region: How Can Remote Sensing Contribute?, Manaus, Brazil, 24-29 June 1990.

Repetto, R., 1988. The forest for the trees? Government policies and the misuse of forest resources, World Resources Institute, Washington, D. C.

Repetto, R. 1990. Deforestation in the tropics. Scientific American, 262(4):36-45.

Rosenqvist, A., S. Murai, and S. Vibulsresth, 1989. Forest change detection - a study of the flooded area in King Amphoe Phipun, Province of Nakhon Si Tammarat, Thailand, Proceedings of Tenth Asian Conference on Remote Sensing, Kuala Lumpur, Malaysia, pp D-2-1 to D-2-8.

Sadowski, F. G. and W. A. Danjoy, 1980. Some observations on the utility of remote sensing for humid tropical forests, Proceedings of the Fourteenth International Symposium on Remote Sensing of Environment, Environmentat Research Institute of Michigan, San Jose Costa Rica, April, pp 1799 - ????

Sicco Smit, G. 1978. SLAR for forest type classification in a semi-deciduous tropical region, ITC Journal, Vol. 1978-3, pp 385-401.

Sicco Smit, G. 1980. SLAR mosaic interpretation for forestry purposes, International Society for Photogrammetry, 14th Congress, Hamburg, W. Germany.

Simonett, D.S., A.H. Strahler, G.Q. Sun & Y. Wang 1987. Radar forest modelling: Potentials, problems, approaches, models, In: Proceedings 13th Annual Conf. of the Remote Sensing Society, University of Nottingham, September 1987, pp. 256-270.

Stellingwerf, D. A., S. G. Banyard, and G. Sicco Smit, 1986. Applications of aerial photographs and other remote sensing imagery in forestry (Tropical regions), ITC Publication Number 5, International Institute for Aerospace Survey and Earth Sciences, P.O. Box 6, 7500, Enschede, The Netherlands, 57 pp (Part 1), 36 pp (Part 2)

Stone, T.A. and G.M. Woodwell 1987. Analysis of forest and forest clearing in Amazonia with LANDSAT and Shuttle Imaging Radar - A data, IGARSS '87 Symposium Proceedings, Ann Arbor, MI., pp 1229-1235.

Stone, T.A, G.M. Woodwell & R.A. Houghton 1989. Tropical deforestation in Para, Brazil: Analysis with Landsat and Shuttle Imaging Radar - A", In: IGARSS '89 Symposium, Vancouver, Proceedings, Vol. 1, pp. 192-195.

Terchunian, A.,V. Klemas, A. Segovia, A. Alvarez, B. Vasconez, and L. Guerrero, 1986. Mangrove mapping in Equador, the impact of shrimp pond construction, Environmental management, 10(3): 345 - 350.

Thompson, M. D., and R. V. Dams, 1990. Forest and land cover mapping from SAR: a summary of recent tropical studies, Proceedings of the Twenty-third International Symposium on Remote Sensing of Environment, Environmental Research Institute of Michigan, Bangkok, Thailand, April 18-25.

Trevett, J.W. 1986. Imaging radar for resources surveys, London, New York.

Werle, D. 1986. The role of spaceborne radar (SIR-A) image interpretation in monitoring tropical forest conversion, RADARSAT Project Office Report, Energy, Mines, and Resources Canada.

Werle, D. 1989a. Potential application of imaging radar for monitoring depletion of tropical forests, Proceedings of 1989 International Geoscience and Remote Sensing Symposium, Vancouver, British Columbia, Canada, pp 1383-1390.

Werle, D. 1989b. Radar remote sensing for application in forestry -- a literature review, Canada Centre for Remote Sensing Report, Ottawa, Canada, 42 pp.

Wilkie, D. S., 1990. Establishing the Okapi Rain Forest Reserve: avoiding human land-use conflicts using satellite image analysis, IGARSS '90 Technical Digest, IEEE Geoscience and Remote Sensing Society.

Williams, D. L., and Coiner, J. C., 1975. Utilization of Landsat imagery for mapping vegetation on the millionth scale, Proceedings of the NASA Earth Resources Survey Symposium, Johnson Space Center, Houston, Texas, pp53-65.

Wilson, E. O., 1989. Threats to biodiversity. Scientific American 261(3):108-117.

Wing, R. S., 1970. Structural analysis from radar imagery, eastern Panama isthmus. University of Kansas Centre for Research CRES Technical Report 133-15.

Woodwell, G. M., R. A. Houghton, T. A. Stone, R. F. Nelson, and W. Kovalick, 1987. Deforestation in the tropics: New measurements in the Amazon basin using Landsat and NOAA advanced very high resolution radiometer imagery.

Wu, S. T., 1985. Analysis of data acquired by the Shuttle Imaging Radar - A and Landsat Thematic Mapper over Baldwin County, Alabama, Proceedings of the 1985 Machine Processing of Remotely Sensed Data Symposium, Purdue University, West Lafayette, Indiana, June 25 - 27, pp 173 - 182.

Table 1. Summary of Optical Applications Results in Tropical Forests

Applications Area	Country	Sensor	Res'n[1]	Reference
Broad veg'n clases				
	Indonesia	MSS	80 m	Stellingwerf et al. 1986
	Columbia	MSS	80 m	Stellingwerf et al. 1986
	Various	MSS	80 m	Baltaxe 1987
	Brazil	MSS	80 m	Novaes 1979
	Bolivia	MSS	80 m	Baltaxe 1980
	Papua N.G.	MSS	80 m	Williams and Coiner 1975
	Philippines	MSS	80 m	Williams and Coiner 1975
	Peru	MSS	80 m	Sadowski and Danjoy 1980
	Ethiopia	TM	30 m	Ekstrand 1986
Vegetation inventory				
	Brazil	MSS	80 m	Keech et al. 1978
Species composition				
	Indonesia	Pan	20 000	Stellingwerf et al. 1986
	Mexico	Pan	30 000	Stellingwerf et al. 1986
	Thailand	Pan	60 000	Stellingwerf et al. 1986
	Australia	Nat. col.	2 000	Myers and Benson 1981
Mangrove Forests				
	Columbia	Pan	45 000	Stellingwerf et al. 1986
	Bangladesh	MSS	80 m	ERIM 1979
	Bangladesh	SPOT	20 m	Khan et al. 1983
Forest damage	Columbia	Pan	20 000	Stellingwerf et al. 1986
Drainage	Indonesia	MSS	80 m	Stellingwerf et al. 1986
Plantation mapping				
	Indonesia	Pan	30 000	Stellingwerf et al. 1986
	Indonesia	Pan	10 000	Stellingwerf et al. 1986
	Brazil	MSS	80 m	Baltaxe 1980
Vegetation change				
	Columbia	MSS	80 m	Stellingwerf et al. 1986
	various	MSS	80 m	Baltaxe 1987
	Brazil	MSS	80 m	Baltaxe 1980
	Thailand	MSS	80 m	Baltaxe 1980
	Brazil	AVHRR	1 km	Malingreau and Tucker 1987
	Brazil	AVHRR	1 km	Nelson and Holben 1986
Land use change				
	Indonesia	Pan	50 000	Stellingwerf et al. 1986
	Columbia	MSS	80 m	Stellingwerf et al. 1986
	various	MSS	80 m	Baltaxe 1987
	Brazil	MSS	80 m	Novaes 1979
Road detection/mapping				
	Mexico	Pan	30 000	Stellingwerf et al. 1986
	Indonesia	MSS	80 m	Stellingwerf et al. 1986
Fire detection	Brazil	AVHRR	1 km	Matson and Holben 1987
	Brazil	AVHRR	1 km	Malingreau and Tucker 1987

[1] For aerial photography ("pan"), the contact scale is used instead of resolution.

Table 2. Summary of SAR Applications Results in Tropical Forests

Applications Area	Country	Band	Res'n	Reference
Road detection	Sarawak	X	6 m	Thompson and Dams 1990
	Peninsular Malaysia	X	6 m	Ahmad et al. 1988
	(Cameroon	L	40 m	Werle 1989a)
Clearcut detection	Cameroon	L	40 m	Werle 1986
	Venezula	L	40 m	Werle 1986
	Indonesia	L	40 m	Werle 1986
	Brazil(?)	L	40 m	Stone & Woodwell 1987
	Columbia	K_a, X, L	10-22, 16, 40 m	de Molina & Molina 1986
	Costa Rica	X	6m	Dams et al. 1987
Clearcut revegetation	Cameroon	L	40 m	Werle 1989a
	Venezuela	L	40 m	Werle 1989a
	Indonesia	L	40 m	Werle 1989a
	Costa Rica	X	6 m	Dams et al. 1987
Settlements	Nigeria	X	30 m	Hunting, 1984
	Paraguay	L	40 m	Werle 1989a
	Indonesia	L	40 m	Werle 1989a
	Sarawak	X	6 m	Thompson and Dams 1990
	Colombia	X	6m, 12m	de Molina and Molina 1989
Agricultural conversion	Paraguay	L	40 m	Werle 1986
	Sarawak	X	6 m	Thompson and Dams 1990
	Peninsular Malaysia	X	6 m	Thompson and Dams 1990
	Colombia	X	6m, 12m	de Molina and Molina 1989
Tree plantations	Guatemala	K_a	10 - 22 m	Dellwig et al. 1978
	Indonesia	L	40 m	Werle 1989a
	Australia	X	12 m	Lowry et al. 1986
	Congo	X	6 m	Thompson and Dams, 1990
	Peninsular Malaysia	X	6 m	Ahmad et al. 1988
Mangrove forests	Indonesia	X, L	40 m	King 1985
	Panama	K_a		Lewis & MacDonald 1973
	Sarawak	X	6 m	Thompson and Dams 1990
	Australia	X	12 m	Lowry et al. 1986
	(Bangladesh	L	≈16 - 33 m	Imhoff et al. 1986)
	(Florida)	L	25 m	MacDonald et al. 1981
Flooding	Bangladesh	L	28 m	Imhoff et al. 1986
	Australia	L	40 m	Werle 1989a
	Indonesia	L	28 m	Ford & Sabins, 1985
	Guatemala	L	25 m	Pope 1987
	Colombia	X	6m, 12m	de Molina and Molina 1989
	Indonesia, Borneo	L	≈ 20 - 30 m	Ford & Casey 1988
Drainage	Nigeria	X	> 30 m	Sicco Smit 1980
	Columbia	K_a, X, L	10-22, 16, 40 m	de Molina & Molina 1986
	Brazil	X, L	16, 40 m	Ford & da Cunha 1985
	Cameroon	L	40 m	Werle 1989a
	Sarawak	X	6 m	Thompson and Dams 1990
Broad vegetation classes	Brazil	X	16 m	Furley, 1986
	Nicaragua	K_a	10-20 m	Trevett 1986
	Togo	K_a	>20 m	Gelnett et al. 1978
	Nigeria	X	30 m	Hunting 1984
	Colombia	X	≈10-22 m	de Molina et al. 1973

Table 2. Summary of SAR Applications Results in Tropical Forests Cont'd

Applications Area	Country	Band	Res'n	Reference
	Colombia			Trevett 1986
	Colombia	K_a,X,L	10-22,16,40 m	de Molina & Molina 1986
	Colombia	X	6m,12m	de Molina and Molina 1989
	Australia	X	6 m	Lowry et al. 1986
	Indonesia, Borneo	L	≈ 20 - 30 m	Ford & Casey 1988
	(Brazil	X	≈16 m	Disperati and Keech 1978)
Forest inventory information	Peninsular Malaysia	X	6 m	Ahmed et al. 1988
	(Nigeria	X	> 30 m	Sicco Smit 1978)
	(Columbia	K_a,X,L	10-22,16,40 m	de Molina and Molina 1986)

Studies in parentheses () report negative findings for that application

Table 3. Basic Characteristics of Optical and Microwave Sensors

Sensor	Mode	Swath(km)	Resolution	Incidence
L-MSS	Standard	185	≈ 80 m	-11° - 11°
L-TM	Standard	185	30 m	-11° - 11°
SPOT/HRV	Multispectral	60	20 m	-31° - 31°
SPOT/HRV	Panchromatic	60	10 m	-31° - 31°
AVHRR	Standard	≈2000	≈1100 m	-45° - 45°
RS-SAR*	Standard	100	28 x 30 m (4 looks)	20° - 49°
RS-SAR	High Resolution	55	8 x 8 m (1 look)	20° - 49°
RS-SAR	Extended	100	28 x 30 m (4 looks)	49° - 60°
RS-SAR	ScanSAR	500	100 x 100 m (8 looks)	20° - 49°

*RS = RADARSAT

Table 4. Summary of Information Requirements and Appropriate Sensors[1]

Broad Scale: Global, continental, national	Agencies concerned:
Typical mapping scales: $1:10^6$ to $1:10^7$ Spatial resolution: 0.1 to 10 km	International organizations Intenational development agencies Global environmental research groups
<u>Information requirement</u>	<u>Appropriate sensor(s)</u>
Broad vegetation classes	NOAA/AVHRR RADARSAT ScanSAR
Vegetation cover/vigour	NOAA/AVHRR
Length of growing season	NOAA/AVHRR
Large area vegetation change	RADARSAT ScanSAR NOAA/AVHRR

Medium Scale: National, regional	Agencies concerned:
Typical mapping scales: $1:10^4$ to $1:10^5$ Spatial resolution: 10 to 1000 m	National, state, and provincial Natural resource, environment, and parks Departments
<u>Information requirement</u>	<u>Appropriate sensor(s)</u>
Topography	Air photo, SPOT/HRV
Vegetation inventories	Air photo, Landsat/TM, RADARSAT/Standard
Mangrove forests	Landsat/TM, SPOT/HRV, RADARSAT/Standard
Drainage networks, standing water	Landsat/TM, SPOT/HRV,RADARSAT Standard
Standing water under canopy	RADARSAT Standard
Roads and settlements	SPOT/HRV, RADARSAT High Resolution
Change detection	SPOT/HRV, Landsat TM, RADARSAT Standard
Forest damage	Air photo, Landsat/TM (based on temperate latitude studies)
Revegetation assessment	Landsat TM, SPOT/HRV
Plantation mapping TM	RADARSAT High Resolution, SPOT/HRV, Landsat
Agricultural conversion (vegetation change)	RADARSAT Standard, RADARSAT High Resolution, SPOT/HRV, Landsat TM
Fire detection	NOAA/AVHRR

[1]In this table we have indicated Landsat/TM and SPOT/HRV where studies have shown that Landsat/MSS is effective, because our experience with forestry applications at temperate latitudes has indicated that customers are usually willing to pay the extra cost for the additional information content of these sensors. We have <u>not</u> indicated aerial photography ("Air photo") for applications which can be done with satellite data because customers generally prefer the much lower cost per unit area of satellite data.

Small Scale: Local

Agencies concerned:

Spatial resolution 1 to 10 m
Typical mapping scales: $1:10^3$ to $1:10^4$

Resource companies, Municipalities, National and local parks administrations, engineering companies, non-governmental organizations

Information requirement	Appropriate sensor(s)
Vegetation species mixes	Air photos, airborne SAR
Wildlife habitat	Air photos, Landsat TM, SPOT/HRV, airborne SAR
Tree diameters and heights	Air photos
Roads, trafficability	Air photos, SPOT/HRV, airborne SAR, RADARSAT High Resolution
Plantation mapping and assessment	Air photos, airborne SAR, SPOT/HRV, Landsat TM, RADARSAT High Resolution

THE EVERGREEN PLAN FOR MONITORING AND MANAGEMENT OF TROPICAL FORESTS

C. N. Specter

Florida International University
Miami, Florida 33199 U.S.A.

R. K. Raney

Canada Centre for Remote Sensing
Ottawa, Ontario, Canada K1A 0Y7

ABSTRACT

The EverGreen Plan is long range, aimed at effective tropical forestry management (using especially spacecraft radar data) before the end of the decade. It has both technical and institutional themes. It builds on basic science and institutional foundations, and is intended to culminate in an effective network of resident technical capability and effective institutional linkages rooted in tropical regions, joined to utilize the information from quantitative observations of the key environmental parameters for appropriate resource management responses. Provision of economic, political, and institutional incentives are incorporated in the Plan, and are intended to overcome those impediments frequently encountered in remote sensing technology transfer programs. This paper elaborates on the rationale for the systems approach and includes a brief description of the ten-year plan for implementation of EverGreen.

INTRODUCTION

The Amazonian region contains a significant proportion of the world's tropical forests, one third of which is found in Brazil. Brazil has taken a leadership role in national and international activities aimed at a better understanding of deforestation processes through improved monitoring. In 1988 the Brazilian government initiated a program called "Our Nature " to establish conservation policies for the country's natural resources (INPE 1990). As part of this program, the Instituto de Pesquisas Espaciais (INPE) conducted a survey of the extent of deforestation in the Brazilian Legal Amazon in 1989. INPE is leading the International Space Year (ISY) Deforestation Project and has proposed a second ISY project, the Synthetic Aperture Radar Deforestation Education Workshops. In order to inform the public about these efforts, INPE has recently initiated a quarterly newlsletter.

These significant activities are representative of an increasing number of private and public responses to tropical deforestation, but there is still no system for monitoring tropical deforestation on a global scale. A contributing factor is the lack of appropriate technology. During the 1980s, the only satellite systems available carried optical sensing systems which have not been able to provide complete and timely coverage due to cloud cover over tropical regions. Beginning in 1991, a series of radar remote sensing satellites will begin operation. These microwave viewing systems can penetrate cloud, fog, and mist. It is timely to prepare for the best use of data from these systems in a global tropical forest monitoring program.

Establishment of an effective indigenous monitoring program will require more than just the provision of radar data and supporting technology. If radar sensing is to be applied successfully to this issue, it must be accompanied by an effective technology transfer program. Such a program will be successful only to the extent that it recognizes and responds to the motivating forces found in developing countries, particularly economic concerns. The systems approach to technology transfer in such circumstances is most apt, but it must go beyond the conventional bounds of remote sensing practice. Within the frame of reference of a given developing country, the systems approach will help to directly relate the information content of data products to local issues of immediate importance. Use of remotely sensed data, much less demand for it, will occur only if it is seen to be essential for effective action.

TECHNOLOGY TRANSFER: A SYSTEMS APPROACH

There are three major schools of science and technology policy which have contributed both to the theoretical literature and to the development of scientific and technological capacities in the developing countries (Weiss and Ramesh 1983). One school emphasizes the building of national scientific enclaves to serve as centers of excellence from which science and technological advances will "trickle down" through the rest of the economy. Another school is based on the fundamental principle that technological resources should be committed based on the most pressing social issues as identified by societal members, a "bottom up" approach.

The third school takes a systems approach to developing technological capacity. This approach begins with an understanding of system objectives, i.e., getting the technology into the hands of the users. Attention is focused on the relevant institutions and the technology transfer networks which connect them. The intended strategy is to improve the flow of technology from developed country donors (getting the technology more cheaply and under less restricted conditions), to and through local institutions (diffusing the technology through the system, developing local expertise), and adapting the technology to local needs. Writers in this school have extended their field of study to include economic and political forces in the environment surrounding the technology transfer process, as these are viewed as having significant impacts on the success of the system and can be influenced by system managers.

Numerous authors have taken this perspective in analyzing technology transfer and diffusion processes (Frame 1983, Rogers 1983, Rogers and Eveland 1975, Robinson 1989, Roman 1980). Likewise, a number of professionals in the field of remote sensing have urged that knowledge gained from remote sensing technology transfer (RSTT) be used to build a conceptual model of the transfer system (Hankins 1977, Levin 1978, Pala 1980, Voute 1982).

In response, a study of remote sensing technology transfer to developing countries was completed recently, based on the systems perspective. The study began with the development of a systems model of the technology transfer process through case studies of the transfer process in Thailand and Zaire. Further research, based on the model and a fifteen year literature review, led to a global survey of experts in the field (Specter 1986). Results of the survey revealed critical factors related to system inputs (the lack of appropriate computer equipment, inadequate data distribution patterns and costs, and the lack of experienced personnel); the transformation process (lack of cooperation and coordination among relevant organizations in developing countries); and environmental considerations (economic and political constraints, and the uncertain future of Earth-observing satellite systems). Later studies have supported the systems perspective as a tool for better understanding of the technology transfer process (Specter and Gayle 1989, Specter 1990).

Employing a systems paradigm to the study of the transfer process has proven successful to the extent that it has led to the identification of system elements and their interrelationships. A more practical result of this approach has been to provide managers in the field with additional knowledge about the system that could assist them in controlling and/or influencing critical elements in order to improve the flow of technology to end users. However, this does not necessarily mean that the information that the technology can provide would be integrated in national decision making processes regarding economic development or improved environmental management. If that is our fundamental goal, we must look beyond the technological system to the role of technology in society, taking a mission-driven, context-oriented approach to objective setting.

ENVIRONMENTAL ISSUES AND SYSTEMS

The human race is facing environmental degradation of global proportions. Many developing countries have experienced massive losses of their major source of economic capital: natural resources. Some hover on the brink of "environmental bankruptcy" (MacNeill 1989). The Club of Rome warned us of these environmental perils through a process of "world modeling", using a systems perspective. These experts began by outlining five major parts of the global predicament: population, pollution, industrial capital, agriculture, and resource depletion. They believed that mankind could no longer deal with such problems individually, but had to attack them in a unified fashion. However, the Club of Rome approach has been criticized for attempting to throw all major problems into one "problematique", making the system far too large and too complicated to encourage action and response (Churchman 1979).

More recently, the World Commission on Environment and Development (WCED) released a report stating that future survivability on this planet rests with our ability to integrate economic and environmental planning in order to achieve sustainable development (WCED 1987). Traditionally these activities have been handled as separate programs by separate groups (MacNeill 1989).

Proponents of the systems approach would argue that this predicament is the result of not having the overall mission clearly in mind when the relevant organizations and networks were established. Some groups have seen the objective as economic development, others have focused on environmental conservation, and those engaged in technology transfer have concentrated their efforts on getting the technology into the hands of the end users. As a consequence, each group's problem-solving context has encompassed a relatively narrow range of organizations, professions, and solutions which are inadequate to meeting the challenge we face.

The systems perspective encourages us to take a broader view. If our mission is to maintain a sustainable resource base in the face of growing economic demands, a systematic response must be designed that brings together experts and organizational resources from various subsystems. One major opportunity for those of us in the remote sensing community to apply this integrative approach is in response to tropical deforestation. Remote sensing technology has a major role to play in the monitoring of tropical forests, and can contribute to sustainable forest management programs, provided that our data collection and distribution efforts are integrated into environmental management and economic development decisions.

RESPONSES TO TROPICAL DEFORESTATION

Losses directly associated with depletion of the tropical forest resource base, including fuel, food, shelter, pharmaceuticals, trade, etc., are tangible, and attempts to quantify these losses have been undertaken (e.g. World Resources Institute (WRI) 1985). Less tangible, but perhaps of more importance, deforestation threatens global ecosystems fundamental to life as we know it. Deforestation is the second largest contributor to the global warming process, (after the burning of fossil fuels), releasing 2 billion tons of carbon dioxide into the atmosphere annually (Houghton and Woodwell, 1989). Whereas the relative importance of tropical biomass in moderating the Earth's atmosphere is a matter of research, there is growing recognition that increase in atmospheric carbon dioxide and other aspects of global change are aggravated by continuing tropical forest depletion (Cowen 1988).

With growing awareness of the tropical deforestation issue, institutional responses have occurred at the international, national, and local level. Some of these initiatives focus on the need to provide adequate monitoring data. Others focus on the need for policy reform, giving consideration to economic, political, and institutional factors. However, there have been few attempts to incorporate remotely sensed data into global natural resource inventory and monitoring activities,[1] nor to tie remotely sensed data to environmental action plans.[2] Here, then, is a real world problem that requires the application of remote sensing technology as part of the solution. Given the new generation of radar satellites that will begin operation in this decade, there is even more reason to harness the technology for tropical forest monitoring.

Tropical deforestation is the most important global problem confronting mankind that is directly observable by environmental surface sensing imaging radar systems. These radar remote sensing satellites will be added to the optical sensing satellites (Landsat and SPOT) and passive microwave radiometric systems (NOAA-7 Advanced Very High Resolution Radiometer (AVHRR)) currently flying. The European Space Agency's Remote Sensing satellite (ERS-1) will fly in 1991; the U.S. Shuttle Imaging Radar-C (SIR-C) is scheduled for launch in 1992, and RADARSAT, a fully operational Canadian system is scheduled for 1994. Ground receiving stations to receive and process the data are being established in several developing countries. These high resolution systems complement the proven global capability of the lower resolution microwave radiometric systems and the optical sensing systems. However, there are no current plans to integrate these systems in an effective global monitoring program, and improved monitoring is only part of the solution.

FROM SATELLITE MONITORING TO EFFECTIVE ACTION

Catastrophic depletion of tropical forests is not the "problem." The real problem may be viewed as our current inability to move from satellite monitoring to effective action. In order to improve institutional responses to this

---

[1] This was the conclusion of many of those who participated in the international conference, Global Natural Resource Monitoring and Assessments: Preparing for the 21st Century, Venice, Italy, 24-30 September 1989.

[2] For example, the advisory group for the FAO Tropical Forestry Action Plan, which includes over 60 tropical countries, has expressed increasing concern over its inability to monitor and evaluate the level of progress being achieved in implementing the Plan.

significant area of global change, we must address three issues in an integrated manner: 1) available data regarding the status and rates of depletion of these resources are often inadequate, insufficient, and unfocused as to economic and political decision making processes at the national and international levels; 2) programs of technology transfer, institution building, and those designed to encourage indigenous capabilities to use the data for environmental analyses within the tropical nations need to be effectively expanded; and 3) economic, political and institutional incentives to encourage use of the data in the service of environmental policies, management, and regulation are lacking. Each of these issues is discussed briefly below.

The Data Base

It is widely believed that changes in policies will not occur without increased understanding of the local consequences of deforestation and degradation. Therefore, improved global monitoring of tropical forests is essential (International Task Force on Forestry Research 1988). Satellite technology is the key to carrying out such a monitoring process, (World Commission on Environment and Development 1987), and it is recognized as such in the science for global change initiatives (Edelson 1988). Ecologists and remote sensing experts have joined together in calling for the establishment of a global monitoring program for tropical deforestation using existing and planned satellite systems (Booth 1989, WRI and the International Institute for Environment and Development 1988).

In such research efforts aimed at redressing the information needs over tropical forests, remote sensing systems such as Landsat and SPOT are being used. However, conventional remote sensing satellites employ optical viewing systems, and thus are limited by optical visibility. As has been proven repeatedly, tropical forests are frequently cloud covered, so that optical remote sensing methods cannot provide the accurate, complete, nor timely coverage required. Radar satellite data can play an important role in providing data that can augment surveys currently underway.

Technology Transfer and Indigenous Capabilities

The effort to provide remote sensing data as input for policy making in the tropical nations would be set most constructively within a broader program of technology transfer and education in order to build indigenous capability to utilize it. Without local motivation, attempts to transfer remote sensing technology to developing countries would encounter numerous obstacles which would have to be overcome if the process is to succeed (Specter 1988).

Economic constraints are a fundamental concern in such a process. The size of capital investment required, coupled with foreign exchange considerations regarding imported information and hardware, are major obstacles to the establishment and operation of monitoring programs in tropical nations. Policy makers need information about the potential role that remote sensing technology can play in addressing their own national tropical forestry issues. Without their support, the success of any tropical forest management effort is questionable. The lack of experienced personnel who have training or education related to the use of remotely sensed data in the developing countries is a serious hurdle to be overcome. Often there is inadequate physical infrastructure to support data processing, analysis, and interpretation. Finally, increased networking and cooperation among the various ministries, agencies, and user groups is a necessary ingredient for success.

Economic, Political, and Institutional Motivations

Within the economic framework, evidence is building that the yields of alternative land uses have been greatly overestimated, while the revenues that could be obtained from standing tracts of forests have been ignored or underestimated (Peters, Alwyn, and Mendelsohn 1989). Also, the negative consequences of large scale development projects have not been quantified (Repetto 1988). In general, given the lack of cost/benefit analyses of current practices, long-term economic considerations are losing out to short-term, special interests, and often illusory gains.

Within the political decision-making framework, efforts to deal with major issues, such as the size of foreign debt owed by tropical nations to private and international banks, often lead to plans and policies which, in effect, further degrade and destroy tropical forests (Smith, Bluestone, and Yanchinski 1988). The situation is complicated by very understandable sovereignty sensitivities concerning the right of each country to control and exploit domestic natural resources. Furthermore, internal political pressures may tempt those in power to consume national forest resources in attempts to solve social and political conflicts, related to poverty, overcrowding, unemployment, and growing dissatisfaction with land tenure polices (Repetto 1988). Government ownership and control of forest resources may lead government officials, special interest groups, and others favored by those in power, to benefit financially from their disposal. In all of these political decision, both at the national and international levels, trade-offs are made by organizations and individuals presumably lacking information about the forest inventory, and the ultimate impact of their decisions leading to resource depletion.

THE EVERGREEN PLAN: A SYSTEMS APPROACH

This reveiw of the problem indicates the need for large scale, multidisciplinary action. Remote sensing technologists must join forces with anthropologists, sociologists, politicians, economists, and bankers in order to fully address the issues raised here. Furthermore, the solution will required a massive commitment of financial and institutional resources. The EverGreen Plan, currently being developed at Florida International University with the cooperation of the Canada Centre for Remote Sensing, is a long range initiative designed to assist tropical countries with forestry management. EverGreen addresses the problem by seeking to capitalize on resources already committed to tropical deforestation monitoring and amelioration, within a program designed to integrate data collection, technology transfer, and responsive action.

Uniqueness of The EverGreen Plan

Any tropical forest observation effort would be enhanced through inclusion of data from radar satellites. Data from the only radar based environmental satellites that have flown to date (SEASAT (1978), SIR-A (1981), and SIR-B (1984)) indicate that spaceborne imaging radars could be used to monitor tropical deforestation. Although the feasibility of this application has been reinforced, there exists rather little effort world-wide to exploit this valuable capability. A forestry radar data base does exist, but it largely excludes tropical data. Many airborne radar missions have been flown in the tropics, but almost exclusively for mapping, or, ironically, for locating stands of large tree specimens for the timber market. In short, there is a job to be done for which systematic spaceborne radar data is eminently suited.

Ground receiving stations to receive and process the radar data expected in this decade are being established in several of the tropical countries where the rates of tropical deforestation are most severe. An Initiative such as The EverGreen Plan is essential to prepare for the effective use of data from these systems in a global tropical forestry monitoring program.

The EverGreen Plan will encourage and capitalize on deployments being planned by remote sensing agencies of experimental airborne imaging radars to tropical forested regions, supported by SAR (Synthetic Aperture Radar) scientists knowledgeable in forestry applications. The program will expand to include data from imaging radar satellites, ERS-1 and SIR-C during the period 1991-1993. The primary value of the use of these data sources will be to prepare for the operational use of satellite SAR data in the latter half of the decade. The first SAR satellite planned to support operational data requirements is RADARSAT, a Canadian mission to be launched by NASA in 1994.

Goals of the EverGreen Plan

In order to provide a coupling between monitoring and management, the EverGreen Plan has scientific, institutional, and policy-related objectives. Achievement of EverGreen's scientific objectives will improve significantly the quality of information available concerning rates of tropical forests' depletion and the types of human activities related to such losses. The scientific objectives of EverGreen are intended to support quantitative remote sensing methodology for tropical forest observation, especially by C-Band radars. The technical objectives are to: 1) coordinate independent investigations directed towards obtaining specific forest radar signatures; 2) compile a listing of tropical forest radar data base, one which, where appropriate, is related to existing temperate and boreal forest radar data bases; 3) identify and qualify key radar and forestry parameters of importance to global monitoring; and 4) encourage and contribute to the development of a strategy for effective tropical forestry monitoring using remote sensing systems in the 1990s.

However, simple availability of forestry information is insufficient by itself. If data collection is to play a significant role in reversing tropical deforestation, the terms of data availability, and local mechanisms for its use must be designed and implemented so that constructive forestry management plans are encouraged.

In light of this perspective, EverGreen's institutional objectives are directed at strengthening individuals and institutions committed to sustainable tropical forestry management practices. Institutional objectives are to: 1) foster establishment of expertise in radar tropical forest observation resident in participating tropical nations; 2) build linkages between participating nations and radar satellite sponsoring nation(s) for on-going tropical forest assessment; and 3) cooperate with appropriate international agencies (such as FAO) engaged in tropical forest ameliorative action, particularly to establish information requirements in support of initiatives such as the Tropical Forestry Action Plan, as well as national and international economic programs.

Even with institution building activities, effective management of tropical forests will not occur unless and until policies and incentives are put in place to stimulate international and local response. Through this third set of objectives related to matters of policy, The EverGreen Plan seeks to: 1) initiate creative national and international policies regarding data availability; 2) encourage the establishment of necessary technology transfer policies from radar satellite launching states; and 3) conduct policy research to identify political, economic, and institutional incentives, tied to terms of data availability, that would encourage a redirection of international and national policies toward sustainable tropical forest environments.

Resources and Responsibilties

The EverGreen Secretariat, headquartered at Florida International University, will call on the abilities and directed energies of two central groups: the international steering committee and the international advisory board. The international steering committee will be comprised of individuals who are internationally recognized for their leadership in issues related to environmental policies and planning. Optimally, five such experts will agree to serve on the committee. Individuals currently being considered include a past official with the United Nations Environment Programme, a U.S. chief executive who previously directed a federal government agency concerned with environmental issues, and the director of a public policy institute concerned with environmental issues.

The international advisory board will be comprised of representatives from each of the three countries which agree to participate in the demonstration projects in Africa, Asia, and Latin America. These individuals will be most likely government officials from ministries of science and technology, or environmental ministries, at sufficiently high levels to commit to program activities and direct implementation. The board will include representatives of the remote sensing nations who would be providing data: e.g., the U.S., Canada, and The European Space Agency.

The EverGreen Timeframe

The overall Plan is divided into four phases. Each phase is comprised of a research component and a networking/implementation component. These are discussed briefly below. Phase I (18 months): Networking activities include establishing an international steering committee to set EverGreen Plan policies; establishing an international advisory board to represent national interests in program implementation; establishing linkages to key, active programs and organizations. Research will be initiated in three areas related to data policies, technology transfer processes, and current patterns of decision making involving trade-offs between environmental and development concerns, and the role that satellite data may play in these decisions. Also, regional workshops will be held in Africa, Asia, and Latin America. Phase II (2-3 years): Field research will be conducted to establish radar data sets for tropical forests; efforts will be made to establish radar capabilities in demonstration project countries, including technology transfer through education, training, and equipment, in order to build indigenous capacities to use the data. Phase III (2-3 years): Demonstration project activities will be carried out and the technology transfer program will be continued. Phase IV (3 years and beyond): An ongoing global monitoring program for tropical forests, with central participation by local decision makers, will be established.

Current Status

The EverGreen Plan is currently is Phase I. Work is underway to bring together a corps of experts to serve on the international steering and advisory committees. The Plan has gained recognition through presentations at international meetings during the past year. Research has been initiated in key areas which will provide foundations for EverGreen's long-term activities. Funding support is being sought for this work.

In addition, progress is being made toward The EverGreen Workshops, to be held in conjunction with regional symposiums in Africa, Asia, and Latin America. Based on a proposal at the International Space Year (ISY) Conference on Education and Applications in early 1990, plans are underway to hold the first workshop in 1991 at the Institute for Space Research in Brazil, in cooperation with Dr. Roberto Pereira da Cunha, Director of Remote Sensing. The workshop will serve as the first in a series of SAR Deforestation Education workshops. The Workshop proposal was most recently presented at the Space Conference of the Americas: Prospects for Cooperation and Development, held in March 1990. As a result, there is growing interest in EverGreen throughout Latin America.

This paper is offered as a vehicle for discussion and to encourage comments and participation from those attending the ISPRS Commission I International Symposium on Primary Data Acquisition. The authors hope to use this opportunity to increase awareness and support for the Plan among Latim American remote sensing experts and others who are concerned with the delicate balance between the management of tropical forest resources and economic development.

BIBLIOGRAPHY

Booth, W. 1989, Monitoring the Fate of Forests from Space: Science, Volume 243, 17 March, pp. 1428-29.

Churchman, C.W. 1979, The Systems Approach, 2nd ed., Delacorte Press, New York.

Cowen, R. 1988, Wheels within Wheels: Mosaic, Vol. 19, No. 3/4, pp. 60-69.

Edelson, E. 1988, Laying the Foundation: Mosaic, Vol 19, No. 3/4, pp. 4-11.

Frame, J.D. 1983, International Business and Global Technology, Lexington Books, Lexington, Mass.

Hankins, D.B. 1977, Building a Model for a Remote Sensing Technology Transfer Program in Northern California, NASA-sponsored final report, Arcata, California.

Houghton, R.A., and G.M. Woodwell 1989, Global Climatic Change: Scientific American, Vol. 260, No. 4, April, pp 36-44.

INPE 1990, INPE Space News, Vol. 1, No. 1, January/February/March 1990, pp. 3-5.

International Task Force on Forestry Research 1988, A Global Research Strategy for Tropical Forestry, Rockefeller Foundation, United Nations Development Programme, World Bank, Food and Agriculture Organization, September, p. 63.

Levin, S. 1978, The Role of Science and Technology in Development: Proceedings of the Twelfth International Symposium on Remote Sensing of Environment, pp. 11-15.

MacNeill, J. 1989, Strategies for Sustainable Development: Scientific American, Vol. 261, No. 3, September, pp. 155-165.

Pala, S. A Working Concept of Remote Sensing Technology Transfer: Proceedigns of the Fourteenth International Symposium on Remote Sensing of Environment, pp. 1653-1660.

Peters, C.M., H.G. Alwyn, and R.O. Mendelsohn 1989, Valuation of an Amazonian Rainforest: Nature, Vol. 339, 29 June, pp. 655-656.

Repetto, R. 1988, The Forest for the Trees? Government Policies and the Misuse of Forest Resources, World Resources Institute, Washington, D.C.

Rogers, E.M. 1983, Diffusions of Innovations, 3rd ed., Free Press, New York.

Rogers, E.M. and J.D. Eveland 1975, Diffusion of Innovations: Perspectives on National R&D Assessment, Technological Innovation: A Critical Review of Current Knowledge, 2, Aspects of Technological Innovation, Consultant Papers, U.S. Department of Commerce, National Technical Information Service, Springfield, Va., pp. 334-337.

Robinson, R.D. 1989, Toward Creating an International Technology Transfer Paradigm: The International Trade Journal, Vol. IV, No. 1, pp. 1-19.

Roman, D.E. 1980, Science, Technology, and Innovation: A Systems Approach, Grid Publishing, Inc., Columbus, Ohio.

Smith, E.M., M. Bluestone, and S. Yanchinski 1988, The Global Greenhouse Finally Has Leaders Sweating: Business Week, 1 August 1988, pp. 74-76.

Specter, C. 1990, An International Space Year Policy for Developing and Newly Industrialized Countries: Space Policy, May 1990 (forthcoming).

Specter, C. 1988, Managing Remote Sensing Technology Transfer to Developing Countries: A Survey of Experts in the Field: Photogrammetria, Vol. 43, No. 1, September 1988, pp. 25-36.

Specter, C. 1986, The Transfer of Remote Sensing Technology to Developing Countries: The Landsat Experience, 1970-1985, University Microfilms International, Ann Arbor, Michigan.

Specter, C. and D. Gayle 1989, Remote Sensing Technology Applications for the Caribbean: Overcoming Economic, Political, and Institutional Obstacles: Proceedings of IEEE International Geoscience and Remote Sensing Symposium '89, Vancouver, Canada, 10-14 July 1989.

Voute, C. 1982, Satellite Remote Sensing for Developing Countries: Prospects and Constraints: Proceedings of an EARSel-ESA Symposium, ESA P-175, June 1982, pp. 196-197.

Weiss, C. and J. Ramesh 1983, Science and Technology Policies in Developing Countries: A Retrospective View: Interdisciplinary Science Reviews, Vol. 8, No. 1, pp. 251-263.

World Commission on Environment and Development 1987, Our Common Future, Oxford University Press, Oxford.

World Resources Institute 1985, Tropical Forests: A Call for Action, Part I, The Plan, Library of Congress 85-51864, World Resources Institute, Washington, D.C.

World Resources Institute and the Institute for Environment and Development 1988, World Resources 1988-1989, Basic Books, Inc., New York.

THE WORLD OZONE DILEMMA:
RESEARCH AND RESULTS WITH REMOTE SENSING

Dr. J.J. Hurtak, Ph.D
Technology Marketing Analysis Corporation
P.O. Box FE
Los Gatos, California 95031 USA

ABSTRACT

In order to study the chemically perturbed region of the Antarctic and the Arctic, NASA initiated airborne and satellite imaging of the ozone depletion through the specialized ER-2 plane (at ~ 18 km) and the modified DC-8-72 aircraft (at ~ 12.5 km) with remote sensing systems onboard. Instruments onboard the ER-2 and DC-8 NASA research aircraft surveyed the atmosphere from various altitudes and instruments on the Nimbus-7 satellite analyzed reflected sunlight. Measurements were designed to gauge not only the extent of ozone depletion over the Antarctic/Arctic, but other chemical changes in the stratosphere. Activities carried out within programs of remote sensing and *in situ* measurements by aircraft are compared with are compared to TOMS onboard the Nimbus-7, as well as Dobson network ground stations.[1] Through these methods, scientists have been extremely successful in mapping the huge hole in the ozone layer that appeared over Antarctica, which is particularly extensive for about two months of each year and to confirm ozone loss in the Arctic area.

1. THE MECHANISMS FOR OZONE DESTRUCTION

Scientists at NASA, the National Science Foundation, the National Oceanic and Atmospheric Administration (NOAA) and other institutions after careful study now believe that the primary triggers of ozone depletion take place when a single atom of chlorine (Cl) combines with O_3 to form molecules of ClO and O_2. In some instances sunlight accelerates the change, focusing on ice crystals in the stratosphere with attached chlorine molecules reacting with ozone yielding O_2. Scientists believe that many of the same conditions of wind, light and temperature that cause the ozone depletion over the Antarctic -- the "ozone hole"-- may also be occurring around the Arctic. In addition, the continual pollution of CFCs and halons appear to add to this phenomena.[2]

Although the key reaction for destruction of ozone takes place when Cl + O_3 react, it is believed that this might begin with the ClO dimer mechanism, where the reaction of ClO + ClO yields Cl_2O_2 which photolyses to atomic chlorine and ClOO and ends with a catalytic destruction of ozone, where atomic chlorine (Cl) reacts with O_3 to form ClO + O_2. Several processes may actually be taking place. For example, the chlorine monoxide dimer could breakdown into Cl_2 + O_2, eventually yielding two atomic chlorine, necessary for the key reaction.

The theory that chlorofluorocarbons (CFCs) could be destroying the ozone layer in the earth's stratosphere was originally presented in 1974 by Dr. F. Sherwood Rowland of the University of California (Irvine) and Mario Molino now at Jet Propulsion Laboratory, California.[3] Their concern was that CFC compounds are chemically inert and could remain in the atmosphere for 40-150 years eventually photolyzing to reactant Cl.

Chemicals are removed from the environments via "sinks," namely photodissociation, rainout, and oxidation. However, the only important sink for CFC-11 and CFC-12 is photodissociation in the mid-stratosphere by solar UV radiation with wavelengths shorter than 230 nm[4] which never reach the lower atmospheres. The CFCs only diffuse when they reach altitudes of 25 to 40 km (with the greatest ozone region lying between 15-35 km). Once they are broken down in the stratosphere, they yield atomic chlorine, which then makes it way back into the lower stratosphere through the ozone layer and finally into the troposphere deposited as hydrochloric acid (HCl).

One must look at the rate of the reactions in the upper atmosphere under full sunlight, as well as with cloud-cover. Quantitatively there is a correlation between the abundance of ClO and the amount of ozone lost. The important factor in the ClO_x chain is that after the chlorine reactant initiates the process of ozone destruction (or the destruction of any odd oxygen, i.e. O_1 or O_3), the Cl is not removed (in a denitrified environment) but is able to once again repeat the process. And each chlorine atom could destroy approximately 100,000 molecules of ozone.[5]

A complete understanding of key chemical reaction rates and photodisassociation products within the catalytic process is still incomplete. If the photolysis products of the ClO dimer are Cl-ClOO, then ozone destruction occurs, but if the products are Cl + O + ClO, then this would not be the mechanism that would

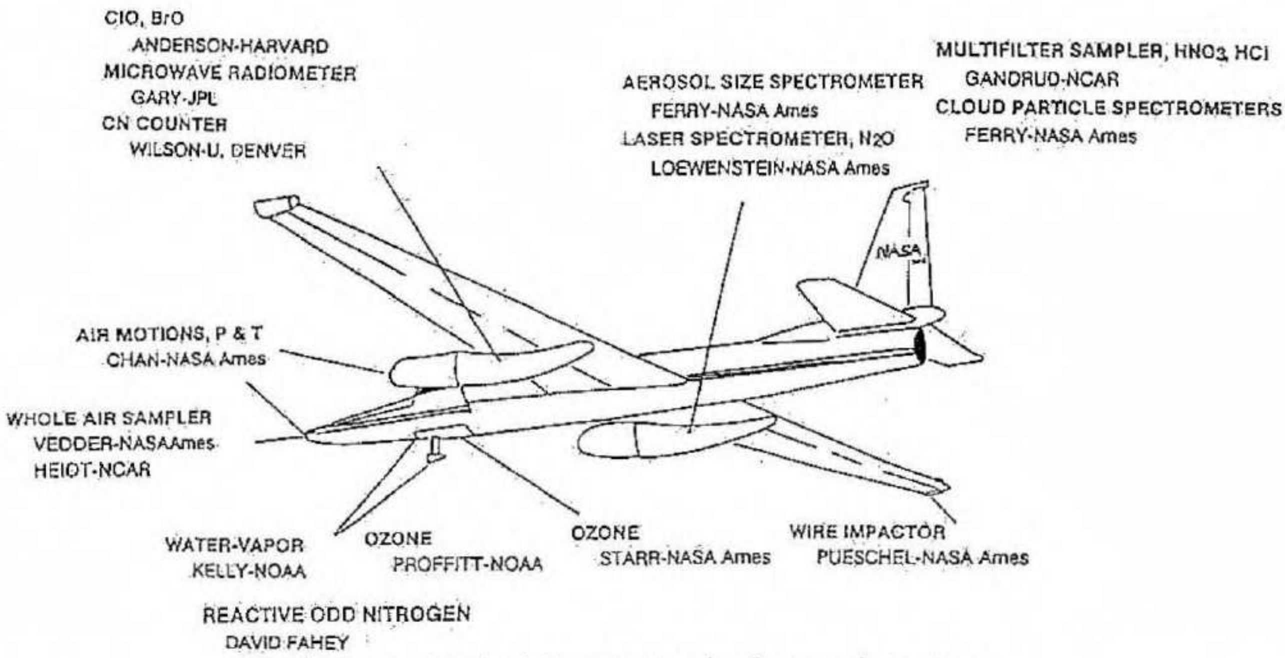

Figure 1. ER-2 with Instrumentation used at AAOE

be destroying the extensive amount of ozone loss observed.

The HCl and $ClONO_2$ that are usually present as nonreactive reservoir species are transformed on aerosols and cloud particles to a form of active chlorine (ClO). The effect of sunlight appears to accelerate the reaction, focusing on ice crystals in the stratosphere with attached heterogeneous (surface) chlorine molecules, creating different amounts of ozone loss at various times of the year.[6] The long polar winter night produces stratospheric temperatures as low as -90°C at 15-20 km which produces Polar Stratospheric Clouds (PSCs). Chemical reactions on their surface are thought to convert hydrochloric acid and chlorine nitrate into molecular chlorine and hypochlorous acid (HOCl) and also separate nitrogen oxides as nitric acid. Then when spring arrives the atomic chlorine is released by the sun, triggering ClO_x chain reactions.

If nitrogen radicals were in abundance, chlorine monoxide would rapidly react to form chlorine nitrate, $ClONO_2$, which like HCl is nonreactive to ozone. Since little NO_x exists to react with ClO, there is no stopping the reaction for 5-6 weeks, causing ozone depletion of 95% in the stratosphere and 60% in all latitudes surrounding the PSCs. The chlorine oxide dimer reaction is thought to account for 75-85% of the ozone depletion in the Antarctic.[7]

2. STRATEGY FOR THE AAOE

The NASA research planes (the DC-8 and modified U-2) utilized between 10 and 13 instruments each in surveying the atmosphere from various altitudes. The flights were based in Punta Arenas, Chile (53°S, 71°W) and flew southward towards the Palmer Peninsula of Antarctica. The AAOE (Airborne Antarctic Ozone Experiment) August and September 1987 was designed to investigate the Antarctic polar vortex. The vortex, a pattern of stable but swirling winds, isolates a large portion of the polar stratosphere. Inside the vortex, air temperatures decrease enough for the formation of type II PSCs (Polar Stratospheric Clouds). Locations of chemically perturbed regions (CPR) within the vortex were made known by the TOMS (Total Ozone Mapping Spectrometer) almost--real-time maps and SAM II measurements of the PSCs.[8]

The DC-8 flew 13 flights in all including extended night flights using lidar measurements with a 308 nm wavelength XeCl-Raman laser having a repetition rate of up to 50 Hz which had its best signal-to-noise ratio in darkness.[9]

The instruments varied according to flight times. The FTIR (Fourier transform IR) required low sun angles, but the NOAA UV/VIS spectrometer used a wide range of angles (including flights 870908-870909) which took place at night during a full moon to measure OClO.[10]

The benefit of the DC-8 was its long-range of 11+ hours flying time to achieve direct penetration of the hole. During the AAOE flights it encountered temperatures colder than its certified limit of -76°C. This problem was overcome by flying lower, or by pumping fuel between the various tanks.[11] Cirrus clouds were found to prevent accurate readings by the FTIR and lidar measuring devices. On one flight (870905) the DC-8 encountered a mini-hole on the outer reaches of the vortex and next to massive PSCs. Some theories indicate that this is not due to large-scale transport of ozone-poor air into the vortex, but relates to anticyclonic flow around the vortex itself creating a low-ozone column.[12]

The 12 ER-2 flights were limited to approximately 6 hours of flying time or 200 nautical miles, reaching their turnaround point by mid-day. The aircraft flew only in sunlight and 72°S (80-90°W) was considered the southernmost part of the flight. (According to TOMS' data, the ozone depletion covers an area from the south pole to approximately 70°S.)[13]

The ER-2 plane has a length of 19 meters and carries extensive payload leaving room for only a single-seat. The pilot must operate all of the instruments that are loaded into the aircraft's wing pods, nose compartment and aft fuselage (See Figure 1).

The plane carried instruments for *in situ* measurements of O_3, chlorine monoxide (ClO), BrO, and NO_y (sum of all odd nitrogen species). In the spear-pod under the wing was a MFS (multifilter sampler) using a cellulose-type filter paper and a Teflon cloth filter which is exposed to the airstream at varying times from 7-55 minutes. The MFS carries up to 22 filters with an 11.4 cm exposure diameter. The filters are held in a linear storage magazine, and are activated by the pilot. The samples which measured sulfate, nitrate, chloride, and flouride abundances were analyzed on base at Punta Arenas immediately after the flight.[14]

The plane also carried a scanning microwave radiometer to measure temperatures above and below the aircraft.

The average potential temperature surface of the flights were of 425 +/- 25K at approx. 18 km. Return flights were sometimes lower in altitude, but followed a similar flight path.[15] Because of weather conditions and movement of the Antarctic vortex in 1987, only three flights were launched while the vortex was close: 870902, 870904, 870909. Other flights during the AAOE had to go off flight track to reach the vortex measuring areas. During the AAOE, there were 6 days when both aircraft flew. These were 870828, 870830, 870902, 870909, 870916, 870921.[16]

The ER-2 also made ferry flights between Moffett Field, California and Punta Arenas, before (870812-15) and after (870929-871003) the scheduled flights over the Antarctic. These flights were extremely important in comparing ozone depletion at mid-latitudes. The equipment onboard the aircraft was calibrated to measure the stratospheric ozone (O_3) which is normally found at a concentration of 10 parts per million, chlorine normally found as a few parts per billion (ppb) with reactive chlorine measured in parts per trillion.

As NASA's Antarctic data was analyzed, large amounts of chlorine monoxide were found at 18 km in altitude. Concentrations of chlorine monoxide (ClO) reached 1 ppb,[17] about two orders of magnitude larger than is found over the temperate zones at the same altitude.

3. AIRBORNE ARCTIC STRATOSPHERIC EXPEDITION

Compared with the Antarctic, PSCs are not as abundant and have a shorter existence due to warmer temperatures in the Arctic. The warmer temperatures (-80°C as opposed to -90°C in the Antarctic) are in part caused by the greater mass of land in the Northern Hemisphere. Only in approximately five of the last 30 winters have January temperatures in the Northern polar region been cold enough for ice clouds to form. The polar vortex is not as constricted and there is little sunlight due to the polar night. However, more than 100 scientists from the U.K., West Germany, Norway, Denmark, and the United States took part in the $10 million dollar six-week ozone study (January-February 1989) in the north polar region sponsored by NASA and NOAA.[18]

Before the flights, scientists knew that the ozone depletion was not as advanced as the hole over the Antarctic and expected a loss in the range of about 2-8% in stratospheric ozone to have occurred over the past two decades.[19] The depletion was anticipated to be greater at higher latitudes and greatest in winter.

The ER-2 and DC-8 planes recorded the chlorine monoxide levels in the Northern stratosphere. The planes were based at Stavanger, Norway (59°N.) and each flew approximately 14 flights. The DC-8 usually targeting the North pole as their turn around point. The Canadians participated by sending experimental balloons into the Arctic stratosphere from Alert Bay, Canada and findings were coordinated with TOMS on board the NIMBUS-7 satellite.

The major part of the expedition was scheduled for the months of January and February, but findings indicated that the expedition should have been scheduled to remain until March or April even though the majority of the PSCs had broken up by mid-February.

4. SURVEY FINDINGS

Ozone measurements have been underway since the 1920s using ground-based ultraviolet spectrometers known as Dobson instruments. An extensive network has now been established with one operating at Halley Bay (Antarctica 76°S) by the British Antarctic Survey team which noted ozone changes as early as the late 1970s.[20]

Significant ozone loss in the Antarctic lower stratosphere during September and October (springtime) were first reported in 1985 by J.C. Farman, et al.[21] This was confirmed in 1986 during the NOZE I expedition that noted evidence of high chlorine chemistry and low nitrogen compounds with ozone levels depleted in the 12 - 20 km region.[22]

4.1 The Antarctic Findings

Within the chemically perturbed region (CPR) of the Antarctic, ClO levels were found to be more than 100 times those expected from mid-latitude measurements. Concentrations where found to be as high as 1.3 ppbv, as opposed to the total 0.7 ppbv chlorine available in the atmosphere in 1965.[23] The CPR areas of the vortex were defined at the abrupt rise in concentration of ClO. The high levels of chlorine monoxide (ClO), however, were not consistent throughout the year. The levels were very low in late winter when there was little sun which has led to the theory that there is a correspondence between the increase in sunlight, the growth of chlorine monoxide, and the decrease in ozone.

Bromide (Br) may also play the same role as reactive chlorine when exposed to ozone, but it does not appear to be the dominant factor. Although, it is now believed that the existence of OClO could be the result of a reaction that started with ClO + BrO. Significantly larger amounts of Br were measured in 1987-88 than previously observed, lending to the belief that some reactions may be taking place.[24]

Recently methane has also been taken as a serious target in both the north and south hemisphere. Findings have shown the increase yearly of about 0.016 ppmv.[25] The incremental greenhouse effect of methane is about 20 times that for CO_2.

When the expedition first arrived in August 1987, a consistent positive correlation or ratio between ClO and O_3 was observed. By the middle of September, the same concentration began dropping at ER-2 altitudes at 70-200 mbar. Instead, a strong anti-correlation developed between ClO and O_3 on both large and small scales within the chemically perturbed region (CPR) of the vortex.[26]

MFS found that sulfate aerosol levels within the CPR are lower than the levels outside the CPR. This would suggest that the air mass inside originated from a different region of the atmosphere and does not indicate any enhancement of sulfate due to periodic volcanic activity.[27]

NASA also found in their ER-2 airborne observations that the atmosphere was not only dehydrated, but also denitrified containing unusually small concentrations of nitrogen radicals.[28] Nitrogen compounds convert reactive chlorine back into its nonreactive form (chlorine nitrate), so the presence of nitric acid clouds are clearly of importance. What was recorded were extremely low values of nitrogen within the chemically perturbed region of the vortex.

The MFS was used to analyze the amount of stratospheric nitrate. Laboratory tests have demonstrated that the filters collect accurate data on nitric acid and $ClONO_2$ as nitrate. These filters also have the ability to analyze the amount of chlorine by collecting Cl from HCl and $ClONO_2$ in the vapor phase and Cl in the particulate phase. Their findings showed that in all cases the amount of total nitrate inside the CPR was less than the amount outside the CPR. Observations made over a 36-day period showed a loss of .06 ppbv total nitrate.[29]

It is clear from the ER-2 flights in the CPR that the region of dehydrified and denitrified air maintained a sharply defined latitude gradient throughout most of the expedition. On a purely meteorological definition, the vortex edge would be well outside the dehydrified, denitrified region.

Specifically, NASA received chemical data on nitrogen in 1986 from both ground-based and airborne experiments. Abundance of NO_2 of 8-12 ppbv was observed outside the chemically perturbed region while 1 to 3 ppbv was observed inside the vortex.[30] NO_2 observations suggest that NO_2 component species are incorporated into polar stratospheric cloud PSC particles. It appears that the nitrous compounds have been taken up by ice crystals, then precipitated out of the atmosphere.

Observations support the picture that NO_y is low because it has been removed from the atmosphere by being taken up in ice crystals which gravitationally settle to much lower altitudes. This picture is supported by observation of low column abundances of HCl and by occasional observations of high levels of nitrate found in the ice particles, and by the visual and lidar observations of high cirrus and PSCs.

The lack of nitrogen compounds also disproves various theories that have been used to explain the ozone hole, such as the solar theory or the cosmic ray theory, etc., that would require high levels of nitrogen oxide.

4.2 The Arctic Results

The recent findings in 1989, during the airborne stratospheric expedition to analyze the chemical composition of the Arctic polar stratosphere found it to be also highly disturbed with the observed abundance of ozone depleting chlorine monoxide radical (ClO) elevated to a factor of 50 in the Arctic stratosphere. The observation added up to a consistent picture with that of the Antarctic data in 1987, believed to be the result of chemical reactions occurring on PSCs that form in the extreme cold regions of the Antarctic region.[31]

Toon also reported that levels of ClO in the Arctic region were as high as 8 ppt which is capable of destroying about 1/2 - 1% of stratospheric ozone per day.[32] It was also discovered that the air in the

Arctic vortex contained PSCs and held extremely low levels of hydrochloric acid and chlorine nitrate which are reservoir species in the stratosphere and would not be involved in ozone destruction. These low levels would indicate that there is a reaction taking place in the Arctic vortex that converts inactive chlorine compounds into active ones. The important factor in the annual amount of ozone depletion in the northern hemisphere could be directly based on the temperature and stability of the vortex.

Unlike the Antarctic, the Arctic showed higher levels of nitric acid which could be converted by sunlight into nitrogen oxides which would reconvert the ClO into an inactive form.

The key factor might be that there are two types of PSC formations. Type I, most common over the Arctic, is composed mostly of $HNO_3 \cdot 3H_2O$ (nitric acid trihydrate) and forms at about -77°C. Type II contain mostly water ice and do not form until the temperatures are closer to -85°C. Type II PSC provide the most active surfaces on which inactive forms of chlorine are converted to reactant forms[33] and they seldom are formed over the Arctic region. However, during the 1989 expedition some Type II PSCs were observed. Scientists now believe that Type I PSC might also contribute, although to a slower pace of ozone destruction or that the chlorine rich air with reactant chlorine might drift into sunlight at lower latitudes to account for the wintertime decrease in ozone.[34]

In the Arctic area, the ClO levels were so high that scientists believe that even after the vortex breaks down, the molecules could be sent out to lower latitudes where there will still be limited ozone destruction depending upon how fast molecular diffusion can bring in NO_x to react with the Cl.

In February, 1989 Canadian balloon experiments over the Arctic measured a fall in ozone of about 25% over Scandinavia which is attributed to an "ozone crater" not an overall net loss. Scientists are not willing to say if this is part of an overall chemical or only meteorological effect because the loss coincided with a cyclone from intermediate latitudes.[35]

5. CHEMICAL VS METEOROLOGICAL THEORIES

Several theories have been put forth, and various causes for the ozone hole have been proposed. There is some direct effect of loss of ozone due to meteorological influences where sunlight, wind and temperature appear to be the controlling factor. One event occurred over the Palmer Peninsula on September 5, 1986 where over a period of 24 hours total ozone decreased by about 10% over an area of approximately 3 million square miles. Such a rapid decrease is difficult to explain chemically.

Lidar measurements from the DC-8 showed low ozone values and extensive aerosol layers between 14 and 15 km in the region of the TOMS minimum of ozone.[36] Such events were spatially correlated with deepening surface pressure lows and marked meridonal flows from middle to high latitudes at lower stratospheric levels.

However, it is also clear that the hole is not purely caused by meteorological factors. Nor is it formed exclusively by an upwelling of low atmospheric materials (in a sustained large scale) from the troposphere to the stratosphere--giving a purely dynamic uplift mechanism to the loss of ozone.

The conclusion is that chemical and meteorological data cannot be separated. An illustration of this difficulty to clearly establish chemical or dynamical mechanisms is the decreasing trends in ozone in regions of ClO outside of the vortex whose magnitudes are comparable to those within the ozone hole vortex. Moreover, downward trends of ozone were observed at the lower altitude regions where ClO concentrations were substantially lower than at 18 km and are not adequate to explain the destruction of ozone in the 14-15 km region.

Low values of CFC-11 (i.e., an aerosol propellant), CFC-113, CFC-12 (i.e., a refrigerant, CF2Cl2), CH_3CCl_3 and N_2O were observed at the upper levels of the ER-2 flight tracks within the chemically perturbed region. The MFS noted that there were consistently higher levels of acidic fluoride concentrations inside of the CPR versus outside of the CPR, showing that the air arrived from a descent from a higher altitude. The ratio of HCl/HF inside the CPR was a consistent ratio of near 1 (0.9 +/- 0.3), indicating a loss of acidic chloride either by the removal of chloride from the airmass or the partitioning of chloride into an unmeasured species.[37] Where the Cl/F ratios outside the CPR are consistently in the 0.5 - 3.0 range of a volume/volume ratio.

A key question is how these values are maintained in the chemically perturbed region? Since 1986, all data appears to correlate with the appearance and formation of PSCs between 16 and 24 km with present calculations taken from 1 µm SAM II showing the formation of type I particles with an aerosol extinction ratio ranging in values from 2 to 50 and type II being those greater than 50.[38] Modeling the proposed availability of free chlorine reactants depends critically on the extent and character of these surfaces which provide active sites for heterogenous reactions liberating reactive halogens whereby effectively immobilizing and depleting the NO_x reservoir.[39] The existence of the PSCs was found to decrease with time after early winter which was attributed to the loss of HNO_3 and H_2O by sedimentation, and directly correlates to the major sequences of ozone depletion at the polar areas.

6. CHANGING THE CHLORINE MOLECULE

Even if we immediately stop the production of all CFCs, we will still be suffering at least for the next 50 years from the chemical effects in our atmosphere. According to Prof. A.Y. Wong et al., from the University of California, Los Angeles, there may be a way of reducing the destruction rate and removing these Cl atoms from the atmospheric ozone region through ion kinetics. Given Gibbs theory on free energy on Cl_x- and NO_x- reactions with ozone which shows that reaction rates of negative ions are slower by several orders of magnitude, where the reaction rate with atomic Cl and O_3 is ΔG = -168kJ/mol the reaction involving Cl^- would be $\Delta G \approx 0$ and the reaction is less than 10^{-12} cm^3/sec.[40]

By using radio frequencies, creating an increase in the electron temperature and density in the atmosphere, an electron could be added to the initial breakdown of halocarbons so the Cl released will not be atomic chlorine but Cl^-. The principle reaction given the conditions and elements in the polar region would then be: $Cl^- + H \rightarrow HCl + e^-$. Depending upon the ambient temperatures the rate from atomic Cl with H is 6.5 x 10^2, the rate would be Cl^- is 9.3 x 10^2. For every 6% decrease in concentration of the most active Cl there is a 1% increase in ozone which is a 3-10% increase in the optical opacity of the layer.[41]

If this proves to be effective and safe for the environment, existing facilities could be used that have high powered ground-based HF transmitters to aid the formation of Cl^-. Ground-based and spaceborne radar have already given us an understanding as to the physical behavior of the ionosphere. At present there are three high powered ionospheric heating facilities in the Western world that could be considered: 1) Tromso, Norway; 2) HIPAS at Fairbanks, Alaska; 3) Arecibo, Puerto Rico. HIPAS (High Power Auroral Stimulation) heater can deliver a peak power of 2MW in 1 ms at a repetition rate of 1 Hz.[42] The purpose of the program at HIPAS has been to understand radio frequency interaction with the ionosphere at both high and low frequencies.

Already in the polar region, there is a large source of free energy (approx. 10^{11} watts) existing in the form of electric fields and currents driven by magnetospheric sources. Using RF from ground-based facilities, the energy of electrons could increase by heating the electrons by the oscillating E-field which could in turn undergo collisions with neutrals. According to Wong, increasing electron temperatures leads to an increase in the vertical downward-pointing electric field which enhances the upward transport of negative ions along the magnetic field amplifying the original power source.[43] The next question then is at what altitude should the heating take place. Since early research has also shown that radio frequencies can reduce ozone production, but mainly in the upper part of the ozone layer (> 70km). It has been shown, however, that a decrease in ozone at the upper atmospheric regions leads to an increase of ozone throughout the ozone regions at mid- and low altitudes.[44]

7. FUTURE SURVEYS

The new systematic look at the ozone-depleting mechanisms and our ability to alleviate them depends on actual experiments, analyses and measurements which have spin-offs for environmental science. A network of ground-based spectrometers in Canada, U.K., Scandinavia (Norway and Greenland) and the Soviet Union will continue to analyze the chemical components of the atmosphere above them by measuring the modifications these chemicals cause in the natural spectrum of sunlight.[45] The monitoring and predicting of changes in the earth's polar environment prompts follow-on studies of world environmental science and increases our sensitivity to the fragile biospheric balance.

Even after the January-February 1989 expedition of the Arctic stratosphere, researchers in Norway and Greenland have continued to release balloons to compile vertical data on the ozone depletion of the stratosphere. In the U.S., TOMS satellite data have continued to be collected over these specific areas. More sophisticated and diverse sensors are also being designed to better understand earth's ozone concentrations.

NASA has proposed a system called Network for The Detection of Stratospheric Change which would span top U.S. facilities from Goddard Space Flight Center to JPL using remote sensors aboard NOAA and Nimbus satellites. NASA has already developed some preliminary equipment which includes using mobile ground laser systems (Table Mountain, California) with orbiting satellites, sounding rockets and balloon sondes. This network will permit earth-based and satellite measurements of mid-latitude ozone trends to be correlated.

The new JPL equipment will make use of excimer lasers to generate ultraviolet light at two wavelengths which are absorbed differently by ozone. Some of this light will be reflected back towards the ground by gases in the atmosphere. A large telescope with very sensitive ultraviolet detectors will collect and measure part of the backscattered light,

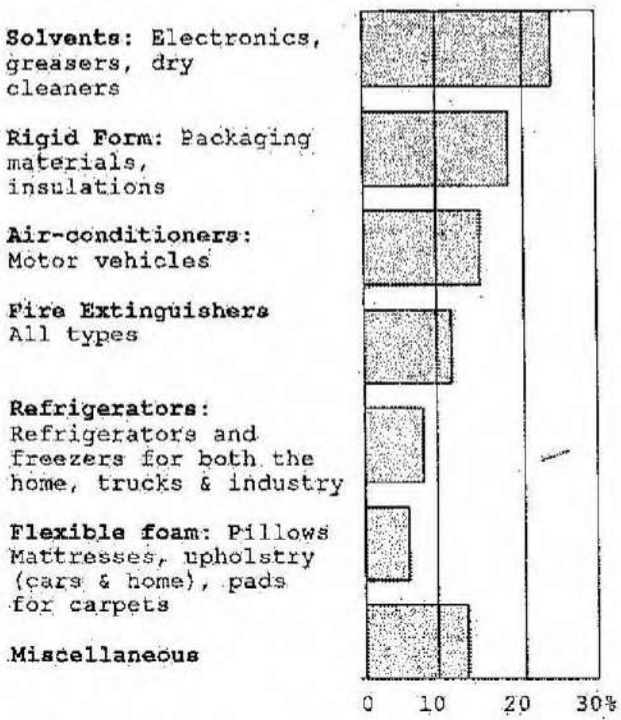

Figure 2: CFCs In The U.S. By Percentage

and the amount of ozone will be calculated by comparing the two return signals.

Europe is also preparing for sophisticated ozone studies through the ERS-1 (Earth Remote Sensing-1) system sponsored by the European Space Agency (ESA). It is scheduled for launch in 1990 in a near polar orbit at an altitude of 780 km. The ERS-1 is to be an end-to-end system with a space and ground segment to provide global oceanic and regional ice/land coverage. Every 3 hours it will deliver standard products that will be used for supporting scientific objectives related to open ocean and coastal zone processes, polar ice regions, global climate, and satellite data processing techniques. It is anticipated that after 2 years of orbit all of the global and regional mission objectives of ERS-1 will have been met.

Another unique system--a European Polar Platform--will be launched with the help of the British Aerospace, Space and Communications Division in Filton Bristol, U.K.[46] This will be a free-flying polar platform that is also a pressurized module which will be attached permanently to a space-station and a man-tended free-flyer. The platform exploits the unique advantages of a non-synchronous polar orbit to give a daily view of the entire globe. These facilities will be operated as complementary parts to address the temporal, spatial, and spectral coverage of the ozone phenomena.

8. GLOBAL CONSEQUENCES

The "greenhouse effect" refers to an incremental increase in infrared absorption within the atmosphere because of the increase of various trace gases. Carbon dioxide has largely been targeted as our greatest problem. Atmospherical concentrations have increased from 315 ppmv in 1957 to 350 ppmv in 1988, which is approximately 1,500 ppbv yearly. This increase does account for half or more of the greenhouse effect. However, increases have also been noted due to CFCs with CFC-11 increasing yearly by 0.011 ppbv and CFC-12 increasing 0.018 ppbv. The important factor is that each molecule of CFC is 10,000 times more efficient in absorbing infrared radiation than that of CO_2.[47]

It has been calculated that our yearly emission of CFCs is on the order of one million tons per year, which translates into an ozone loss 10^5 times larger. Sayeh El-Sayed from Texas A&M University recorded observations at Antarctica's Palmer Station and measured the photosynthetic rate of marine phytoplankton at four different UV conditions. His study showed that when compared to phytoplankton raised under ambient light, those exposed to the enhanced UV reduced their photosynthetic rate 35 to 75 percent depending on the source of the plants. This shows that where the UV levels are high (upper one or two meters in the ocean) the plants are substantially reducing their productivity.[48]

The current NASA investigations are beginning to reveal the inadequacy of the Montreal Protocol (UNEP-Sept 1987) strategy which called for only a 50% reduction in CFC production (20% reduction by 1994; and 30% by 1999).[49] New NASA reports on ozone have now shown the ozone depletion occurring at a faster rate than previously recognized in scientific models. EPA estimates that even with the Montreal Protocol, chlorine levels in the atmosphere could rise to a high of 8 ppb from the present +/- 2.7 ppb.

After additional expeditions were sent to the North Pole in 1989, 81 nations met at Helsinki in May of 1989 and adopted a declaration calling for a complete phase-out of CFC's by the year 2000, and a ban on the use of the destructive compounds halons. This activity went beyond the Montreal Protocol which was adopted principally by the United States, Mexico and 37 other nations in 1987, calling for countries to cut in half their production and use of CFCs by 1999.

Many less developed nations such as China and India have yet to make either commitment because of their own concerns about the cost of discarding equipment which uses CFCs. To overcome this dilemma, the Helsinki declaration calls for provisions to assist developing countries through funding and transfer of technology.[50]

In this recent strategy, countries have also shown support for setting limits on other harmful chlorine containing chemicals such as methyl chloroform and carbon tetrachloride. Until the new declarations of Helsinki are ratified, perhaps as early as April 1990, the Montreal Protocol sets the only standards being enforced in countries that signed the agreement. Although it is far from sufficient, many countries have also made cuts well ahead of time due to public concerns, mainly in the area of aerosol cans and foam packaging. Three of the largest producers of CFCs, U.K., West Germany and the U.S. have agreed to press for an 85% reduction in CFC production. However, less developed nations (approx. 16% of world production) have fewer restrictions and are not currently making steps to stop production.

Even if we stopped all production of CFCs, the problem could be with us for the next century. Chief research scientist for both expeditions, Robert Watson is now convinced that the current terms of the Montreal Protocol are insufficient. Under the Montreal Protocol, chlorine will increase from 3 ppb in the atmosphere today to 6 ppb by the end of the century. Each year chlorine is added takes 10 additional years to remove it.

CFC-12 is the most widely used chlorofluorocarbon. This year chemists at Du Pont, the inventors of CFCs, have developed two new alternative compounds to replace CFC-113 which is the common cleaning agent in electronics and other industries. One of the new compounds is called HCFC-124, but will still take a minimum of four years before it could be used widely in commercial applications.[51]

The initial findings set forth by the EPA suggests that each 1% depletion of ozone leads to a 2-3% increase in skin cancer among fair-skinned people.[52] There is already a large data base indicating that UV-B (280-320nm) is stressful to biological life even at current levels. Suppression of the immune system due to UV-B may also be a factor in the development of skin cancers.[53]

What is known is that the continued destruction of ozone could have global ramifications which would start with the disruption of the food chain of marine bacteria. However, as we continue to analyze the data that we have acquired and explain the picture that we have developed, we will be in a better position to address the important questions of long-term effects on the human race. On the other hand tropospheric ozone abundance has accounted for about 90% of U.S crop losses from air pollution, as well as playing a significant role in forest decline.

9. CONCLUSIONS

Concentrations of CFCs and halocarbons are rising faster than most greenhouse gases and such products manufactured as Halon 1301 and 1211 (fire retardants) both contribute to greenhouse warming, as well as stratospheric ozone destruction.

According to findings, 1987 was the worst year to date with 50% of the ozone over the Southern continent destroyed during the early spring. The conclusion of scientists who worked on the Arctic expedition is that the northern ozone layer is "primed for destruction" although there is little evidence that it would accelerate at the rate found in the Antarctic. The prime culprit is chlorine monoxide and recent findings have also shown that PSC can help them accelerate the ozone destruction. Reduced ozone in the stratosphere can also result in less heating of the environment and further reductions in temperatures, which may allow for more extensive formations of PSC over longer periods of time.

Reducing the emissions of CFC will reduce the greenhouse effect, because there is indication that they could be accounting for as much as 15-20% of the global warming. The world ozone dilemma requires a unified approach between environmental scientists, energy experts, and futurists using multi-disciplines of science which concern the resources of the planet for the next generation of mankind.

REFERENCES

1. "Has Stratospheric Ozone Started to Disappear?" Science Vol 237 July 10, 1987, p. 14

2. Rowland, F. S, et. al. "Variations Since 1978 in Tropospheric Concentrations of Halocarbons: CCl_3F, CCl_2F_2, CCl_4, CH_3CCl_3 Symposium Proceedings of WMO Technical Conference on Observation and Measurement of Atmospheric Contaminants Vienna, Oct. 1983.

3. Rowland, F.S. and Molina, Mario, "Stratospheric Sink for Chlorofluoromethanes: Chlorine atom-catalysed destruction of Ozone" Nature Vol 249, No. 5460 June 28, 1974, pp. 810-812.

4. Rowland, F.Sherwood, Science, vol. 239, pp. 36.

5. Rowland, F. Sherwood, "Chlorofluorocarbons and the Depletion of Stratospheric Ozone" American Scientist, Vol 77, January-February 1989, p. 36.

6. McCormick, M.P., "Persistence of Polar Stratospheric Clouds in the Southern Polar Region" Journal of Geophysical Research, Vol 94, No. D9 August 30, 1989, pp. 11,241-11,251.

7. Rowland, F. S. American Scientist, Vol 77, p. 43

8. Tuck, A.F. et al. "The Planning and Execution of ER-2 and DC-8 Aircraft Flights Over Antarctica, August and September 1987" Journal of Geophysical Research, Vol 94 August 30, 1989, pp. 11,181-2

9. Steinbrecht, W., et al. "Lidar setup for daytime and nighttime probing of stratospheric ozone and measurements in polar and equatorial regions." Applied Optics vol 28, No. 17 Sept. 1, 1989, pp. 3616-24.

10. Wahner, A. et. al. "Remote Sensing Observations of Nighttime OClO Column During the Airborne Antarctic Ozone Experiment, Sept 8, 1987." Journal of Geophysical Research, Vol 94, No. D9 August 30, 1989, pp. 11,405-9

11. Tuck, A.F., op cit, p. 11,183

12. McKenna, D.S. et al "Diagnostic Studies of the Antarctic Vortex During the 1987 Airborne Antarctic Ozone Experiment: Ozone Miniholes" Journal of Geophysical Research, Vol 94 August 30, 1989. pp. 11,641-68

13. McIntyre, M.E. "On the Antarctic Ozone Hole" Journal of Atmospheric and Terrestrial Physics, Vol 51. No.1 1989, p. 39.

14. Gandrud, B.W. "Filter Measurement Results From the Airborne Antarctic Ozone Experiment" Journal of Geophysical Research, Vol 94, August 30, 1989, p. 11,286.

15. Gandrud, ibid, p. 11,287.

16. Tuck, op cit., p. 11,193.

17. Warner, op cit., 11,405

18. Zurer, P.S. "Arctic Ozone Loss: Fact-Finding Mission Concludes Outlook is Bleak," Chemical and Engineering News March 6, 1989, p.29

19. Zurer, P.S. "International Effort to Examine Arctic Ozone Loss Gets Under Way." Chemical and Engineering News January 2, 1989 pp. 30-32

20. Komhyr, W.D. and Grass, R.D. "Dobson Spectrophotometer 83: A Standard for Total Ozone Measurements, 1962-1987" Journal of Geophysical Research, Vol 94, No. D7 July 20, 1989, pp 9847-60.

21. Farman, J.C., et. al. "Large losses of total ozone in Antarctica reveal seasonal ClO_x/No_x interaction, Nature, Vol 315 1985, pp. 207-210.

22. Film documentation with Dr. Robert Watson, NASA Headquarters chief on the Upper Atmospheric and Research and Tropospheric Chemistry, Washington DC, 1987.

23. Proffitt, M.H. "A Chemical Definition of the Boundary of the Antarctic Ozone Hole" Journal of Geophysical Research, Vol 94, August 30, 1989, 11,437

24. Wahner, A.R. Jakoubek, et. al.,"Remote Sensing Observations of Nighttime OClO Column During the Airborne Antarctic Ozone Experiment, September 8, 1987" Journal of Geophysical Research Vol. 94, August 30, 1989, pp. 11,482-11.

25. Blake, D.and F. Sherwood Rowland, "Continuing Worldwide Increase in Tropospheric Methane," 1978-1987, Science, Vol 239, pp. 1129-1131.

26. Film study by NASA Ames, Mountain View, California, covering the 1987 Airborne Expedition of the ER-2 team stationed in Chile.

27. Gandrud, B.W., op. cit., pp. 11,296.

28. Proffitt, M.H., op.cit., pp. 11,437.

29. Gandrud, B.W., op. cit., 11, 293.

30. Kelly, K.K. et al., "Dehydration in the Lower Antarctic Stratosphere During Late Winter and Early Spring, 1987," Journal of Geophysical Research vol 94 August 30, 1989, pp. 11,317-11,357.

31. Film documentation with Dr. Robert Watson, NASA Headquarters chief on the Upper Atmosphere and Research and Tropospheric Chemistry, Washington, DC, 1987.

32. Toon, O.B.,P. Hamill, R.P.Turco, and J. Pinto. 1986. "Condensation of HNO_3 and HCl in the winter polar stratospheres," Geophys. Res. Lett. 13:1284-87.

33. Zurer, op. cit., March 6, 1989,p. 30.

34. Fahey, D.W., et. al., "In Situ Measurements of Total Reactive Nitrogen, Total Water, and Aerosol in a Polar Stratospheric Cloud in the Antarctic," in Journal of Geophysical Research, vol. 94, No. D9, pp. 11,313.

35. Rowland, F. Sherwood, "Chlorofluorocarbons and the Depletion of Stratospheric Ozone," American Scientist, Jan.-Feb. 89, pp. 36

36. McKenna, D.S. et al., op. cit., pp. 11,641-2

37. Gandrud,B.W. op. cit., pp. 11,295.

ECO-CLIMATE MAP FOR GLOBAL MONITORING

Shunji Murai and Yoshiaki Honda
Institute of Industrial Science
University of Tokyo
7-22 Roppongi, Minato-ku, Tokyo 106
JAPAN

ABSTRACT

Though Köppen's climatological map is widely known all over the world, a new climatological and ecological zoning system should be developed in order to monitor the global change of vegetation. The new zone is named "Eco-Climate map". Generation of a vegetation map based on Global Vegetation Index and weather data is presented in this paper. The 7 typical patterns of monthly vegetation activity are analyzed from Global Vegetation Index. Climatological and ecological characteristics are classified from these patterns. This vegetation map is a base of Eco-Climate map.

KEY WORDS : Eco-Climate map, Global vegetation index, weather data

1. INTRODUCTION

Nowadays, the global change of the climate is one of the most important problems for the human society, and this change can be detected from the condition of the Earth's vegetation. Global Vegetation Index (GVI) indicates the weekly condition of the Earth's vegetation. GVI, which is produced from NOAA's (United States National Oceanic and Atmospheric Administration) AVHRR sensor (Advanced Very High Resolution Radiometer), is used as a tool to study the continental and global-scale patterns of the Earth's vegetation. The monthly change characteristic of the vegetation can be classified by dividing GVI into 7 typical vegetation patterns. A new vegetation map based on these vegetation patterns has been made.

2. DATA and METHODOLOGY

2.1 DATA

The data which have been used in this study consist of :

a) Monthly maximum value of GVI from January 1983 to December 1987.
The original GVI data which indicates the weekly density and vigor of the green vegetation is the resampling data of the Normalized Vegetation Index (NVI) for the whole Earth (except parts above 75 degrees latitude north and below 55 degrees latitude south). The NVI is determined by the following equation :

$$NVI=(Ch2-Ch1)/(Ch2+Ch1)$$

where Ch1 and Ch2 are the data from channel 1 (visible red band) and 2 (near infrared band) of the AVHRR. The spectral response of the five AVHRR channels is shown in table 1.

b) Monthly average values of temperature, rainfall and moisture from January 1983 to December 1987, provided by the Japanese Meteorological Agency, detected at 2344 observation stations all over the world.

Table 1 The spectral channels of the AVHRR

Channel	wavelength (micrometer)
1	0.58 ~ 0.68
2	0.725~ 1.10
3	3.55 ~ 3.93
4	10.30 ~ 11.30
5	11.50 ~ 12.50

2.2 METHODOLOGY

In climatology, the classification methods of the climate are as follows:

1) The method based on the climate factor
2) The method based on the characteristic of the climatological index
3) The method based on the vegetation
4) The method based on natural phenomena (except for the vegetation)

In this paper, the method based on the vegetation is used. Aforemetioned Köppen also used this method when he made his famous climatological map. In general, this method is separated into :

(1) A method based on the elements of the vegetation
(2) A method based on the life forms of the main vegetation

In case of the study of global-scale patterns of the vegetation, the second one is widely used and so also in this paper.

The outline of the method which used in this study is (Fig.1) :

1st Step:

120 stable stations were selected from 2344 observation stations. The stability was computed in this study to avoid unstable stations. The stability was computed as follows;

$$SMVC=\sum_{y=83}^{87}\left(\sum_{m=1}^{12}(NVI_{y,m}-\dddot{NVI})^{2}\right)$$

SMVC :The stability of the monthly vegetation change

$\dddot{NVI}$:Average NVI for 5 years (1983~1987)

$NVI_{y,m}$:Maximum NVI (year:y, Month:m)

2nd Step:

7 typical monthly change patterns were selected from the patterns of the monthly GVI data of those stable stations. They are tropical forest, evergreen forest, deciduous forest, tundra, grassland, semi-desert and desert.

3rd Step:

Minimum distance classification method was applied for all pixels. In this classification, the monthly change pattern was normalized by using the peak month of vegetation index.

4th Step:

This step was to avoid data under abnormal climate conditions. When we observe the climate value that has never been observed in this 30 years, the climate can be called abnormal climate. The data around the observation station (where abnormal climate was observed) was avoided. Then the vegetation map was made using the normalized average data for 5 years.

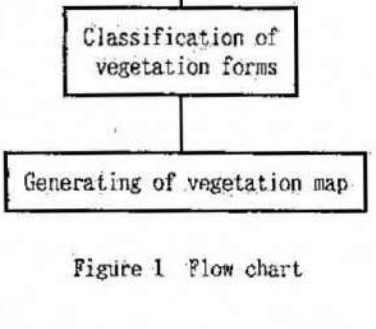

Figure 1 Flow chart

3 RESULTS

3.1 7 typical patterns of monthly vegetation change

7 typical patterns of monthly vegetation change are shown in Figure 2. The vertical and horizontal axes in Figure 2 indicate the NVI and the months respectively.

The NVI curve of tropical forest in Figure 2 shows the characteristics of tropical forest. The curve is almost constant at about NVI 0.3, so it is easy to classify them to be Af (tropical rain forest) in Köppen's climatological map. The NVI curve of evergreen in Figure 2 shows the characteristics of evergreen leaved forest. This NVI curve has a small difference in NVI between summer and winter and only has one peak of NVI per year. The NVI curve of deciduous forest shows the characteristics of dense forest in Figure 2. This NVI curve has a big difference in NVI between summer and winter and only has one peak of NVI per year. The NVI curve of tundra in Figure 2 shows the characteristics of tundra. The NVI curves of grassland in Figure 2 show various patterns. These observation points are grassland in Köppen's climatological map. The NVI curve of desert in Figure 2 shows that there is almost no vegetation and the curves show almost constant low NVI. They are BW (desert) in Köppen's climatological map. The last one is the NVI curve of semi-desert. It has a small peak of NVI.

3.2 A NEW VEGETATION MAP

Figures 3 are generated based on the 7 typical monthly vegetation change patterns. Zone No.1 is tropical forest, zone No.2 is evergreen forest, zone No.3 is deciduous forest, zone No.4 is tundra, zone No.5 is grassland, zone No.6 is nearly desert and zone No.7 is desert. The border between grassland and desert runs parallel with the latitude. Because of the abnormal climate, there is big difference in Africa and South America between 1984 and 1985. The areas of vegetation form are shown in Table 2 year by year. The area of forest is about 30% (including tropical forest), and the area of desert and semi-desert about 30%.

4 CONCLUSIONS

The results of this study lead to the conclusions;

(1) It is easy to distinguish desert from other kinds of vegetation.

(2) It is easy to distinguish tropical forest from other kinds of vegetation.

(3) It is difficult to classify grassland into steppe, savanna, prairie etc.

(4) Under abnormal climate, the patterns of the monthly vegetation change also becomes abnormal.

Further research should be paid attention to the classification of grassland into more categories. Then Eco-Climate map will be generated based on this vegetation map, climate information, soil map, geological map.

REFERENCES

1 Kuniji Yoshioka, Vegetation geography, Kyoritu publishing company, 1973
2 Masatoshi Yoshino, Climatology, Taimei-do, 1978
3 Noriyuki Nasu, Atmosphere and Ocean, Japan broadcast publishing association, 1986
4 Hideo Iwaki, Introduction of ecology, Japan broadcast publishing association, 1986
5 Global vegetation index users' guide, Satellite Data Services Division U.S.Department of Commerce, 1986
6 W.Köppen, Das geographische System der Klimate, Kraus reprint 1972

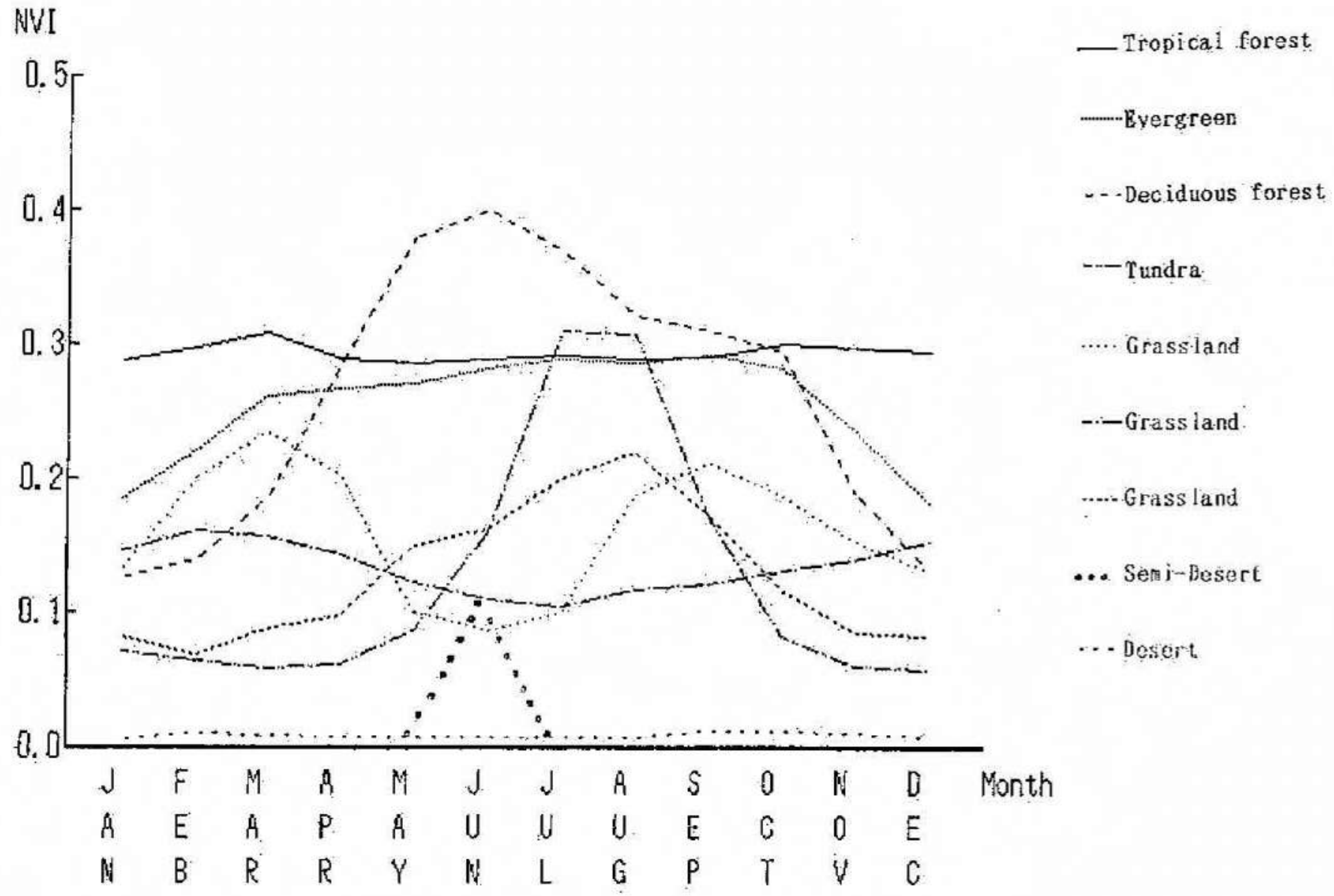

Figure 2 7 typical patterns of monthly vegetation change

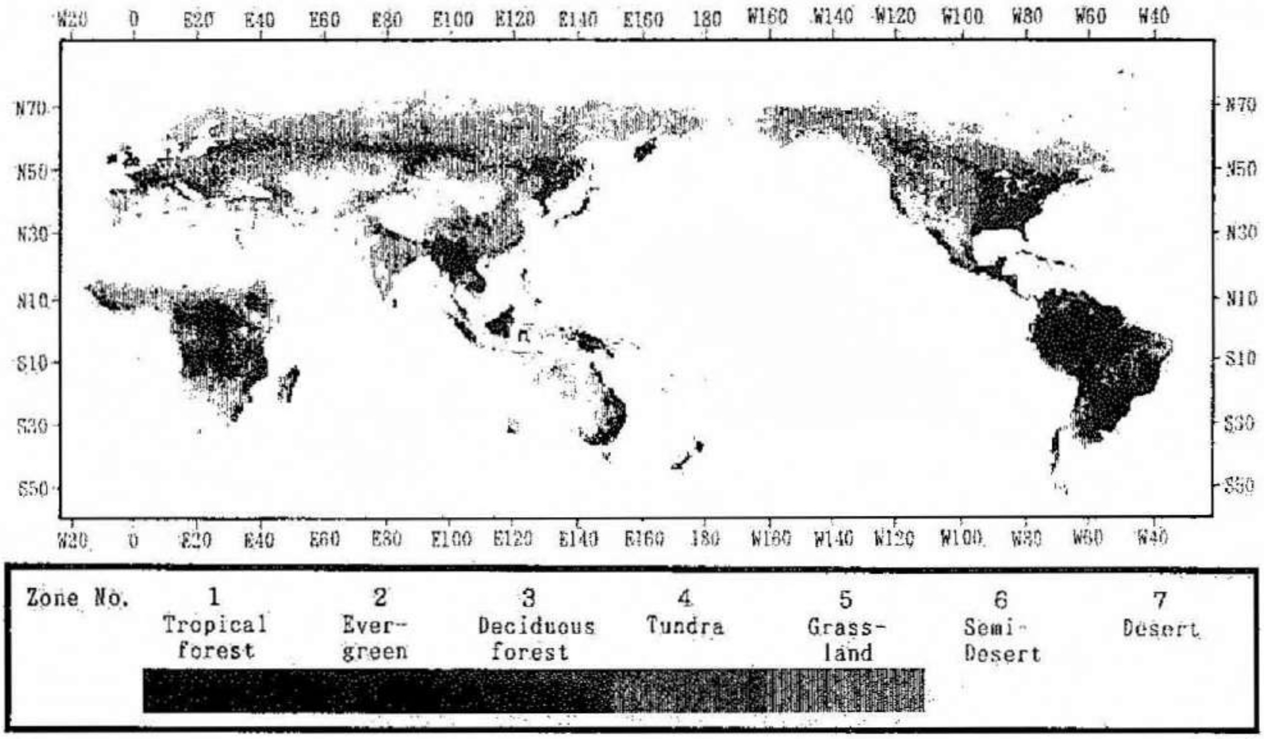

1983 Vegetation Map (Fig.3)

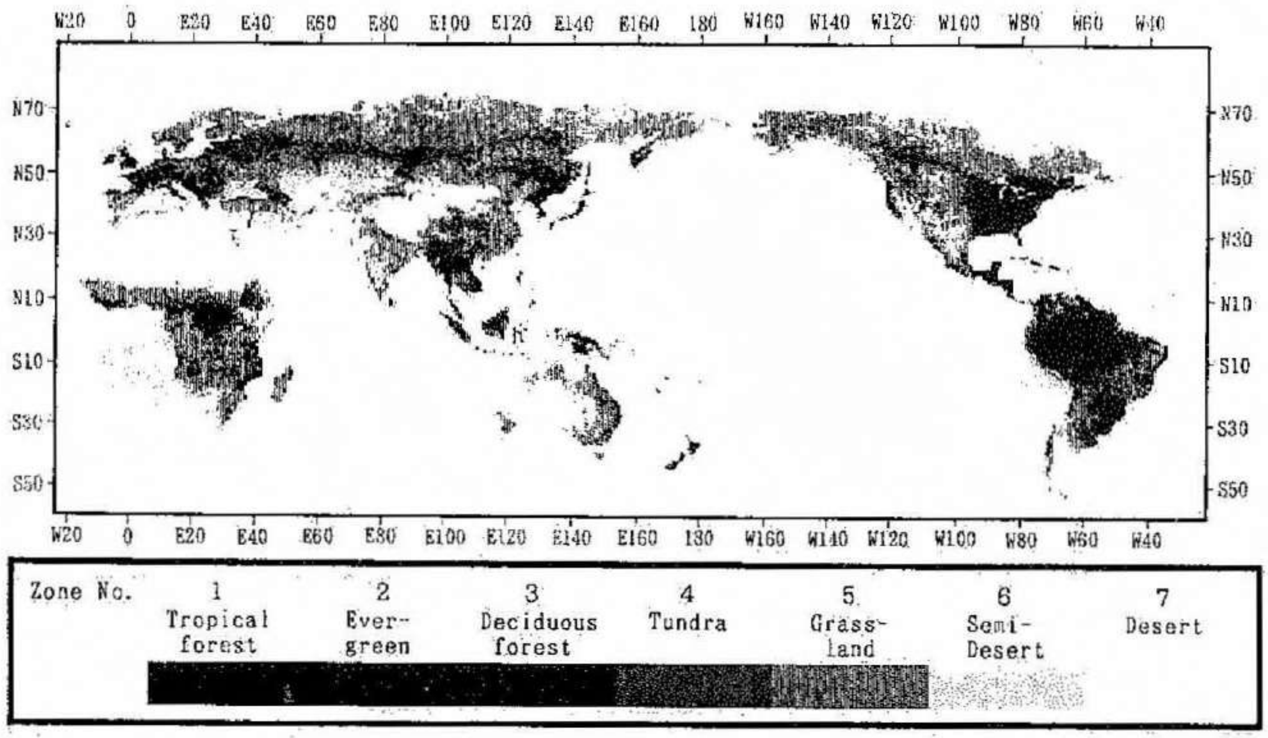

1984 Vegetation Map (Fig.3)

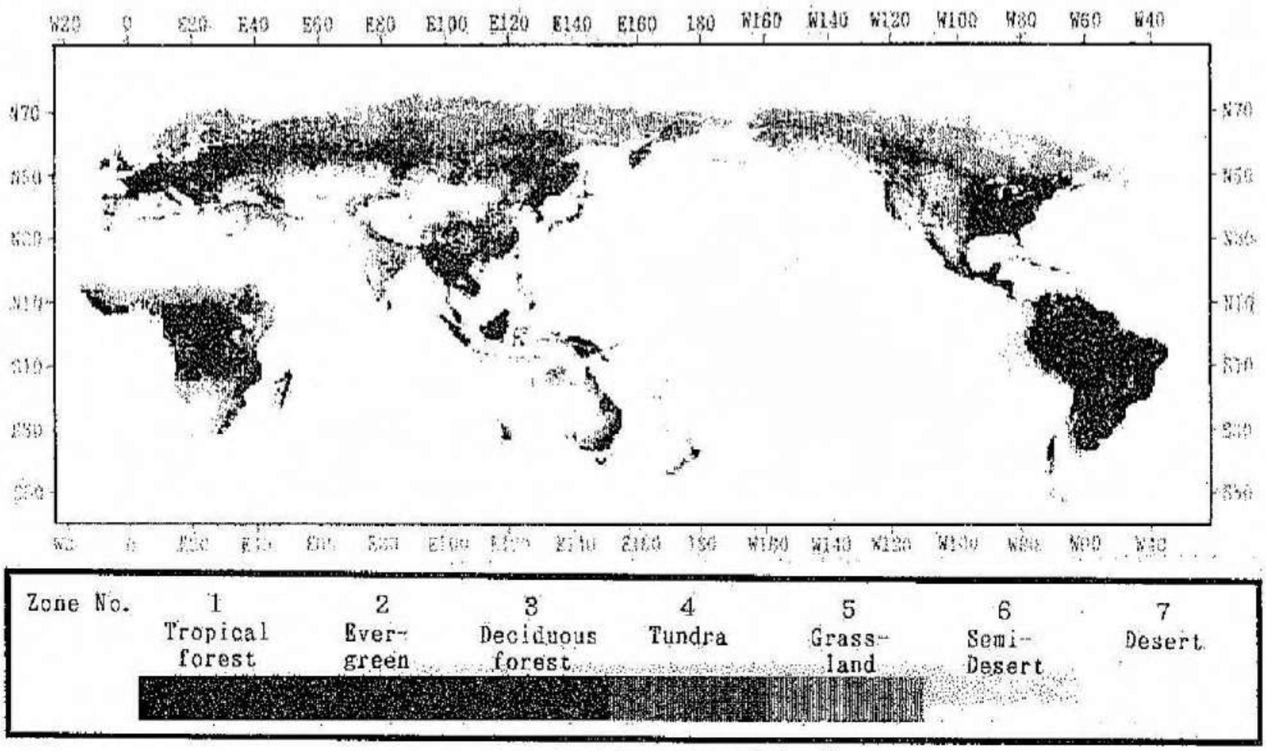

1985 Vegetation Map (Fig.3)

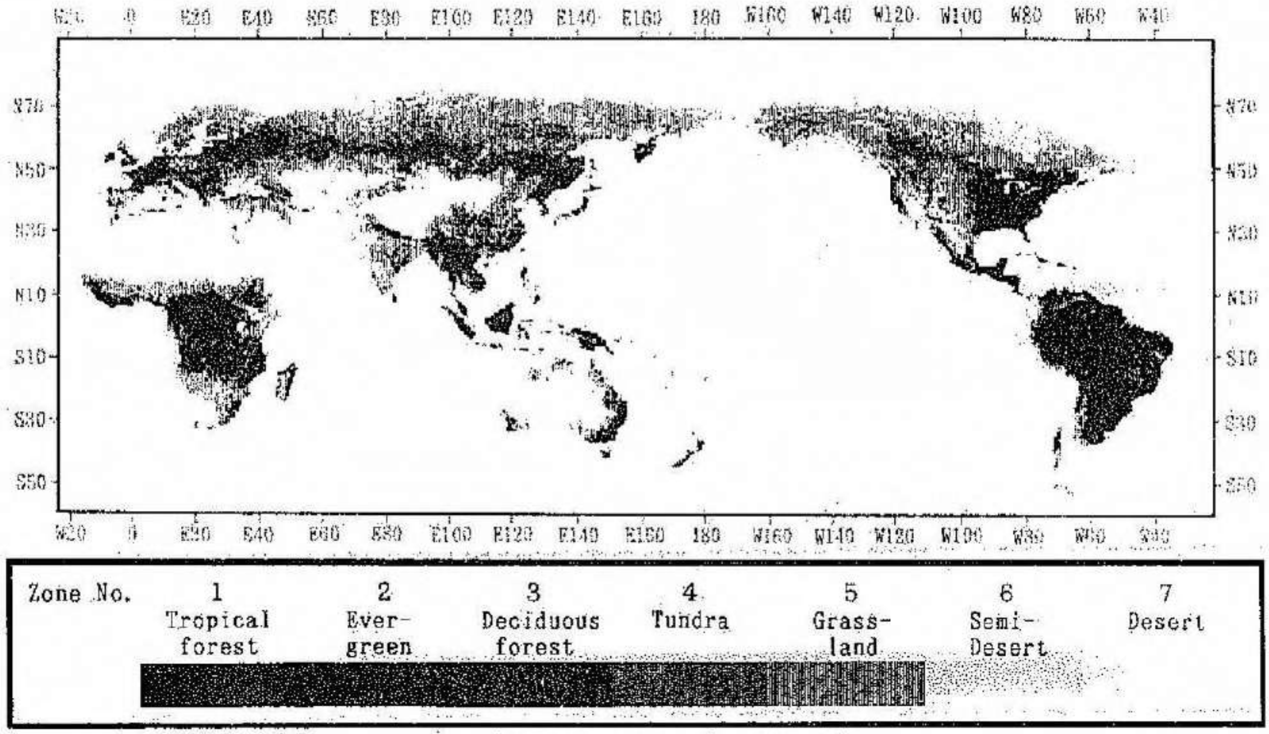

1986 Vegetation Map (Fig.3)

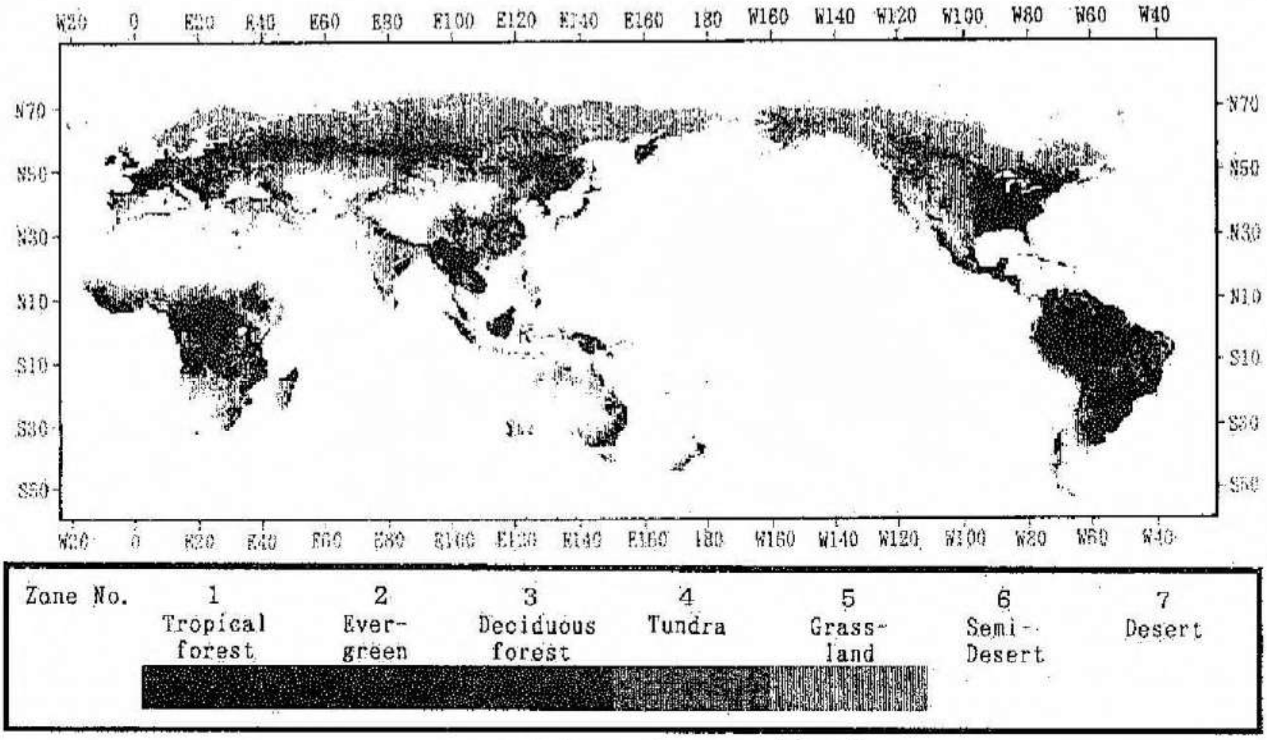

1987 Vegetation Map (Fig.3)

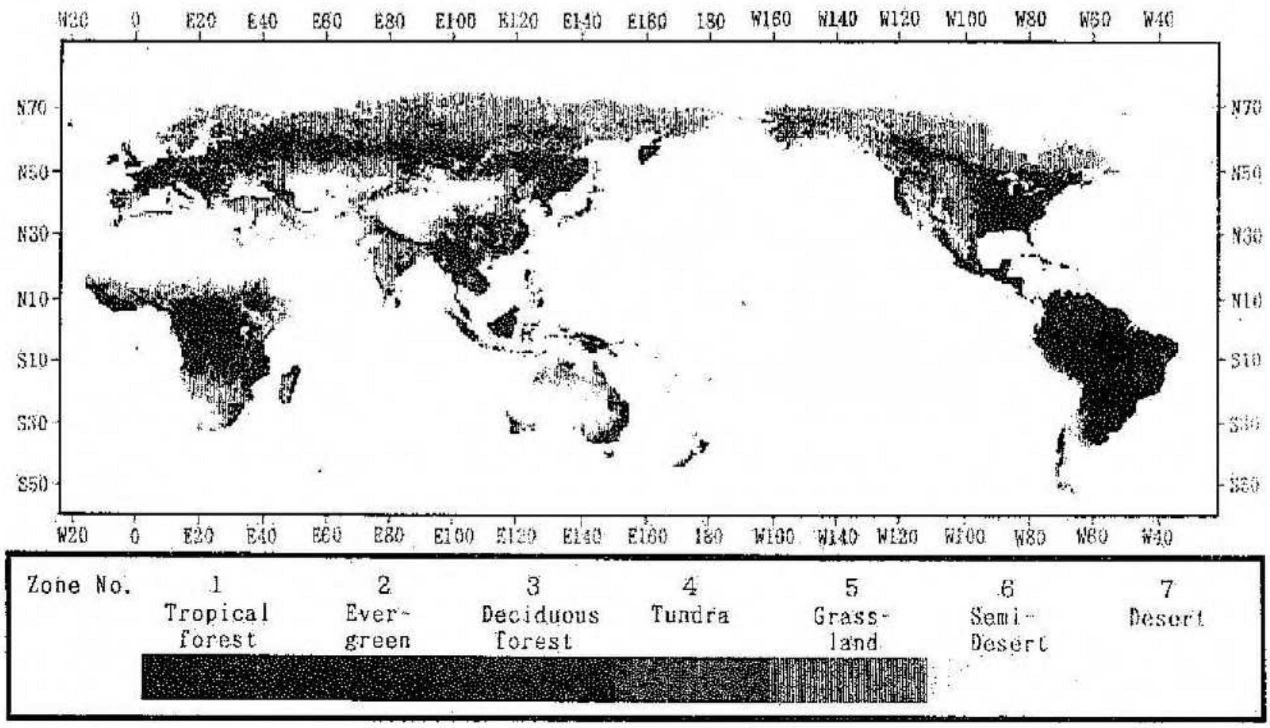

Vegetation Map (Fig.3)

Figure 3 Vegetation Map

Table 2 Classification of Vegetation

Vegetation in 1983

Region	Trop. Forest	Ever-green	Forest	Tundra	Grass-land	Semi-desert	Desert	Total
Asia Europe	680 1.23	2440 4.23	6533 11.83	2293 4.15	24212 43.84	9413 17.05	9655 17.48	55226
Oceania	155 1.83	937 11.01	632 7.44	0 0.00	2337 27.47	3654 42.96	790 8.29	8507
North America	357 1.48	1261 5.20	4513 18.61	356 1.47	10688 44.07	6129 8.01	948 3.91	24253
South America	2502 14.48	6725 38.04	2458 14.58	0 0.00	3499 20.25	1053 6.10	1008 5.84	17274
Africa	195 0.67	2589 8.87	4016 13.75	0 0.00	8346 28.58	3312 11.34	10746 36.80	29204
Total	3890 2.89	13953 10.38	18151 13.52	2649 1.97	49082 36.50	23563 17.52	23147 17.21	134464

Upper:1000 km² Under:%

Vegetation in 1984

Region	Trop. Forest	Ever-green	Forest	Tundra	Grass-land	Semi-desert	Desert	Total
Asia Europe	191 0.35	1945 3.52	9096 16.47	2641 4.78	23085 41.76	7939 14.38	10359 18.74	55226
Oceania	17 0.20	555 6.52	286 3.36	0 0.00	3114 36.60	4052 47.63	484 5.69	8507
North America	110 0.45	829 3.42	5727 23.61	530 2.19	10725 44.22	4347 17.93	1983 8.18	24253
South America	668 3.86	7222 41.81	1786 10.34	0 0.00	3499 20.25	5255 30.42	1333 7.72	17274
Africa	14 0.05	1568 5.37	2605 8.92	0 0.00	9948 34.06	3482 11.92	11586 39.67	29204
Total	1001 0.74	12119 9.01	19499 14.50	3171 2.36	52107 38.75	21154 15.73	25413 18.91	134464

Upper:1000×km² Under:%

Vegetation in 1985

Region	Trop. Forest	Ever-green	Forest	Tundra	Grass-land	Semi-desert	Desert	Total
Asia Europe	1096 1.98	1965 3.56	12006 21.74	3300 5.97	19684 35.64	7476 13.54	9701 17.57	55226
Oceania	374 4.39	879 10.33	423 4.98	0 0.00	1824 21.45	3974 46.72	1032 12.13	8507
North America	475 1.96	1409 5.81	6052 24.95	628 2.59	9556 39.40	4259 17.56	1874 7.73	24253
South America	5840 33.81	5297 30.66	1692 9.79	0 0.00	2371 13.73	1033 5.98	1041 6.03	17274
Africa	557 1.91	3542 12.13	4291 14.69	0 0.00	7406 25.36	3229 11.06	10179 34.85	29204
Total	8341 6.20	13091 9.74	24464 18.19	3928 2.92	40842 30.37	19971 14.85	23827 17.72	134464

Upper:1000×km² Under:%

Vegetation in 1986

Region	Trop. Forest	Ever-green	Forest	Tundra	Grass-land	Semi-desert	Desert	Total
Asia Europe	1435 2.60	2355 4.26	11772 21.32	2727 4.94	19813 35.88	7214 13.06	9910 17.94	55226
Oceania	348 4.09	836 9.83	436 5.13	0 0.00	1635 19.22	4383 51.52	869 10.21	8507
North America	504 2.08	1499 6.18	6035 24.88	537 2.21	9876 40.72	4044 16.67	1758 7.25	24253
South America	5982 34.63	4993 28.90	1565 9.06	0 0.00	2613 15.13	1039 6.02	1081 6.26	17274
Africa	676 2.31	3579 12.25	4297 14.71	0 0.00	7286 24.95	3033 10.38	10334 35.39	29204
Total	8946 6.65	13261 9.86	24105 17.93	3264 2.43	41223 30.66	19712 14.66	23953 17.81	134464

Upper:1000 km² Under:%

Vegetation in 1987

Region	Trop. Forest	Ever-green	Forest	Tundra	Grass-land	Semi-desert	Desert	Total
Asia Europe	1272 2.31	2623 4.75	11139 20.17	3438 6.23	20956 37.94	6756 12.23	9042 16.37	55226
Oceania	326 3.83	844 9.92	294 3.45	0 0.00	2093 24.61	4494 52.83	456 5.36	8507
North America	462 1.90	1569 6.47	6111 25.20	862 3.55	9997 41.22	4139 17.06	1114 4.59	24253
South America	4177 24.18	6165 35.69	1923 11.13	0 0.00	2890 16.73	1293 7.48	825 4.78	17274
Africa	416 1.42	3262 11.17	4529 15.51	0 0.00	7247 24.82	3561 12.19	10188 34.89	29204
Total	6654 4.95	14463 10.76	23997 17.85	4300 3.20	43184 32.12	20243 15.06	21624 16.08	134464

Upper:1000×km² Under:%

Vegetation

Region	Trop. Forest	Ever-green	Forest	Tundra	Grass-land	Semi-desert	Desert	Total
Asia Europe	1823 3.30	2745 4.97	13882 25.14	3322 6.02	18566 33.62	6558 11.87	8330 15.08	55226
Oceania	426 5.01	990 11.64	389 4.57	0 0.00	1972 23.18	4443 52.22	287 3.38	8507
North America	603 2.49	1874 7.73	6516 26.86	884 3.65	9551 39.38	3914 16.14	912 3.76	24253
South America	6448 37.33	5223 30.24	1505 8.71	0 0.00	2151 12.46	1261 7.30	685 3.96	17274
Africa	873 2.99	3988 13.66	4734 16.21	0 0.00	6674 22.85	3287 11.25	9647 33.03	29204
Total	10173 7.57	14820 11.02	27027 20.10	4207 3.13	38915 28.94	19462 14.47	19860 14.77	134464

Upper:1000×km² Under:%

MONITORING DEFORESTATION IN THE TROPICS WITH NOAA AVHRR AND LANDSAT DATA

Thomas A. Stone, Research Associate
and
Peter Schlesinger, Research Assistant
The Woods Hole Research Center
P. O. Box 296
Woods Hole, Massachusetts
02543 USA

ISPRS Commission 1, Manaus June 1990

ABSTRACT:

Numerous authors have suggested the use of combined AVHRR and LANDSAT data for monitoring tropical forest area and rates of change. Each sensor has its own advantages; the AVHRR data has very high temporal resolution with a daily revisit cycle and Landsat TM data has high spatial and spectral resolution. To monitor forest changes over areas the size of continents we must either sample with LANDSAT or sample with LANDSAT and then use the AVHRR data to scale-up our estimates. Using both satellite systems combines high temporal resolution and high spatial resolution.

We have examined the use of combined LANDSAT and AVHRR data to define areas and rates of deforestation in both West Africa and in Brazilian Amazonia. In Amazonia, we have examined the region of Maraba in Para, the state of Mato Grosso and the state of Rondonia and have found significant correlations between the percentage of forest and non-forest determined from the LANDSAT data and the AVHRR data.

KEY WORDS: Tropical Forests, Deforestation, NOAA AVHRR, LANDSAT TM

1. INTRODUCTION

Tropical forests are being cleared now at rates that are about double the estimated 1980 rate of 113,000 km^2yr^{-1}(Houghton 1990, Blasco and Achard 1990). Forests are being cleared for agriculture, timber products, pasture and for land speculation. Detrimental impacts include the loss of soils and uncounted numbers of plant and animal species, disruption of local and, potentially, regional (Lean and Warrilow 1989) and global climate patterns (Shukla et al. 1990). The current rates of change may mean near complete and perhaps irreversible loss (Shukla et al. 1990) of the tropical forests for many regions of the world over the next few decades. Already, some countries which were formerly rich in forests now have no primary forest left. Given such rapid change over large areas it seems clear that both extensive and detailed investigations of tropical forests of the globe must occur before they are lost.

Because the changes that are occurring are rapid and cover large areas the only way to quantify the process may be through the use of satellite data. The areas are too large to rely only on high resolution data such as that from the French Satellite Probatoire pour l'Observation de la Terre (SPOT) or the LANDSAT Thematic Mapper (TM). Several authors (Woodwell et al. 1987, Iverson et al. 1989, Tucker et al. 1984) have advocated taking advantage of the high temporal frequency of the U. S. National Oceanic and Atmospheric Administration's Advanced Very High Resolution Radiometer (NOAA AVHRR) data and the high spatial resolution of TM and or SPOT data. We explore here one method of combining these two types of data.

We have in the past used AVHRR classifications and a simple scale-up procedure in Rondonia to convert the area cleared as defined by TM or MSS data to cover an entire state (Woodwell et al. 1987). For this we defined the area cleared as determined from the LANDSAT data and then classified AVHRR data for a comparable area. Assuming the forest/non-forest classification from the LANDSAT data was correct, we scaled the AVHRR data accordingly. In this first instance, the scaling factor was very close to unity.

In a second effort with the NASA Goddard Space Flight Center we used UNESCO vegetation maps and the AVHRR data to stratify the state of Mato

Grosso and to serve as a basis for sampling with LANDSAT data. (Nelson et al. 1987, Stone et al. in prep.) The number of fires in pixels determined from the AVHRR Channel Three (3.5 microns) were assumed to be correlated to deforestation. We found, however, a weak correlation between the AVHRR fire "counts" and the area deforested and hence view the results from the Mato Grosso work as unsatisfactory in determining the total area deforested and the rate of deforestation.

A third effort in the state of Rondonia used a supervised maximum likelihood classification of AVHRR data to estimate the area deforested (Stone et al. submitted). This estimate was very close to the estimates of others (Tucker pers. comm.) but later examination of a detail of the AVHRR data and a co-registered TM image showed a discrepancy of a least 15%. This led to the conclusion that the use of AVHRR data alone overestimated the total area cleared. That our estimates for the entire state were similar to those of other authors could have been either a coincidence or due to offsetting over- and under-classification of deforestation over the much larger area of the entire state (243,000 km^2).

We report here a new effort to understand the relationships between AVHRR and LANDSAT data classifications for the area of forest and clearings in a portion of West Africa, where only patches of tropical moist forest remain and in Brazilian Amazonia, where an estimated 90% of the forest remains uncut (Tucker et al. 1990).

2. WEST AFRICA

2.1 Data and Methods

The data for this portion of the work were supplied by UNEP/GRID/GEMS as part of a project to develop common techniques for the understanding of forested regions in the tropics. This dataset, consisted of one AVHRR Local Area Coverage (LAC) image of West Africa and a LANDSAT TM image of a portion of Ghana in which there were forest reserves. The LAC data was from 13 January 1987 and the LANDSAT TM data was from 20 December 1986 (scene no. Y510240946, Path Row 195/055 Quadrant 4).

The first step was to register the LAC data to a map. We choose as our base map a 1:3,000,000 scale map of West Africa with a Lambert Conformal Conic projection (Defense Mapping Agency 1983). After determining more than 50 common ground control points in the map and LAC data and creating a transformation matrix the LAC data were co-registered with the map using and ERDAS-PC image processing system. After this step each 1.1 by 1.1 km pixel in the LAC data had a unique geographic coordinate.

The second step was to register the TM data to the same map base as the AVHRR data using more than 50 control points. This resulted in each TM pixel (30 by 30 m) also having a unique geographic coordinate. Unfortunately, the TM data had some relatively severe striping and a narrow range of DN values for the forested region.

We then sampled as many as possible cloud-free blocks of AVHRR and TM data. We chose LAC blocks of 20 by 20 pixels (approx. 480 km^2), classified those blocks, and then compared those classifications with classifications of cloud-free TM data of the same area (740 by 740 TM pixels).

Initially, 9 blocks of 480 km^2 each were classified using a supervised maximum likelihood classification algorithm. The total area sampled was then 4,320 km^2 or 25% of the total common area of LAC and TM data of 17,500 km^2.

2.2 Results West Africa

When we performed a linear regression between the percent of forest determined from TM and the percent of forested determined from the AVHRR data, the correlation or R^2 was 0.68 (Figure 1). The supervised maximum likelihood classification of LAC data generally underestimated the amount of forest and consequently overestimated the amount deforested (Figure 1). Also, as the percentage of forest declined (as defined from the TM data) the apparent error in the LAC data classification increased and underpredicted the amount of forest and therefore overpredicted the amount of deforestation. The difference between the mean TM maximum likelihood classification and the mean LAC maximum likelihood classification of the percentage of forest (TM percent forest less LAC % forest) was 24%.

3. AMAZONIA, BRAZIL

3.1 Maraba Region, Para, Data and Methods

The state of Para is the second largest Brazilian state in Amazonia, covering about 1,248,000 km^2. Originally, 88% of Para was covered by upland or terra firme tropical moist forest. By 1975, some 8,650 km^2 of the forest had been cleared; by 1978 the area cleared had increased by 160% to 22,445 km^2 (Tardin et al. 1980). By 1980 the area cleared had increased another 50% to 33,900 km^2 (fide Fearnside 1984) or about 3% of the total area, and of the area of forests of Para. Tardin and DaCunha (1990) estimated that by 1988 about 88,700 km^2 of Para had been recently deforested.

For this portion of the work we focussed on the Maraba region of Para. This region has been undergoing colonization and industrial development for the last two decades. In addition to a rapid influx of colonists, the world's fourth largest hydroelectric reservoir, Tucurui, which covers about 2,200 km^2 and the world's largest high grade iron ore deposit, Carajas, have both been opened in the region within the last decade.

We acquired NOAA9 AVHRR LAC data (5 bands) from July 30, 1988 and INPE LANDSAT TM data (bands 3,4,5) from July 6, 1988 (Scene ID 5-23123C005 Path-Row 223/63). To co-register the data sets we used a 1:2,500,000 scale map from the Grandas Projetos Carajas (CIMI et al. 1986). Seventy-five control points were selected and a transformation matrix was created to rectify the AVHRR data to the map. Many common points (60-75) were found between the map-rectified AVHRR and file coordinates of the LANDSAT TM to co-register the LANDSAT TM and AVHRR imagery to the same coordinate system. A window of analogous map coordinates and dimensions was created. The TM window (16,235 km^2) chosen was 3151 X 5727 pixels (94.5 km X 171.8 km) and the LAC window (15,942 km^2) was (93.5 km X 170.5 km). The two windows differ in area by about 2% due, partially, to different pixel sizes and co-registration error.

As described earlier for West Africa, we sampled all available cloud-free blocks of AVHRR data and TM data. We again chose LAC blocks of 20 by 20 pixels (approx. 480 km^2), classified those blocks, and then compared those classifications with classification of cloud-free TM data of the same area (740 by 740 pixels). Ten blocks of 480 km^2 were classified using a supervised classification algorithm. The total area sampled was then 4800 km^2 or about 30% of the total common area of LAC and TM data of 16,000 km^2.

3.2 Results, Maraba Region, Brazil

When we performed a linear regression between the percent of forest determined from TM and the percent of forested determined from the AVHRR data the correlation was quite strong (R^2 = 0.93). It is apparent from Figure 2 that the supervised maximum likelihood classification of LAC data that we used always underestimated the percent forest and overestimated the percent of deforestation. This finding was in agreement with our previous work in Rondonia (Stone et al. in prep.) and in West Africa where it appeared that a supervised classification of LAC data underestimated the percent forested and overestimated the percent deforested. It is also apparent in this region that as the percent of forest declined (as defined from the TM data) the error in the LAC data increased and underpredicted the amount of forest and overpredicted the amount of deforestation.

4. DISCUSSION AND SUMMARY

With both of these data sets, West Africa and Amazonia, a supervised maximum likelihood classification of the AVHRR data consistently resulted in underestimating the percent forest and therefore overestimating the amount of deforestation. For West Africa the average error was about 24% while for Amazonia the average error was about 13%. The linear regression between the West African TM and LAC block forest classifications had an R^2 of about 0.68 while the linear regression between the Amazonian TM and LAC classification had an R^2 of about 0.93. The two regressions differ because of the weakening of the relationship between the LAC and TM estimates of the percent of forest as the amount of forest declines below about 50%. Another way of saying this is that the less forest there is, the lower would be one's confidence in the use of AVHRR data to define the amount of forest.

We also combined the results of the block classifications of the West African and Amazonia research to look for a generalized relationship between AVHRR and TM classifications. Combining the West African and Amazonian data sets has the advantage of allowing us to examine a fuller range of types and amounts of forest clearing. In the Maraba region of Brazil, all blocks examined were greater than 50% forested according to the TM data classification. In the West African data sets about half the blocks were more than 50% forested and half were less than 50% forested according to the TM data classification. These results should be considered preliminary, however, because of the vast differences in the land use between the two regions.

The method described above is appropriate for large regions and for the purposes of monitoring the area and rate of forest clearing. It is not a substitute for the detailed investigations required for national or local planning or for understanding forest composition and land use styles. Also, from the results shown here, the method becomes weaker as the amount of forest declines.

The majority of the sources of error in this method are due to the large pixel size and the amount of geometric distortion inherent in AVHRR LAC data. The large pixel size of the AVHRR makes it difficult to register and immediately introduces a minimum error of at least half a pixel or about 500 m. The large pixel size also makes the choice of training sites difficult and makes the acquisition of ground reference data more important than it might if one were using only high resolution data. The geometric distortion in raw AVHRR data is difficult to correct. The 95% confidence interval for the combined data sets indicates that use of the regression should be accurate within a range of +/- 11% to +/- 5%. Despite these problems, however, it is important to remember that for 17 tropical countries the estimates from different sources of the amount of deforestation that had occurred by 1980 differed by 25 to 100% (Molofsky et al. 1986).

5. CONCLUSIONS

Combining the data sets (Figure 3) leads us to several preliminary conclusions. As mentioned before it appears that the quality of the LAC maximum likelihood classifications for forest areas declines as the percent of forest declines. Also, that in areas of less than about 50% forest cover that LAC estimates of forest are expected to be even less reliable. Finally, it appears that when there is less than about 35% forest that using the LAC data alone may not classify any forest at all. In these regions, the use of high resolution data and ground reference data is even more important.

One essential route to improving our understanding of the size and change or loss of critical ecosystems such as tropical moist forests is through the use of remotely sensed data. We could have had the information we now require available to us on a yearly basis for the last decade. A global forest inventory that pays particular attention to tropical forests could be completed within two to three years using current data and technology. The expected error for such an inventory would be about of 20% to about 5% but would be a substantial improvement to our current understanding of the area and rates of loss of tropical moist forests globally.

6. REFERENCES

Blasco F. and F. Achard, 1990. Analysis of Vegetation Changes using Satellite Data. pp. 303-310 in A. F. Bouwman [ed.], Soils and the Greenhouse Effect, John Wiley and Sons, Inc., Chichester, 574 pp.

CIMI, CEDI, IBASE and GhK, 1986. Areas Indigenas E Grandes Projetos Carajas. Technische Fachhochschule, Berlin.

Defense Mapping Agency 1983. Map of West Africa #505000 [A000340] 12-83.

Fearnside, P. M., 1984. A Floresta Vai Acabar. Ciencia Hoje 2(10):42-52.

Houghton, R. A., 1990. The Global Effects of Tropical Deforestation, Environ. Sci. Technol. 24(4):414-422.

Iverson, L. R., Cook, E. A., and R. L. Graham, 1989. A Technique for Extrapolating and Validating Forest Cover across Large Regions: Calibrating AVHRR Data with TM Data. International Journal of Remote Sensing 10(11):1805-1812.

Lean, J. and D. A. Warrilow, 1989. Simulation of the Regional Climatic Impact of Amazon Deforestation. Nature 342:411-413.

Molofsky, J., Hall, C. A. S. and N. Myers, 1986. A Comparison of Tropical Forest Surveys. TR032, DOE/NBB-0078. U.S. Department of Energy, Washington, D.C. 66 pp.

Nelson, R. F., Horning, N. and T. A. Stone, 1987. Determining the Rate of Forest Conversion in Mato Grosso, Brazil Using LANDSAT and AVHRR Data. Intl. Jour. of Remote Sensing 8(12):1767-1784.

Shukla, J., C. Nobre, and P. Sellers, 1990. Amazon Deforestation and Climate Change. Science 247:1322-1325.

Stone, T. A., Brown, I. F., and G. M. Woodwell, submitted. Estimates of Land Use Change in Central Rondonia, Brazil By Remote Sensing. Journal of Forest Ecology and Management.

Stone, T.A., R. A. Houghton and G. M. Woodwell, in prep., Steps toward a global appraisal of the area of forests and the rates of deforestation using satellite imagery.

Tardin, A. T.,D. C. Lee, R. J. R. Santos, O. R.de Assis, M.P. Barbosa, M. Moreira, M. T. Pereira, and C. P. Filho, 1980. Subprojecto desmatamento convenio IBDF/CNP-INPE (Instituto De Pesquisas Espaciais, Sao Jose Dos Campos, Brazil), 44 pp.

Tardin, A.T. and R. P. DaCunha, 1990. Evaluation of Deforestation in the Legal Amazon using LANDSAT-TM Images, INPE-5015-RPE/609. 38 pp.

Tucker, C. J., Holben, B. N. and Goff, T. E., 1984. Intensive Forest Clearing in Rondonia Brazil as Detected by Satellite Remote Sensing. Remote Sensing of the Environment 15:255-261.

Tucker, C. J. 1989. personal communication regarding his analysis of 1987 AVHRR data of Rondonia.

Tucker, C. J., W.W. Newcomb, and T. Grant, 1990 [abs.]. Satellite Estimation of Tropical Deforestation in the Amazon Basin of Brazil. Chapman Conference on Global Biomass Burning: Atmospheric, Climatic, and Biospheric Implications. p. 15.

Woodwell, G. M., Houghton, R. A., Stone, T. A., Nelson, R. F., and W. Kovalick, 1987. Deforestation in the tropics: New measurements in the Amazon basin using LANDSAT and NOAA AVHRR imagery. Jour. of Geophysical Research - Atmospheres 92(D2):2157-2163.

7. ACKNOWLEDGEMENTS

Funding for this research and for imagery acquisition was provided by the W. Alton Jones Foundation and by the Conservation, Food, and Health Foundation.

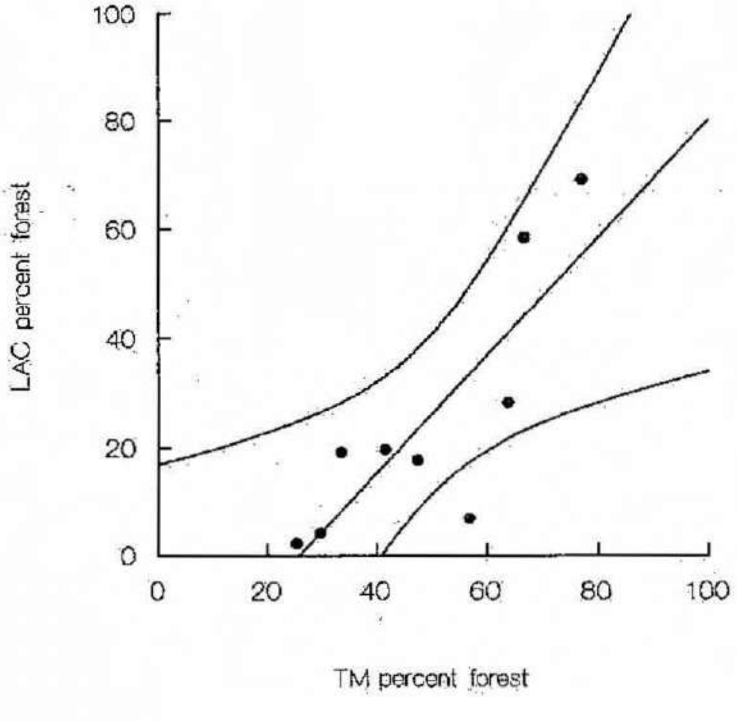

Figure 1. Ghana, West Africa. Relationship between the percent forest determined from maximum likelihood classifications of 20 by 20 LAC pixels areas (480 km^2) and maximum likelihood classification of the same region with coincident and co-registered TM data. Each of the 9 points equals 480 km^2 classified with both LAC and TM data. The linear regression line and 95% confidence interval are plotted. $R^2 = 0.68$. It appears that areas with less than 50% forest are poorly classified when using AVHRR data and areas with less than 25% forest may appear from AVHRR data to have no forest all within them.

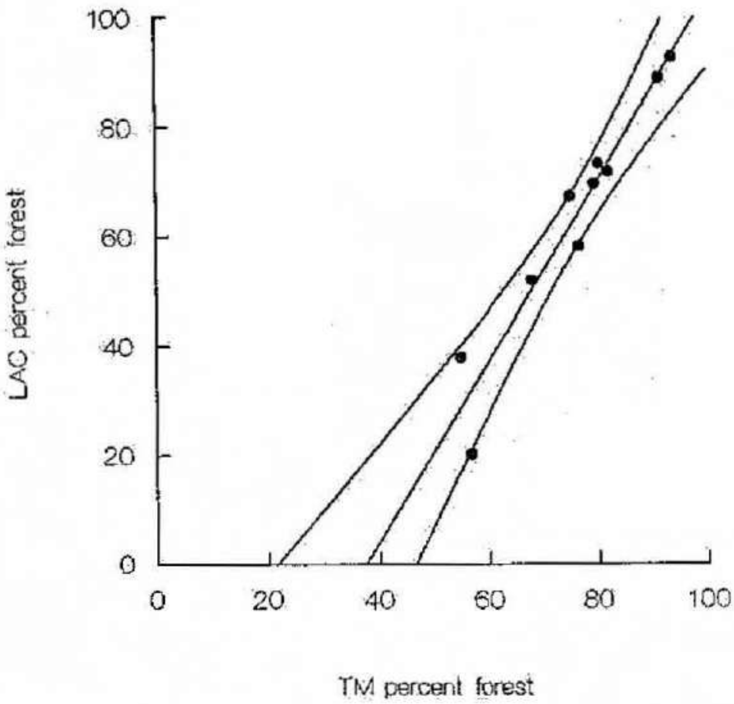

Figure 2. Maraba Region, Para, Brazil, Amazon Basin. Each of the 10 points equals 480 km^2 classified with both LAC and TM data. $R^2 = 0.93$. The linear regression line and 95% confidence interval are plotted.

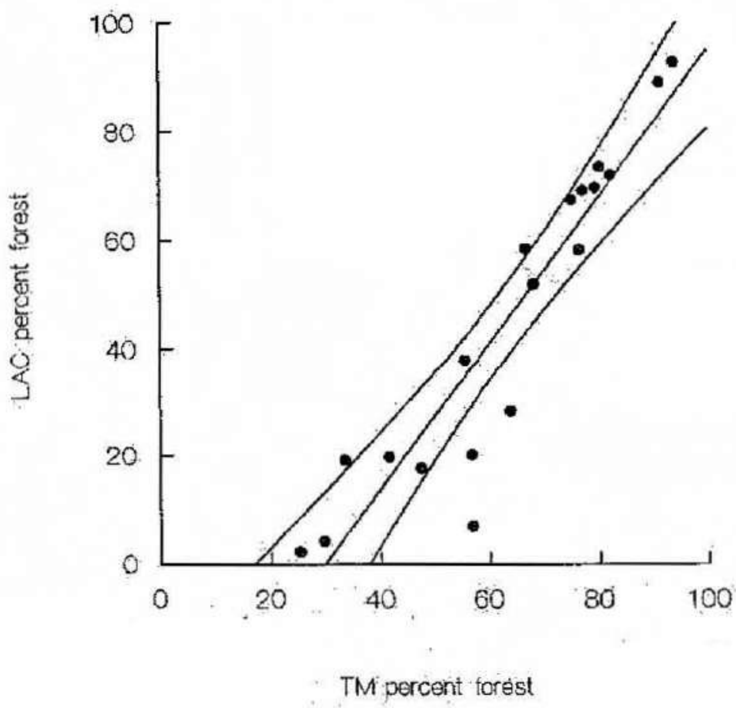

Figure 3. Combined West African and Amazon Basin Data. Each of the 19 points equals 480 km^2 classified with both LAC and TM data. $R^2 = 0.87$. The linear regression line and 95% confidence interval are plotted. In almost all cases using a supervised maximum likelihood classification of the first three AVHRR channels results in an overestimation of deforestation when compared to the LANDSAT TM data.

UTILIZATION OF THE SHUTTLE IMAGING RADAR (SIR-C) FOR MONITORING CHANGE IN THE AMAZON

John C. Curlander, JPL, USA

ABSTRACT:

This paper describes the upcoming Spaceborne Radar Laboratory (SRL-1) experiment to be flown aboard the NASA Space Shuttle in 1992. This experiment features a multi-frequency, multi-polarization synthetic aperture radar, SIR-C, that is capable of performing a variety of geophysical measurements over a large region of the Amazon independent of cloud cover and time of day.

The SIR-C instrument, the first fully polarimetric radar to be flown in space, will measure target characteristics over radar frequency, polarization, incident wave geometry and season (3 missions). This extended target signature can be used to derive quantitative characteristics about the forest canopy (relative biomass) and the underlying soil (water content).

This paper will review the characteristics of the SIR-C instrument, describe the planned data products (with examples from SIR-A, SIR-B and NASA DC-8 aircraft) and present an overview of the types of geophysical analysis algorithms that can be applied to the polarimetric SAR data.

(Original not received in time for publication)

Technology

MOMS-02: POTENTIAL OF A NEW SENSOR FOR PHOTOGRAMMETRY AND REMOTE SENSING

Hans-Peter Bähr and Hermann Kaufmann

University of Karlsruhe, Institut of Photogrammetry and Remote Sensing

7500 Karlsruhe, Englerstr. 7, FRG

Abstract:

The German MOMS-02 sensor to be flown on NASA's space shuttle Mission D2 in 1992 presents a challenge for applications in photogrammetry and remote sensing. The flexibility of radiometric and geometric resolution, combined with a sophisticated stereo system offers new methodologies for data processing.

Starting out from this point, the paper discusses basic possibilities and limitations of advanced automation for digital image processing.

KEY WORDS: MOMS-02, Acquisition-modes, Knowledge-based Systems.

1. DEFINITION OF THE PROBLEM

When LANDSAT was launched in 1972, the Multispectral Scanner (MSS) was the only operative satellite-borne earth observation system - apart from some very low resolution weather satellite systems. The four MSS channels were highly correlated, and therefore data selection did not present a mayor problem to the user. This has changed very much during the past 10 years, since LANDSAT-TM and SPOT-HRV are available on a global scope, providing extended multispectral and stereoscopic data at a higher resolution than MSS and in multitemporal mode.

Since various remote sensing systems being more and more available, there is still a growing trend in putting national systems into orbit, like the German MOMS-02 sensor. Though MOMS-02 is an experimental system operating in shuttle orbit, the general question is raised, how the user may determine the appropriate data mode for his specific application. This question goes far beyond MOMS, because choice of the sensor and selection of spectral bands, geometric resolution, definition of the appropriate season and possible repetition cycles are basic matters for most applications. The more variable the possible data modes are, the more complicated their correct selection turns out to be.

The thesis treated in this paper is: The correct data mode selection has to be done computer-assisted by a knowledge-based system.

Analyzing this problem, the complexity is evident. Therefore, we will restrict to MOMS-02 and not include different sensors into the discussion. Even regarding only MOMS-02, the task seems to be very demanding, as five bands (including a panchromatic channel) and three simultaneous strips are produced. The different viewing geometry of the three strips allows stereoprocessing, but beyond that offers additional radiometric information of the observed terrestrial surfaces.

At the long run, knowledge-based systems for data selection are a contribution to automatization. Automatization covers the entire area of computer-controlled processing. In remote sensing it is not restricted to image processing as such - the user in future has to be assisted by intelligent systems offering alternatives during the **whole** procedure. The question of well-directed data selection is only the first step, representing the link between data acquisition and data processing.

2. MOMS-02 SYSTEM- AND FLIGHTPARAMETERS

MOMS, acronym for Modular Optoelectronic Multispectral/Stereo Scanner, is an Earth sending CCD-instrument using the "pushbroom" scan principle (Meißner, 1988). it is a second generation system being developed by Messerschmitt-Bölkow-Blohm GmbH (MBB) under contract to the German Aerospace and Research Establishment (DLR), funded by the German Ministry of Research and Technology (BMFT). MOMS-02 will be flown in the framework of D2 mission scheduled for 1992 aboard NASA's space shuttle in an 28,5° inclination orbit. The instrument is designed with an along-track, simultaneously acquired forward, nadir and backward looking stereo capability and four spectral bands in the visible and near infrared range (Ackermann et. al., 1989).

The stereo capability is provided by one nadir and two tilted modules 21,95° fore and aft of nadir. The ground instantaneous field of view (GIFOV) at a nominal shuttle orbit at 160 nautical miles will be 4.49m by 4.49m for the nadir module (band 5) and 13.47m by 13.47m for both forward (band 6) and aft (band 7) of nadir looking modules. All three stereo devices have an equivalent **panchromatic bandpass from 520nm to 760nm** (Fig. 1) that is optimized for reflectance properties of vegetation, rocks and soils, and allows recording of a certain penetration depth in water bodies (Kaufmann et. al., 1989).

The GIFOV of the four spectral bands, placed in the visible and near infrared will be 13.47m by 13.47m. Optimization of all four bands (Fig. 1) is well balanced on the basis of reflectance characteristics of vegetational and Fe-bearing targets (Kaufmann et. al., 1989).

Band 1 (530nm-575nm) is placed within the blue absorption of vegetation that is mainly caused by chlorophyll and carotenoid concentration. It is most valuable for hydrologic applications, the detection of changes in pigment ratios, to distinguish paved surfaces from their surroundings and to differentiate among Fe-bearing minerals, rocks and soils. **Band 2 (530nm-575nm)** is centered at the reduced level of vegetational pigment absorption, the "green peak". It can be used to detect progressive states of senescence or stress and to differentiate among rocks and soils containing ferric and ferrous iron. **Band 3 (650nm-685nm)** is located at the principal absorption peak for chlorophyll-a molecules associated with the photosynthetic light trap. In combination with band 4 it is most useful for biomass estimations. **Band 4 (770nm-810nm)** is placed into the high reflectance plateau of vegetation, and data derived from it can be related to biomass, state and type of cellular arrangement, density, geometry and water content of a vegetation canopy. Additionally it should provide somewhat more detailed information about iron-beared rocks and soils that can be derived from existing operational sensors in these wavelength range (Fig. 2).

The possibility of combined multispectral and stereoscopic data acquisition provides new ways for data evaluation. This is true especially for those scopes, where the spatial information renders major contributions to the solution of a problem.

MODE	NADIR MODULE # 5A, 5B + SWATH (km)	TILTED MODULES # 6,7 + SWATH (km)	SPECTRAL BANDS # 1,2,3,4 + SWATH (km)
I	5A+5B 37.6	6,7 37.6	——
II	——	——	1, 2, 3, 4 78.1
III	——	6, 7 78.1	3, 4 78.1
IV	——	6 78.1	1, 2, 4 78.1
V	——	7 78.1	2, 3, 4 78.1
VI	5A 26.9	——	2, 3, 4 43.4
VII	5A 26.9	——	1, 3, 4 43.4

Table 1:
Operating bands and associated swaths of seven selectable modes for MOMS-02 on D2-mission. The channel marked as outlined in each actual mode will be transmitted as video-signal during operation.

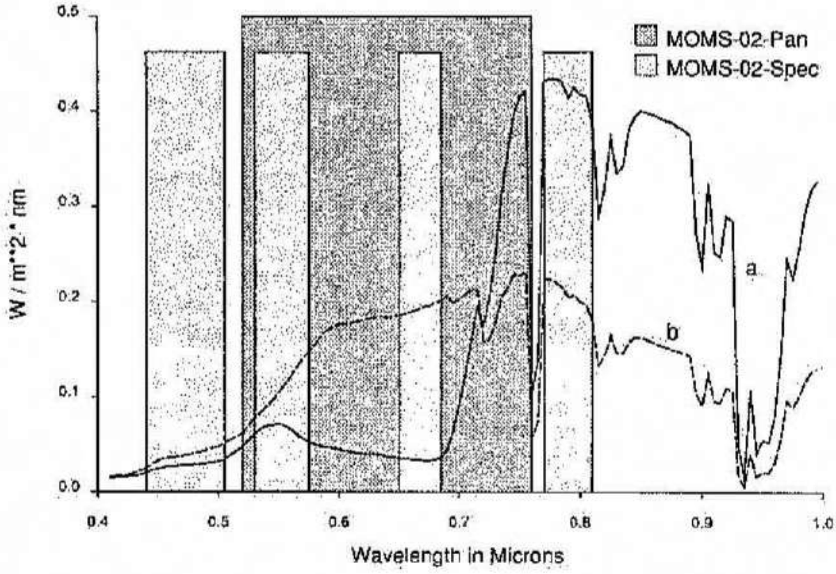

Fig. 1:
Nominal bandpasses of spectral and panchromatic bands of MOMS-02. (a) meanradiance spectra of vegetational targets, (b) meanradiance spectra of Fe-bearing targets after the spectral properties of a mid-latitude, mid-summer atmosphere (LOWTRAN-6) has been applied.

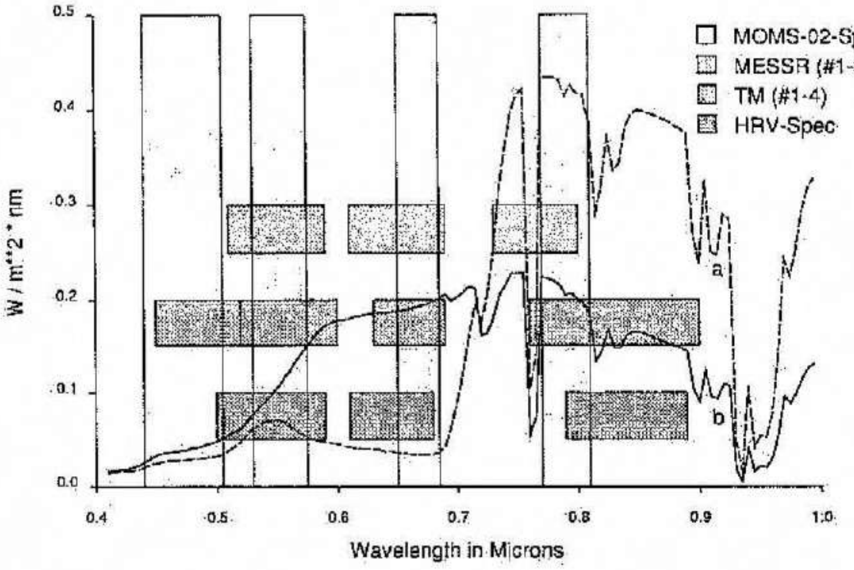

Fig. 2:
Comparative illustration of nominal bandpasses of MOMS-02, SPOT - High Resolution Visible Instrument (HRV), LANDSAT - Thematic Mapper (TM) first four bands, MOS - Multispectral Electronic Self-scanning Radiometer (MESSR) first three bands. Bandpasses are overlain by spectra of Figure 1.

Data will be stored on HDDT tape during the mission. Due to limitations in data transfer, MOMS-02 cannot operate all channels simultaneously, but will be recording in one of seven different acquisition modes (Tab. 1).

The swath-width of the system will be up to 37.6 km for the panchromatic nadir module and up to 78.1 km for all remaining channels (Tab. 1).

3. DESIGN OF A KNOWLEDGE-BASED SYSTEM FOR MOMS-02 DATA SELECTION

Knowledge consists of facts, rules and heuristics. A human operator in general does not exactly separate the different levels of knowledge but integrates all when generating a decision. For computer-assisted decisions however, all components have to be thouroghly placed within an expert system.

Such a system was designed at the Institute of Photogrammetry and Remote Sensing (IPF) for the purpose of architectural photogrammetry in order to determine cameras and geometrical configurations (BEHR, et al., 1988). This task is very similar to MOMS data selection: Both applications deal with data acquisition, and the geometric configuration of the imagery is very important for the next steps. Moreover, the specific application may vary, standardized procedures do not seem appropriate, and for subsequent data processing many alternatives are available. On the other hand, for both satellite-born MOMS-02 and for terrestrial photogrammetry many restrictions exist a priori:

- imagery simply not being existent (MOMS) or
- required configurations not being possible (photogrammetry).

The components of an expert system are shown in Fig. 3.

Regarding Fig. 3, we will explain the most important components:
The core of an expert system consists of an inference computer, which draws conclusions from knowledge of different structure. The most flexible procedure for data processing is the "blackboard principle", a non-hierarcial, parallel working program system. Although basically any programming language may be used for taking the decisions, rule-based languages like PROLOG (CLOCKSIN and MELLISH, 1981) offer many advantages. Instead of defining procedures by conventinal algorithmic languages - which work sequentially -, rule-based languages take facts and rules for drawing logical conclusions.

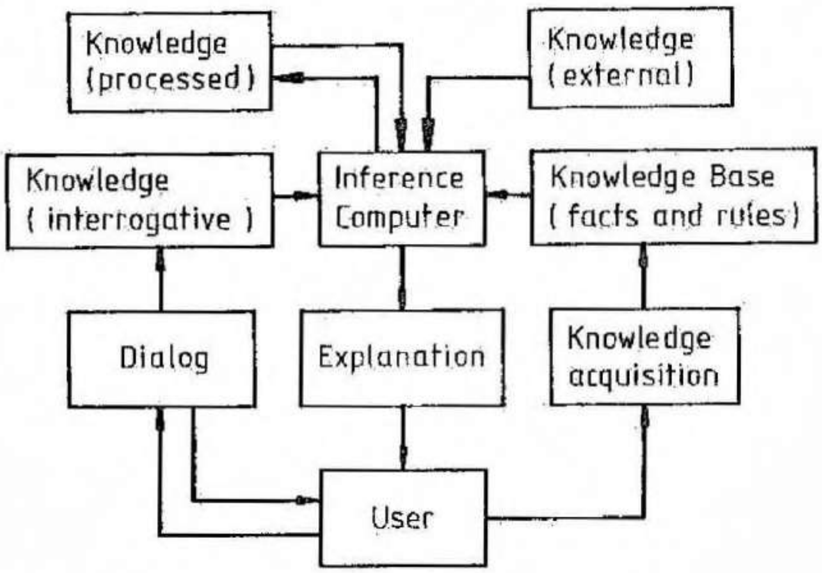

Fig. 3 Components of a general expert system (after SESTER, 1987)

We will take an example for PROLOG - like programming of the inference computer regarding the MOMS mode structure.

```
/*Facts*/

  F (c6, m1).
  F (c6, m3).
  F (c6, m4).

  A (c7, m1).
  A (c7, m3).
  A (c7, m5).

  N (c1/2/3/4, m2).
  N (c3/4, m3).
  N (c1/3/4, m4).
  N (c1/3/4, m5).
  N (c2/3/4, m6).
  N (c1/3/4, m7).


/*Rules*/

  Stereo 1(X,Y):-  /* X and Y allow
first order stereoplotting*/
        F(X,J),    /* if X is forward
view of J*/
        A(Y,K).    /* and Y is aft
view of K*/


  Stereo 2(X,Y):-  /* X and Y allow
2nd order stereoplotting*/
        F(X,J),    /* if X is forward
view of J*/
        N(Y,K).    /* and Y is nadir
view of K*/


  Stereo 2(X,Y):-  /* X and Y allow
2nd order stereoplotting*/
        A(X,J),    /* if X is aft
view of J*/
        N(Y,K).    /* and Y is nadir
view of K*/

  (including J = K)
```

First, *facts* have to be defined. The list shows 3 different types:

F ("forward mode")
A (" aft mode")
N ("nadir mode").

The parameter list includes the available channels (c 1/2/3/4; c6; c7) as well as the modes m1 ... m7.

The *rules* show 2 options for stereo viewing: "Stereo 1" means a combination of F and A ("1st order"), and "Stereo 2" of F and N or A and N, respectively ("2nd order"). The PROLOG formulation of *rules* shows the advantage of a declarative language for taking logical decisions. Only 3 very short lines are necessary to formulate the complex procedures. Taking a procedural language, for instance FORTRAN, the program would look very confusing.

For "Stereo 2" two "or" alternatives are valid simultaneonsly.
The example treats all stereo cases which may occur for MOMS-02. If J = K we have the "trivial" case i. e. stereo effect is possible within one mode at one orbit.

The given example presents an inference procedure by a PROLOG program. The knowledge, however, has to be defined outside of the inference computer.

Fig. 3 shows the link between the inference computer and the other components. There exist many alternatives for introducing knowledge. For MOMS-02, "external knowledge" seems to be most important, as it consists of a list from available data. This includes information about available data for different locations and different modes.

Besides this, the user introduces "interrogative knowledge", working on a specific projekt. One may for instance form "interrogative knowledge" for surfaces suffering from desertification: By a dialog procedure the operatur will transmit human know how about appropriate channels and seasons into the system.

4. CONCLUDING REMARKS

Since MOMS-02 is an experimental system on a shuttle platform, users may expect only relatively few data. Consequently, an expert system in order to assist channel and mode selection, seems rather exaggerated, as not many alternatives will exist in practice. But even for MOMS-02 the determination of appropriate image data for stereoviewing turns out to be rather complicated, when several orbits and different modes are feasible. The task of the inference computer solved by a PROLOG program showed clearly the complex conditions.

However, the complexity still grows considerably when various sensor systems are included, and this is more and more the case in practice. Operational earth observation systems are LANDSAT-TM, SPOT and the photographic KFA-1000. In the years to come we will certainly have an increasing number of those observation systems.

In a first step a general catalogue of all systems should be generated in order to facilitate appropriate data selection. In a second step data selection should be done problem-oriented. This means taking a knowledge based system in order to assist human decisions. This may partly lead to a fully automated process for data selection.

There are, however, many restrictions: The most severe consists in not existing human knowledge about the potential of sensor-parameters, like geometric resolution, spectral bands and configuration of imagery. "Image understanding" requires knowledge about the natural process to be observed. There is generally a big lack of detailed models for describing natural processes appropriately.

References

ACKERMANN, F.; BODECHTEL, J.; DORRER, E.; EBNER, H.; KAUFMANN, H.; KOCH, B.; KONECNY, G.; LANZL, F.; SEIGE, P.; WINKENBACH, H., and ZILGER, J.; 1989, MOMS-02/D2 Wissenschaftsplan. **DLR/PT-Bericht**, Bonn, FRG, 75p.

BEHR, F-J., SESTER, M., and RINGLE, K., 1988, Komponenten von Expertensystemen, aufgezeigt am Beispiel eines Expertensystems zur Unterstützung photogrammetrischer Bauaufnahmen. Bildmessung und Luftbildwesen, **56/88**, 217-226.

KAUFMANN, H.; MEISSNER, D.; BODECHTEL, J., and BEHR, F-J., 1989, Design of spectral and panchromatic bands for the German MOMS-02 sensor. Photogrammetric Engineering and Remote Sensing, **55/6**, 875-881.

MEISSNER, D., 1988, Preliminary design review of MOMS-02 for D2 mission. **Doc.No: MOMS-02.PR.0010**, DLR/MBB, 104p.

SESTER, M., 1987, Entwurf und Implementierung eines Expertensystems zur photogrammetrischen Bauaufnahme. Diploma Thesis IPF, University of Karlsruhe, 69p.

CLOCKSIN, W.F., and MELLISH, C.S., 1981 Programming in PROLOG. Springer, 279p.

CAPABILITIES OF A NEW RADAR SYSTEM BASED ON ADVANCED SENSOR TECHNOLOGIES

J. P. Aguttes, CNES, France

ABSTRACT:

The wellknown all weather capability gives a decisive advantage to RADAR for all the applications having temporal requirements (surveillance, renewable resources...). The other points of interest are in the specific RADAR radiometric sensitivity for the morphology and the water content (geology, hydrology, vegetation) and in the inherent high geometric performance in terms of resolution and positioning (cartography, surveillance...). These properties complement the ones of optical imagery rather than compete with them. As one of the main actors of space remote sensing, CNES considers the RADAR as a way to consolidate applications already served by optics as well as to develop specific new applications.

There are also imaging properties introduced by the emerging RADAR technologies. Active antenna concepts allow high image product versatility and high system efficiency, a same system can serve most of the RADAR applications.

Economical value for the applications, advanced technology for the sensor, efficiency for the whole system, these are the key points of the CNES approach for the implementation of a new program in the 2000's.

The paper exposes the different aspects of the ongoing preliminary phase: application thematic investigation, technology and concept validation, system and mission trade-offs.

(Original not received in time for publication)

AN X-SAR EXPERIMENT FROM THE SHUTTLE: GROUND TECHNOLOGY AND APPLICATIONS (*)

G. Braconi, F. Lamberti,
Selenia Spazio S.p.A.
Roma, Italia
F. Corsi,
Tesis, Italy,
ISPRS Commission I

At the beginning of 1992, an experimental American/European mission for SAR data acquisition will take place. This mission will be characterized by several new aspects, that is multifrequency and multipolarization acquisition, together with the capability of multiparameters imaging radars (i.e. with varying look angles, receiver gains, pulse repetition frequencies).

The mission will consist of two radars, to be flown on a Shuttle, operating the first in C and L-band (SIR-C) and the second in X-band (X-SAR).
This paper presents the capabilities of the X-SAR Ground Station (G.S.) related to these new aspects for the radar setting and instrument controlling during the mission.

The X-SAR G.S. Control Section will be able to determine the most suitable radar commands according to the scientists' requirements. This will allow to obtain SAR images having the spatial and radiometric properties as requested by the scientist. Further, on the basis of the incoming telemetry data, it will be possible to modify some radar parameters.

Another important aspect of the X-SAR G.S. will concern the Processing Section facilities. These will allow a real-time SAR processing and the storing of the resulting images.

The catalogue of SAR images will be distributed to the scientists on VHS cassettes, in order to verify the capability or the multifrequency/multipolarization system SIR-C/X-SAR and the possible fields of application.

KEY WORDS: X-SAR, Ground Station, Mission Planning, Processing, Primary sites.

1. INTRODUCTION

The joint mission SIR-C/X-SAR, foreseen for the summer of 1993, will provide a powerful tool for scientific studies of the earth, and it will represent a significant step in the evolution of advanced spaceborne imaging radars.

It will provide:

- the first opportunity of simultaneous multifrequency radar imagery from space;
- the first spaceborne imaging radar with simultaneous multipolarization capability;
- the first multiparameters acquisition, to supply coverage in different times according to several illumination geometries.

The first experiment of a Shuttle-based imaging radar was held in 1981, with the SIR-A, an L-band, HH polarized radar. This was a fixed parameters radar. The collected images showed the importance of developing systems allowing multiple acquisitions in order to classify terrain features.

The second experiment, the SIR-B, in 1984, was an improved version of SIR-A providing a multi-look-angle radar system. This allowed data acquisition at various angles from 15 to 65 degrees on successive days. The images were used for stereo mapping and for the production of curves of backscatter as a function of incidence angle for different terrain types.

After several years of delay, due to the tragedy of the Shuttle Challenger in 1986, the joint mission SIR-C/X-SAR now represents the next step towards the development of more sophisticated technologies to satisfy the increasing scientific requirements. The two payloads will be commanded and monitored by two separate ground teams.

The aim of this paper is to describe the X-SAR Ground Station with respect to the facilities provided to accurately plan and control the whole mission. So, after a short description of mission characteristics, emphasis will be given to the Ground Station functional description and to all the facilities to be used to integrate and harmonize the scientific requirements in the mission operations.

(*) The work described in this paper is part of a project developed under a contract from Italian Space Agency (ASI) to Selenia Spazio, within an international co-operation between ASI and the Deutsche Forschungsanstalt fur Luft und Raumfahrt (DLR), for the realization of the X-SAR Space Segment and Ground Segment.

2. MISSION CHARACTERISTICS.

As mentioned above, the SIR-C/X-SAR mission will allow data acquisition with multiple frequencies, polarizations and parameters. In fact, the SIR-C will operate both in L and C-band with HH, VV, HV or VH polarizations, while the X-SAR will operate in X-band with VV polarization.

In both cases it will be possible to vary the incidence angles by electronically steering of the antenna beam for the SIR-C and mechanical tilting for the X-SAR. Therefore it will be possible to image simultaneously selected sites at 23-cm, 6-cm and 3-cm wavelengths.

The SIR-C/X-SAR payloads will be launched aboard the Space Shuttle into a nominally circular orbit with an inclination of 57 degrees at an average altitude of 225 km. This orbit configuration will allow about 1-day repeat cycle with a small westward drift. In this way a given site can be imaged during the mission with several different parameters. The SIR-C/X-SAR mission will also include two flights, planned at eighteen months interval, to record the effect of seasonal and climatic changes.

This will offer the scientists a wide range of experiments to be performed in the areas of geology, hydrology, vegetation science and oceanography. A series of 45 sites has already been selected by the American and European Science team, including the fields of application and the experiments to be performed. Ground Truth activities, as well as the use of corner reflectors or active calibrators, will therefore be scheduled in order to achieve valuable results in the interpretation of SAR images.

Owing to the orbit characteristics, it will be possible for each site to determine a list of opportunities, that is all the allowed passes of the Shuttle over the sites. This information can be used to determine the schedule for data acquisition under variable illumination conditions.

The activity to be performed in the Ground Station is therefore very important to select the most appealing opportunities and the best radar commands, with the final goal of producing a big variety of images, having satisfactory characteristics.

3. X-SAR GROUND STATION DESCRIPTION.

The X-SAR Ground Station will be characterized by a series of computers and software tools in order to guarantee the successful monitoring and control of the on-board antenna and the data acquisition during the whole mission. Owing to the short duration of the mission, 8 days, the X-SAR Ground Station shall be able to react to mission variations and X-SAR system anomalies in near real-time, so maximizing the scientific results also in case of contingencies.

To fulfill this requirement, the X-SAR Ground Station has been decomposed in two main sections, the Control and the Processing Sections (Figure 1).

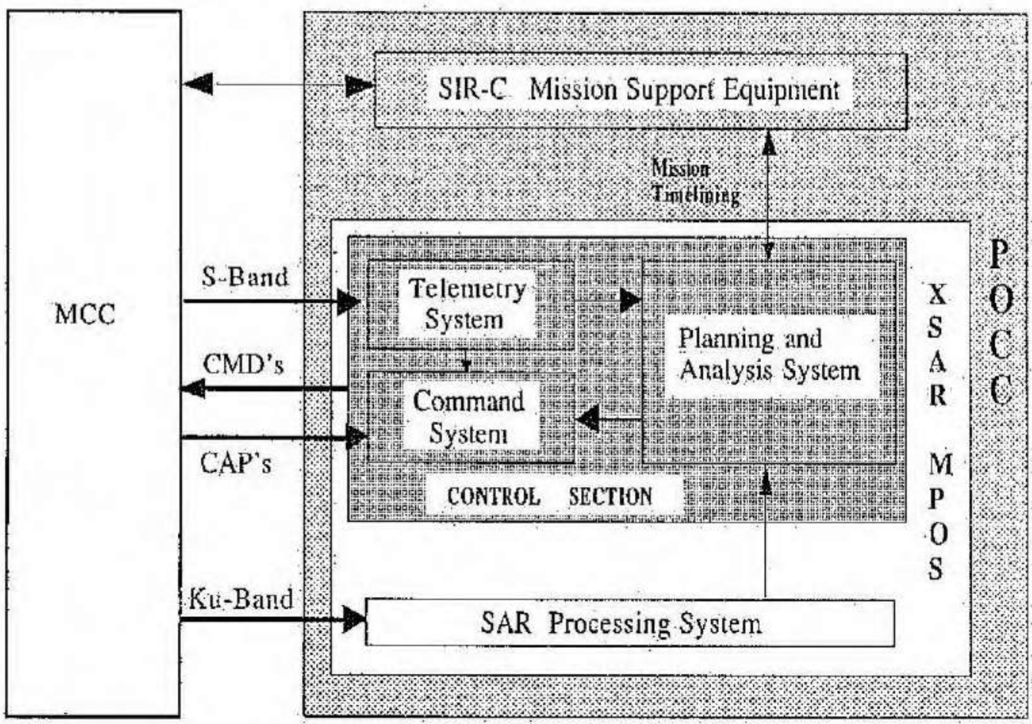

FIGURE 1 - X-SAR Ground Station Functional Description

The Control Section performs the following functions:

- mission planning;
- instrument monitoring and control.

It includes the following systems:

- Planning and Analysis System (PAS), which plans and updates all the mission events. It also analyses incoming telemetry data to derive radar corrections in real time.
- Telemetry System (TS), which receives and displays telemetry data to monitor the X-SAR instrument status.
- Command System (CS), which sends commands to the Mission Control Center for uplink to X-SAR and receives Command Acceptance Pattern (CAPs) ensuring the correct storage of commands on board,
- Telemetry and Command Simulators, which simulate the telemetry date and the interface with the Mission Control Center, in order to test the Telemetry and Command System and to train the operation teams.

The Processing Section performs the following functions:

- raw data acquisition;
- real time date processing and display.

It encompasses the following systems:

- SAR Processing System, which processes the 45 Mbps Ku-band SAR data to generate real-time images of the illuminated sites.
- High Rate Data Simulator, which simulates Ku-band data to test the SAR Processing System and to train the operation teams.

The X-SAR Ground Station will operate both prior and during the mission:

- the pre-mission activity is mainly related to the creation of the mission timeline, that is the complete list of all the operations and events for every minute of the mission. The mission timeline will include the optimal radar settings for all the sites to be imaged and the corresponding command blocks. The creation of the mission timeline will be coordinated by both X-SAR and SIR-C teams.

  During this phase, the simulators will work to test the critical parts of the Ground Station, i.e. the Telemetry, Command and SAR Processing Systems. They will also be used to train the operation teams, in order to make them familiar with the equipment and the foreseen operations.

- During the mission, the X-SAR Ground Station activities will be devoted to the monitoring of the instrument and to data acquisition.

  The mission timeline will be updated each time the Orbiter deviates from the preplanned position with the new sets of radar commands.

  Further, the Telemetry System will check X-SAR parameters, issueing warnings to the operation team in case of anomalies. Also the uplinked commands will be continuously monitored to verify that they have been correctly received by the on-board equipment. The SAR Processing System will be used during the Ku-band data transmission to produce real-time images of the selected sites. These images will be stored as a film on VHS cassettes so creating a preliminary catalogue of the mission.

4. X-SAR GROUND STATION FACILITIES

The activities performed in the Ground Station have been conceived in order to match, as far as possible, all the scientists' requirements and to strictly cooperate with them during each phase of the mission.

To this aim, both the Control and the Processing Sections will be characterized by tools which allow to take into account scientists' requests, trading-off the application related problems with the mission constraints, and to present the results of acquisition to the users for immediate verification.

Let now examine in detail for each section the related functions.

4.1 Control Section Facilities.

In order to create a mission timeline fully adherent to the scientific aspects, the Control Section will offer the following capabilities:

- selection of primary sites;
- selection of radar parameters;
- real-time correction of radar configuration.

An important new aspect for the mission is represented by the fact that all the abovementioned functions can be performed both in a fully automated way and in a manual modality, under operation team control, according to the time constraints for the planning.

The selection of primary sites represents an important step during the planning. In fact, only for the selected sites the radar acquisition will be scheduled and therefore an accurate trade-off has to be performed between site characteristics and mission constraints.

To this aim the function will be based on the following information:

- list of test sites with the related description, such as site extent, best times of day for imaging, look direction, incidence angles, ground truth activities, calibration procedures. Further, each test site is characterized by a parameter, the "site priority", which expresses the scientific relevance for the site under investigation.

- List of all the data take opportunities, that is all the imaging opportunities provided by the selected orbit, together with the related illumination geometry (incidence angle, Shuttle position, look direction, etc.)

- Details of mission constraints, such as Shuttle attitude, time required to perform manoeuvres, time required to modify antenna pointing, time required to modify the on-board instrument configuration.

The selection will be performed by using several criteria, which can be chosen by the operational teams. These criteria can be based on the scientific aspects of the mission and so they will use the site priority and the number of opportunities foreseen for the site. Further, the criteria will also take into account mission details and in this case the selection will be performed to minimize manoeuvres or antenna rotation. The operation team will be given full visibility of the available opportunities and attitudes either to monitor selection results or to intervene in the selection phase (Figure 2). In both cases it will be possible for the users to examine the results of each procedure by means of statistic tables reporting, for each selected criterium, the observable sites and the discarded ones. Further, it will be possible to suggest the Mission Control Center a complete schedule for the Shuttle attitude in order to maximize the number of primary sites.

The selection of primary sites represents together with the selection of the radar parameters, the "kernel" of the planning phase. In fact only for primary sites the related radar commands will be determined and uplinked.

As stated before, this mission foresees multiparameter acquisition, so allowing the optimization of radar parameters on the basis of the Shuttle geometry and user's requests.

The selection of radar parameters is performed using as input data the primary sites, the related illumination geometry and the scientist's requirements, together with the X-SAR instrument characteristics. The aim of this phase is both to provide the most suitable radar configuration for each primary site and to calculate the corresponding image performances.

A radar configuration will consist of the following parameters:

- Pulse Repetition Frequency (1240-1860 Hz)

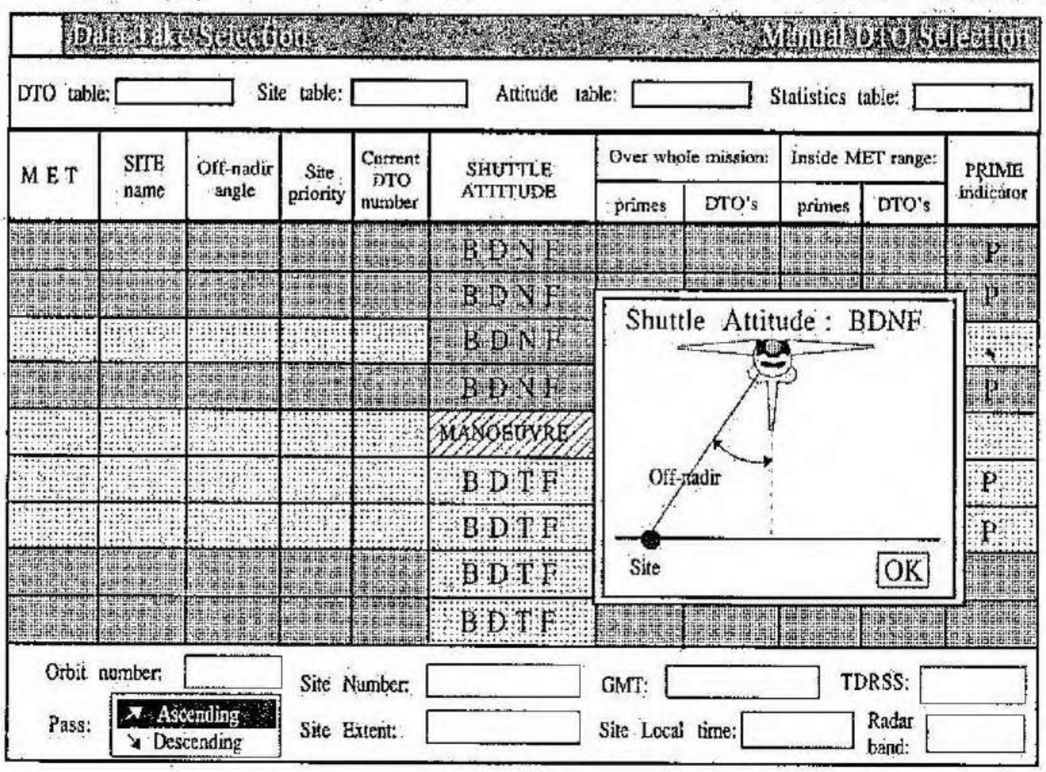

FIGURE 2 - Primary Sites Selection

- Antenna Tilt Angle (0-90 degrees in 1 degree step)

- Bits per Sample (8/12)

- Chirp Bandwidth (9.5/19 MHz)

- Receiver Gain (0-40 dB in 2 dB step)

- Data Window Position (depending on PRF BPS and chirp bandwidth and commandable in steps of 9.95 microsec);

The radar configuration will be selected according to the scientist's requirements which are provided by means of the following data package:

- wide swath (coarse resolution, low PRF, 8 bits per sample);

- high spatial resolution (fine resolution, low PRF, 12 bits per sample);

- high radiometric performance (coarse resolution, high PRF, 12 bits per sample).

Each user will specify in advance which package is to be considered for the radar setting determination procedure. At the end of the calculation, the list of the most suitable radar parameters will be presented to the user, ranked according to the selected package (Figure 3). Though the calculation is fully automatic, the final choice is left to the operation and science teams.

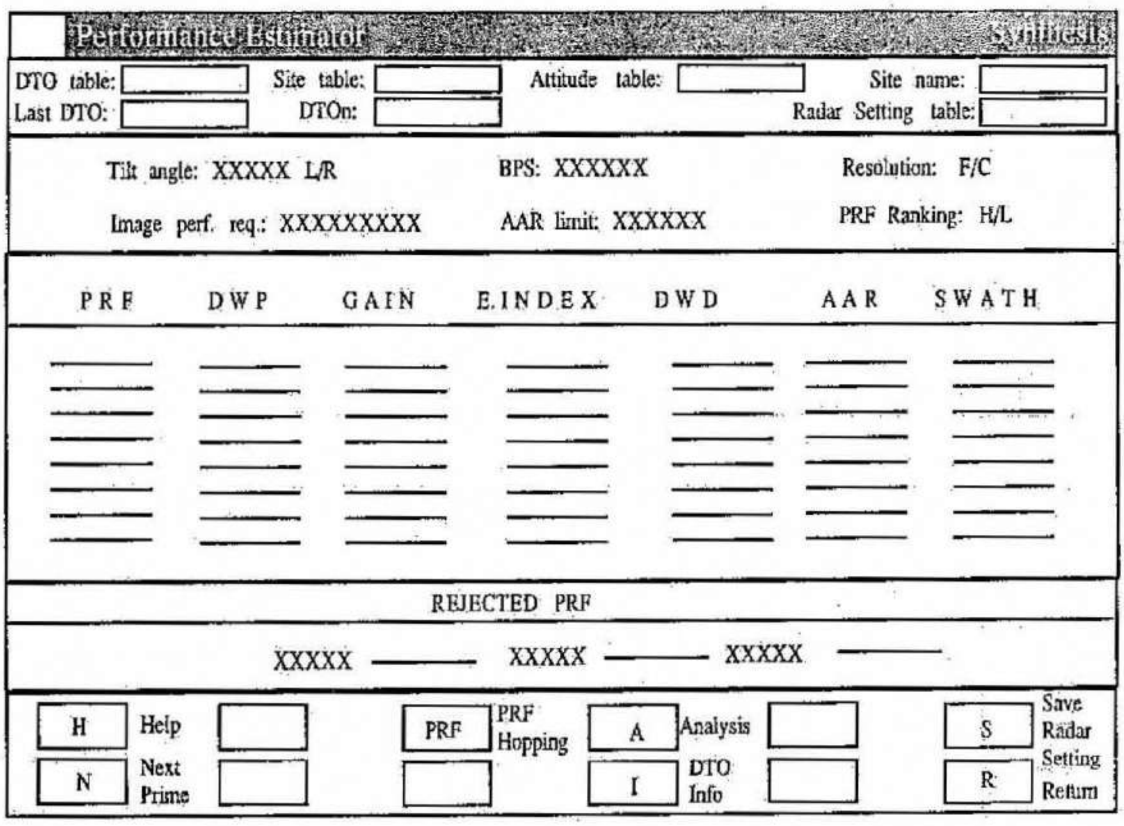

FIGURE 3 - Radar Setting Selection

A support to the selection of the radar setting will be provided by the determination of the performance curves for each radar configuration. In fact, the following image quality functions will be calculated:

- ambiguity ratio;
- spatial resolution;
- radiometric resolution;
- dynamic range.

All these curves will be displayed to the users (Figure 4), also allowing to compare performances related to different radar configurations. Further, each scientist can provide performance requirements in advance and so it can be checked if a selected radar configuration provides the image performances as requested. In case of poor results the scientist can suggest the operation team different packages so determining configurations and related performances, until good compromises have been reached.

This interactive approach is the basis for the hardware configuration of the Control Section, where a large use of workstations is foreseen. The workstations will be connected by a Local Area Network to a Central Computer where a relational data base will be resident. In this way, each console will access all the planning information and the science team will have the capability to follow each phase, also supporting the operation team.

Another important new facility provided by the X-SAR Control Section is the capability to modify the radar parameters in real time. This task will be performed by means of an intensive monitoring of the telemetry data, in particular of the echo profile, which expresses the strength of the return signals.

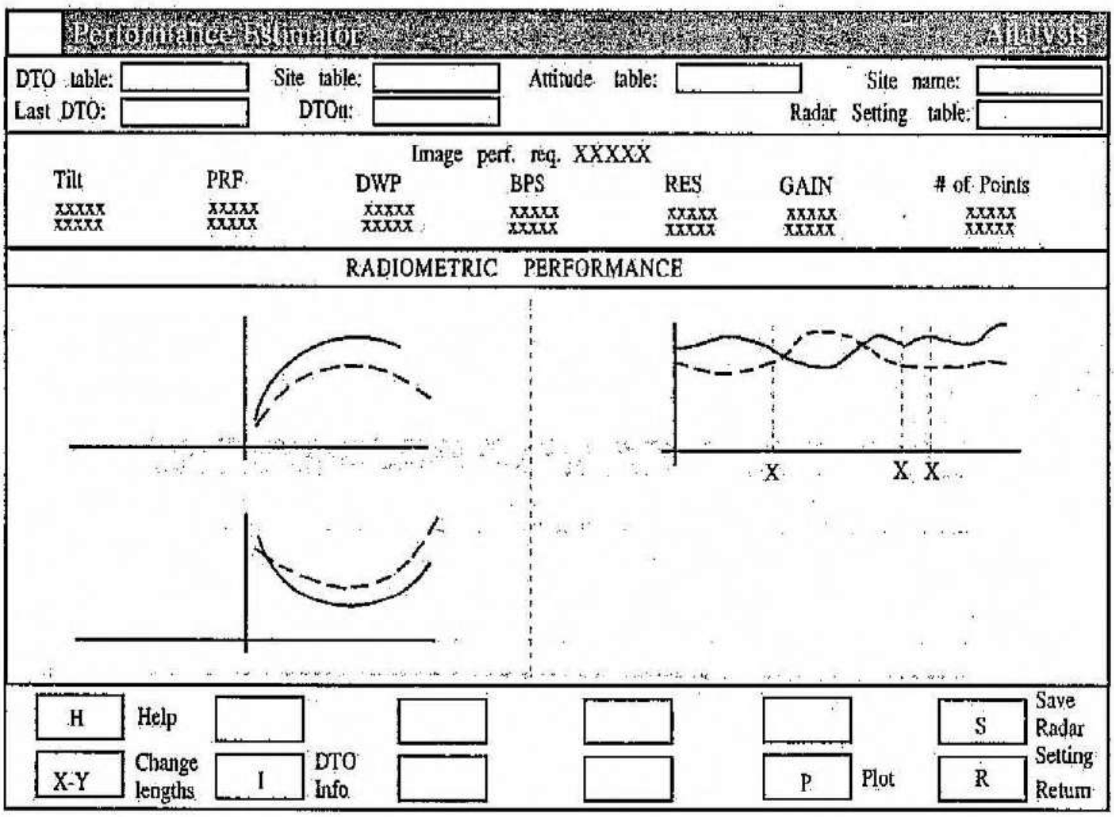

FIGURE 4 - Analysis of Image Quality Functions

The operation team will be given the capability to monitor the echo profile on a screen (Figure 5) superimposing on the curve the site position, the planned data window position and the expected nadir return. In this way it will be possible to monitor whether the gain has been properly selected or the data window has been correctly positioned with respect to the site.

This procedure is completely automated and so the resulting corrections for gain and data window are immediately presented to the operator. In this way, a corrected radar setting can be uplinked to the on-board instrument. Though only for the receiver gain and data window position it will be possible to calculate corrections, all the other parameters will be modified in real time if required by the science of operation team, to face particular contingencies.

4.2 - Processing Section Facilities.

As mentioned above, the Processing Section will produce real-time images of the selected sites. This will be achieved by means of a Quick Look Processor(*) which will process the deformatted raw radar data in real time and will display the resulting images on a high resolution monitor.

The X-SAR Processing Section will offer the capability to both store the raw radar data on CCT to be deliverable to the scientists and to record the preliminary output from the QLP on VHS cassettes by using a commercial videorecorder. Due to the strict time constraints, the QLP will only produce very draft images, without performing any preliminary correction. In any case by creating a catalogue on cassettes, the scientists would be immediately aware whether the acquisition has been successful. At the moment the creation of a catalogue is foreseen just at the end of the mission. Anyway, for the second and third launches the preparation of a catalogue will be performed in near-real time. In this case, some input information for the the replanning cycle can be provided. The user will infact require some modification to the timeline, if possible, in order to replan new acquisitions for the sites under investigation.

The Processing Section will also offer the capability to analyse off-line processed radar data to determine the corresponding power spectra and histograms, to assess the quality of data acquisition.

5. CONCLUSIONS.

Though the X-SAR Ground Segment has been conceived to operate in such a way to fulfil scientific expectations, our effort is to improve the present configuration in order to overcome some limitations, especially for the Processing Section.

The future trend will be so devoted to the realization of more sophisticated Quick look Processor, capable to provide corrected images for the sites in near real-time. The use of more complex algorithms will also be evaluated in order to determine, on the basis of processed data, system features such as antenna pattern that can be correlated to the radar configurations. This will provide quick reactions to any contingency and a more accurate determination of the resulting corrections.

6. ACKNOWLEDGMENTS.

We would like to thank ASI people for the support provided to the presentation of this paper. We also thank Dr. M. Musmeci (SeS) for his kind help in the realization of the graphics.

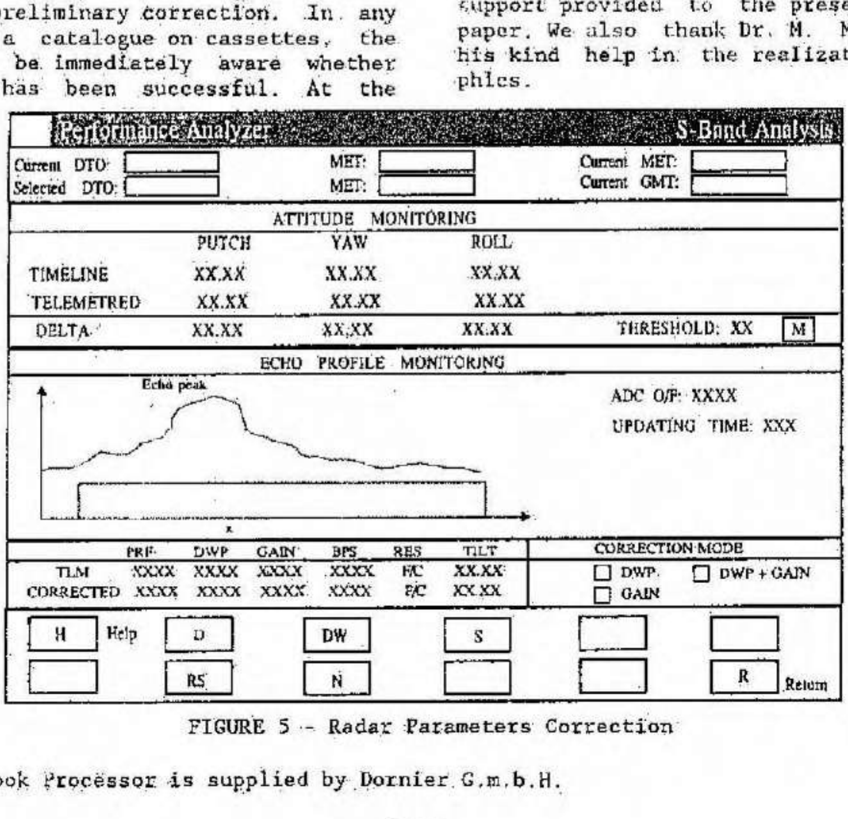

FIGURE 5 - Radar Parameters Correction

(*) The Quick Look Processor is supplied by Dornier G.m.b.H.

references were not intended to be a complete review of the literature available on the subject, they provide a general background for the focus of this paper.

For decision making, forest planners and managers need current information which can be manipulated in a flexible way (Hegyi 1985). The basic ingredients of such a land information system are: geo-referenced base, cadastral and thematic maps within the context of a geographic information system, cost effective change detection procedures, and flexible data management algorithms. Examples of such systems are the forest inventory data base of British Columbia (Hegyi and Quenet 1983, Hegyi 1988) and New Zealand (Kirkland 1985), the resource information management project in Thailand (Beaudoin 1988), GIS strategic projects in the Nordic countries (Tveitdal and Hesjedal 1989), remote sensing and GIS applications in Asean countries (Mok et al 1988), and the forest change classification project in northern Florida (Hoffer and Lee 1989).

Forest inventory and monitoring techniques have experienced some dramatic changes during the past 30 years, driven by technology, needs, local conditions and public pressure for information on resources other than forestry. The long standing leadership of the European practices have been challenged by the rapidly evolving technology. In particular, North American foresters, faced with extensive areas of unknown forests, have turned to remote sensing techniques, computers, and geographic information systems to aid in the design of forest inventory and monitoring projects.

In recent years, considerable attention has been focused on global monitoring. The need for monitoring renewable resources on a global basis is well documented by Hilderbrandt (1983) and Singh and Laniy (1983), and on a national basis by Schmid-Haas (1983), Lund (1983), Hagglund (1983) and Hegyi (1983). Geographic information systems have perhaps made the greatest impact on forest inventory and monitoring practices and their operational implementation has received considerable attention (Tomlinson 1989, Hegyi 1989).

FOREST INVENTORY AND MONITORING TECHNIQUES IN CANADA

A review of forest inventory and monitoring techniques used in Canada indicates that numerous alternative methods are available, depending on needs and local conditions. However, there are a number of components that are common to most inventories, such as planimetric and cadastral maps, administrative boundaries, thematic forest cover and environmental sensitivity maps, road networks, information on other resources and land use options. In addition, cartographic maps containing digital elevation data and change monitoring information are essential requirements of modern forest management.

Geographic information and satellite image analysis systems are becoming an integral part of forest inventory. The requirement of stand or area specific information further confirms the strong role of GIS in inventory practices. These new tools have a major effect on the statistical techniques that may be used for the inventory, as well as on data management and retrieval practices.

Given the available modern technology, forest inventory projects in Canada include the following components:

1. Essential components of forest inventory projects are the base maps. Starting with planimetric maps, ownership, cadastre and administrative boundaries are entered to form the base map. Automation of this process with GIS is cost-effective and provides the opportunity of storing the various sources of information as levels, facilitating further manipulations with thematic and topographic information. In cases where planimetric base maps are not available, geometrically corrected satellite imagery provide a practical alternative.

2. Most management unit inventory projects use vertical aerial photographs at 1:15,000 or 1:10,000 scales. These photographs are interpreted to provide descriptions of forest cover. For example, in areas where the number of species within homogeneous strata are less than five, individual species composition may be determined to the nearest 10%. Otherwise species groups or other relevant ecological units may have to form the description of the forest cover. Date of stand establishment or age, if available, and total height (e.g., average height of 100 largest stems per hectare) of the leading species is estimated next. In order to improve the estimation of volumes of individual stands, some measure of stocking is important, such as crown closure to the nearest 10% or stems per hectare. In addition, other relevant information is included in the attribute list, such as site index or site type, estimated volume, stand history, etc.

3. Using ground control information and field samples, the interpretation of aerial photographs is confirmed. Photo centres and the boundaries of homogeneous types are transferred onto base maps either photogrametrically or directly into the GIS. High quality forest cover maps can then be prepared with the aid of the computer.

4. Sampling systems which are considered most cost-effective and efficient involve both large-scale photo and ground samples. Experience indicates that 70 mm stereo photos at 1:500 scales are highly suitable for the estimation of photo volumes. Random distribution of photo samples is preferred, with the aim of representing adequately the major population groups. A sub-sample of the areas selected for photo samples can then be chosen randomly and visited on the ground for detailed measurements. Ground and photo samples are analyzed according to procedures outlined under multi-phase sampling (Loetsch and Haller 1973).

5. In addition to the formal statistical analysis, volume

equations are derived from the sample data base, using independent variables which are compatible with the classification system. This approach allows volume estimation on an individual stand basis, a capability that is becoming increasingly important in multiple and integrated resource management.

6. The major advantages of using a GIS for processing the inventory data are that the thematic forest cover and multi-resource levels can be combined with cadastre, administrative boundaries, and other relevant levels of information that are available in digital or geo-referenced forms. Using either vector or raster based overlay procedures, areas of resultant polygons can be determined and the results displayed graphically, including colour enhanced thematic maps. As well, the statistical data may be manipulated in a flexible manner to provide a wide range of summaries.

7. An integral part of any forest inventory is growth projections. In Canada several approaches, are used including deterministic volume equations with time as one of the independent variables, stochastic models, and simulation models. The use of expert systems in growth projections will likely pick up momentum and may replace conventional approaches to a large degree.

The above described procedure is enhanced by the use of satellite image data. For example, supervised classification of thematic mapper imagery can provide useful information for the planning of forest inventory projects, including both the classification and sampling. Furthermore, if funding for aerial photography is limited, or due to weather conditions, parts of the area may not be covered by conventional photography, satellite image analysis has the potential of providing a lower resolution alternative for implementing projects.

For resource monitoring and change detection, satellite data provide perhaps the most cost-effective solution. Imagery obtained at two different times and subjected to multi-temporal analysis, provides opportunities far beyond the capabilities of any of the conventional techniques. Changes detected can be transferred to existing forest cover maps, or entered directly into the GIS. A more sophisticated option is to use an integrated satellite image analysis and geographic information system to monitor and manage change data.

TECHNOLOGICAL CHALLENGES FOR RESOURCE INVENTORIES

Traditionally, large field parties have been used to survey the land. Medium and small scale aerial photographs have provided opportunities to examine large areas in terms of such interest parameters as timber types, land forms, geological formations and agricultural uses. Extensive ground surveys have changed gradually to multiphase and multistage sampling designs, and for quality control. As the resolution of airborne remote sensing products has improved, even more field work has been substituted with large scale aerial photographs and photo sampling has become a new challenge to statisticians. Information that could only be obtained in the past from ground surveys, can now be closely approximated with the combination of extensive photo and limited ground sampling, used within the context of double sampling, or even higher order multiphase sampling designs. This was possible by correcting or "ground truthing" estimates from photographs from the sample measurements made on the ground.

Satellite imagery, such as the early versions of Landsat multispectral scanner data, has become fairly popular in a relatively short period of time, mainly because large areas can be covered frequently at lower cost than with conventional photographs. However, its low resolution has reduced its use mainly to monitoring changes, except in research and development environments, where claims have been made beyond its operational capabilities. With the advent of Thematic Mapper products, both spatial and spectral resolution have improved considerably, and the operational usefulness of spaceborne scanner products have increased. In addition, the release of SPOT data has shown resolution capabilities that can match conventional aerial photographs in many areas.

The major technological challenge of the 90's will be, however, the replacement of conventional aerial photographs with high resolution airborne scanner data, such as MEIS. When analyzed and colour enhanced, MEIS products can appear as if they were large scale aerial photographs, but have the main advantage of being in digital form. Once a library of spectral signatures can be compiled for such applications as forestry, agriculture, geology, land use, land production capability and environmental sensitivity, high resolution airborne scanner imagery will challenge aerial photo interpretation in a manner similar to the replacement of manual drafting by GIS.

The development of remote sensing technology has, in the past, occurred as a joint effort between researchers and resource managers. This development has not progressed as fast as it could have, mainly because both the users and those who have had major control on funding the new technology, have learned their resource management skills in a more conventional and manual environment for data acquisition. Hence, remote sensing techniques, especially those involving satellites, have undergone some scepticism and even resistance.

However, with the increasing concerns by the public about the environment and the changes that are being inflicted upon the land base, resource managers will be subject to scrutiny at a scale previously unimagined. Rightly or wrongly, practices previously considered acceptable and even cost effective, will be challenged. And the chances are that the challengers will have up-to-date information about the land base, using remote sensing technology, combined with powerful geographical information systems. In addition, in many cases the resource managers' own data will be used as the base, over which space and airborne scanner data will be displayed, showing the adverse effects on the environment.

Entrepreneurs working with land information systems are just a few steps away from setting up data marts, where, on floppy disks, information may be purchased about most parts of the world. Conflicts of land use and resource management practices, whether involving forestry, mining, agriculture or range, will be dealt with in the 90's from a new power base: current information, which can be manipulated at ease to highlight areas of concern.

Availability of information about the natural resources of a region, province or country has created further problems or challenges. Surveillance of natural resources by competitors could become an active industry, creating both marketing and legal problems.

GIS AS THE INFORMATION SERVER

Information that is being accumulated about our resources and environment is constantly increasing. A large portion of the data is already in digital form and is georeferenced. As new descriptive statistics are becoming available at frequent intervals with remote sensing techniques, the size of the data base will create major information management problems. Geographic information systems have the functional capabilities of acting as information servers as well as data managers.

For example, in British Columbia, a relatively large number of GIS installations have been initiated, many of which are PC-based, using 386 machines with at least 80 megabytes of storage. Most of these systems have been acquired to carry out contract work for the expanded forest inventory program. However, some of the consultants and contractors involved in this program are seeking expansion to other disciplines, such as land use allocation, environmental monitoring and mining. As the momentum of the digital conversion of land information increases, PC-based systems could become limiting factors to production and throughput. Provided that the healthy economic climate of this high tech industry continues in British Columbia, expansion of GIS installations from PCs to workstations and to more powerful processors, such as microVAX and VAX computers, will occur. Alternatively, the PC industry will advance in response to this demand, and microcomputer systems will be available to address increasing processing needs.

The projected expansion of the GIS industry will result in further decreases in cost for digital conversion, as well as for the management and distribution of land-related information. In fact, this expansion will likely move to a situation where a few wholesale distributors of land information feed the data to retailers, who will turn it into products that can be examined in a user friendly manner, perhaps even with home computers.

CONCLUSIONS

Public pressure on resource managers, to justify their decisions with respect to land use and environmental issues, will result in increased applications of remote sensing and GIS technologies. Demands for land-related information will increase and the data distribution industry will expand. A more informed public, and, in particular, special interest groups, will help to resolve some of the existing land use conflicts.

At the same time, readily available data can become powerful weapons against decisions which are contrary to public interest.

Conventional aerial photographic products will be replaced by airborne multispectral scanner data in resource management, while the use of satellite imagery will expand in global environmental monitoring. Remote sensing technology will become the principal tool for data acquisition. GIS, on the other hand, will be used for the management and distribution of georeferenced land information.

REFERENCES

Avery, T. E. 1975, Natural Resources Measurements, McGraw-Hill Book Co., New York.

Anon. 1988, Report of a Workshop: GIS: Geographic information systems, ESCAP/UNDP, Bangkok, Thailand.

Anon. 1989, Proceedings: Challenges for the 1990s GIS, Ottawa, Canada.

Bickford, C. A. 1952, The sampling design used in the forest survey of the Northeast: Journal of Forestry, Vol. 50, pp. 290-293.

Beaudoin, M. 1988, The Landsat Thailand project resource information management system in Thailand: Overview and trends in GIS systems, In Report of a Workshop on GIS: Geographic Information Systems, ESCAP/UNDP, Bangkok, Thailand.

Bell, J. F. and T. Atterbury, ed. 1983, Proceedings: Renewable resource inventories for monitoring changes and trends, Oregon State Univ. Corvallis.

Brann, T. B., House, L. O., and H.G. Lund, ed. 1981, Proceedings: In-place resource inventories: principles and practices, Univ. Maine, Orono.

Bruce, D. and F. X. Schumacher 1942, Forest Mensuration, McGraw-Hill Book Co., New York.

Cochran, W. G. 1953, Sampling Techniques, John Wiley & Sons, New York.

Cunia, T. 1974, ed. Proceedings: Monitoring forest environment through successive sampling, IUFRO S4.02, Syracuse, New York.

Frayer, W. E. 1979, ed. Proceedings: Forest resource inventories, Vol I and II, Colorado State Univ., Fort Collins.

Freese, F. 1962, Elementary forest sampling, Agriculture Handbook No.232.

Fries, J. 1974, ed. Proceedings: Growth models for tree and stand simulation, IUFRO S4.01-4, Stockholm, Sweden.

Hagglund, B. 1983, The new national forest survey, In Proceedings: Renewable resource inventories for monitoring changes and trends, Oregon State Univ. Corvallis.

Hegyi, F. and R. V. Quenet, 1983, Integration of remote sensing and computer assisted mapping technology in forestry: Canadian Journal of Remote Sensing, Vol. 9(2), pp. 92-98.

Hegyi, F. 1983, Mapping and satellite image analysis for forest inventory, In Proceedings: Renewable resource inventories for monitoring changes and trends, Oregon State Univ. Corvallis.

Hegyi, F. 1985. Opportunity for increasing the scope and efficiency of forest planning through high technology, In Proceedings: Twelfth Commonwealth Forestry Conference, Victoria, Canada.

Hegyi, F. 1988, Key factors in an operational GIS for land use planning, In Report of a Workshop on GIS: Geographic Information Systems, ESCAP/UNDP, Bangkok, Thailand.

Hegyi, F. 1989, The role of GIS in Provincial inventories, In Proceedings: GIS 89: A wider perspective, Vancouver, Canada.

Hildebrandt, G. 1983. Needs for monitoring renewable resources and national ecosystems - a global prospective, In Proceedings: Renewable resource inventories for monitoring changes and trends, Oregon State Univ. Corvallis.

Hoffer, R. M. and K. S. Lee, 1989, Forest change classification using Seasat and Sir-B satellite Sar data, In Proceedings: IGARS'89 Quantitative Remote Sensing: An Economic Tool for the Nineties, Vancouver, Canada.

Husch, B., Miller, C. I., and T. W. Beers 1972, Forest Mensuration, The Ronald Press Co., New York.

Johannsen, C. J. and J. L. Sanders, 1982, ed. Remote sensing for forest management, Soil Conservation Society of America, Ankeny, Iowa.

Kirkland, A. 1985, Data needs and recent developments in resource management and planning, In Proceedings: Twelfth Commonwealth Forestry Conference, Victoria, Canada.

Loetsch, F. and K. E. Haller, 1973, Forest Inventory, Vol. I and II, BLV Verlagsgesellschaft, Munchen.

Lund, H. G. 1978, ed. Proceedings: Integrated inventories of renewable natural resources, Univ. Arizona, Tuscon.

Lund, H. G. 1983, Change: now you see it - now you don't, In Proceedings: Renewable resource inventories for monitoring changes and trends, Oregon State Univ. Corvallis.

McPhalen, J. 1989, ed. Proceedings: GIS 89: A wider perspective, Vancouver, Canada.

Mok, S. T., Anis, Z., and A. Ramlee, 1988, Promoting remote sensing and GIS applications in Forestry in Asean, In Proceedings: Ninth Asian Conference on Remote Sensing, Bangkok, Thailand.

Schmid-Haas, P. 1983, Swiss continuous forest inventory, twenty years experience, In Proceedings: Renewable resource inventories for monitoring changes and trends, Oregon State Univ. Corvallis.

Singh, K. D. and J. P . Lanly, 1983, A review of FAO's contributions to assessment and monitoring of tropical forest resources, In Proceedings: Renewable resource inventories for monitoring changes and trends, Oregon State Univ. Corvallis.

Snedecor, G. W. and W. G. Cochran 1956, Statistical Methods, The Iowa State College Press, Ames.

Spurr, S. H. 1948, Aerial Photographs in Forestry, The Ronald Press Co., New York.

Spurr, S. H. 1952, Forest Inventory, The Roland Press Co., New York.

Tomlinson, R. F. 1989, Geographic information systems - challenges for the 1990s, In Proceedings: Challenges for the 1990s GIS, Ottawa, Canada.

Tveitdal, S. and O. Hesjedal, 1989, GIS in the Nordic countries, Proceedings: GIS 89: A wider perspective, Vancouver, Canada.

Ware, K.D. and T. Cunia, 1962, Continuous forest inventory with partial replacement of samples, Forest Science Monograph 3.

Weller, B. S. 1983, ed. Proceedings: Automated cartography: international perspectives on achievements and challenges, Vol. I and II, Auto-Carto Six, Ottawa, Canada.

LASERS: A NEW TECHNOLOGY FOR AIRBORNE PROFILING OVER FORESTED AREAS

J. Blair, B. Hlasny and J. Schleppe, McElhanney Geosurveys Ltd., Vancouver, B.C., Canada

ABSTRACT

Airborne Profile Recording systems for digital terrain acquisition have now been replaced by laser technology combining integrated components which include standard cartographic cameras and small tracking cameras, precise altimetry and GPS positioning. McElhanney has recently completed a contract covering the islands of Kalimantan and Sulawesi in Indonesia providing vertical control and aerotriangulation for 1:50,000 map production. This contract required the installation of a high altitude laser system mounted onboard a fixed wing aircraft, to provide photo identifiable vertical points which were transferred to mapping photography. The laser system, designed by Holometrix of Cambridge, Massachusetts is the first privately owned high altitude unit to be integrated and designed specifically for such mapping applications. A total of 11,000 line kilometers were flown in four months over heavy forested terrain providing true ground data to inaccessible areas. Project field operations, profile results and vertical transfer methodology are presented in this paper.

KEY WORDS: Airborne Laser Profiling, Hardware and Software Integrations

1. INTRODUCTION

Airborne profile recording (APR) for topographic surveys were first undertaken in the late 1940's with particular application to heavily forested and remote areas. The early systems were radar units providing profile accuracies of approximately 10 metres. These systems were used extensively providing vertical control on projects throughout the world for map productions at small scales such as national 1:250,000 and 1:50,000 series.

Recently with the advent of LASER technology, more accurate systems have been developed, and APR is being used not only in mapping applications, but also in hydrographic surveys, route profiling, forest inventory, water quality sensing, reservoir planning and volume determination.

McElhanney's development of an integrated laser system came from the company's involvement in a large survey and mapping program in Indonesia. This program is being carried out as the Resource Evaluation Aerial Photography Project (REAP) and was designed to set up a physical and institutional capability in Indonesia to handle the development of their natural resource, particularly forestry, mining and oil and gas exploration. Canadian aid has sponsored the project over 3 phases commencing in 1979. Phase 1 was the establishment of horizontal and vertical control points using Doppler satellite observations to form a base for 1:50,000 mapping. This was completed by McElhanney in 1981 (A total of 238 stations established covering all of Kalimantan, Sulawesi and some of the southern islands). Phase 2 provided aerial photography coverage and Phase 3 has provided densification of vertical control using the laser APR, for aerotriangulation and numerical adjustment of the final map compilation.

The APR for use on Phase 3 was developed to provide high altitude terrain profile data at an economical cost using fixed wing aircraft. The system was developed for portability and to operate in relatively small aircraft with standard aerial camera ports. It is designed to acquire ground profiles for applications such as route profiling, cross-sectioning, vertical control for topographical mapping and the creation of a DEM base.

2. APR PROFILING AND SYSTEM COMPONENTS

APR equipment, when mounted and operated in an aircraft (airplane or helicopter), measures vertical profiles of terrain with respect to a reference isobaric surface.

The aircraft flies along a constant pressure altitude anywhere from 1,000 to 30,000 feet above the ground level. Pulses of LASER energy (travelling at the speed of light 186,230 mi/sec) are transmitted in a narrow beam and the elapsed time between transmission and return is a measure of the distance between the aircraft and the ground. These measurements are reproduced as a continuous line or profile of a narrow strip of ground traversed by the aircraft. A Barometric Reference Unit (BRU) senses deviations of the aircraft either up or down from a constant pressure level. The flight path of the aircraft is recorded by a tracking camera (70 mm frame or continuous strip camera), or other onboard navigation system.

After adjustments to remove pitch, roll, BRU deviation and isobaric surface slope, and to adjust the terrain profile to ground datum, the profile is used to provide vertical control for mapping or other DEM applications.

The McElhanney airborne laser system consists of five separate sensors, four of which are interfaced to the central processing unit and each drawing power from the central power distribution module. The system is essentially a passive data collector with the only control being over the tracking camera. The central computer waits for information from the altimeter, pitch/roll meter and the laser. It in turn triggers the tracking camera shutter and advances it based on operator inputs. It stamps all information coming in with a time tag, allowing it to later reassemble and correlate the data at the post processing stage. A description of each component is given below. Figure 1 illustrates the interfacing of the components.

3. COMPUTER

The central processing unit for the laser system is the McElhanney designed M CAT.DC powered (19-30 volts) navigation computer. The M CAT includes a 20 Mbyte hardcard, a 1.2 Mbyte, 5.25 inch floppy drive and a 720 Mbyte, 3.5 inch micro-floppy drive. The system display monitor is an ASK LCD flat screen and graphics adapter. The computer is shock resistent and rack mountable.

4. LASER PROFILER

The laser used by the McElhanney system is the ACCI PRAM IV Model LRY-1000 pulsed laser, which was designed specifically for high altitude airborne service, and for easy mounting in an aircraft.

The laser has a peak power rating of 114 mjoules and can operate at speeds of 5, 10 and 20 pulses per second at ranges up to 6000 metres. Range accuracy of the laser is 0.1 metre. A 28V DC power is provided for operation from the aircraft.

The PRAM IV profiler is interfaced to the M CAT computer via a RS-232 port.

5. DIGITAL ELEVATION COMPUTER

The laser system utilizes a Davidson Elevation Computer Model D101 as a barometric pressure altitude reference. The solid state unit incorporates pressure and temperature sensors in a software controlled unit. The pressure sensor is connected to the aircrafts static system. Vertical resolution is 0.1 metre.

6. TRACKING CAMERA

The system's tracking camera is a Hasselblad 500 EL/M 70 mm format camera complete with an autowinder, a 50mm super wide angle lens and a detachable 120 exposure film magazine. The film magazine is equipped with a built in DA-1 serial interface and a detachable DE-32 Datapac which allows the system to automatically annotate the 70 mm tracking film with date, time, roll number and frame number. The frame interval is controlled by the central computer based on the operator selected ground speed, flying height and forward overlap.

7. PITCH AND ROLL METER

The MDL TRIM Cube Model 40S provides pitch and roll information for the laser system. It is a two axis inclinometer using electrolytic gravity sensors with a single chip micro-computer used to demodulate the sensor information and produce a serial data stream. The unit has a range of 40° and an accuracy of 0.25 degrees.

8. DATA COLLECTION

Program MAPR V1.0 is used by the McElhanney system for the real-time collection of APR data. As data is read by the program it is time tagged and then stored in a unique device file on the hard disk. There is a file created for each of the devices, which include the laser, altimeter, camera and pitch/roll meter. The time tags allow the post processing section of the program to later reassemble the data and correlate it for adjustment and profile display.

9. POST PROCESSING AND ADJUSTMENT

For post processing the APR data, the M CAT computer is interfaced to a Okidata Microline 320 high speed dot matrix graphics printer and to a Houston Instruments Hipad Plus Model 9012 digitizing tablet and cursor.

At the end of each days flying all data collected is inspected for completeness. The data is processed through program MAPR and the unadjusted profiles are inspected for: annomalies; poor laser tracking of water surfaces (necessary for profile adjustment); large gaps in data; proper exposure and firing of tracking camera.

A linear correction is determined for each profile which corrects the line's initial datum error and the elevation discrepancy at the end of the line. The operator would inspect the unadjusted profile and input the time, raw elevation and the controlling elevation for the control points or sea level at the start of the line and end of the line or APR traverse. The program then automatically computes a translation component in metres which corrects for the line's initial datum error and a scaling component in metres per second. In addition, the operator can enter intermediate points into the adjustment and it will give misclosures for these points along with intermediate correction values. The operator is then free to interpret the results and enter the values most suitable as corrections for later profiling of the APR data. A printout of each profile adjustment is made and logged along with a graphical representation of the APR lines or traverses and the corrections. Corrections entered by the operator for each line if satisfactory, were then saved in an initialization file which is stored for each line and can later be recalled when the data is to be inspected. This eliminates the need to re-enter the correction components and reduces the possibility of operator error.

To facilitate point selection along the profile the program utilizes a digitizing tablet and cursor. The operator digitizes a left and right photocentre on the tracking film, after which he can digitally display elevations, altitude, roll and pitch along the profile as the cursor is moved within the tracking film. This coupled with the stereo images on the tracking film allow the operator to identify features and transfer them to the mapping photography for mensuration. Selected points are also entered automatically into a log file by pressing one of the cursor keys.

Printouts of the profiles are available using a high speed dot matrix printer. The operator has the option to print one profile only or the entire line (at any scale).

10. APR PROJECT APPLICATION

The Indonesian project provided a real test for both hardware and system capability. Terrain in Kalimantan and Sualwesi varied from low level swamp and jungles to densely forested mountains, with temperatures consistently in the low 30's and high humidity. Elevation varied from sea level to more than 3000m.

Weather was the major contributing factor in profile production. Generall flight missions were achieved during the morning before any cloud build up developed. Extreme heat haze and cloud affects laser penetration and restricts identification on aerial photography.

Flight profile lines were chosen to meet mapping specifications for vertical point density and to also follow the geography of the land so that major features such as mountain ranges, rivers, lakes and coastal areas were easily identifiable. Daily flight planning was critical to ensure planned flight paths were covered and profile gaps were fully completed.

Profile lines commenced and terminated on points of known elevation such as sea level, lakes, rivers or large open areas. Additional check and common points were tied to along the flight path to improve closure accuracy and detect any blunders. After each days mission, all profiles were verified and adjusted prior to the next days mission planning.

Profile data and aerial photography were forwarded to photogrammetrists. They made the vertical point selection, identification on the 70m film and transfer to the mapping photo was completed. The results were processed through the aerotriangulation adjustment program PATM which verified the elevation value with the identified point selected.

11. CONCLUSIONS AND RESULTS

The laser system proved very effective over heavily forested areas such as tropical jungle. Approximately 20% of laser penetration was achieved through the heavy foliage providing an accuracy, after misclosure adjustment, of 0.5 to 1.0 metre.

12. REFERENCES

Blair, J.D., and McLellan, J.F., 1984, Route Profiling in Australia Using an Integrated Inertial and Laser Profiling System; The Australian Surveyor.

Dalton, B., 1989, Indonesian Handbook; Moon Publications.

Department of Energy, Mines and Resources, Surveys and Mapping Branch, 1973, Specification for aerial Survey Photography.

Holometrix, Inc., 1989, PRAM IV LRY-1000 Airborne Laser Profiling System: Operation and Maintenance Manual.

McElhanney Geosurveys Ltd., 1989, APR Operations Guide.

McElhanney Geosurveys Ltd., 1989, MAPR – McElhanney's Airborne Profile Recorder Operating Manual.

McElhanney Geosurveys Ltd. 1988, Inception Report, Resource Evaluation Aerial Photography Project Phase III, Airborne Profile Recording, Aerial Triangulation.

Thomson, D.B. and Rais, J., 1981, The Indonesian REAP Doppler Satellite Network.

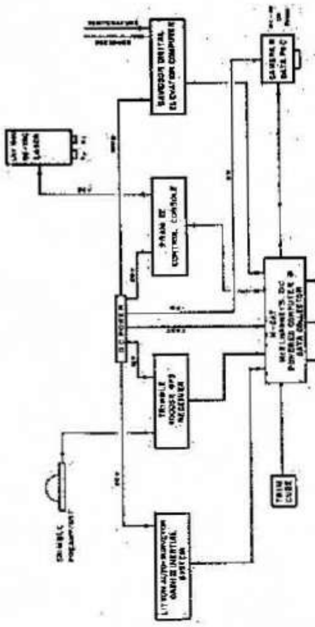

APR (MAPR) SCHEMATIC DIAGRAM

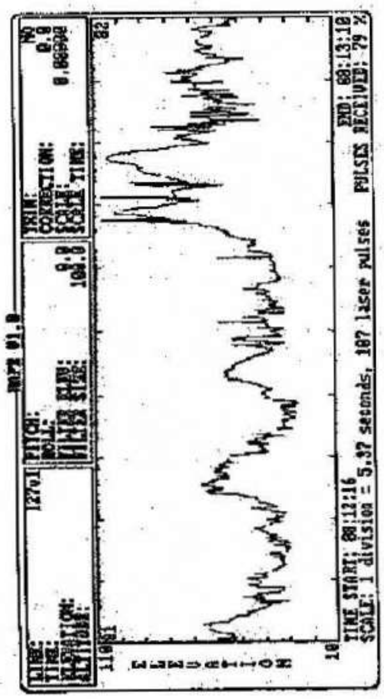

REAL TIME PROFILE PRINTOUT